

**Biomechanical Study of Upper Limb Activities
of Daily Living**

by

Pei Lai Cheng BEng, MEng

This thesis is submitted in partial fulfilment of the requirements for the degree of
Doctor of Philosophy in the Bioengineering Unit, University of Strathclyde.

May 1996

**Bioengineering Unit
University of Strathclyde
Glasgow**

The copyright of this thesis belongs to the author under the terms of the United Kingdom Copyright Act as qualified by the University of Strathclyde Regulation 3.49. Due acknowledgement must always be made of the use of any material contained in, or derived from , this thesis.

ABSTRACT

The kinematic and kinetic characteristics of arm movement during four activities of daily living: lifting a weight, driving a steering wheel, opening/closing a door and cutting were investigated in this study by using a human movement analysis system comprising a 6 camera Vicon motion analysis system, a 6 component strain-gauged transducer, a specially designed and instrumented steering wheel simulation system, a door and a cutting plate.

The most important achievements of this study are: (1) Implementation of the residual analysis technique into a computer program to filter the noisy kinematic data at an auto-selected cut-off frequency for each data sequence. (2) The development of a new method of representing the velocity and acceleration of points of interest using the phase plane presentation.

It was found that driving is the most complicated activity investigated in this study according to the range of arm movement. From the kinetic results, it was found that the order of difficulty of the four activities can be arranged as cutting, door opening/closing, lifting, and driving according to the magnitude of the maximum resultant total shoulder moment. The difficulty of the lifting activity increased with the weight to be lifted and the height of lifting. It was also found that the major component of the shoulder moment is the flexion/extension moment for most of the activities except driving, therefore it is concluded that having sufficient shoulder flexion/extension strength is most important for conducting most upper limb activities of daily living. In addition, the results of this study provide information for improving the understanding of the biomechanics of the upper limb activities and for clinical reference.

Acknowledgements

Without the assistance, encouragement and patience of many individuals my research project would never have been completed.

I would like to first thank Professor **John P. Paul** for giving me the opportunity to conduct this research in the Bioengineering Unit.

I would also like to thank Professor **J. C. Barbenel**, the head of Bioengineering Unit, for allowing me to use the facilities in the Bioengineering Unit.

I am extremely grateful to Dr. **A. C. Nicol**, my supervisor, for his guidance, constructive criticism, invaluable advice and encouragement given to me throughout this project.

I would also like to express my appreciation to the assistance given to me by the staff of the Bioengineering Unit, in particular Mr. **A. J. Tullis** (electronic technician), Mrs. **S. M. M. Nicol** (computer advisor), **David A. Robb** and **Robert Hay** (mechanical technicians), and Miss **Joan D. Wilson** (secretary).

The financial support of the Overseas Research Student Award, David Livingstone Bursary and University of Strathclyde Scholarship are greatly appreciated.

I am deeply indebted to my wife Heqing for her patience, understanding, and encouragement. Many thanks also to my parents and the members of my family for their understanding and support.

TABLE OF CONTENTS

Abstract	iii
Acknowledgement	iv
Table of Contents	v
Chapter One: Introduction	1
Chapter Two	
Literature Review on Biomechanical Studies of Upper Limb Activities and Related Researches	4
2.1 Functional Assessment of Activities of Daily Living	4
2.2 Biomechanics of Ergonomic Problems	10
2.2.1 Biomechanical Basis of Ergonomics	10
2.2.2 Some Ergonomic Problems	13
2.3 Anthropometry	26
2.3.1 Body Segment Link Length Measurement Method	27
2.3.2 Body Segment Mass	28
2.3.3 Determination of Mass Centre Location	29
2.3.4 Segment Moment of Inertia	30
2.4 Biomechanical Models	32
2.4.1 Link Segment Model	32
2.4.2 Musculoskeletal Model	35
2.5 Joint Loads	36
2.5.1 Joint Intersegmental Forces	36
2.5.2 Joint Intersegmental Moments	37
Chapter Three	
Literature Review on Human Movement Analysis Methods	38
3.1 Kinematic Analysis of Human Movement	38
3.1.1 Position and Orientation	38
3.1.2 Rotation	39
3.1.3 Angular Velocities and Accelerations	43
3.2 Kinematic Measurement Methods	46
3.2.1 Photographic Technique	46
3.2.2 Optoelectronic Techniques	47
3.2.3 Goniometry	50

3.3	Kinetic Measurement Methods	50
3.3.1	Ground Reaction Measurements	51
3.3.2	Hand Forces Measurements	52
Chapter Four		
	Experimental Work	55
4.1	Vicon Motion Analysis System	55
4.2	The Force Transducer	56
4.2.1	Modification of Pylon Transducer	56
4.2.2	Calibration of the Transducer	57
4.2.3	The End Adapter Design	62
4.3	Instrumentation	62
4.3.1	Instrumented Driving Wheel	62
4.3.2	Instrumented Door	65
4.3.3	Instrumented Cutting Plate	66
4.3.4	The Books Used for Lifting Activities	66
4.4	Test Procedures	66
4.4.1	Setting Up the Measuring System	66
4.4.2	The Landmark System	67
4.4.3	Measurement of Body Parameters	68
4.4.4	Lifting a Book	69
4.4.5	Driving the Steering Wheel	70
4.4.6	Door Opening and Closing	70
4.4.7	Cutting	71
4.5	Data Acquisition and Pre-processing	71
Chapter Five		
	Theoretical Aspects of the Research	73
5.1	Data Processing	73
5.1.1	FIR Filter Design	74
5.1.2	Choice of the Cut-off Frequency - Frequency and Residual Analysis	75
5.1.3	Time Normalisation	79
5.2	Determination of Joint Centres and Segment Coordinate Systems	80
5.2.1	Joints Centres	80
5.2.2	Segment Coordinate Systems	82
5.3	Kinematic Analysis	88
5.3.1	Joint Motion	88

5.3.2	Numerical Differentiation	89
5.3.3	Angular Velocity and Acceleration	89
5.3.4	Angular Orientations of the Upper Arm and Elbow Angle	90
5.4	Kinetic Analysis	91
5.4.1	Gravitational Force	91
5.4.2	Inertial Forces and Moments	92
5.4.3	Forces and Moments Measured by Transducer	93
5.4.4	Joint Intersegment Forces and Moments	95
5.5	Determination of Axial Rotation Angles of Limb Segment	96
Chapter Six		
Results and Discussions		
		108
6.1	Lifting Activity	108
6.1.1	Kinematic Results and Discussions	109
6.1.2	Kinetic Results and Discussions I - Shoulder Forces and Moments	118
6.1.3	Kinetic Results and Discussions II - Elbow Forces and Moments	125
6.2	Door Opening and Closing Activity	130
6.2.1	Kinematic Results and Discussions	130
6.2.2	Kinetic Results and Discussions	131
6.3	Driving Activity	133
6.3.1	Kinematic Results and Discussions	134
6.3.2	Kinetic Results and Discussions	135
6.4	Cutting Activity	136
6.4.1	Kinetic Results and Discussions	137
6.5	Summary of Shoulder and Elbow Moments of Four Activities	139
6.5.1	Summary of Shoulder Moments of Different Activities	139
6.5.2	Summary of Elbow Moments of Different Activities	142
Chapter Seven		
Conclusions and Recommendations		
		144
7.1	Conclusions	144
7.2	Recommendations for Further Work	148
References		
		150
Appendix A		
		167
Appendix B		
		170
Appendix C		
		172

Chapter One

Introduction

Activities of daily living (ADL) are an essential part of everyone's life. The quality of one's life is influenced by the ADL which one can undertake. Assessment of the ability of doing ADL is one of the common practices of clinicians, physiotherapists, and rehabilitation engineers (Law 1993, Law & Letts 1993). In the assessments, biomechanical parameters are important factors to be considered. However, in most previous practical assessments, these factors were often assessed qualitatively (Merbitz et al. 1989, Christiansen 1993), because the biomechanical characteristics of most activities are still unknown especially for upper limb activities. Precise assessment of the ability of doing ADL requires that the biomechanical characteristics of each activity be described quantitatively, which will depend on fully understanding the biomechanical behaviours of each activity. Some of the most important and fundamental biomechanical factors for describing each activity involve the range of movement of the limb segment and joint; the linear and angular velocities and accelerations of each limb segment; the forces and moments on the joints; the influence of inertial, gravitational effects and external loads on the joint forces and moments. To know these factors each activity must be investigated individually.

In industry, work related pain and musculoskeletal disorders and injuries of the shoulder region rank the second highest occurrence in clinical frequency following low back pain (Caillict 1981). Most of the work related injuries occur in the light manual material handling and light manipulations in many industrial occupations. Generally, there are three main causes of work related injuries (Bammer & Blignault 1987), rapid repetitive movements, less frequent but more forceful movement, and static loading. The causes are usually illustrated by a number of risk factors which may be different from one occupation to another. The determination of the risk factors is based on the understanding of the characteristics of the specific job. To know the characteristics of each job a biomechanical task analysis must be performed.

The advancement of modern technology and the development of human movement analysis methods provide an effective way of performing the activity or task analysis to give the biomechanical information required by the clinicians, physiotherapists, rehabilitation engineers, and ergonomists in their clinical practices and work designs for the diagnosis,

treatment and prevention of the musculoskeletal disorders and injuries, also for the assessment of the ability of doing of ADL.

The purpose of this study was to investigate the kinematics of arm movements, the loads (forces and moments) which act on the upper limb joints, and the influence of different effects on the loads of upper limb joints during some upper limb activities. A large number of upper limb activities in daily living and in the working place need to be investigated, and it is not realistic to investigate all of these activities in a limited period of time. Therefore selecting some common and representative activities for investigation was necessary. In this study four upper limb activities are investigated, lifting a weight, opening and closing a door, operating a steering wheel, and cutting with a knife. The choice of these activities is based on the following considerations (details are given in Chapter Two).

First the lifting of a light weight by one arm-hand to different heights is one of the most frequently conducted activity in daily living and in various working places such as the home, office, library, supermarket etc. However lifting activities have not been well investigated and understood especially in the three-dimensional situation. Little biomechanical information is known up to date.

Second, the door opening/closing activity can be characterised as pushing and pulling which is another most frequently conducted activity in daily living and work place. Most previous studies of pushing and pulling activities are limited to finding out the maximum isokinetic pushing and pulling strength in various conditions (Nicholson 1989). However, the real pushing and pulling activity is a dynamic process, and is performed below the maximum isokinetic strength. The dynamic characteristics of the pushing and pulling activity have not been well understood.

Third, in the modern world, driving is becoming a more and more important part of one's life as a daily activity or as an occupational task. The ability to drive is one of the important concerns for disabled people such as people after stroke, handicapped people and people with arthritis whether they wish to do shopping, get to work, visit friends or go on holiday. On the other hand, driving as an occupational task can cause musculoskeletal disorders (Kompier et al. 1987, Porter et al. 1992). To assess the driving ability of disabled people and to find out the causation of musculoskeletal disorder or discomfort of driving, it is essential to know the magnitude of control forces for driving and then to understand how the

forces and moments act on the hand and joints of the upper limb during driving. The study of driving performance has become one of the major areas of ergonomics and rehabilitation engineering, but most previous studies of driving activity are related to the visual, cognitive, and perceptive control abilities etc. The biomechanical information is very scarce in the literature. The full, dynamic, 3-D biomechanical picture of the driving activity is still not clear and is therefore required.

Fourth, a large portion of neck and shoulder pain occurs in sedentary work such as electro-mechanical assembly work, office work and working at computer terminals etc (Chaffin & Andersson 1984). Since this kind of work needs a small range of arm movement, neck and shoulder pain are caused by maintaining static muscle contractions. Previous studies are limited to measuring muscular activity and the biomechanical data on the joint forces and moments are still unknown. Therefore cutting at the sitting position is investigated in this study as one of the sedentary actions.

Finally, from the kinematic point of view, the arm movements during lifting, door opening/closing, driving, and cutting activities can be considered as up-down, forward-backward, rotational, and static dominated movement, respectively. Therefore the four activities can cover the major types of arm movements occurring in daily living and in the work place.

The thesis is presented in seven chapters including this introduction. Chapter Two reviews the biomechanical studies of upper limb activities and some related researches. Human movement analysis methods and measuring techniques are reviewed in Chapter Three. Chapter Four describes the experimental works conducted in this study. The analytical methods used in this study are given in Chapter Five. A new method developed in this study for determining the axial rotation angles of limb segments is given in the final section of Chapter Five. The results are presented and discussed in Chapter Six and Chapter Seven lists the conclusions and recommendations for further work.

Chapter Two

Literature Review on Biomechanical Studies of Upper Limb Activities and Related Research

Upper limb activities can be divided into two categories, the activities for daily living and the activities of occupational or industrial related. In this chapter the various methods that are currently used in rehabilitation engineering for assessing the ability of doing daily activities are discussed in the first section of functional assessment of activities of daily living. The biomechanical studies of some occupational related activities are discussed in section two as biomechanics of ergonomical problems. The discussion of some fundamental topics of biomechanical studies such as: anthropometric data measurement, biomechanical modelling, joint loads calculation are given in the remaining sections of this chapter.

2.1 Functional Assessment of Activities of Daily Living

Although the term activities of daily living or ADL has been in use for more than forty years since first published by Edith Buchwald (1949), a physiotherapist in 1949, who used it to refer to an assessment checklist, a generally accepted definition has not been found by the author to date. The difficulty of giving a proper definition to the activities of daily living is that a variety of people are doing a wide variety of activities daily. The people can be grouped from children, youth, adult to elderly people, from healthy people to those with disabilities, from persons at the work place to persons at home. The activities can range from the activities of basic living to the activities of working, from indoor activities to outdoor activities, from activities of upper limb to activities of lower limb, from activities of the central nervous system to the mobility of the body, from the activities for self-care to the activities for leisure. However, the lack of an appropriate definition of ADL does not prevent its use in many scientific fields.

The expectations of patients to improve their ability of doing ADL and from healthy persons to improve their quality of life stimulate the ADL related studies. Many ADL related research results are published each year in different journals by researchers from different fields. It is tedious to make a global review on all aspects of these investigations and is beyond the scope of this review. Since a reliable and valid assessment of the client's status

PULSES Profile (Adapted)

BARTHEL INDEX

	With Help	Inde- pendent
1. Feeding (if food needs to be cut up — help)	5	10
2. Moving from wheelchair to bed and return (includes sitting up in bed)	5-10	15
3. Personal toilet (wash face, comb hair, shave, clean teeth)	0	5
4. Getting on and off toilet (handling clothes, wipe, flush)	5	10
5. Bathing self	0	5
6. Walking on level surface (or if unable to walk, propel wheelchair)	10	15
*score only if unable to walk		
7. Ascend and descend stairs	0*	5*
8. Dressing (includes tying shoes, fastening fasteners)	5	10
9. Controlling bowels	5	10
10. Controlling bladder	5	10

A patient scoring 100 BI is continent, feeds himself, dresses himself, gets up out of bed and chairs, bathes himself, walks at least a block, and can ascend and descend stairs. This does not mean that he is able to live alone: he may not be able to cook, keep house, and meet the public, but he is able to get along without attendant care.

(Mahoney & Barthel 1965)

P—Physical condition: includes diseases of the viscera (cardio-vascular, gastrointestinal, urologic, and endocrine) and neurologic disorders:

1. Medical problems sufficiently stable that medical or nursing monitoring is not required more often than 3-month intervals.
2. Medical or nurse monitoring is needed more often than 3-month intervals but not each week.
3. Medical problems are sufficiently unstable as to require regular medical and/or nursing attention at least weekly.
4. Medical problems require intensive medical and/or nursing attention at least daily (excluding personal care assistance only).

U—Upper limb functions: Self-care activities (drink/feed, dress upper/lower, brace/prosthesis, groom, wash, perineal care) dependent mainly upon upper limb function:

1. Independent in self-care without impairment of upper limbs.
2. Independent in self-care with some impairment of upper limbs.
3. Dependent upon assistance or supervision in self-care with or without impairment of upper limbs.
4. Dependent totally in self-care with marked impairment of upper limbs.

L—Lower limb functions: Mobility (transfer chair/toilet/tub or shower, walk, stairs, wheelchair) dependent mainly upon lower limb function:

1. Independent in mobility without impairment of lower limbs.
2. Independent in mobility with some impairment in lower limbs; such as needing ambulatory aids, a brace or prosthesis, or else fully independent in a wheelchair without significant architectural or environmental barriers.
3. Dependent upon assistance or supervision in mobility with or without impairment of lower limbs, or partly independent in a wheelchair, or there are significant architectural or environmental barriers.
4. Dependent totally in mobility with marked impairment of lower limbs.

S—Sensory components: Relating to communication (speech and hearing) and vision:

1. Independent in communication and vision without impairment.
2. Independent in communication and vision with some impairment such as mild dysarthria, mild aphasia, or need for eyeglasses or hearing aid, or needing regular eye medication.
3. Dependent upon assistance, an interpreter, or supervision in communication or vision.
4. Dependent totally in communication or vision.

E—Excretory functions (bladder and bowel):

1. Complete voluntary control of bladder and bowel sphincters.
2. Control of sphincters allows normal social activities despite urgency or need for catheter, appliance, suppositories, etc. Able to care for needs without assistance.
3. Dependent upon assistance in sphincter management or else has accidents occasionally.
4. Frequent wetting or soiling from incontinence of bladder or bowel sphincters.

S—Support factors: Consider intellectual and emotional adaptability, support from family unit, and financial ability:

1. Able to fulfill usual roles and perform customary tasks.
2. Must make some modification in usual roles and performance of customary tasks.
3. Dependent upon assistance, supervision, encouragement or assistance from a public or private agency due to any of the above considerations.
4. Dependent upon long-term institutional care (chronic hospitalization, nursing home, etc) excluding time-limited hospital for specific evaluation, treatment, or active rehabilitation.

PULSE TOTAL: BEST SCORE IS 6. WORST SCORE IS 24.

(Granger *et al.* 1979)

plays an extremely important role in the clinical therapeutic process, the review in this section will be limited in the methods of evaluation and assessment of ADL. Attention will also be given to the activities of the upper limb.

Assessment of ADL

In the field of rehabilitation engineering and occupational therapy, the activities of daily living are commonly divided into those that are more simple, called ADL, and that are more complex, referred to as instrumented activities of daily living (IADL). Law (1993) gives some examples of ADLs as bathing, feeding, toileting, and transfers, and IADLs as housework, shopping, budgeting, and cooking meals. In the following discussions, the ADL and IADL will not be distinguished, and only ADL will be used, because in the biomechanical point of view, it is difficult to say whether bathing or cooking is more difficult without considering the physical conditions of individual subjects.

The ADL are often assessed by indices or scales. The first reference to an "assessment of every day activities" was reported by Sheldon in the *Journal of Health and Physical Education* in 1935 (Feinstein *et al.* 1986). Since that time, many indices and scales have been developed by rehabilitation professionals and occupational therapists. Some of them are well known and are often used such as: Barthel Index (Mahoney & Barthel 1965), Index of ADL (Katz *et al.* 1963), Klein-Bell ADL scale (Klein & Bell 1982), PULSES Profile (Granger *et al.* 1979), Level of Rehabilitation Scale (LORS-II) (Carey & Posavac 1982), and Edinburgh Rehabilitation Status Scale (Afflect *et al.* 1988).

Each of the indices includes a number of items which will be scored, the scores on each item will be summed to get the total scores of assessment of the ADL. These indices or scales have often been developed with different conceptual bases, including different items and scaling. In order to get inside these measurements of ADL, two examples are given here.

The Barthel index, a traditional assessment of physical disability, is established on the assessment of capacity to perform various activities of daily living. It includes ten items and different values are assigned to different activities. The scores on the Barthel index range from 0 to 100, 0 indicating total dependence and 100 total independence in self-care and mobility.

The PULSES Profile has six components, each component is scored by a four point rating scale from 1, intact and independent of help from another person, to 4, fully dependent,

for each function of the component area. The total scores range from a low of 6 to a high of 24, the higher the score, the more dependent the person. A score of 6 represents essentially unimpaired independence.

Problems exist in these measurements when occupational therapists use them in clinical practice. Questions, which have been raised on the currently used assessment of ADL, are summarised as follows.

First, most therapists assess and treat ADL skills, but have difficulty deciding which assessment to employ, because so many ADL measurement scales are available. Although most instruments are designed to quantify information for one of three general purposes: description, prediction, or evaluation of ADL (Law & Letts 1993), each instrument has its own specified purpose and client. Only a few indices can cover two or three of the purposes such as the Barthel Index (Mahoney & Barthel 1965) and the PULSES Profile (Granger *et al.* 1979).

Second, most measurements use summed ordinal scales, which have an inherent problem of lack of comparability because different items and scoring systems were used in these measurements (Merbitz *et al.* 1989). Problems also arise when scores are totalled and clients are compared on the basis of totals. For example, if there are 10 items on an ADL scale that is scored on a 4-point rating scale, one client could score 2 on each item for a total score of 20; another client could score 4 on three items, 3 on one item, and 1 on five items and also achieve a score of 20. Thus two persons could receive the same total score although their functional profiles, which have important implications for occupational therapy, are quite different. Although the use of summed ordinal scores is an attempt to create a quantitative index of ability, the fundamental problem is that the summing of qualitative ordinal counts to create total score does not result in a number that is a valid means of making quantitative comparison of performance. The solution of the problem needs a real quantitative assessment of ADL which should be based on the precise results of biomedical and biomechanical studies of each activity.

Third, the scores of items of ADL scales are obtained by self-report by the client in a questionnaire form, or from the direct observations of therapists on the client's performance. The accuracy of the reports from patients may be influenced by their psychosocial conditions. The assessment of observations from therapists may conflict with client's self-report about the

same activities, because not only the skill or expertise are involved in these observations, but also the client's perspective, value, and effort are not considered. Reports in the literature provide evidence that there are significant differences between ADL scores reported by an individual and those reported by service providers (Edwards 1990, Kivela 1984, Rubenstein *et al.* 1984). A survey by Chiou and Burnett (1985) also demonstrated that patients and therapist may value ADL functions very differently. It is still not clear how to deal with these differences.

Fourth, the occupational therapy functional assessments can be focused on physical performance component (PPC) evaluation or occupational performance evaluation. PPC evaluations include neuromuscular tests (e.g. strength, range of motion, muscle tone) and motor test (e.g. gross motor coordinate, fine dexterity, praxis). However, the evaluation of occupational performance purposed to assess the ability of doing activities (e.g. ADL) rather than components of the activities. In the mid-1970s, occupational therapy assessment tended to focus on physical performance component evaluation, whereas assessment of occupational performance played a secondary role (Mathiowetz 1993). The reasons for PPC evaluation taking priority over occupational performance evaluation on occupational therapy assessment and treatment was reviewed by Mathiowetz (1993). For example, the arrangement of priority was evident in treatments, where primary focus was on remediation of PPC deficits, whereas the remedy of occupational performance deficits was secondary. The assumption was that if PPC deficits could be normalized, then deficits in occupational performance would also be remedied. Another reason for the priority of PPC was the lack of occupational performance assessment to evaluate change in functional status. The ADL evaluations of the mid-1970s were highly subjective and assessed change qualitatively, whereas many of the PPC assessments (e.g. strength, range of motion, and dexterity) were objective and could be reported quantitatively. It was deemed more important by therapists to report objective data on a related variable than to report subjective data on occupational performance.

Recently, it has been recommended that the PPC evaluation should play a secondary role in occupational therapy assessment, and the occupational performance should play a primary role (Mathiowetz 1993, Christiansen 1993, Fisher 1993). The reasons that support the opinion are summarised as follows (Mathiowetz 1993):

- The value of occupation or purposeful activity in preventing and mediating dysfunction has been and is a core concept of occupational therapy (AOTA. 1979).

- Occupational performance is the central focus of all developing models in occupational therapy (Reed & Sanderson 1983).

- The study of the human as an occupational being is the focus of the new discipline of occupational science (Clark *et al.* 1991).

- Theoretical approaches outside the occupational therapy profession (e.g., the ecological approach to perception and action) emphasise the study of human behaviour during the performance of functional tasks in the natural environment (Reed 1982).

- The health care system is demanding that occupational therapy (and rehabilitation programs in general) document their efficiency in terms of changes in functional performance.

- School therapists must document the effectiveness of their treatment in terms of educational or functional performance changes.

The gap existing between evaluations of performance and performance component should be bridged. There is increasing agreement that occupational therapy's unique contribution to function is through emphasis on occupational performance (Christiansen 1993). It needs to shift the evaluation of assessment of ADL from the functional component domain to the performance domain. Also, it is necessary to develop new and better methods to assess ADL to serve occupational therapy practice and researches. The questions are:

- What is the strategy for developing the new assessment?
- What is the structure of the new assessment?
- What kind of activities should be involved in the new assessment?
- How to relate the performance and components of performance in new assessment?
- How to prove the validity and reliability of the new assessment?

The answer to these questions is a great challenge to the occupational therapists, rehabilitation professionals and related researchers, because limited research results have been reported to identify the relationship between performance and performance component. More efforts are required and more multidisciplinary investigations should be done, in which biomechanical research should play an important role to find out how the movement components contribute to the specified performance, which components dominate a specific activity, and how much effort and energy should be consumed to complete an activity.

To reach the goals, some initial considerations should be adopted in the future assessment and researches.

First, the performance based assessment should involve the measurement of performance components, because a simple activity may be conducted by the combination of a number of performance components. For example, shopping involves the activities of going out, accessing the supermarket (opening door), selecting an item (lifting and lowering a weight), and counting etc. A number of arm movement components are required to conduct these activities, such as flexion-extension, adduction-abduction, and internal-external rotation. The combination of the performance components is an optimum process for conducting an activity. An activity may be mainly controlled by one or two functional components and adjusted by others. For example, one can lift a weight in the sitting position by flexing one's arm and adjusting the hand position to the proposed site by adducting, abducting, and/or rotating the arm. Dysfunction of some functional components may be compensated by other functional components. For example, if you have shoulder pain and can not rotate your arm, you still can move your body to reach your target.

Second, the upper limb activities, lower limb activities, and whole body activities should be investigated and assessed respectively (Trombly 1993). The upper limb and lower limb have different functions. Upper limbs provide the primary ability of transferring one's hand from place to place to perform a multitude of tasks on which one's survival depends. Two major functions of the lower limb are body weight supporting and locomotion. The activities of upper limb and lower limb influence the different aspects of one's life and should have different weight on the assessment of the ability of ADL. A wheelchair user may have a great ability to conduct many desired activities by using the upper limbs in the sitting position despite the difficulty of self-transportation.

Third, the activities to be assessed should be carefully selected. Both low level and high level activities should be involved. Here, the low level activities are referred to, in the biomechanical view, as activities which need less strength, less power to conduct and have a small range of motion; and will be controlled by less motion components. In contrast the activity which uses much strength, has a large range of motion and is controlled by more motion components is referred to as a high level activity. It is obvious that the low level

activities are more important for disabilities and most of the healthy people than the high level activities. The perspective of the client should also be considered.

Fourth, quantitative assessment of ADL should be based on the quantitative descriptions of each of the performance components. Many biomechanical studies are required in this aspect, such as how much upper limb strength is needed to lift a light weight to different heights, to open a door, to do a simple cutting and to drive a car *etc.* How the loads act on each joint of the upper limb, how the weight and the inertial effects influence the joint loads, and how much of the range of movement of the upper limb are needed for conducting these activities.

2.2 Biomechanics of Ergonomic Problems

The concept of ergonomics was introduced in 1949 as a title for the interdisciplinary teamwork between various human scientists. It was started by a group of English scientists, primarily psychologists and physiologists, and the originator of the name was the marine psychologist Murrell (Ivergård 1982). The word is derived from the Greek *ergon* meaning work and *nomos*, whose nearest meaning is natural law or system. The conjunction of *ergon/nomos* was also used in classical Greek times for a worker's protection law, probably the world's first Safety at Work Act.

Ergonomics has been defined as an applied science concerned with the characteristics of people that need to be considered in designing and arranging things that they use in order that people and things will interact most effectively and safely (Griffin 1992). The primary aim of ergonomics is to optimise the functioning of a system by adapting it for man's abilities and needs. This implies attaining the best man-machine performance possible in the conditions, without causing injury or unnecessary wear and tear, and producing working conditions which are as comfortable and positive as possible.

2.2.1 Biomechanical Basis of Ergonomics

Originally it was known that ergonomics is based on human biological science: anatomy, physiology, and psychology (Singleton, W. T. 1972, Tichauer, E. R. 1978). In general terms, anatomy is concerned with the structure of the body (the size and the way it is constructed), physiology is concerned with the function of the body (biological processes that

maintain it), and psychology is concerned with behaviour (the adaptive responses of this organism to its environment). With expansion of the researches of ergonomics and the development of other scientific and technologies disciplines, a number of scientific disciplines have made great contributions to ergonomics. The rapid progress of the researches of biomechanics provided a number of new methods and instruments for ergonomics studies. Some ergonomic researches are conducted by using biomechanical methods. In fact, a book by professor E. R. Tichauer is entitled *The Biomechanical Basis of Ergonomics* (Tichauer, 1978). Ivergard (1982) also divided Ergonomics into two main areas, *Biomechanical Ergonomics* and *Information Ergonomics*. Biomechanical ergonomics covers the type of system where man's muscular power is involved.

The following discussions in this chapter will be limited to researches of biomechanical aspects of ergonomics, especially for the upper limb.

The researches in a number of subdisciplines of biomechanics contribute to the different aspects of ergonomics, while the combinations of methodologies of subdisciplines of biomechanics provide a direct way to the studies of performances of ergonomics concerned. The subdisciplines of biomechanics involve anthropometry, kinesiology, biomechanical modelling etc.

- **Anthropometry** is the empirical science that attempts to define reliable physical measures of a person's size and form for anthropological comparison. Engineering anthropometry stresses the application of these measurements in developing and evaluating engineering drawings and produces mock-ups to assure that the drawings are suitable for the intended user (Roebuck, Korea, and Thomson, 1975). Work-space designs are largely based on such data. At present, over 300 different human size and form variables have been statistically tabulated for US., European, and Asian populations (Webb Associates, 1978a).

The ergonomist, therefore, will use anthropometric data to ensure, quite literally, that the measure or the environment fits the person. Whenever the human operator has to interact with the environment it is important to have details of the dimensions of the appropriate body part. Overall stature is an important determinant of, for example, room size, door height, or cockpit dimensions; the dimensions of pelvis and buttocks limit the size of hatch openings or seats; the size of the hand determines the dimensions of controls and supportive stanchions;

while it is necessary to have details of arm reach to be able to position control consoles at appropriate distances. The list of possible examples is almost endless.

Another use of anthropometric data is in biomechanical models. Biomechanical models are often used in the analysis of industrial tasks. The accuracy of the analysis clearly depends on the reliability of anthropometry measures. Without it, biomechanical models to predict human reach and space requirements cannot be developed.

Some of the most often used anthropometry parameters in industry design and biomechanical models include the body-segment link length, body-segment volume and weight, body-segment mass centre locations, and body-segment inertial property. The development of measurement methods used to acquire anthropometric data and predicting the anthropometric data on the living body will be discussed in more detail in section 2.3.

Kinesiology is the complete study of human movement (Barham, 1978). Therefore kinesiology is concerned with one of the most complex of all phenomena associated with the complex of all living organisms - the movement behaviour of the human being. Kinesiology can be divided into kinematics and kinetics (Chaffin and Andersson 1984). The kinematics describes motions of the whole body or major body segments independent of forces that cause the movement and the kinetics describes the forces causing the movement. Kinematic variables include angular and linear displacement, velocities and accelerations; kinetic variables include both internal and external forces.

Kinematic and kinetic variables are widely used in the ergonomics related literature to describe human motions in everyday activities; human performances in industry tasks; working postures; the mobility of the human body; the range of motion of body segments; muscle strength, endurance and fatigue. These subjects can be divided into three parts (Barham, 1978). The first part is confined to the mechanical foundations of human motion and is primarily concerned with the fundamental methods and principles of mechanics involved in the kinematic and kinetic analysis of human motion. The second part, sometimes called anatomical or structural kinesiology, pertains to a study of the structures and mechanical functions of the specific muscles, bones, and joints that form the movement or motor apparatus of the human body. The third part, primarily concerned with the detailed analysis of specific motor skills, deals with how the different body segments and joint actions are linked together in the proper sequence for the most effective and efficient production of total body

movements. It is too ambitious to make a review on the whole area of human movement and is beyond the scope of this thesis. However, because the kinesiological knowledge is a prerequisite to the development of biomechanical models and their applications, the kinematic and kinetic analysis methods will be discussed separately in chapter three. The researches of muscle forces and joint loads will be reviewed in section 2.5, while some ergonomics concerned problems will be reviewed at the end of this section.

The Biomechanical Model is one of the most effective tools in biomechanical studies which enables the researchers to get into the inside of the biomechanical system, when the characteristics of some variables inside the system can not be determined by direct observations or measurements. For example, internal forces at the joints can rarely be measured directly, but by using biomechanical models it is possible to predict the internal forces from the measured external forces. The components of the models are adjustable to fit the environment to be described. Each time a model does not predict a system's behaviour correctly, certain parts of the model can be rationally changed, thus gaining insight into the complex nature of the real system.

When biomechanical models are used, they are the representations that can be understood. Since human biomechanical system is very complex, such representation may require gross simplifications and assumptions. The simplifications and assumptions adopted by the biomechanical models control the range of their applications. The development of biomechanical methods will be reviewed in detail in section 2.4.

2.2.2 Some Ergonomic Problems

Among the various ergonomic problems, occupational musculoskeletal injury due to manual material handling is perhaps the most important one. For this reason, the biomechanical studies of general manual material handling are discussed in the first part of this section. The focus of the second part of this section is on the reports of epidemiological studies of upper limb injuries. A brief review of biomechanical studies of some upper limb activities is given in the final part of this section.

2.2.2.1 Manual material handling

Manual material handling (MMH) remains a frequent activity in modern industries. Many MMH tasks (lifting, pushing, pulling, and carrying) are physically demanding to the worker. However, if the tasks are carried out incorrectly, they may result in at least musculoskeletal disorders and discomfort or at the worst permanent disability. It was reported (Tichauer 1973) that almost one-third of all disability injuries at work (temporary or permanent) are related to manual handling of objects. The high incidence of musculoskeletal disorders associated with MMH is a well recognised health problem.

The lifting activity is the major task of Manual Materials Handling. It has been a focus of attention amongst the ergonomics and biomechanics research communities for some 20 or more years (Buckle et al. 1992). Numerous studies have been published which describe the epidemiological, biomechanical, physiological and psychophysiological natures of the act of lifting. Most of the studies aimed to assess the lumbar loads because the high prevalence of back disorders is usually found in jobs involving very frequent heavy lifting (Andersson 1981).

The early model-based analysis of typical load manipulation tasks were mainly limited activities symmetrical to the median sagittal plane (e.g. Morris et al. 1961, Bejjani et al. 1984, Chaffin 1969, Ayoub and El-Bassoussi 1976, Freivalds et al. 1984, Jager et al. 1984). The symmetric lifting refers to the posture of lifting of loads by two hands in the sagittal plane (Chaffin and Andersson 1984). Though the biomechanical analysis of the sagittal plane lifting is the simplest and easiest, the symmetrical lifting was involved in the NIOSH (1981) *Work Practices Guide for Manual Lifting* as the recommended posture of lifting, because of the support from research findings on the safety and stability of the posture. However, the act of lifting could not be restricted in only the sagittal plane. In actual working situations in industry, the worker is constrained by workplace rather than by laboratory simulation and the working postures adopted are often asymmetrical and require whole exertions in a free-style manner. To investigate the asymmetrical lifting or the lifting that are not restricted in the sagittal plane, the three dimensional biomechanical analysis is required.

Previously, the static spatial biomechanical models have been developed by Schultz et al. (1982), and Chaffin et al. (1977) to assess the compression forces on the L4/L5 or L5/S1 intervertebral disc in different lifting postures. The problem with a static approach, noted by

Freivalds et al. (1984) is that the actual dynamic loading can be underestimated by as much as 40%. The clear differences (Leskinen 1985, McGill and Norman 1985) in the results calculated with static and dynamic models show that dynamic aspects should be taken into account when lifting work is analysed with biomechanical models (Leskinen 1985).

Recently, dynamic three-dimensional (3D) analysis on the various aspects of lifting activities have been reported (Frigo 1990, Kromodihardjo and Mital 1987, Jager and Luttman 1992). It should be mentioned that the tasks investigated in these and the above mentioned studies were all conducted by two hands in a standing posture. These tasks were generally referred to as heavy manual material handling (or lifting). The intensive studies have greatly improved our understanding of the nature of the heavy manual material handling, such as, the action of loads on the lumbar spine and the joints of lower limb; the muscle activity; the inertial effect on the joint loads; the stability of different lifting postures; the lifting strength and the acceptable handling limit for different group of people at various situations etc.. The direct results of previous efforts were reflected and condensed in a variety guidelines (NIOSH 1981, 1990, Davis and Stubbs 1980, ILO 1988, HSC 1988, Waters *et al.* 1993). There are however still some limitations in these guidelines (Buckle *et al.* 1992).

The other approach proposed for safer and more efficient manual handling is through the training programme of manual handling operation which is based on biomechanical principles and the findings of biomechanical studies. It has been proved that proper training programmes could significantly improve the physical capacity, such as endurance time, and static and dynamic muscular strength (Guo et al. 1992). However, there has been no convincing evidence that such training has effected any significant reduction in low back episodes (Rowe 1983) and much applied research needs to be done in this area (Kroemer 1992).

In industry, the contemporary wave of automated work handling has significantly decreased the number of human tasks which require heavy muscular force. Despite this increase in automation, human manual power is still required for different task manipulations, especially for light manipulations. These activities involve repetitive movements, and produce muscular tension on the shoulder and neck area, and are usually associated with musculoskeletal disorders (MSDs) on the upper limb and neck area. The researches relevant to upper limb musculoskeletal disorders will be reviewed in the following section.

2.2.2.2 Epidemiological studies of musculoskeletal disorders of upper limb

Musculoskeletal disorders (MSDs) of the upper limb are the prime disablers of working adults (Putz-Anderson 1988) in many industry professions. In literature, different names were used to describe these work-related problems (Ranney 1993). In Australia and Canada they are referred to as repetitive strain injuries (RSI). In America they are called cumulative trauma disorders (CTD) and in Scandinavia, occupational cervicobrachial disorders (OCD). In the following, the term of musculoskeletal disorder or work-related injury will be used as a general description of the problems and some specific terms such as rotator cuff (RC) tendinitis and carpal tunnel syndrome will be used to describe the symptoms on different areas.

The shoulder is the most frequently injured joint of the upper limb. It was recognised that the occurrence of shoulder pain ranks second in clinical frequency to low back and neck pain (Cailliet 1981). Recent studies have shown the prevalence of shoulder pain syndromes to be elevated in many working populations. Herbert *et al.* (1984) found the prevalence of supraspinatus tendinitis in shipyard welders to be 18.3% compared with 2% in clerks employed by the same company. The Prevalence of rotator cuff (RC) tendinitis and/or bicipital tendinitis in grocery store checkers was found to be 15% in contrast to a 4% level in non-checkers (Baron *et al.* 1990). The prevalence of regular discomfort in the shoulder region in a population of chicken processing workers was found to be 9% (Buckle 1987). In that study the employees' lifetime prevalence of shoulder discomfort or pain was determined to be 42%. Punnett *et al.* (1985) found the prevalence of persistent shoulder discomfort in garment workers to be 19.6%. The prevalence of discomfort or pain in the shoulder region of newspaper employees composing and editing on computer terminals was reported to be 11% (Burt *et al.* 1990). The prevalence of shoulder pain in other occupations have been reported, such as assembly (Fine *et al.* 1987), and shoemaking (Serratos-Perez *et al.* 1993).

In addition to the high prevalence of discomfort in the shoulder region, many employees in industry also suffered from elbow, wrist and hand pains. Statistics Canada (1991) reported that in 1989 there were 20,637 work related injuries of elbow, wrists, hand and fingers. In a review paper, Bammer & Blignault (1987) give out some examples of the prevalence of musculoskeletal problems on the forearm and hand, such as: about 50% of Finnish butchers were found to suffer from carpal tunnel syndrome; in a sample of 152 food packers in Finland,

Table 2.1 Factors suggested by the Task Force on Repetition Strain Injury in Australian Public Service (1985) to influence the incidence of RSI (Bammer & Blignault 1987).

Associated Factors	
1.	FEATURES OF WORK TASK Occupation/kind of work Physical demands of work Job design Design of equipment Training in use of equipment Opportunities for rest breaks rate of work Pressure of work
2.	FEATURES OF WORKPLACE Physical features of workplace Social context of work
3.	RESPONSE TO WORK AND WORKPLACE Attitudes to the job Stress responses to work Method/approach to task
4.	WORKER CHARACTERISTICS Physical (age, sex, level of fitness, associated physical symptoms) Psychological (personality, anxiety level emotional reactivity) Work history (years of service, experience/skill in task) Life outside work (opportunities for recuperation)
5.	WIDER SOCIAL CONTEXT Cultural attitudes to work Economic factors Attitudes to health and sickness Workers' compensation
Change Factors	
1.	CHANGE IN DEMAND Return to work after a break Increase in workload Change in equipment Reduced tolerance to stress
2.	CUMULATIVE EFFECTS Chronic fatigue Response to musculoskeletal symptoms

56% were found to have muscle-tendon syndromes of the hands and forearms; and 37% of data processing operators in one Australian study had hand, wrist and arm pain daily. The prevalence of MSDs can not be limited to these occupations. The syndromes are often found on different areas of the upper limb for different persons in the same occupation or workplace. It is difficult to write a list of each occupation in which the prevalence has been found and how serious a problem it is. However it is evident that the occurrence of work-related injuries of the arm has increased in recent years (Kvarnström 1983, Herbert *et al.* 1984, Louis 1990).

The cause of the musculoskeletal disorders of the upper limb is of great concern to researchers, ergonomists, clinicians, employers, bankers (Meyer 1987), and even policy makers of government (Kiddicoal & Ellis 1987) because of the high cost of the disorders. There is general agreement that there are 3 main causes of work-related injuries (Bammer & Blignault 1987): rapid repetitive movements, less frequent but more forceful movement, and static loading (i.e. the work that muscles must do to hold the body or parts of it in certain positions). In a statistical analysis, Stock (1991) concluded that specific disorders of tendon and tendon sheath, together with carpal tunnel syndrome, can be found that are causally related to repetitive forceful work. In fact, the term like RSI and CTD are not diagnoses, but *statement of causation* (Ranney 1993) and imply that repetitive tasks may cause an injurious strain. Such a term is necessary for a full diagnosis. First, the injured tissue must be identified, then the nature of the pathology, and finally the cause (Ranney 1993).

The cause can be illustrated by a number of risk factors. Some factors suggested by the Task Force on Repetition Strain Injury in Australian Public Service (Bammer & Blignault 1987) are shown in Table 2.1. These factors give a general view of the problem. Each item in Table 2.1 may involve some variables. However these factors in Table 2.1 can not be used directly because the risk factors in one occupation may be different from another. The risk factors corresponding to a specific job must be identified before it is used in the prevention of work-related injuries. The determination of risk factors is based on the understandings of the characteristics of the job. To know the characteristics of each job, some form of task analysis must be performed to establish that the forces at work were necessary and sufficient to cause the injury. The task analysis must show that specific structures could be injured and the physical examination must show that these structures were injured, but not others (Ranney 1993). To do so requires some knowledge of ergonomics, tissue biomechanics, pathology,

surface anatomy, and functional anatomy. Because the objective of this research and a number of risk factors are biomechanically related, the biomechanical studies of upper limb activities will be reviewed in the following.

2.2.2.3 Biomechanical studies of some upper limb activities

In modern industries, most of the light manual handling work and office work require repetitive movements of the upper limbs. Some of the major biomechanical factors associated with work-induced upper limb injuries include the working posture of the upper limb, the weight of materials to be handled, the loads acting on the joints of the upper limb, the inertial effect of the upper limb on the joint loads, the speed of movement of the upper limb and the muscular activities. The quantitative descriptions of these biomechanical factors in different tasks need intensive biomechanical studies of task analysis.

Sedentary work

Sitting is the main working posture adopted in the electro-mechanical assembly work, office work and working at computer terminals etc. The possibility of neck and shoulder muscle pain arising in the kinds of sitting work posture have already been discussed (Bjelle et al. 1979, Kvarnström 1983). Because the arm usually moves in a small area during sedentary work, the neck and shoulder pain of sitting workers can be caused by the maintained static muscle contractions (Hagberg et al. 1984) or called static loading. The loads on the upper limb joints for sitting work can be influenced by the sitting posture, the arm position, the table height, the inclination of the working table, the arm support and ergonomic aid. Inadequate working postures can also cause neck and shoulder pain.

In previous studies, the shoulder loads were assessed by measuring the muscular activity through electromyographic (EMG) signals (Herberts et al. 1980, Harms-Ringdahl & Ekholm 1987, Schüldt et al. 1986, Schüldt et al. 1987). The problem with these studies is that the EMG signal measured on one muscle may involve the activities of adjacent muscles. It is difficult to eliminate the cross effect from the measured signals to distinguish the activities from one muscle to another for giving a reliable relationship between the EMG signal and single muscle force. Another problem is that different muscles were measured in these papers and the EMG signals were given in different forms. It is therefore difficult to compare these

results. Alternatively the loads on the upper limb can also be compared by the joint forces and moments in different working postures. Unfortunately there was no biomechanical data on joint forces and moments given in these papers.

Lifting of light weights

There are many jobs, particularly on assembly line operation and sorting tasks, where frequent lifting of light loads to different heights is required. Such lifting activities do not usually impose high biomechanical and metabolic demands, but rather impose a localised load on muscles of the upper extremities. Hence, for jobs requiring upper extremity lifts, it is suggested that the weight, the vertical and horizontal location of the end point of the lift are the important factors. Habes et al. (1985) investigated the effect of height, weight and reach of arm lifting on the muscle fatigue. In their test, two levels of weight were lifted to two heights at two reach levels. The two levels of weight are 80 and 40% MVC (Maximum Voluntary Contraction) which is the subject's maximum isometric vertical pull-strength measured at shoulder level with the arm fully outstretched. The two heights are the eye and substernal levels, and the two levels of reach are the arm fully extended and the half reach which was defined as the distance midway between wrist and elbow. They found that the most fatiguing task variable was weight. At the heavier of the two weight levels, weight significantly increased the EMG amplitude of the deltoid, biceps and brachioradialis muscles. Significant increases in the EMG amplitude of the biceps were also found when the variable of height was adjusted to the higher of the two levels. There was a similar effect on the EMG level of the deltoid muscle when reach was at a maximum.

In task designs, the moderate and maximum weights of lifting to suitable height and reach point are always the requested variables. Habes et al. (1985) suggested that the ideal weight to be lifted at near maximum reach and height requirements should be less than 40% MVC and an acceptable weight level should be less than 80% MVC even under low height and reach requirements. It should be mentioned that the MVC measured by Habes et al. (1985) was for two arms, and the lifting is also conducted by two arms. The averaged masses lifted at 40 and 80% MVC were 3.28 and 6.46kg respectively. However, in most sitting work the objects were usually lifted by one arm. Unfortunately, the recommended weight for arm lifting, especially for one arm lifting, at sitting posture is still not available. Again, the loads

on the joints of upper limb for arm lifting are also required when investigating the causation of work-induced upper limb disorders because the joint forces and moments are likely to be equilibrated by a muscular moment of equal dimension and is directly related to compression forces and muscular contractions applied at the joint (Schultz et al. 1982).

Giroux et al. (1992) investigated the net shoulder joint moment (which was not clearly defined) and muscular activity during light weight handling at the sitting position. They found that the vertical displacement conditions induced higher muscular loads on the shoulder than the horizontal weight displacement conditions. It is therefore reasonable to pay more attention to the studies of the vertical weight lift task than the horizontal weight handling at sitting position. However, Giroux et al. (1992) did not find any significant difference in integrated normalised net shoulder joint moment between horizontal and vertical displacement of light weight handling. The reason may be that only one height and weight level were tested in their paper, and only sagittal plane shoulder moments were calculated. The weight handled in Giroux's test was selected as 15% of the maximal lift weight, which was determined for each subject by adding 1.14 kg increment for successive horizontal displacements until there was a disturbance in motion such as trunk and head motions. The average handled mass was 2.04 kg, but it was not stated whether this was handled by two arms or one arm in their paper.

The full understanding of how the loads act on the shoulder joint and how the shoulder loads are affected by the weight and height during arm lifting in the sitting position need more intensive, three dimensional and dynamic, biomechanical studies, especially for one arm lifting of different weights to several heights.

Driving

Driving is one of the important daily activities and occupational tasks in the modern world, and the study of driving performance has become one of the major areas of ergonomics and rehabilitation engineering. Many people want to drive, but safe driving needs very sophisticated skills that require good visual, cognitive, perceptive and physical control abilities in a highly dangerous environment using sophisticated and expensive equipment. It is therefore essential that all drivers, both able-bodied and disabled, should be able to show that they are capable of driving in all sorts of driving conditions and that they are physically capable of

controlling the car. The attention of this review will be focused on the studies of the physical and biomechanical aspects of driving activity.

The ability to drive is one of the most important concerns for disabled people, such as people after stroke, handicapped people and people with arthritis (Lings and Jensen 1991, Haslegrave 1991, Cornwell 1987) whether they wish to do shopping, get to work, visit friends or go on holiday. On the other hand, driving as an occupational task could cause musculoskeletal disorders (Kompier et al. 1987) or discomfort (Porter et al. 1992).

To assess the driving ability of disabled people and to find out the causation of disorder or discomfort of driving, it is essential to know the magnitude of control forces for driving, and then to understand how the forces and moments act on the hand and joints of the upper limb during driving. This information is very scarce in the literature.

The primary controls in a vehicle are the steering wheel, brake and accelerator. The steering force is applied to the steering wheel by the hand of the person in driving. In different driving conditions, the steering forces can vary greatly. For instance, steering forces are highest during low speed manoeuvres, as when parking a car, and both force and movement are quite low for most of the time spent on the road. The driver may therefore have to be capable of exerting higher forces and different models of cars have different ranges of steering forces (MIRA 1979). In a study of the muscular strength required to drive a motor car, Asmussen et al. (1964) measured 47 standard models of the more common types of cars and found the range of control forces shown in Table 2.2, in which the mean steering force for a stationary car is 88 ± 26 N. These were 1963-64 models of cars and there will obviously be different from modern cars. They were then in a position to compare these loads with the forces which a group of disabled drivers were able to apply and to investigate the relationship between the demand and ability in driving these cars.

Table 2.2 Control Force (N) in Range of Cars in Denmark 1963-64 (Asmussen et al. 1964)

	Brake	Clutch	Gearshift	Steering Wheel (Car stationary)	Handbrake
Mean load	186	167	33	88	255
Standard deviation	58	40	17	26	90

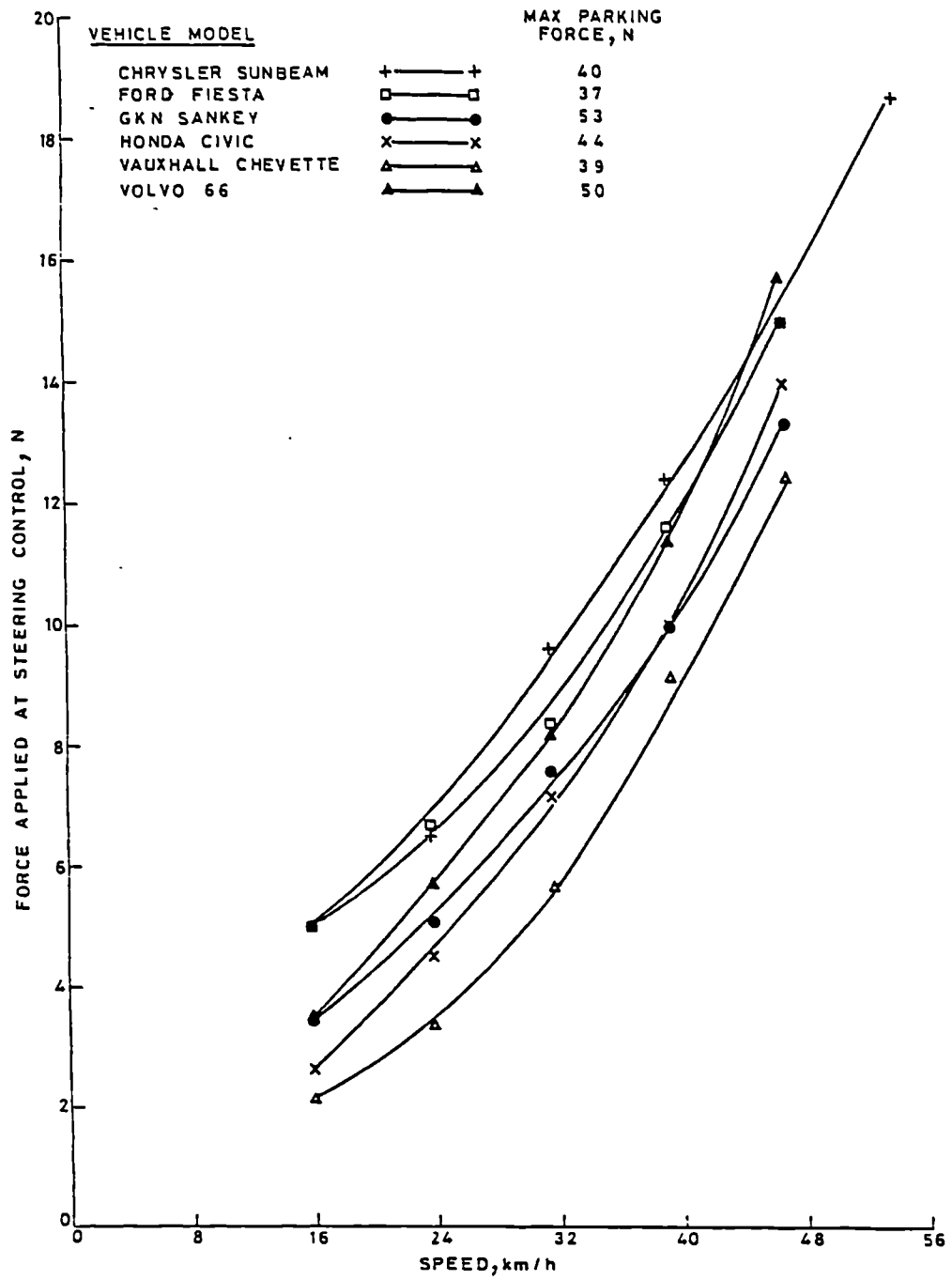


Figure 2.1 Variation of steering force with speed on a 32.9m turning circle (MIRA 1979).

MIRA (1979) measured the steering forces that were applied by each of two hands at the rim of the steering wheel of 6 models of production cars. The variation in steering force with speed for each car is shown in Figure 2.1. The maximum load (parking force) needed to turn the wheel from lock to lock while the car is stationary is also shown in the inset table. It can be found that the maximum parking force on one hand for two hand driving ranged from 37-53N. Thus the maximum steering force applied by two hands for parking would be approximately doubled to 74-106 N. These results provide a reference for assessing the driving ability of disabled people. The steering forces obtained by MIRA (1979) were measured by strain gauge transducers in production cars during road driving. However it is not clear how the steering force is exerted on the rim of the steering wheel. Because the force acting on the steering wheel is a spatial vector, both its magnitude and direction can be changed with the turning of the steering wheel. Unfortunately the three dimensional and continuously monitoring of steering force on a production car has not been found in the literature.

MIRA (1979) also measured the brake force of six models of production cars, but only one car was fitted with a hand operated control. It was found that the hand operated brake force was in the lightest of the six cars, and it required 75 N of hand brake force to produce a deceleration of 0.7g. The hand control is relatively simpler than the steering wheel control, because hand control is only a push-pull activity, and hand brake force requires no more than 75% the of person's maximum strength in operation (Bøgh and Poulsen 1967). While the operation of the steering wheel is more complicated than hand control, it will need the combination of flexion-extension, abduction-adduction, and internal-external rotation of the arm movements. It needs not only the push-pull strength but also the gripping and rotational strength.

The next question is how the driver's capabilities can be measured and matched to the demand of the standard car or modified controls, but relatively little research has been done in this area. Bøgh and Poulsen (1967) studied the demand-ability relation for 50 handicapped motorists at the Polio Institute in Copenhagen by measuring their maximum isometric force while performing movements similar to those used during actual driving. They also measured the same movements in their subjects' own cars, and found that the handicapped motorists in a considerable number of cars were subjected to a very high degree of stress. For instance, in

declutching, able-bodied motorists used only 6% of their maximum strength, while some of the handicapped motorists required as much as 65% of their maximum strength, and two-thirds had to use between 25 and 50%. The measurements in this study were carried out with strain gauge dynamometers attached to the controls in both the car seating mock-up and the individual cars.

MIRA (1979) assessed the capabilities of groups of severely disabled people with various types of handicap, measuring the maximum isometric force which they could apply to a steering wheel and brake control applied by foot or hand. The measurements of steering forces were made on five points around the circumference of the wheel, which provided an assessment of each subject's ability to reach and turn the wheel throughout its full range of travel.

In assessing the driving ability of people after stroke, Lings and Jensen (1991) measured 46 individuals suffering from left-sided hemiparesis and 67 with right-sided hemiparesis after stroke by means of a mock car. In their test, 11 items were measured which involved the manual grip strength, the maximum force applied when depressing pedals, the maximum forces applied when operating the hand brake, the maximum isometric force applied with hands in freely chosen positions when trying to turn the steering wheel when it is locked, the direction of steering wheel turn, and the steering wheel turning speed. The results were then compared with 109 healthy controls.

In summary, the previous assessment of driving ability were based on the measurements of maximum isometric force applied on the rim of the steering wheel, the grip strength and the maximum isometric push-pull strength. These measurements give some ideas of how much the control strength of disabled people or some kinds of patients have. The problem is that the maximum isometric strength can not be sustained for a long time for disabled people. Although there are few occasions for a driver to keep a high force for a long time on road driving, the highest steering force is needed for low speed manoeuvres, but it may be difficult for disabled people to exert a high force for even a very short period. The question is that if the maximum isometric strength of a patient has matched some standards, can it be said that the physical condition of the patient is suitable for driving. The question can also be asked in another way as whether the isometric strength tested in the static condition can be used to

assess a dynamic process. The question can not be answered, because the dynamic measurement of steering force has not been reported in the literature.

The other problem is that previous measurements of driving ability were tested on the mock car or simulating systems. Koppa et al. (1978) also developed a device using a simple spring scale to measure the maximum isometric steering forces for handicapped drivers. These devices can not be used to measure the dynamic steering force, nor simulate the driving resistance. To measure the steering force dynamically, a new simulating system is required which should be able to provide a resistive torque to simulate the real driving condition and be able to measure the three dimensional forces and moments on the hand for holding the steering wheel. The loads on the joints of the upper limb should also be considered when assessing the driving abilities. To find out the joint loads and to consider the inertial effect of the mass of arm, the motion of the arm should also be recorded.

Pushing and Pulling

Pushing and pulling are the most frequently used manual handling activities after lifting. It has been of continual concern to those planning efficient use of workplaces and to those attempting to prevent unnecessary injury and illness in industry. Unlike the act of sagittal-plane lifting, pushing and pulling capabilities have been studied only within a very limited scope. Furthermore, estimates of the number of injuries that occur during pushing or pulling of loads are not complete, though approximately 20% of overexertion injuries have been associated with pushing and pulling (NIOSH 1981).

The maximal pushing and pulling strength depends on a number of factors. It would appear from the work of Fox (1967) and Kroemer & Robinson (1971) that the effect of friction (μ) between foot and floor on push and pull static strength capability is of primary importance. They collectively showed that healthy young males can only exert a mean force of approximately 200N if μ is about 0.3. With μ greater than 0.6, the mean push or pull strength capability increases to 300N for the same group, according to Kroemer & Robinson (1971).

Martin & Chaffin (1972), Ayoub & McDaniel (1974), Lee (1982), and Davis & Stubbs (1978) reported that the vertical height of the handle against which one pushes and pulls is of critical importance. In the experimental strength study of Ayoub and McDaniel (1974), the elbows and rearward knee were kept straight for the exertions. This resulted in the

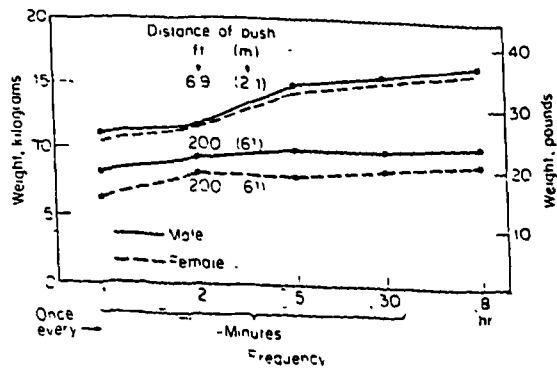


Figure 2.2

Maximum weights chosen as acceptable by 90 percent of a sample of female and male industrial workers for a pushing task at shoulder height, at different frequencies, for two distances. (Source: Snook, 1978, tables 5, 6, 7, 8, pp. 975-978.)

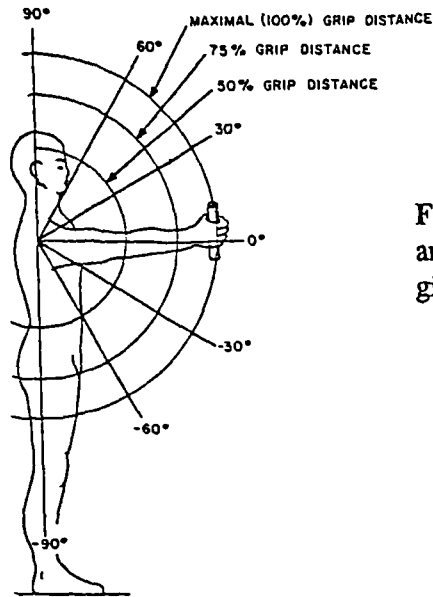


Figure 2.3 Arm postures used in one arm strength study, the results are given in Table 2.3 (Rohmert 1966).

Type of Exertion	Arm Angle (deg)	Location of the Handgrip (see Figure 8.5)		
		At Percentages of Maximal Grip Distance		
		50%	75%	100%
Force (N)				
Push outward, horizontal	30	71	108	142
	0	133	156	178
	-30	125	135	142
	-60	125	142	160
Pull inward, horizontal	30	85	98	116
	0	102	116	129
	-30	125	134	138
	-60	102	125	151
Push to the left, horizontal	30	156	136	107
	0	187	147	107
	-30	187	151	116
	-60	147	136	116
Push to the right, horizontal	30	107	98	93
	0	136	111	89
	-30	147	120	98
	-60	111	102	93
Lift, vertical	30	125	107	85
	0	151	116	80
	-30	222	178	125
	-60	280	227	182
Press down, vertical	30	338	258	182
	0	249	178	147
	-30	156	147	136
	-60	173	160	142

Table 2.3 Maximal right-handed static forces exerted on vertical hand grip by standing young male subjects (Rohmert 1966).

recommendation that the optimal height for a handle to be pushed or pulled should be approximately 91 to 114 cm (i.e., about hip height for males), above the floor. Davis and Stubbs (1978) developed recommendations for pushing and pulling limits based on abdominal pressure measurements. These experiments also disclosed a larger force capability when the hands were at hip height than raised to shoulder or above.

Martin and Chaffin (1972) predicted that maximum push or pull forces could be obtained on a high-traction surface with the hands in a slightly lower position (about 50 to 90 cm) from the floor. This lower posture allows a person to lean further forward when pushing, or backward when pulling, effectively, with such extreme postures, the risk of falling forward or backward is greatly increased if the foot suddenly slips. In this regard, Lee (1982) performed a set of dynamic push and pull experiments and found that the predicted compression forces were less when the hands were approximately 109 cm above the floor, compared with either 152 cm or 66 cm.

The maximal pushing and pulling capability can also be affected by sex, age, the distance of pushing and pulling, and the frequency of pushing and pulling (Snook 1978, Nicholson 1989). Snook (1978) found that the maximum acceptable force was greater for shorter pushing distances. A similar result was found by Ciriello et al. (1993) for the pulling task. The relationship between maximum acceptable loads of pushing task and the pushing frequency were given by Sanders and McCormick (1987) from Snook's data, which is shown in Figure 2.2.

In some situations of manual handling, especially for light weight handling, the task has to be handled by one hand. One hand handling, including one hand pushing and pulling, with the loads at one side of body, is usually referred to as asymmetric handling (Chaffin & Andersson 1984). It is obvious that the maximum acceptable capability of asymmetric pushing and pulling is different from that of the sagittal plane pushing and pulling. The problem is more complicated than the symmetric handling, therefore three-dimensional analysis is required.

A study of one handed strength in the standing position was made by Rohmert (1966). Five healthy young males of average anthropometric dimension were used in the experiment. Right-hand strength was measured in various positions, as indicated in Figure 2.3. Six strengths were measured while the subject was erect with feet parallel and 30 cm apart. The

means of the resulting strength data are shown in the Table 2.3. The results demonstrate the complexity of asymmetric exertions, with postures and force direction interacting to create large variations in the mean value. Clearly, if the left hand and the feet were allowed to assume different bracing configurations, the values generally would be expected to increase and be more varied than in Table 2.3. A recent and more complex set of data can also be found in Kuhlmann's (1986) book.

In summary, the need to understand pushing and pulling activities in industry is recognised since many overexertion and fall injuries appear to be related to such activities. It is also clear that many biomechanical factors interact to alter push and pull capabilities. At present, there is only a limited amount of data and modelling of these common activities, thus any design limits must be carefully interpreted. Asymmetrical exertions appear to be more hazardous to the musculoskeletal system than symmetrical exertions (Kumar 1980). It is conceded, however, that biomechanical and epidemiological data do not exist to quantify this belief and to define specific limits for asymmetric activities. The present data, either incomplete or given in the complex forms, are difficult to use in industrial safety design. Otherwise, the task analysis and daily activities analysis should be conducted to obtain more knowledge of the loads on the joints of the upper limb in practical situations. Even more important is the lack of knowledge regarding dynamic loading of the musculoskeletal system, which often is concomitant with an asymmetric manual material handling.

2.3 Anthropometry

Anthropometry is the science of the physical measurement of size, weight, and proportions of the human body to determine differences in individuals and groups. Anthropometric data are fundamental to occupational biomechanics. A number of anthropometric parameters, such as the body-segment link length, the mass and mass centre of the body segment, and the body segment inertial properties must be known before the biomechanical models can be used.

Active interest in the mass, volume, and centre of mass of the human body and its segments has been demonstrated by numerous investigators over the past 200 years (Clauser et al. 1969). These investigators have developed and used a wide variety of techniques in their studies with varying degrees of success. A complete review of the history of the development

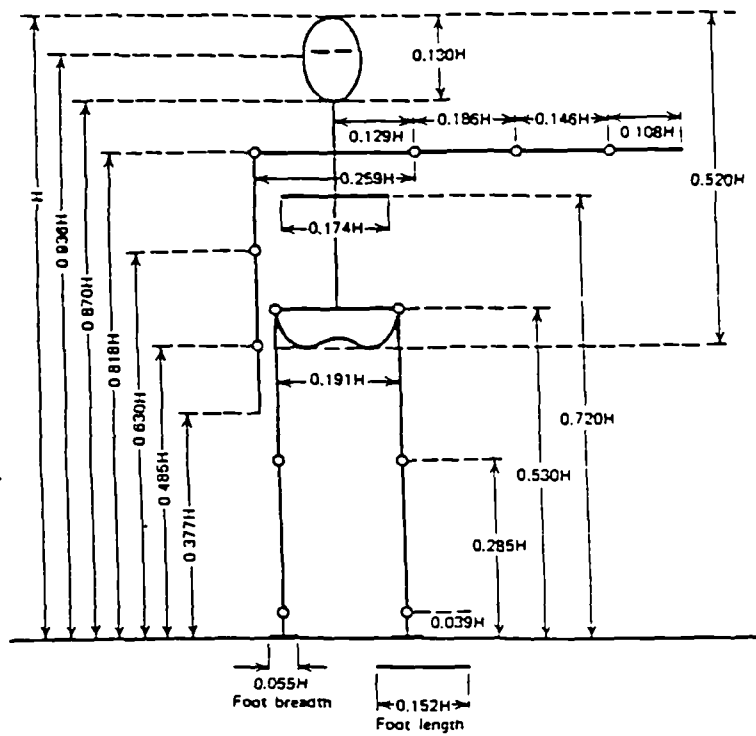


Figure 2.4 Body segment lengths expressed as a fractions of body height H (Drillis and Contini 1966).

is beyond the scope of this thesis. In the following section, only some currently used methods of measurements of the anthropometric parameters will be discussed.

2.3.1 Body-segment Link Length Measurement Methods

The most basic body dimension is the length of segments between each joint. The measurement of the length of various body segments in a linkage system assumes that the segments are connected at easily identifiable joints. Clearly this assumption is better for limbs than for the torso, neck and head segments. Even so, the identification of segment joints for the limbs can be difficult, because the bony landmarks are often covered by muscle and fat tissue, especially at the shoulder and hip joint.

The location of joint centres of rotation has been estimated on dissected cadavers by anthropometrists (Braune and Fischer 1889, Dempster 1955). Knowing the joint centres of rotation, link lengths can be defined as the distance between the projected centres. These link lengths have been correlated with distances measured between palpable bony landmarks located near the joint centres-of-rotation of interest, which have been carefully defined in literature (Webb Associate 1978b). Thus, if one is attempting to define the length of a person's forearm link, using palpable bony landmarks at either end of the ulna or radius, an estimate acceptable for most occupational biomechanical studies can be obtained by measuring between these reference points and multiplying by a given proportionality factor given in Table 2.4. The joint centre location and link definitions of the upper limb are given in Table 2.5.

The link length data, derived on living subjects with reference to surface landmark measurements, have also been statistically regressed onto a subject's stature. An average set of segment lengths expressed as a percentage of body height was derived by Drillis and Contini (1966) as shown in Figure.2.4. These segment proportions serve as a good approximation in the absence of better data, preferably measured directly from the individual.

Table 2.4 Upper limb link length to bone length ratios (Dempster1955)

Segment	Link-to-length ratio (%)
Humerus link Humerus length	89.0
Radius link Radius length	107.0
Hand link (wrist centre to centre of mass) Hand length	20.6

Table 2.5 Joint centre locations and link definitions (Webb Associates 1978)

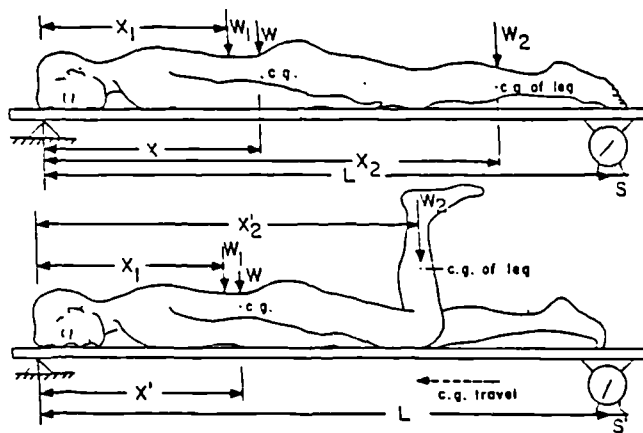
Glenohumeral	Midregion of the palpable bony mass of the head and tuberosities of the humerus; with the arm abducted about 45° relative to the vertebral margin of the scapula, a line dropped perpendicular to the long axis of the arm from the outermost margin of the acromion will approximately bisect the joint.
Elbow	Midpoint on a line between (1) the lowest palpable point on the medial epicondyle of the humerus, and (2) a point 8 mm above the radial (radiohumeral junction).
Wrist	On the palmar side of the hand, the distal wrist crease at the palmaris longus tendon, or the midpoint of a line between the radial styloid and the centre of the pisiform bone; on the dorsal side of the hand, the palpable groove between the lunata and capitate bones, on a line with metacarpal bone III.
Upper Arm Link	The straight line between the glenohumeral and elbow joint centres of rotation.
Forearm Link	The straight line between the elbow and wrist joint centres of rotation.
Hand Link	The straight line between the wrist joint centre of rotation and the centre of mass of the hand.

2.3.2 Body Segmental Mass

Not only are body tissues mechanically stressed by external loads carried, pushed or pulled on the job, but the effect of gravity on the mass of the body segments creates body weight related stress. These weight related stresses can be of considerable magnitude in certain postures, such as in sedentary work. A simple example is holding an arm straight out. The shoulder muscles become rapidly fatigued and the posture cannot be maintained. Knowledge of the distribution of body mass throughout the body, therefore, is of importance in determining the effect of gravity on various musculoskeletal areas.

The body segment mass can be determined by three main methods; the volumetric method, reaction change method and coefficient method. Using the volumetric method, the determination of the segment mass from its volume is based on the assumption that the segment density is known or can be determined if the density of the whole body is known. The segment mass is then proportional to the product of the volume and the density (Drillis & Contini 1966).

The reaction change method for estimating the segment mass has been described by Williams & Lissner (1962), Drillis & Contini (1966) and Miller & Nelson (1973). Essentially it consists of the determination of the reaction force of a board while the subject lies at rest on it. The board is fixed at one end and supported at the other by a scale or other type of force



IF MASS CENTER LOCATIONS ARE KNOWN, THEN SEGMENT WEIGHT PREDICTED FOR FOOT AND SHANK BY:

$$W_2 = \frac{L(s-s')}{(x_2 - x_2')}$$

IF SEGMENT WEIGHT IS KNOWN, THEN MASS CENTER (C.G LOCATION) CAN BE PREDICTED BY BALANCING SEGMENT OVER JOINTS, WHICH FOR FOOT AND SHANK YIELD:

$$x_2 = \left[\frac{L(s-s')}{W_2} + x_2' \right]$$

Figure 2.5 Estimation of body segment weight and mass centre location using reaction change method (Chaffin and Anderson 1984).

transducer. The reaction board provides a means to determine the segment mass by applying the static equilibrium principle that requires the sum of moments around any point in a force system, while in equilibrium, to be zero. By having a person assume two different positions on the reaction board and if the location of the segment mass centre is known, one can solve for the segment mass using a procedure described in detail by Williams and Lissner (LeVeau 1977). Figure 2.5 presents the basic procedure for determining the segment mass for the combined shank and foot segments.

The method of coefficients (Braune & Fischer 1889) is a way of presenting the segment mass data. The segment masses have been correlated with total body mass by a number of investigators. Drillis and Contini (1966) measured the segment mass of twelve living subjects by the reaction change method using a highly sensitive apparatus. The segment masses were given in percent of the total body mass and compared with the results of five investigators. Finally an average segment mass from six investigators was given in the percent of total body mass as shown in Table 2.6. These results of segment mass as a ratio of total body mass not only give a general idea of the proportion of segment mass in the body mass, but also provide a quick way of finding the approximate values of segment mass for particular subjects.

Table 2.6 Average segment mass in percent of the total body weight (Drillis & Contini 1966)

<i>Segments</i>	<i>Mass in percent of the total body mass</i>
<i>Head, neck and trunk</i>	<i>55.4</i>
<i>Extremities</i>	<i>44.6</i>
<i>Upper extremities</i>	<i>11.3</i>
<i>Upper arms</i>	<i>6.2</i>
<i>Forearms</i>	<i>3.6</i>
<i>Hands</i>	<i>1.5</i>
<i>Lower Extremities</i>	<i>33.3</i>
<i>Thighs</i>	<i>20.9</i>
<i>Shanks</i>	<i>9.2</i>
<i>Feet</i>	<i>3.2</i>

2.3.3 Determination of Mass Centre Location

In the biomechanical analysis of movements, it is necessary to know the location of the segment mass centre which represents the point of application of the resultant force of gravity acting on the segment.

The segment mass centre location can be measured by suspension, reaction change, compound pendulum and segment zone methods. By the suspension method, the frozen section was suspended from a pin that was systematically reinserted until a point of balance was

determined. The reaction change method can also be used to determine the segment mass centre location in cases where the segment mass is known. The compound pendulum method has been described by Drillis et al. (1964). The segment zone or immersion method is based on the assumption that the segment volume and mass centre are coincident, these, according to Bernstein (1967) are in very close agreement. A simple method, as Miller and Nelson (1973) noted, of determining the approximate centre of mass on the long axis of the segment is to immerse the limb to its proximal end using a second catch tank to measure the volume of water displaced. Withdraw the limb slowly until half the volume first displaced is returned. The water level at this point on the limb, assuming uniform segment density, bisects the mass centre.

The segment mass centre position of living subjects have also been obtained by Drillis and Contini (1966) using the segment zone-immersion method. Their results were then combined with the previously published data to give an overall average value of segment mass centre distance from the proximal joint as a

Table 2.7 Average location of mass centres from proximal joint in percent of segment length (Drillis and Contini 1966)

<i>Segment</i>	<i>Distance in percent of segment length</i>
<i>Entire Arm</i>	43.1
<i>Upper Arm</i>	46.1
<i>Forearm and Hand</i>	42.0
<i>Forearm</i>	42.5
<i>Hand</i>	43.3
<i>Entire Leg</i>	41.5
<i>Thigh</i>	42.7
<i>Shank and foot</i>	46.7
<i>Shank</i>	40.4
<i>Foot (from heel)</i>	44.3

percent of the segment length as shown in Table 2.7. Although similar results have been reported (Clauser et al. 1969, Contini et al. 1970) and the segment mass centre location have been given by various regression equations, the data of Drillis and Contini (1966) are sufficient to allow quantitative biomechanical analysis of industrial tasks.

2.3.4 Segmental Moment of Inertia

The inertial property of the segment, such as moment of inertia (second moment of mass), must be considered in the dynamic analysis of human movement. The moment of inertia of a segment with respect to any axis of rotation is defined as:

$$I = m_1 r_1^2 + m_2 r_2^2 + \dots + m_n r_n^2 = \sum_{i=1}^n m_i r_i^2 \quad \text{or} \quad \int r^2 dm \quad (2.1)$$

where m_i is a discrete quantity of mass, r_i is the distance from the mass to the axis.

Previously, the segmental moments of inertia of cadaver and living subjects have been determined by a number of investigators using various methods. These investigations have been reviewed by Berme and Cappozzo (1990). Perhaps, the most comprehensive set of data of segment moment of inertia was that collected by Chandler et al. (1975). Their study dealt with the determination of segment principal axes of inertia. These data provide an opportunity to relate segment principal moment of inertia values to standard anthropometric measurements.

Recently, the data of Chandler et al. (1975) have been re-analysed by linear and non-linear regression equations (Hinrichs 1985, Yeadon and Morlock 1989). The non-linear regression equations, suggested by Yeadon and Morlock (1989), for the non-torso segmental moments of inertia I_z and I_t about the longitudinal and transverse axes passing the mass centre are given by:

$$I_z = k_1 p^4 h \quad (2.2)$$

$$I_t = \frac{1}{2} I_z + k_2 p^2 h^3 \quad (2.3)$$

where linear measurements are in m and moments of inertia are in kgm^2 , for segments with three perimeters the mean perimeter is calculated as $p = (p_1 + 2p_2 + p_3) / 4$, and for the hand $p = (p_1 + p_2) / 2$. The definition of anthropometric variables of the upper limb are given in Table 2.8. The values of k_1 and k_2 for the upper limb are given in Table 2.9. It has been proved that these non-linear equations are superior to the linear equations and that the non-linear equations can provide reasonable estimates of segmental moment of inertia even when the anthropometric measurements lie outside the sample range of Chandler et al. (1975) (Yeadon and Morlock 1989).

Table 2.8 (Yeadon and Morlock 1989)

Segment	Variable	Definition
Upper arm	h	Length: shoulder centre to elbow centre
	p_1	Perimeter below axilla
	p_2	Perimeter: maximum
Forearm	p_3	Perimeter: elbow
	h	Length: elbow centre to wrist centre
	p_1	Perimeter: elbow
Hand	p_2	Perimeter: maximum
	p_3	Perimeter: wrist
	h	Length: wrist centre to tip of finger III
	p_1	Perimeter: wrist
	p_2	Perimeter: metacarpal-phalangeal joint

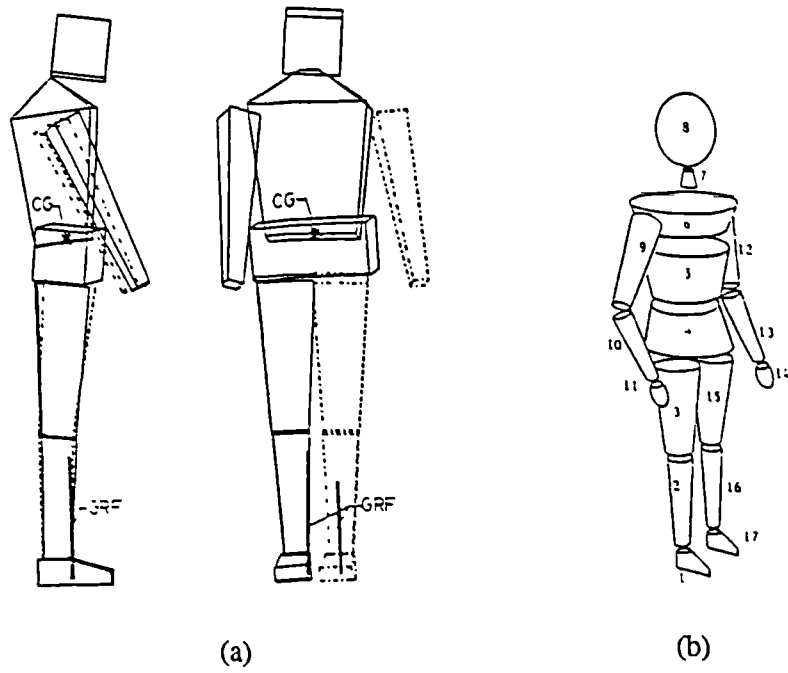


Figure 2.6 Whole body link-segment models
(a) 11 segments model (Riley et al. 1990)
(b) 17 segment model (Amirouche et al. 1990)

Table 2.9 (Yeadon and Morlock 1989)

Segment	k_1	k_2
Upper arm	0.979	6.11
Forearm	0.810	4.98
Hand	1.309	7.68

2.4 Biomechanical Model

Because of the impossibility of direct measurement of joint forces and moments on living subjects, the necessity of using biomechanical models to obtain the joint forces and moments becomes evident. The biomechanical models of dealing with the loads can be divided into two categories, the link-segment models and the musculoskeletal models. The link-segment models are usually used in the biomechanical studies of human movement to obtain the inter-segment loads and kinematic information of each segment from external loading. The musculoskeletal models try to relate muscle forces and joint forces with the inter-segment load.

2.4.1 Link-segment Models

The link-segment models assume that the human body is composed of a number of rigid segments which are connected at joints. In biomechanical applications, the number of segments can be varied based on the anatomical structure, the nature of movement permitted for each segment, the purpose of various studies and the characteristics of the problem to be solved. The whole human body system has been modelled by 11, 15, 17 and n segments (Riley *et al.* 1990, Hanavan 1964, Dapena 1981, Hatze 1980, Amirouche *et al.* 1990, and Marshall *et al.* 1985). As an example, the 11 and 17 segments whole body models are given in Figure 2.6. The 11 segments model was used by Riley *et al.* (1990) for the investigation of the relationship of posture to balance. It can be found that in this model the upper limb was modelled as one segment. However, in the analysis of upper limb activities, the upper limb is often modelled by three (as seen in the model of Amirouche *et al.*) or two segments. In two segment models, the forearm and hand are considered as one segment, and the upper arm as another segment. The three segment model of the upper limb considers the upper arm, forearm and hand each as a single segment, which are connected at wrist, elbow and shoulder (with

trunk) joints. It is clear that to find the inter-segment loads on the shoulder, elbow and wrist during upper limb activities, the three segment upper limb model must be used.

2.4.1.1 Two-dimensional static model

The inter-segment forces and moments can be obtained by solving the equilibrium equations of each segment. In planar static problems, there are three equilibrium equations for each segment, therefore three unknowns can be determined from the external loads. The external loads include the external forces on the segment and the gravitational force of the segment acting on the mass centre. The gravitational force and mass centre location of segment can be estimated by using the method described in section 2.3, the external forces can be measured directly by force transducer as discussed in section 3.3.2.

2.4.1.2 Three-dimensional static model

Two dimensional coplanar models are very useful in the evaluation of many occupational tasks. In some cases a person will use only one arm for lifting, pushing and pulling an object, while the other arm is used to counterbalance or stabilise the rest of the body. In such a situation the external forces acting on the body must be treated in three dimensions and the forces are considered to be non-coplanar. In three dimensional link-segment static models there are six equilibrium equations for each segment, therefore, six unknowns can be determined. In three dimensional space, the joint forces and moments on each joint can be split into three force components and three moment components on the three orthogonal axes. Thus, by using the proceeding in sequence method, which starts the analysis at the point of application of external loads (often hand) and proceeds in sequence solving the equilibrium equations for each body segment, the three force components and three moment components can be calculated from six equilibrium equations of each segment. The complexity of the problem is obvious. In creating the equilibrium equations, not only must the three dimensional loads on the hand and the positions of joints in the three dimensional space be known, but there is also the need to specify a reference axis system for each segment, in order to properly express the joint forces and moments in anatomical axes. This requires that the measurement of the hand forces and the recording of the joint positions and segment directions should be done in three dimensions. The basic understanding of vector algebra is

also necessary to solve the three dimensional force and moment system. The descriptions of the measuring system and computing techniques will be given in the later chapters.

2.4.1.3 Dynamic model

In dynamic analysis of the joint loads, the contributions of the inertial effects of segments must be considered. The inertial effects of segments are caused by the translational and rotational accelerations of each segment, which are called the inertial forces and inertial moments, respectively.

The inertial force of a segment is related to the mass of the segment and the translational acceleration of the segment. The inertial force of a segment can be expressed by *the d'Alembert's principle* as:

$$F_{inertial} = -ma \quad (2.4)$$

where a is the acceleration vector of mass centre of the segment, $F_{inertial}$ is the inertial force vector acting at the mass centre of segment in the opposite direction to the acceleration vector of the mass centre.

The inertial moment of a segment is related with the angular momentum of the segment and the distribution of mass relative to the axis of rotation (mass moment of inertia of segment). The relationship can be given by using *d' Alembert's principle* as:

$$M_{inertial} = -\dot{H}_c \quad (2.5)$$

where, $M_{inertial}$ is the vector of inertial moment about the mass centre of the segment, H_c is the angular momentum about the mass centre, and

$$H_c = \{I\} \cdot \omega \quad (2.6)$$

where $\{I\}$ is the inertia tensor and ω is the instantaneous angular velocity vector. At present, the kinematic parameters in Equation 2.4 to 2.6 are mostly obtained by using the numerical differentiation techniques on the displacement data because there is no satisfactory method to measure the kinematic parameters directly in the multi-linkage system. The above analysis is based on the rectangular Cartesian coordinate system fixed to the moving body segment. To incorporate the inertial effects into the joint load, it is only necessary to consider the inertial forces and moments as additional external loads acting on the mass centre of the segment. The inter-segment forces and moments can be solved at each time instant as a static problem. The method is called the inverse dynamics approach and has been widely used in the

biomechanical analysis of human movement. Details of this method have been given by Roberson & Schwertassek (1988) and Berme & Cappozzo (1990).

2.4.2 Musculoskeletal Model

Although the link-segment model provides an effective way of finding the inter-segment forces and moments, there are only six independent equations for each segment. However, in each joint system the number of unknown muscle forces, joint forces and constraint relationships exceeds the number of available motion equations. Mathematically, this is an indeterminate system. Thus a separate equilibrium must be satisfied at each joint, and a number of simplifying assumptions are necessary in order to resolve the indeterminate problems

In developing the musculoskeletal model it is necessary to firstly identify each muscle around the joint being investigated and then determine the positions of the origin and insertion points of each muscle. Also the muscle length, direction (muscle force line) and cross-sectional area of the muscle should be measured. In order to determine the magnitude and direction of each muscle force, some assumptions have been made that the muscle force acts at the origin and insertion points along the muscle force line (between origin and insertion point) and the magnitude of muscle force is related to its cross-sectional area. Several muscle wrapping correction techniques have been used (Nicol 1977, Van der Helm *et al.* 1992, Runciman 1994) to determine the muscle force line for the muscles passing over and around other anatomical structures.

To reduce redundant muscle variables, muscles with similar function, anatomic insertion and orientation can be grouped together (Paul 1967, Morrison 1967, Chao & An 1990). Most authors (e.g. Högfors *et al.* 1987, van der Helm *et al.* 1992, Wood *et al.* 1989a, b) divide large muscles into convenient portions, which represent more or less functionally distinguishable parts. So far, the most often used method to solve these indeterminate systems is the optimisation technique. The determination of muscle forces by using finite element methods have also been reported (van der Helm *et al.* 1992, van der Helm 1994), where the muscles have been assumed as truss or curved-truss elements.

Among the upper limb joints, the shoulder is the most complex system from the biomechanical point of view, as it consists of three bones (humerus, scapula, and clavicle) and

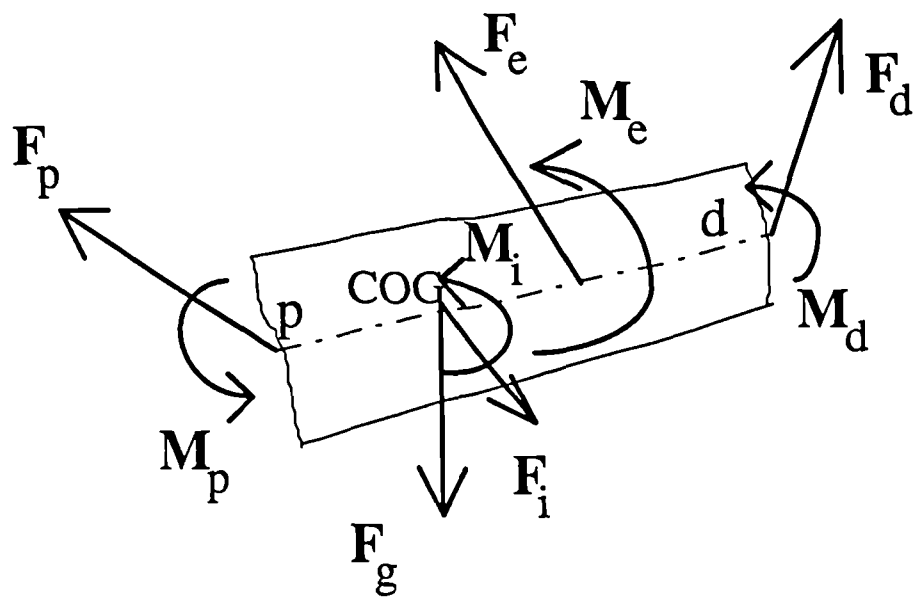


Figure 2.7 A free-body diagram of the standard link-segment model

F_p	Intersegmental Force at distal end of the link-segment
M_p	Intersegmental Moment at distal end of the link-segment
F_d	Intersegmental Force at proximal end of the link-segment
M_d	Intersegmental Moment at proximal end of the link-segment
F_g	Gravitational force of the link-segment
F_i	Inertial force of the link segment
M_i	Inertial moment of the link-segment
F_e	External force on the link-segment
M_e	External Moment on the link-segment

more than 20 muscles. Although a number of efforts have been made to model the shoulder complex (e.g. Poppen & Walker 1978, Pronk 1987, Engin & Tümer 1989, Tümer & Engin 1989, Karlsson & Petersson 1992, van der Helm *et al.* 1992, van der Helm 1994, Runciman 1994), to date, no biomechanical shoulder model exists that is capable of predicting all of the musculoskeletal forces and no model exhibits the flexibility required for the dynamic analysis of different positions and loads. The problem is that on living subjects, it is very difficult to precisely find the three-dimensional positions and directions of scapula and clavicle relative to the trunk and humerus by using surface markers, because of the errors caused by the skin movement between the skin and underneath bones. The difficulties also come from the determination of the changes of the position of muscle insertion points, the changes of muscle force line directions and muscle length, while the arm is in motion. Therefore much effort is needed to incorporate the link segment model and musculoskeletal model together to suit the demand of dynamic analysis of joint loads and muscle forces. At present for the above reasons, the link-segment models are often used in the biomechanical analysis of human movement.

2.5 Joint Loads

To understand how the loads are transmitted through each joint and how the joint forces and moments are generated are the major concerns of biomechanists in investigating the human movement and musculoskeletal injuries. Knowledge of some fundamental concepts such as net joint moment, intersegment forces, joint contact forces (bone on bone force), and muscle forces are necessary for dealing with the interactions between the segments. The full descriptions of the forces transmitted at the hip joint was first given by Paul (1967a, b).

2.5.1 Joint Intersegmental Forces

Joint intersegmental forces (say joint forces) are the resultant forces transmitted between body segments, and are the resultant of all external, gravitational and inertial forces developed on the parts of the body to one side of the joint being considered. It can be easily illustrated by the free body diagram as shown in Figure 2.7. The relationship of the inter-

segmental force, external, gravitational and inertial forces is expressed by the vector equilibrium equation of the segment as:

$$\sum \mathbf{F}_p + \mathbf{F}_{others} = 0 \quad (2.7)$$

where $\mathbf{F}_{others} = \mathbf{F}_e + \mathbf{F}_g + \mathbf{F}_i + \mathbf{F}_d$ (2.8)

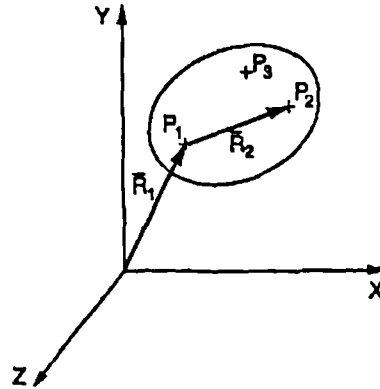
and \mathbf{F}_p is the joint intersegmental force at the proximal end of the segment, \mathbf{F}_d is the intersegmental force at the distal end of the segment. When the other forces (\mathbf{F}_{others}) on the segment are known, the inter-segmental force at the proximal end can be easily found from Equation (2.7). In the three-dimensional situation, Equation (2.7) can be expressed by a set of three independent equations corresponding to the three axes of an orthogonal coordinate system. This orthogonal coordinate system is usually determined according to the anatomical structure of the segment. Therefore, the magnitude and direction of inter-segmental force can be fully determined in a three-dimensional space.

2.5.2 Joint Intersegmental Moments

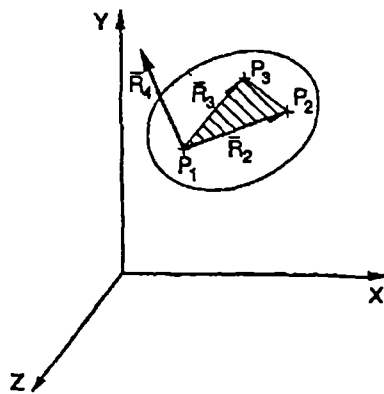
Similar to the inter-segmental force, the inter-segmental moment (net joint moment) is the resultant moment at one end of a segment. The intersegmental moment at the proximal end (\mathbf{M}_p) of the segment is balanced by the external moments (\mathbf{M}_e) on the segment, the intersegmental moment at the distal end (\mathbf{M}_d), the inertial moment (\mathbf{M}_i) of the segment, and the moments caused by the forces on the segment (\mathbf{M}_{forces}). The vector moment equilibrium equation of the segment is given as:

$$\sum \mathbf{M}_p + \mathbf{M}_e + \mathbf{M}_i + \mathbf{M}_d + \mathbf{M}_{forces} = 0 \quad (2.9)$$

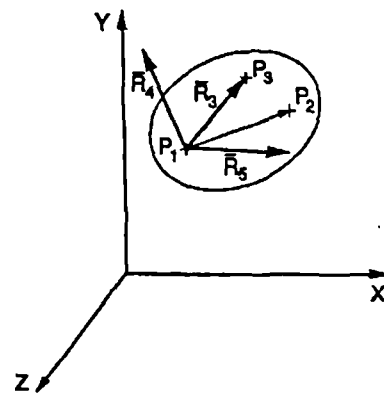
In the three dimensional analysis, three independent moment equilibrium equations can be used to calculate the three components of the intersegmental moment at the proximal end of the segment from the known forces and moments on the segment and distal end of the segment.



(a)



(b)



(c)

Figure 3.1 Determination of a local coordinate system of rigid body in the three-dimensional space by the coordinates of three non-collinear points on the rigid body. Where (X, Y, Z) is the reference coordinate system. P_1 , P_2 , and P_3 are the three non-collinear points on the rigid body.

(a) Three non-collinear points on a rigid body define the position and orientation of the rigid body in the three-dimensional space.

(b) Two vectors \bar{R}_2 and \bar{R}_3 define a plane by their cross product, \bar{R}_4 is the vector normal to this plane.

(c). The cross product of \bar{R}_2 and \bar{R}_4 define \bar{R}_5 , thus giving three mutually perpendicular vectors.

Chapter Three

Literature Review on Human Motion Analysis Methods

In this chapter the general description of kinematic analysis methods of rigid body movement and its application in human movement studies is given. The various methods of measuring the kinematic and kinetic data of human motion are also discussed.

3.1 Kinematic Analysis of Human Movement

Kinematics is the study of body motion without reference to the forces causing this motion. The complete kinematics of any segment in a three-dimensional spatial system requires 18 data variables (Winter 1990). These include the position vectors, linear velocity and acceleration of the segment's centre of mass, angular orientation, angular velocity and angular acceleration of the segment in two planes. In order to describe these kinematic variables, a convention or coordinate system is required. Using a non-moving inertial system, the absolute motion of the segment can be described. On the other hand, with the local coordinates attached to each segment, relative motion between segments can be calculated.

3.1.1 Position and Orientation

The first step to describe the motion of a body is to define the location and orientation of the body in the three-dimensional space which is usually called the reference frame. In kinematic analysis, bodies are assumed to be rigid. That is, they do not deform, and therefore, the distance between any two points of a body does not change. The rigid body assumption enables the location and orientation of a rigid body to be represented by the location and orientation of a body-fixed coordinate system which is usually called the local coordinate system, local frame or segment frame. The local coordinate system can be easily defined by the coordinates of three points on the rigid body in the reference frame (Alexander and Colbourne 1980, Berme et al. 1990). Figure 3.1 depicts how the coordinates of the three points on the rigid body are used to find a mutually orthogonal coordinate system (local frame) fixed to the body. This principle has been widely used in biomechanical studies of human movement, in which the appropriate landmarks of each segment should be carefully

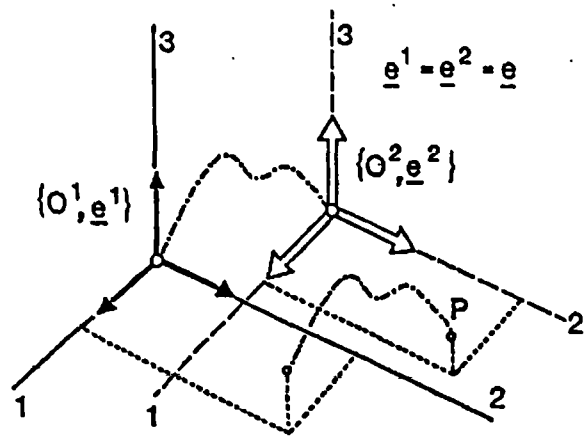


Figure 3.2 Translation keeping a fixed orientation.

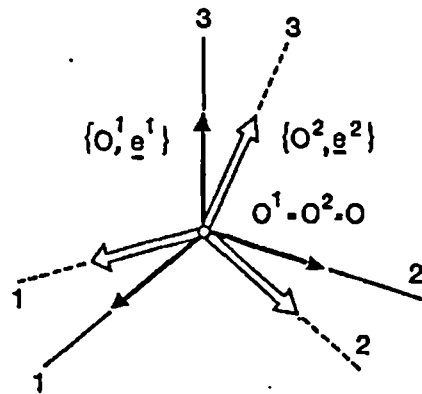


Figure 3.3 Rotation of frames with a common origin.

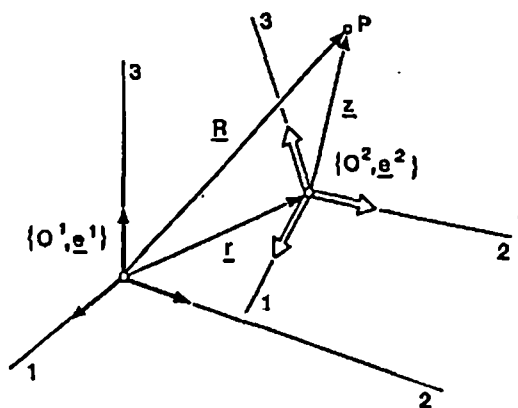


Figure 3.4 General motion composed of translation and rotation.

chosen on the principle that the local frame defined by these landmarks coincides with the anatomical axes of the segment.

In the following discussions the reference frame will be noted as $\{O^1, \mathbf{e}^1\}$, where O^1 is the origin of the reference frame and \mathbf{e}^1 is the unit vectors of it:

$$\mathbf{e}^1 = (\mathbf{I}, \mathbf{J}, \mathbf{K})^T \text{ or } (1, 2, 3)^T \quad (3.1)$$

Similarly, the local frame will be noted as $\{O^2, \mathbf{e}^2\}$, and:

$$\mathbf{e}^2 = (\mathbf{i}, \mathbf{j}, \mathbf{k})^T \text{ or } (1, 2, 3)^T \quad (3.2)$$

The motion of the local frame with respect to a reference frame can be regarded as composed of two simple motions called translation and rotation. Motion during which the relative orientation of the \mathbf{e}^2 and \mathbf{e}^1 does not change is called translation as shown in Figure 3.2. When O^2 remains in a fixed location with respect to O^1 the motion is called rotation as shown in Figure 3.3 (where $O^2 = O^1$). The most general motion of a rigid body can be composed of these two simple motion as shown in Figure 3.4.

The translation of a moving frame is determined by the location of its origin in the reference frame which is expressed as $\underline{\mathbf{r}}$ as shown in Figure 3.4. The orientation of the local frame relative to the reference frame can be expressed by the direction cosine matrix as:

$$\mathbf{e}^2 = A^{21} \mathbf{e}^1 \quad (3.3)$$

where A^{21} is the direction cosine matrix between the two frames. The superscripts to A denote the frames which are connected. Equation (3.3) can be explained as that the frame \mathbf{e}^2 can be obtained from the \mathbf{e}^1 frame by a rigid rotation of the latter. The explicit form of direction cosine matrix A^{21} is written as:

$$A^{21} = \begin{bmatrix} a_{11} & a_{12} & a_{13} \\ a_{21} & a_{22} & a_{23} \\ a_{31} & a_{32} & a_{33} \end{bmatrix} = \begin{bmatrix} \mathbf{i} \cdot \mathbf{I} & \mathbf{i} \cdot \mathbf{J} & \mathbf{i} \cdot \mathbf{K} \\ \mathbf{j} \cdot \mathbf{I} & \mathbf{j} \cdot \mathbf{J} & \mathbf{j} \cdot \mathbf{K} \\ \mathbf{k} \cdot \mathbf{I} & \mathbf{k} \cdot \mathbf{J} & \mathbf{k} \cdot \mathbf{K} \end{bmatrix} \quad (3.4)$$

Although there are nine elements in the direction cosine matrix, only three of them are independent as the sums of squares for rows and for columns equal 1. These three independent elements along with the three terms of the position vector comprise the six variables needed to completely describe the physical location and orientation of the segment.

3.1.2 Rotation

Having found the orientation and location of frame \mathbf{e}^2 relative to the reference frame \mathbf{e}^1 , the next question is how the body rotates from \mathbf{e}^1 to \mathbf{e}^2 , or how to describe the process of

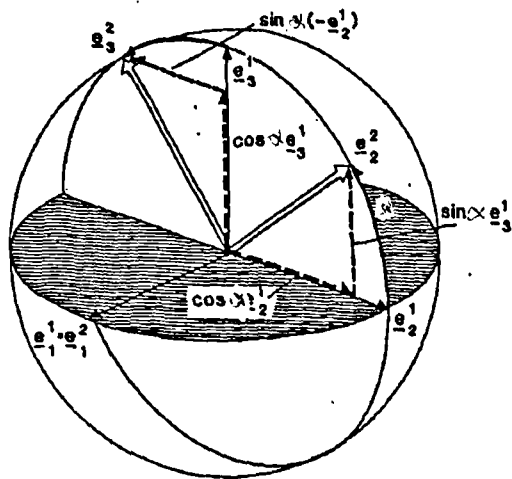


Figure 3.5 Canonical rotation about 1-axis

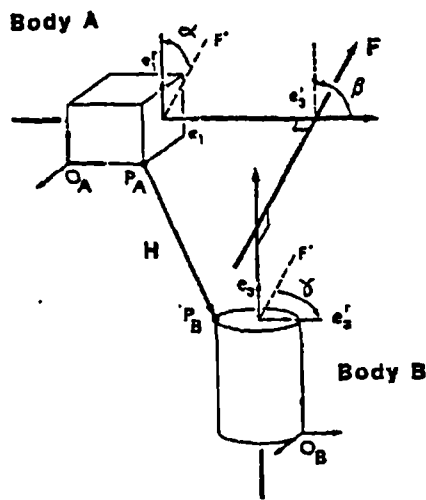


Figure 3.6 The general joint coordinate system composed of three axes. Two axes are embedded in the two bodies where relative motion is to be described. These axes which have unit base vectors e_1 and e_3 , are called body fixed axes. The third axis, F , is the common perpendicular to both body fixed axes. Since the common perpendicular is not fixed to either body and moves in relation to both we call it the floating axis. The unit base vector for the floating axis is e_2 (Grood and Suntay 1983).

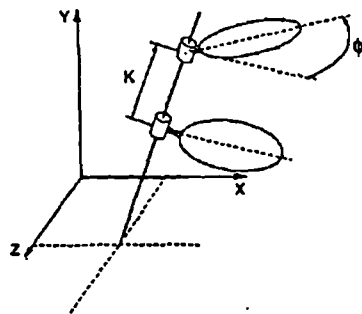


Figure 3.7 Motion a moving body from position 1 to position 2 with respect to a fixed system can be expressed as a rotation ϕ about and a translation K along a unique axis called the screw axis.

rotation from e^1 to e^2 . Euler showed before the middle of the 18th Century that rotation is a motion with three degrees of freedom, so it requires only three independent variables to describe it. The most widely used parameters for this purpose are angle variables.

The simplest case is the rotation about one axis of the reference frame which is called *elementary rotation* or *canonical rotation*. Figure 3.5 shows the rotation about the axis of e_1^1 through an angle α . The direction cosine matrix describing this rotation is denoted as:

$${}^1A(\alpha) = \begin{bmatrix} 1 & 0 & 0 \\ 0 & \cos \alpha & \sin \alpha \\ 0 & -\sin \alpha & \cos \alpha \end{bmatrix} \quad (3.5)$$

In this notation for canonical rotation, the superscripted prescript identifies the axis of rotation, in this case, 1-axis, and the argument specifies the angle of rotation here α . Analogously, rotation about 2-axis and 3-axis lead to:

$${}^2A(\beta) = \begin{bmatrix} \cos \beta & 0 & -\sin \beta \\ 0 & 1 & 0 \\ \sin \beta & 0 & \cos \beta \end{bmatrix} \quad (3.6)$$

$$\text{and } {}^3A(\gamma) = \begin{bmatrix} \cos \gamma & \sin \gamma & 0 \\ -\sin \gamma & \cos \gamma & 0 \\ 0 & 0 & 1 \end{bmatrix} \quad (3.7)$$

The above three canonical rotations have been proved to be independent and the three variables are α , β , and γ . In fact if the third rotation is repeated around the first axis instead of around the third axis, it is still an independent variable. In this case the three variables are α , β , α . Therefore any general rotation represented by the general direction cosine matrix can be described by a sequence of the three elementary rotations and the general direction cosine matrix can also be built by the multiplication of three direction cosine matrices of elementary rotation. For example, for the α , β , γ sequence rotation, the general direction cosine matrix can be built by ${}^1A(\alpha)$, ${}^2A(\beta)$, and ${}^3A(\gamma)$ as:

$$A = {}^3A(\gamma) {}^2A(\beta) {}^1A(\alpha) \quad (3.8)$$

in which the order of matrix multiplication of ${}^1A(\alpha)$, ${}^2A(\beta)$, and ${}^3A(\gamma)$ is the opposite of the order of angles of rotation α , β , γ . A complete proof of this can be found elsewhere (Roberson & Schwertassek 1988). Knowing the direction cosine matrix A from section 3.1, the rotation angles of α , β , and γ of the α - β - γ sequence rotation can be calculated

from equation (3.8). Other sequences can also be built. All together, there are twelve possibilities for a sequence of three independent rotations (Roberson & Schwertassek 1988). There is no universal standard of choice in the general literature, but some of them are widely used which will be discussed below.

3.1.2.1 Euler and Cardan angles techniques

The rotation angles followed by the 313 sequence rotation are universally known as the Euler angles. This type of rotation is usually referred to as α , β , α -type rotation. Another type of rotation is the α , β , γ -type rotation, in which each rotation occurs about an axis whose index differs from that of all previous axes. The angles in the α , β , γ sequence are called Cardan angles in Biomechanics and German literature (Woltring 1991, Tupling and Pierrynowski 1987). However, in literature, the Cardan angles were also included in the "Euler angles" (Chao 1980, Selvik 1989).

There are several disadvantages when utilising this system of defining three-dimensional segment and joint kinematics. Rotation angles in this technique are order dependent. Because of this and as a result of a lack of a standardised set of rotation axes, comparison of kinematic results between studies is often cumbersome. Visualisation of this analysis technique is difficult especially when segment orientation is well removed from the anatomical position. Gimbal-lock and singularity is an embedded problem of this technique, although it can be avoided in some cases (Woltring 1991). Perhaps the fatal disadvantage of using the Euler or Cardan angles method is that the rotation of human segments and joints is not used in the way prespecified by the ordered Euler or Cardan angles. Therefore, the sequence-independent method has attempted to describe the rotation of human segments and joints and is discussed in the following section.

3.1.2.2 Floating axis technique

Grood & Suntay (1983) developed a coordinate system with three nonorthogonal unit base vectors, which are denoted as \mathbf{e}_1 , \mathbf{e}_2 and \mathbf{e}_3 as shown in Figure 3.6. Two of the axes, called body fixed axes, are embedded in the two bodies whose relative motion is to be described. Their direction is specified by unit base vectors \mathbf{e}_1 in body A and \mathbf{e}_3 in body B. The fixed axes move with the bodies so that the relationship between them changes with the

motion. The third axis F is the common perpendicular to the body fixed axes. Therefore its orientation is given by the cross product of the unit base vectors, which define the orientation of the fixed axes, $e_2 = e_3 \times e_1 / |e_3 \times e_1|$. The common perpendicular is referred to as the floating axis, because it is not fixed in either body and moves in relation to both. The coordinate system is referred to as the floating axis system. The rotation angles corresponding to each base vector are α , β , and γ . The direction and sense of the reference lines are described by unit vectors e_1' and e_3' in each body and are taken to be perpendicular to the fixed axis also shown in Figure 3.6. The floating axis system has been used in the knee joint kinematic analysis (Grood & Suntay 1983), where the clinical description of three-dimensional rotation of the knee joint: flexion-extension, abduction-adduction and external-internal rotation were described by α , β , and γ respectively.

The advantage of using this system for the description of spatial rotation of anatomical joints is that the angular rotation does not have to refer back to the neutral position of the joint because the rotational sequence can be totally independent and the measurement can be easily related to anatomical structures. However, it is important to recognise that two of the rotational axes in this system are nonorthogonal when the joint departs from its neutral position. Consequently, the system is difficult to use in the kinetic analysis. Angular velocity and acceleration have to be transformed into a set of inertial axes in terms of the Eulerian angles defined (An & Chao 1984).

3.1.2.3 Screw axis technique

Regardless of how the motion takes place, the displacement of a moving body relative to a fixed body from position 1 to position 2 can always be expressed by a rotation about, and a translation along a unique axis in space (Chasles's Theorem). This axis is called the screw axis or the helical axis as shown in Figure 3.7. Complete parameterization of the relative position and orientation of a coordinate system includes: the coordinates of the screw axis intersection with a known plane, screw axis orientation and translation along and rotation about the screw axis of the moving coordinate system. These parameters can be determined as long as four points are known relative to a laboratory reference system before and after a motion. Details of the calculation can be found elsewhere (Kinzel et al. 1972a, Small et al. 1992, Berme et al. 1990).

There are several disadvantages with the screw axis technique. The screw axis rotation magnitude is not comparable to other methods except in special cases. Translational information is not directly comparable with any other system. Correlation of the analysis parameters to clinical joint motion parameters is difficult. Also the determination of the screw displacement axis is highly sensitive to measurement error. The ratio of error increases exponentially with decreasing displacement (Crippen et al. 1982, Kinzel 1973).

3.1.3 Angular Velocity and Acceleration

The complete description of the kinematics of a moving body should involve the parameters of linear and angular velocities and accelerations. These parameters are also required in the kinetic analysis of the moving body. In classical mechanics, rigid body kinematics principles state that the velocity of any point may be expressed with respect to the velocity of any other point on the same body as:

$$\mathbf{v}_i = \mathbf{v}_j + \bar{\omega} \times \bar{\mathbf{r}}_{ij} \quad (3.9)$$

where $\bar{\omega}$ is the angular velocity vector of the body and $\bar{\mathbf{r}}_{ij}$ is the relative position vector between any two points (point i and point j). Because the relative position vector on a rigid body remains constant with time, the linear velocity \mathbf{v}_j of point j can be found by numerical differentiation on the position data of point j which can be measured by the techniques described in the following section. If the angular velocities are known, the velocity \mathbf{v}_i of point i, can be easily found from the above equation. However, in principle, the procedure is not reversible. The unique solution for $\bar{\omega}$ can not be found from the known velocities of two points and the relative position between them.

Several experimental and numerical methods have been used to bypass the problem so that the components of the angular velocity and acceleration may be determined for a rigid body in space. Some investigators (Chao 1980, Bober et al. 1987) have used the principles of goniometry to study relative joint motions. Triaxial goniometers allow the three-dimensional relative angular motion of a joint to be recorded over time. The angular velocity and acceleration of a joint may then be computed by differentiating the relative joint angles. Such a technique may include errors due to misalignment or misplacement of the goniometer at the joint, errors due to soft tissue motion and the possibility of discomfort when studying an injured population. Another drawback of this method is that only angular variables are

recorded for the limb segment; absolute positions, linear velocities and linear accelerations remain unknown.

Another technique occasionally used to record the motion of a body segment is the accelerometer. Morris (1973) used six accelerometers to develop a method for defining the motion of the shank during gait, numerically determining the position, linear velocity, angular velocity and the associated direction cosines from the linear acceleration measurement but he overlooked cross-sensitivity of the instruments. Padgaonkar et al. (1975) and Mital et al. (1979) showed that nine linear acceleration measurements were necessary to completely define the three-dimensional motions of a rigid body. One major limitation of the accelerometer technique is that the sensitivity of the accelerometers to extraneous noise allows the artefacts to be included in the data due to building vibrations and soft tissue motions. The other limitation is their sensitivity to gravity which requires knowledge of their inclination to the vertical to correct for this. Either that or a 6 accelerometer inertial navigation system is required. Also, the recorded linear accelerations are measured relative to the position of the accelerometer on the limb, the absolute positions remain unknown.

Many investigators prefer using experimental techniques that record the positions of specified targets placed on the body segments. This method of recording motion yields three-dimensional positions, linear velocities and linear accelerations, but is hindered by the non independence of the equations to solve for the components of angular velocity and angular acceleration vectors. In two dimensional problems, this restriction is often overcome by analysing planar representations of the rigid bodies in question, removing the unknown direction of angular velocity and acceleration, leaving only the magnitude of these vectors as a variable. In the three-dimensional case, Alexander and Colbourne (1980) developed a method to calculate the angular velocity of a moving segment by using the relative position and velocity vectors of two points on the segment with respect to a third point on the same segment. The formula is:

$$\bar{\omega} = (\mathbf{v}_1 \times \mathbf{v}_2) / (\mathbf{v}_1 \cdot \mathbf{r}_2) = (\mathbf{v}_2 \times \mathbf{v}_1) / (\mathbf{v}_2 \cdot \mathbf{r}_1) \quad (3.10)$$

where $\bar{\omega}$ is the angular velocity vector of the segment, \mathbf{r}_1 , \mathbf{r}_2 , \mathbf{v}_1 , \mathbf{v}_2 are the relative position and velocity vectors respectively of two points with respect to the third point on the same segment. The problem of this method is that when one relative velocity vector is perpendicular to other relative position vector i.e. $\mathbf{v}_1 \cdot \mathbf{r}_2 = \mathbf{v}_2 \cdot \mathbf{r}_1 = 0$, singularity will occur. To avoid this

problem, the three points on the segment should be carefully selected for the specified pattern of motion of studied.

Verstraete & Soutas-Little (1990) used a least squares method to solve for the three-dimensional components of the angular velocity and acceleration of a limb segment from experimentally recorded three-dimensional position data. The calculation of this method is complex and the accuracy of the results calculated by this method depends on the number of targeted position points which have been measured and the number of position vector equations to be solved. As it was concluded, a minimum of four targets, forming six relative position vector equations, should be used to produce the best results for both the angular velocity and angular acceleration.

Another method of finding the angular velocity and acceleration of a moving body is to use the relationship between the time derivative of the direction cosine matrix and the angular velocity of the moving body. This relationship is called the Poisson equation which can be expressed as (see Roberson & Schwertassek 1988, Berme et al. 1990):

$$d(A^{21})/dt = \dot{A}^{21} = -\tilde{\omega}^{21}A^{21} \quad (3.11)$$

where A^{21} is the direction cosine matrix of frame 2 (body fixed frame) with respect to frame 1 (laboratory fixed reference frame), \dot{A}^{21} is the time derivative of A^{21} . The right superscripts on ω show that the angular velocity is to be considered to be the angular velocity of frame 2 with respect to frame 1, and left superscript indicate that the angular velocity is written in frame 2. The $\tilde{\omega}$ is just a symbol for calculation in which the components of angular velocity were involved. The explicit expression of equation (3.11) can be written as:

$$(\dot{A}^{21})(A^{21})^{-1} = - \begin{bmatrix} 0 & -\omega_z & \omega_y \\ \omega_z & 0 & -\omega_x \\ -\omega_y & \omega_x & 0 \end{bmatrix} \quad (3.12)$$

Because $(A^{21})^{-1} = (A^{21})^T$, then equation (3.12) become:

$$\begin{bmatrix} \dot{a}_{11} & \dot{a}_{12} & \dot{a}_{13} \\ \dot{a}_{21} & \dot{a}_{22} & \dot{a}_{23} \\ \dot{a}_{31} & \dot{a}_{32} & \dot{a}_{33} \end{bmatrix} \begin{bmatrix} a_{11} & a_{21} & a_{31} \\ a_{12} & a_{22} & a_{32} \\ a_{13} & a_{23} & a_{33} \end{bmatrix} = - \begin{bmatrix} 0 & -\omega_z & \omega_y \\ \omega_z & 0 & -\omega_x \\ -\omega_y & \omega_x & 0 \end{bmatrix} \quad (3.13)$$

From equation (3.13), the components of angular velocity of frame 2 with respect to frame 1, written in frame 2, can be obtained as:

$$\begin{aligned}
\omega_x &= -(a_{21}\dot{a}_{31} + a_{22}\dot{a}_{32} + a_{23}\dot{a}_{33}) \\
\omega_y &= -(a_{31}\dot{a}_{11} + a_{32}\dot{a}_{12} + a_{33}\dot{a}_{13}) \\
\omega_z &= -(a_{11}\dot{a}_{21} + a_{12}\dot{a}_{22} + a_{13}\dot{a}_{23})
\end{aligned}
\tag{3.14}$$

The advantages of this method are the simplicity of its calculation and independence of rotational sequence. Only information of the direction cosine matrix is required to calculate the angular velocity of a moving segment, then the angular acceleration can be easily obtained by numerical differentiation of angular velocity. The method has been used by a number of authors (Gagnon & Gagnon 1992, Ramey & Yang 1981, Kromodihardjo & Mital 1987).

Finally, there are especially important properties of angular velocity which need to be mentioned which state that interchanging the rotating frame and the reference frame, the angular velocity reverses its algebraic sign, i.e. ${}^1\omega^{12} = -{}^2\omega^{21}$.

3.2 Kinematic Measurement Methods

In biomechanics of human movement, measuring kinematic data is the basis of any further kinematic and kinetic analysis. Many techniques have been used to collect the kinematic data, among them the most frequently used photographic techniques, optoelectronic techniques and electrogoniometer measurement are discussed in this section.

3.2.1 Photographic Technique

The earliest scientific studies of human movement were reported by Marey in 1873 (see Steindler 1953, and Begg et al 1989), who used serial photography to study locomotion. Using the photographic techniques, the entire movement can be recorded on a single photographic plate (Chronophotography), or the movement at each instant in time be recorded on separate frames (cinematography). The pattern of movement can then be represented by the 'stick diagram' which is obtained by photographing the subject in movement with bright reflective strips affixed on the subject's segments (Marey 1873, Murray 1964). In order to enhance contrast of the pictures and smoothly identify the anatomic position of the body a number of special markers have been used. These landmarks may be passive (e.g. bright reflectors with stroboscope used by Murray 1964) or active (e.g. LEDs used by Cappozzo 1981).

Chronophotography is one of the most economical and simple techniques to measure movement in human locomotion research with the advantage of providing all the information on a single photographic plate and giving rapid assessment if a Polaroid camera is used. With

an electric strobe of high flash frequency it is possible to record high speed movement. However, there are several disadvantages for the chronophotographic method. Image overlapping is a major problem when movement overlaps or when a point is more or less stationary, strobe flash may influence the subject to produce a non-natural gait pattern, LEDs may restrict movement.

The overlap problem can be overcome by using cinematography techniques. Using cinematography, the movement of the human body can be filmed at pre-selected time intervals (film rate) (Eberhart & Inman 1947, Bresler & Frankel 1950, and Paul 1967). The selection of film rate is dependent on the camera used and the objective of the studies. It has been suggested (Winter 1990) that for movements such as walking or for slower movements, an inexpensive camera at 24 frames per second appears to be quite adequate. Simon (1981) concluded that 50 frames per second was perhaps the best for analysing walking gait. For high speed movement, such as sport, higher film rate should be used. In most studies, more than one camera was often used (Eberhart & Inman 1947, Bresler & Frankel 1950, and Paul 1967). This enables the three-dimensional positions of landmarks to be recorded. The recorded body segment displacements can be obtained by digitization of cinematographic film (Sutherland & Hagy 1972). Whilst this technique may be suitable for research purposes, it is unsuitable for routine clinical use because manual data reduction is a time consuming and tedious process (Davis 1988). For film, the turnaround time for film development may be a problem, also the possibility of film distortion and errors in framing.

3.2.2 Optoelectronic Techniques

Since the 1960's, various alternatives for cinematography have been developed. Among these, a number of optoelectronic systems have become available both commercially and academically. These systems can be interfaced directly with a computer to overcome the disadvantages of cinematography. The digitization of image coordinates is automatic, and some systems can also provide hardware identification of multiple landmarks. A wide range of software is available for 2D or 3D reconstruction of stick figures etc. Some of the currently available optoelectronic systems are discussed briefly below.

Television or Video/computer system (VICON)

Although several television/computer systems have been developed independently (Furnée 1967, Winter et al. 1972, Jarrett 1976), they share the same basic principles. The spatial coordinates of markers are derived from the position in the television camera scan of the video signal produced by markers. This depends on digitizing either the complete video signal or the coordinates when a marker is detected in the video signal. In the latter case, two digital counters are used to register the ordinate line number from the start of each field and time lapse period from the start of each scan respectively. When a marker is amplitude detected in the video signal the states of these two counters are sampled, giving a marker's position in the TV raster.

The commercial and computerized video-system VICON (Oxford Metrics Ltd, Oxford, UK) was first developed by Jarrett (1976) and Andrews (1981) in the University of Strathclyde, and has been available since 1982. It can accommodate up to seven video-cameras, and it uses retro-reflective markers which are affixed to the body, in combination with infrared, stroboscopic illumination. A ring of IR LEDs is mounted around the lens of each camera, and the LEDs give a short light flash at the end of each video scan. In this fashion, image blur caused by fast movement is avoided. A comprehensive software package (for use on PDP11 and VAX computers) is provided, allowing 3-D camera calibration, data collection, reduction, and sorting (landmark identification) of raw image data, 3-D landmark reconstruction, smoothing and differentiation, and graphics. Additional data channels are available for synchronized collection of EMG and force-plate data. The number of landmarks can be very high and is mainly limited by the disk transfer rates for data storage. A considerable asset of the system is the passive nature of the landmarks (no wires), and the availability of a comprehensive, well-designed software package.

It should be emphasised that, when using the VICON system, the distance between markers should be sufficiently large so that error propagation from measured marker coordinates to the transformation matrix is minimal. Each marker must be viewed by at least two cameras at any moment of measurement for getting a continuous trajectory of the marker. Disadvantages are the processing time required for reduction of data and for operator-supervised sorting. Also installation of the system is very expensive, and it can only be used in the laboratory under suitable conditions.

The SELSPOT system

SELSPOT-II system (SElective light SPOT recognition, trademark of SELCOMAB, Partille, Sweden) relies on the lateral photoeffect (Lindholm & Öberg 1974, Woltring 1975, Woltring and Marsolais 1980) for determination of the positions of a light image on a semiconductor photodetector. It can use up to 16 SELSPOT cameras (telemetric or hardwired) with active light emitting diode (LED) markers attached to anatomical landmarks, a signal processing unit and a controlling computer. The active LED markers are pulsed sequentially from the controlling unit providing the computer with automatic identification of markers. The advantages of SELSPOT are the (limited) possibility to use the system in daylight situations, the much higher spatial resolution, the high resolution in time, and automatic landmark identification. Disadvantages are the use of active (wired) markers and the sensitivity to marker light reflections: since the lateral detector senses the centroid of the incident light distribution, any indirect image due to reflections on neighbouring surfaces (adjacent limbs, ground, wall, ceiling) will influence the position estimate for the directly observed light source.

CODA-3 system

The CODA-3, for Cartesian Optoelectronic Digital Anthropometer (trademark of Charmwood Dynamics Ltd, Loughborough, Leic, UK) use an optical scanning technique (Güth et al. 1973, and Heinrichs 1974) and coloured retroreflective landmarks on the subject. Two mirrors rotate about vertical axes which are spaced 1 m apart. A third mirror is positioned halfway between these mirrors, and it rotates about a horizontal axis which intersects the two vertical axes. A line of light is projected onto each mirror, and the reflected lines sweep through space because of the mirror rotations. Whenever a retroreflective landmark is hit by a light beam, colored light is reflected back into the scanning mirror. Time and color are determined via splitting optics, diffractive gratings, and optoelectronic circuitry, and these provide unique direction and identification information.

The advantages of the system with respect to the SELSPOT and VICON systems are the passive nature of the landmarks, the high spatio-temporal resolution, and the real time availability of 3-D landmark coordinates. Disadvantages are the limited number of markers (8-12) due to difficulties in distinguishing the landmark colors, and the fixed stereobase which

limits the depth range. A new version of this system CODA mpx30, can use up to 28 markers at a minimum sampling rate of 200Hz, but the number of markers which can be used decreases with the increase of the sampling rate.

3Space™ Isotrak™ system

The 3Space™ Isotrak™ system (Polhemus Navigation Science Division, McDonnell Douglas Electronics Company, Hercules Drive P.O. Box 560, Colchester, VT, 05446, USA) is an electro-magnetic device for the measurement of the position and orientation of a sensor in space. It consists of three components: a system Electronics Unit (SEU), a source, and a sensor. Both source and sensor are connected to the SEU by cables. The source emits and the sensor detects a low frequency magnetic field. The SEU contains all the analogue circuitry to generate and sense the magnetic fields as well as the hardware and software to control the analogue circuitry, digitise the signals, and perform the calculations to compute the position and orientation of the sensor.

It was reported (AN et al. 1988, Hindle et al. 1990) that this system has high position and angular resolutions, and relatively easy and simple to operate. This system has been used to measure the back movement (Hindle et al. 1990, Buchalter et al. 1989, Buchalter et al 1986). However, since the magnetic tracking system was constructed based on the principle of electromagnetism, any material with magnetic or electric characteristics could, therefore, possibly affect and distort the output of the system. Systematic test to identify the effects of a metallic object on the output of the coordinate and rotation of the sensor are required before application of the device to kinematic analysis involving metallic artificial joint.

3.2.3 Goniometry

One of the commonly used method for kinematic measurement of human movement is goniometry that measures the joint angle changes. Various types of goniometers are available for example, electrogoniometers (Johnson & Smidt 1969, Chao 1980, Kinzel et al. 1972b), Polarised light goniometers (Mitchelson 1977) and flexible electrogoniometers (Nicol 1987a, 1987b). The most obvious advantage of goniometry is that a large amount of angular displacement data can be obtained instantaneously without tedious data reduction procedures. Moreover, it is fairly cheap and relatively easy to use for clinical routine work. Planar rotation

is recorded independent of the plane of joint movement. However, goniometry suffers some disadvantages. First of all, the accuracy of the system is limited by the accuracy with which the exoskeleton follows the movement of the internal structure. Secondly, it may require an excessive length of time to fit and align, and the alignment over fat and muscle tissue can vary over the time of the movement. Thirdly, if a large number of goniometers is fitted, movement can be encumbered by the straps and cables. Finally more complex goniometers are required for joints that do not move as hinge joints.

3.3 Kinetic Measurement Methods

Kinetic analysis of human movement during various activities requires that forces on body segments should be determined. These forces include gravitational forces, external forces, muscle and ligament forces. The gravitational forces can be found from a full kinematic description and accurate anthropometric measures that have been described in previous sections. The muscle and ligament forces can be assessed experimentally by electromyography records (EMG) or theoretically by solving equilibrium equations of each segment or joint. In solving these equilibrium equations, the external forces must be known. The external forces usually act on the foot during standing, walking, or running and on the hand during conducting various activities of daily living or on the body due to aerodynamic wind effects. The experimental methods of measuring these external forces are discussed in this section.

3.3.1 Ground Reaction Measurements

The force on the foot has a distribution of pressure under the foot, while the resultant of the distributed forces can be represented by a three-dimensional force vector, called the ground reaction force, acting at the centre of pressure.

Force plate

The external forces are usually measured by force transducers. There are many kinds of transducers such as: strain gauge, piezoelectric, piezoresistive, capacitive. All these transducers work on the principle that the applied force causes a certain amount of strain within the transducer and the strain is recorded as an electrical signal proportional to the

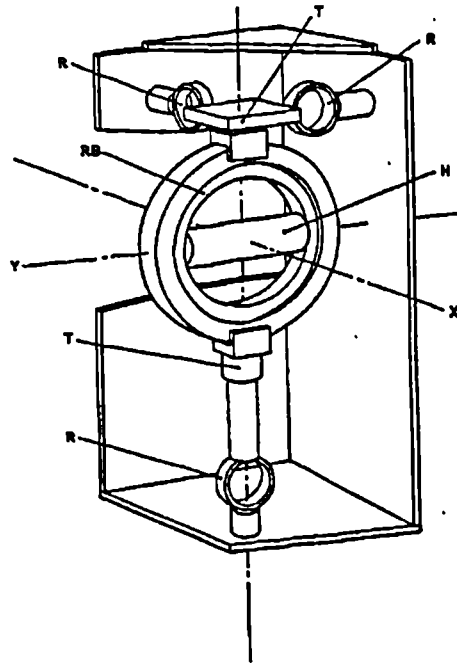


Figure 3.8 Triaxial hand force measurement system developed by Pinder et al. (1993), where X, Y, Z are the x, y, z axes, H is the handle, R are ring transducers, T are thrust bearings, and RB is the ring bearing.

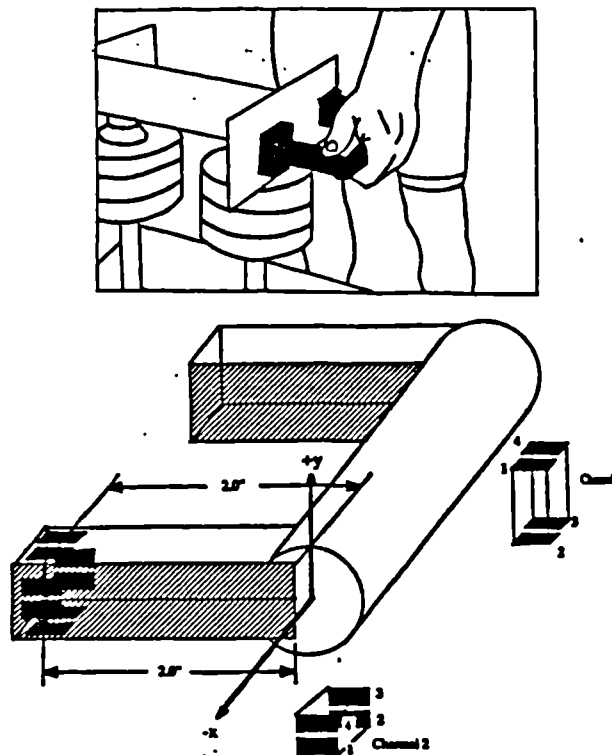


Figure 3.9 Strain gauged handle for measuring the hand forces of lifting activity. The shaded handle is enlarged below to show detail of the gauges mounted on the handle (Danz and Ayoub 1992).

applied force. The force plate is a special transducer to record the ground reaction force of the foot automatically when the foot contacts it. Among the various kinds of force plate, the Kistler force plate is the most widely used one in which piezoelectric sensors are used. A cast aluminium rectangular plate is supported on a platform below. At each corner there is a stack of three quartz transducers, corresponding to vertical, fore-aft, and lateral forces, respectively. Therefore, the forces in three orthogonal directions can be measured. From these forces, the turning effect or moment about various axes can be derived and the centre of foot pressure can be deduced if necessary.

At present, the force platform is a common device in gait analysis to find out the joint forces and moments of lower extremities. Because the force platform has the advantage of stability, accuracy and can provide the fundamental information about the three-dimensional reaction forces, it has also been used for biomechanical studies of some upper limb activities. de Looze et al. (1993) using the ground reaction forces measured by force platform (Kistler, 9281B) calculated the joint moments at the lower back for lifting and lowering tasks but their study was limited to the sagittal plane. For asymmetrical lifting and lowering activities, the triaxial net muscular moments at the L5/S1 joint were computed by Gagnon & Gagnon (1992) from the external forces measured by two force platforms. Donkers et al. (1993) investigated the elbow joint load during push-up exercise by measuring the location and magnitude of loads applied to the hand using a force platform. In the investigation of muscular mechanical energy expenditure in manual materials handling, Gagnon & Smyth (1991) using a sagittal plane segments model calculated the shoulder and elbow joint moments from the ground reaction force measured by force platform.

Although the force platform can be used for the study of some upper limb activities, it is obvious that the viability and validity of using it in a wide range of upper limb activities is limited. First the force platform is usually fixed on the ground and upper limb activities are rarely conducted at this level. Second, for upper limb activities, it is obvious that the external loads are directly transferred through the hand to the upper limb joints. This process can be easily analysed by upper limb link-segments models in cases where the external loads on the hand are known. In contrast with this, the transfer of loads from foot to the upper limb joints is more complicated than from hand to the upper limb joints. Although Gagnon & Smyth (1991) used 'foot to shoulder, elbow' procedure, too many simplifications were involved in

their study. Comparison could not be found to prove the equivalence of the 'hand to elbow, shoulder' and the 'foot to shoulder, elbow' procedures. Therefore, the most appropriate way to analyse the loads on upper limb joints for a variety of activities is to measure the hand loads directly.

3.3.2 Hand Forces Measurements

Hand force is the interaction between hand and the objects to be moved or controlled by the hand. Various methods of measurement of hand forces are used for the different kinds of activities and different objects.

In clinical practice, the magnitude of forces that can be exerted by the hand is assessed as the hand strength involving push/pull, pinch and grip strength which has been measured by various dynamometers or testing devices (An et al. 1980, Jones, et al. 1985, Pronk & Niesing 1981, Forthergill et al., Clarke, et al. 1991). Most of the devices for measuring hand strength in clinical use are single purpose, i.e. can only measure the push/pull, pinch or grip strength respectively. Arguments still exist in whether the grip strength should be measured as a pressure or as a force (Ellis & Cutts 1992, Kondrake 1985). In fact, hand force is a three-dimensional action, single push/pull or grip strength information can not describe the hand strength completely. Pinder et al. (1993) developed a triaxial force measurement system of measuring the three components of hand force in three perpendicular directions as shown in Figure 3.8. The handle of this system can rotate about three axes to allow the subject to move the handle to the most preferred orientation for the direction in which he or she wishes to exert force. This prevents the transmission of moments due to the flexion/extension, pronation/supination or ulnar/radial deviation of the wrist. Therefore the moments exerted by the hand can not be measured by this system. Using this system to measure hand strength, subjects must learn to exert a force in a given testing direction (Fothergill et al. 1993). The forearm posture of subjects can sometimes be constrained by mechanical links and the framework that support the handles. Like other dynamometers used in clinical applications for measuring hand strength, this system was designed for measuring isometric strength, it is difficult to measure the hand forces dynamically for a wide range of real activities.

Strain gauge technology is the most widely used tool for force measurements, because it is accurate, sensitive, versatile, has a linear output, is easy to use and has low cost. Strain

gauges can be either bonded on the sets of interest of any object to be measured or bonded on a single unit to construct a force transducer. Danz & Ayoub (1992) measured the hand forces for a floor to knuckle lifting task by mounting two sets of four strain gauges on the handle of the weight to be lifted (Figure 3.9). The hand forces in vertical (in sagittal plane direction, positive direction towards the head of the lifter) and horizontal (in the transverse plane direction, position away from the body of the lifter) directions were measured. Because the movement of the lift was not recorded and involved in the analysis, their results were only the approximate results of neglecting the tilt effect of the weight. It may be appropriate to use the strain gauged handle to measure the hand forces in the two hand, heavy weight sagittal plane lift activity such as investigated in Danz & Ayoub's study. However, there may be problems for using the strain gauged handle to measure the hand forces of one hand, light weight lift activity. First, the handle may influence the real lifting postures. Second, the weight of the handle may exert an additional load on the hand. This load may become a significant factor when the lifted weight is relatively small.

Nicol (1977) measured the forces on the hand during a table-pull activity by using a six-channel strain-gauged transducer (Berme et al. 1975) for the measurement of forces and moments transmitted through lower limb prostheses. The six channels of the transducer can measure simultaneously three components of force and three components of moment acting at the centre of the transducer. Because of its small size and bolted endplate, it is suitable for many applications. However additional adapters must be designed so that it can be fixed on the different objects for use in this project. Detail of the design work will be given in section 4.2.

Chapter Four

Experimental Work

Two main instruments were used in the experimental work of this study. A Vicon motion analysis system was used for measuring the dynamic positions of landmarks affixed on the body of the subject, the force transducer, and the book. The description of the Vicon motion analysis system currently used in the biomechanics laboratory of Bioengineering Unit is given in the first section. A force transducer was used for measuring the hand forces and moments. The modification and calibration of a pylon transducer and the design of an end-adaptor of the transducer are given in the second section. In the third section, the design of the force transducer instrumented steering wheel, door and cutting plate are described. The details of the test procedure of four activities are given in the fourth section. The data acquisition and pre-processing are described in the final section of this chapter.

4.1 Vicon Motion Analysis System

A six camera Vicon motion analysis system (Oxford Metrics Ltd, UK) was used in this study for measuring the three-dimensional coordinates of discrete points within a predetermined laboratory space. To accomplish this it uses 6 CCD cameras, each viewing the measurement space from a different angle. Each camera emits pulsed infrared light at 50Hz, and monitors the reflection of this light from retroreflective markers in its field of view. If this information from two or more cameras with respect to the measurement space is known, the three-dimensional coordinates of the marker centre can be calculated.

The motion analysis system operates at a predetermined operating frequency. This results in dynamic marker movement being represented as a series of static marker positions. Each of these sets of static marker positions is referred to as a frame of data. The frequency used for this study was 50 Hz. Up to 40 markers can be used and each marker must be viewed by at least two cameras to keep a continuous trace of the marker. Up to 40 additional analogue data channels can be connected to the A-D converter and then to the system for synchronised collection of data. The Vicon system is operated via a micro VAX 3100 computer using either the VT340 terminal or the adjacent Amstrad PC 2086/30 computer.

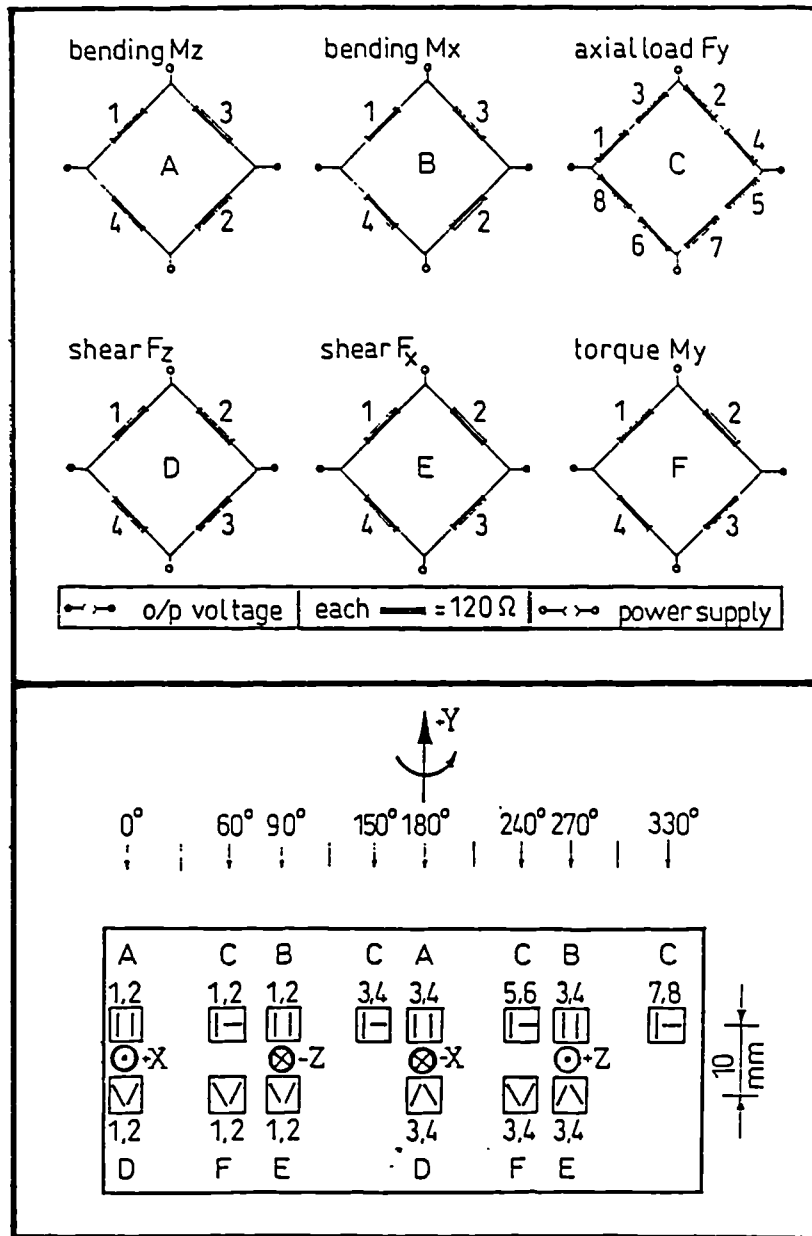


Figure 4.1 Gauging diagrams of the pylon transducer

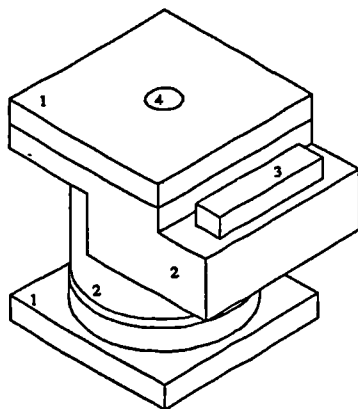


Figure 4.2 Modified pylon transducer

- (1) Square endplate
- (2) Impact protection cover and socket holder
- (3) Socket fixed on the socket holder
- (4) Central bolt hole

After the test, collected data can be transferred to the computer centre main frame system for further analysis.

The use of the Vicon motion analysis system includes four steps, calibration, data collection, reconstruction, and identification. The details of these steps used in this study are given in the final two sections of this chapter.

4.2 The force Transducer

4.2.1 Modification of Pylon Transducer

In order to measure the hand loads during various activities a force transducer was made. The main structure of the force transducer is the same as the 'shorter pylon transducer' described by Berme et. al (1975) because of its small size and suitable range of load measurements. The main part of the pylon transducer is a strain-gauged tube with 14 electrical resistance strain gauges bonded to the surface. The gauges were placed at two levels and distributed around the circumference at different angles as shown in Figure 4.1. The gauges forming 6 full bridges allowing the 3 forces and 3 moments to be measured by 6 nominally independent channels.

The original transducer was designed to be placed in the shank of a below or above knee prosthesis for measuring the forces transmitted by the prosthesis. Two circular endplates were bolted to the flanges at both ends, each providing a threaded central bolt hole for quick and easy fitting within the prosthesis. A number of grooves were made on the surface of the endplate. Because the principal loads transmitted by the prosthesis are the axial force and anterior-posterior moment, the structure of the circular endplate provided an effective way of transmitting the loads from the prosthesis to the transducer for measuring the loads. However, for a wide range of activities investigated in this study, the hand forces may act in many directions, for example the principal force and moment may be transmitted to the transducer as a shear force and torque. In order to make a solid and secure means of attachment between the transducer and other objects used in this project and to provide an effective transmission of the loads in any directions, a pair of square endplates with a central bolt hole were designed as shown in Figure 4.2. The outer dimension of the transducer was 58mm×73.5mm×72mm.

4.2.2 Calibration of The Transducer

The force transducer must be calibrated before it could be used experimentally. Generally two approaches can be used for transducer calibration, linear and non-linear. A complete review of both techniques is presented by Magnissalis (1992). Magnissalis draws the conclusion that a non-linear approach may be marginally more accurate but that the added complications and expense are not justifiable for a transducer of this type.

A linear calibration approach assumes that each output signal can be expressed as a linear combination of the applied load components. The signal for each output channel of the transducer would then be the linear combination of the combined effects of the loading. Mathematically this would take the form:

$$\begin{aligned}
 SFx &= m_{11}Fx + m_{12}Fy + m_{13}Fz + m_{14}Mx + m_{15}My + m_{16}Mz \\
 SFy &= m_{21}Fx + m_{22}Fy + m_{23}Fz + m_{24}Mx + m_{25}My + m_{26}Mz \\
 SFz &= m_{31}Fx + m_{32}Fy + m_{33}Fz + m_{34}Mx + m_{35}My + m_{36}Mz \\
 SMx &= m_{41}Fx + m_{42}Fy + m_{43}Fz + m_{44}Mx + m_{45}My + m_{46}Mz \\
 SMy &= m_{51}Fx + m_{52}Fy + m_{53}Fz + m_{54}Mx + m_{55}My + m_{56}Mz \\
 SMz &= m_{61}Fx + m_{62}Fy + m_{63}Fz + m_{64}Mx + m_{65}My + m_{66}Mz
 \end{aligned} \tag{4.1}$$

where the SFx, SFy, SFz, SMx, SMy, SMz, are the six output signals, Fx, Fy, Fz are the three force components applied along each of the three axes of the transducer coordinate system, Mx, My, and Mz are the three moment components applied around each of the three axes of the transducer coordinate system, and $m_{11} \dots m_{66}$ are the linear coefficients to be determined during the calibration procedure. Equation 4.1 can be written more simply as:

$$[S]=[M][L] \tag{4.2}$$

where the [S] and [L] are column vectors representing the bridge output voltages and the input loads, respectively. The matrix [M] is a square matrix relating the applied loads to the measured output signals in which each diagonal element relates one loading component and its contribution to the output signal of the corresponding channel. Non-diagonal elements represent the cross-effects.

In normal practice, the purpose is to find the loads applied to the transducer from the recorded output signals. From Equation 4.2 the load [L] can be expressed as :

$$[L]=[C][S] \tag{4.3}$$

where $[C]=[M]^{-1}$ is the inverse of matrix of [M] and is called the calibration matrix.

Determining the calibration matrix involves first calculating the components of matrix [M]. This is done by loading each of the channels of the transducer and measuring corresponding output signal voltages. Many different loading formats have been used for previous calibration of the pylon transducer and they were reviewed by Magnissalis (1992). After using an Instron materials testing machine for calibration of a pylon transducer, and comparing with other methods, Magnissalis (1992) indicated that standard dead-weights are more appropriate for this purpose, because they rely on fewer components and the friction can be more readily quantified.

Ideally, step-increased dead-weight loads should be applied to each transducer channel independently, the resulting six output signals for each load could then be analysed using linear regression to determine the corresponding 6 components of a column of matrix [M]. In order to get the minimal cross-effects due to the misloading on non-purposed channels during calibration a set of highly accurate loading devices is required. Alternatively, combinations of loads on different channels have been used for calibrating the pylon transducer in the Bioengineering Unit (Lawes 1982, and Grant-Thompson 1977, Hall 1996). These combinations include combined shear force and bending moment, combined axial load and bending moment, and combined shear force, bending moment and torque. A pure axial loading, a pure torque and combined shear force and moment were used in this study.

For the purpose of calibration and later use of the transducer, the bridge voltage and the gain of amplifier for each channel which were used are shown in Table 4.1.

Table 4.1 Parameters of the force transducer

	Ch-1	Ch-2	Ch-3	Ch-4	Ch-5	Ch-6
Bridge voltage	3V	6V	3V	3V	3V	3V
Gain of amplifier	2000	2000	2000	500	1000	500

Axial load calibration

In axial load calibration, an axial loading frame reported by Lowe (1969) was used as shown in Figure 4.3. The axial compression force W was loaded on the y axis of the transducer by means of weights on the top disc. The point loading was guaranteed by the use of two steel balls at the interface between transducer and the frame. Five loads from - 49.05N

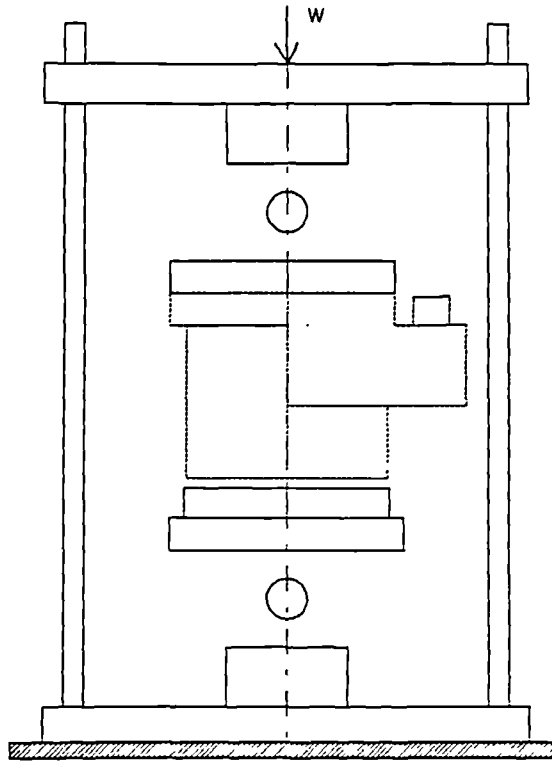


Figure 4.3 The set-up for the axial load calibration

Figure 4.4 Calibration results of axial loading

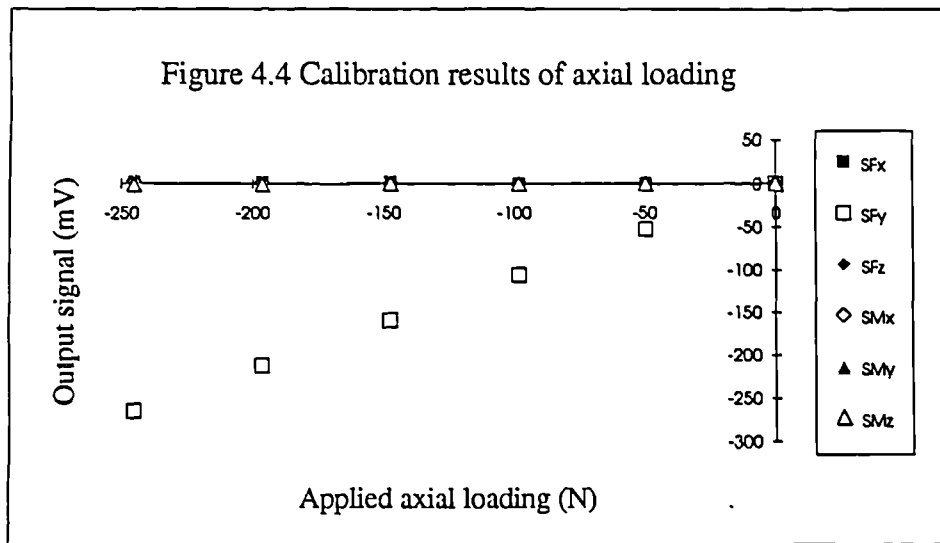
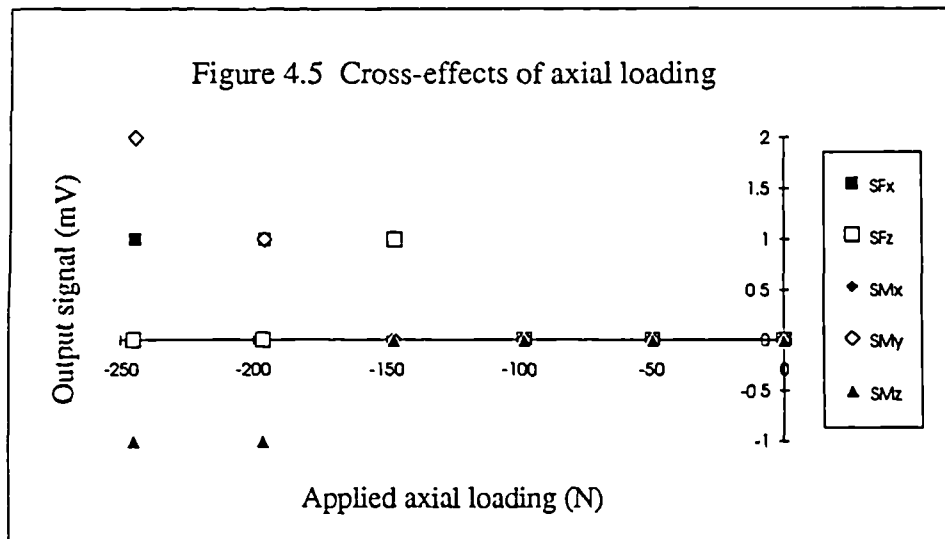


Figure 4.5 Cross-effects of axial loading



(5kg) to - 245.25N (17kg) were applied. The output signals of the six channels corresponding to each load were recorded in mV. A linear regression analysis was conducted on the output signals of each channel against the applied loads, respectively. Six coefficients of column 2 of matrix [M] were determined. The main effect and cross-effects of the axial loading calibration are shown in Figure 4.4 and Figure 4.5 respectively. The regression results are given in Table 4.2.

Calibration of torque

For applying a torque to the transducer, one end of the transducer was vertically fixed and a special machined bar was horizontally attached on the other end of the transducer. Two vertical forces with equal magnitude were applied in opposite directions on each end of the bar, producing a zero resultant shear force and a pure torque on the transducer. As shown in Figure 4.6, the upward force (on the right side of the bar) was applied to the bar by using a pulley, cable and suspended weight system. The downward force (on the left side of the bar) was applied by simply suspending a weight using a cable. Exchanging the position of the pulley system with the simply suspended weight, a torque in the opposite direction was applied. The magnitude of the applied torque is $2 \cdot d \cdot W$. Six torques (3 in each direction) valued $\pm 9.81\text{Nm}$, $\pm 19.62\text{Nm}$, and $\pm 29.43\text{Nm}$ were applied. All six output signals were recorded for each applied torque. Linear regression analyses were conducted on the output signals of each channel against the torques producing six coefficients of column 5 of matrix [M]. The calibration results and cross-effects are shown in Figure 4.7 and Figure 4.8. The regression results are given in Table 4.2.

Calibration of shear forces and bending moments

For shear forces and bending moments calibration, a cantilever system was used as shown in Figure 4.9 and Figure 4.14, in which the transducer was fixed at one end, and a aluminium tube fixed to the other end constructing a cantilever system. The weight was suspended at a distance d' and d'' from the centre of the transducer applying a shear force and a bending moment on the transducer. Two combinations are required to calibrate two shear forces and two bending moments channels, they are $F_x\text{-}M_z$ combination and $F_z\text{-}M_x$ combination.

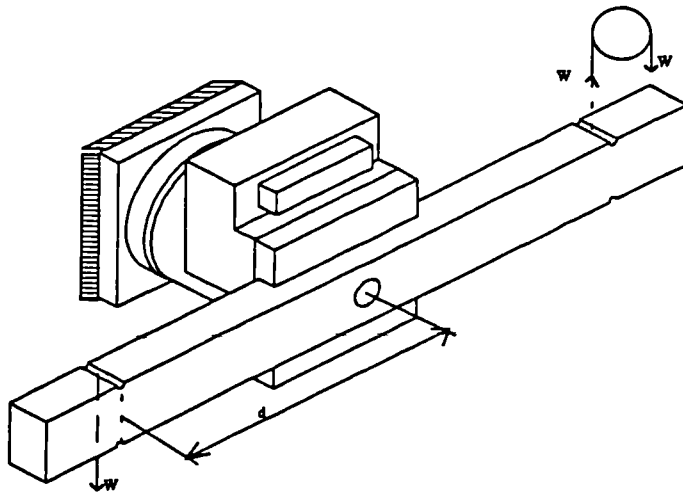


Figure 4.6 The set-up of torque calibration

Figure 4.7 Calibration results of M_y

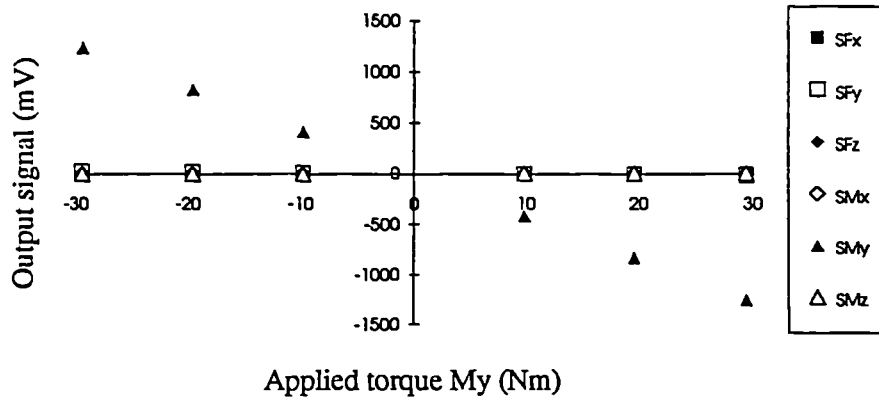


Figure 4.8 Cross-effects of M_y

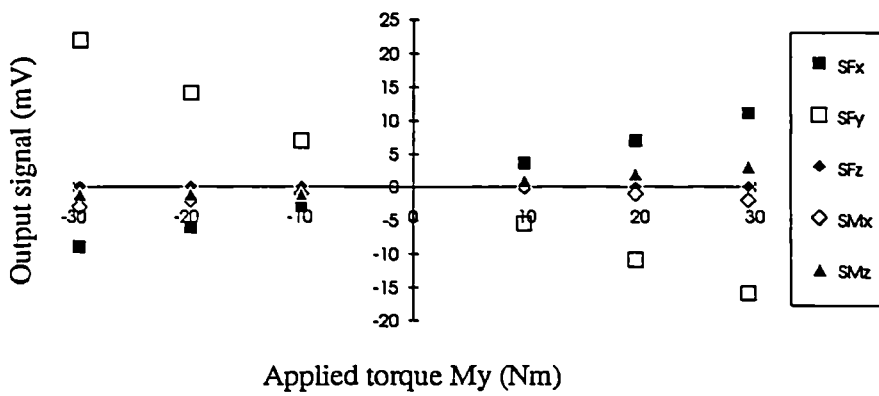


Table 4.2 Regression results of calibration of the force transducer

Variable (y - x)	Correlation coefficient	x - coefficient	Se of x coefficient	Se of y estimate	constant	no of obs.
SFx - Fx	0.999935	2.084004	0.009727	3.411190	-2.85100	8
SFy - Fx	0.998740	0.084603	0.001735	0.608590	1.25000	8
SFz - Fx	-0.996661	-0.048204	0.001612	0.565370	1.18750	8
SMx - Fx	0.0	0.0	0.0	0.0	0.0	8
SMy - Fx	0.0	0.0	0.0	0.0	0.0	8
SMz - Fx	-0.998865	-0.049947	0.000972	0.341029	0.25050	8
SFx - Fy	-0.866025	-0.006116	0.002039	0.316228	-0.30000	5
SFy - Fy	0.999993	1.076453	0.002354	0.365148	-0.40000	5
SFz - Fy	0.0	0.0	0.0	0.0	0.0	5
SMx - Fy	-0.883883	-0.010194	0.003114	0.483046	-0.90000	5
SMy - Fy	-0.883883	-0.010194	0.003114	0.483046	-0.90000	5
SMz - Fy	0.866025	0.006116	0.002039	0.316228	0.50000	5
SFx - Fz	-0.996801	-0.026451	0.000866	0.303657	-0.12475	8
SFy - Fz	0.989730	0.070180	0.004138	1.451196	2.60038	8
SFz - Fz	0.999993	2.080632	0.003164	1.109443	1.34406	8
SMx - Fz	0.960807	-0.011991	0.001412	0.495356	0.34406	8
SMy - Fz	0.0	0.0	0.0	0.0	0.0	8
SMz - Fz	0.054873	-0.000437	0.003250	1.139792	-1.32575	8
SFx - Mx	-0.999896	-1.669378	0.009846	0.170916	0.0	8
SFy - Mx	0.998114	0.528529	0.013271	0.230386	-0.50000	8
SFz - Mx	0.960003	0.123270	0.014678	0.254796	-0.18750	8
SMx - Mx	0.999999	30.597476	0.010314	0.179044	-0.31250	8
SMy - Mx	0.0	0.0	0.0	0.0	0.0	8
SMz - Mx	-0.942281	-0.127298	0.018466	0.320569	0.25000	8
SFx - My	0.998974	0.336756	0.007633	0.396225	0.58333	6
SFy - My	-0.997629	-0.642566	0.022164	1.150505	1.75	6
SFz - My	0.0	0.0	0.0	0.0	0.0	6
SMx - My	0.483494	0.021844	0.019774	1.026436	-1.5	6
SMy - My	-0.999997	-42.19819	0.055162	2.863460	-1.16667	6
SMz - My	0.960031	0.072812	0.010614	0.550973	0.5	6
SFx - Mz	-0.979359	-0.422178	0.035572	0.617517	0.99999	8
SFy - Mz	-0.999896	-0.834688	0.004922	0.085451	-4.2E-06	8
SFz - Mz	0.999896	0.417344	0.002461	0.042725	2.1E-06	8
SMx - Mz	0.0	0.0	0.0	0.0	0.0	8
SMy - Mz	0.0	0.0	0.0	0.0	0.0	8
SMz - Mz	0.999993	30.583746	0.045546	0.790658	-1.74985	8

Se:Standard error

For combined Fx and Mz calibration, the weight was suspended along the x-axis of the transducer (Figure 4.9). From Equation 4.1, the six output signals can be expressed as:

$$S'_i = m_{i1}Fx + m_{i6}M'z \quad i=1,6 \quad (4.4)$$

$$S''_i = m_{i1}Fx + m_{i6}M''z \quad i=1,6 \quad (4.5)$$

where i denotes the channel number, S'_i represent the 6 measured output signals when the weight was suspended at the distance d' from centre of the transducer, the corresponding bending moment is $M'z = -Fx \cdot d'$. S''_i represent the 6 measured output signals when the weight was suspended at the distance d'' from centre of the transducer and $M''z = -Fx \cdot d''$. The x, y, z axes of the transducer are also shown in Figure 4.9. The signals of S'_i and S''_i involve the combined effects of Fx and $M'z$ (in S'_i) and $M''z$ (in S''_i). Therefore, in order to determine the coefficients m_{i1} and m_{i6} , the output signals corresponding to each input load of Fx and Mz should be found. By solving Equations 4.4 and 4.5 the following equations can be obtained:

$$S_{i1} = m_{i1}Fx \quad (4.6)$$

$$S_{i6} = m_{i6}Mz \quad (4.7)$$

$$\text{where } S_{i1} = \frac{1}{2} \left[S''_i + S'_i - \frac{M'z + M''z}{M''z - M'z} (S''_i - S'_i) \right] \quad (4.8)$$

$$S_{i6} = S''_i - S'_i \quad (4.9)$$

$$Mz = M''z - M'z \quad (4.10)$$

the S_{i1} represent the 6 output signals corresponding to each Fx loading, S_{i6} represent the 6 output signals corresponding to each Mz loading, here Mz is the difference of the two bending moments $M''z$ and $M'z$ applied at the centre of the transducer (Equation 4.10). From Equation 4.6 and 4.7, it can be seen that the coefficients m_{i1} and m_{i6} can be determined by regressing S_{i1} against Fx and S_{i6} against Mz. The regression results are given in Table 4.2.

For the complete Fx-Mz calibration, four loads were applied in each direction at two distances from the centre of the transducer. The corresponding output signals S'_i and S''_i were recorded. S_{i1} , S_{i6} and Mz were calculated using Equations 4.8 to 4.10. The regression analyses were conducted on S_{i1} against Fx and S_{i6} against Mz obtaining 12 coefficients in column 1 and 6 of matrix [M]. The calibration results and cross-effects for Fx and Mz loading are given in Figure 4.10 to Figure 4.13.

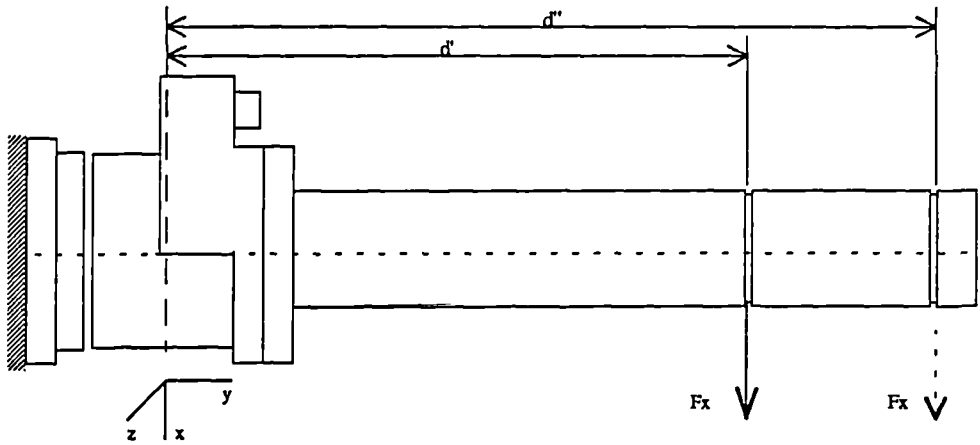


Figure 4.9 The set-up of F_x - M_z calibration

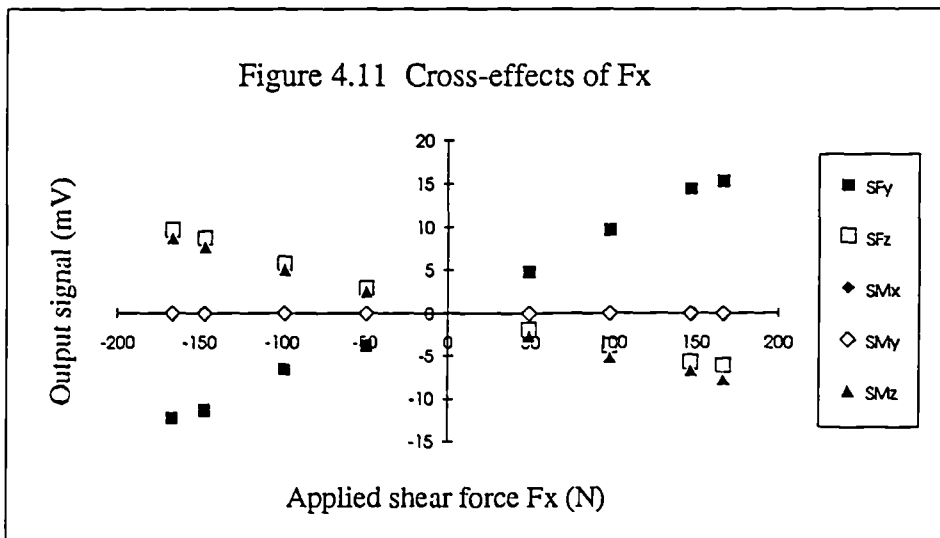
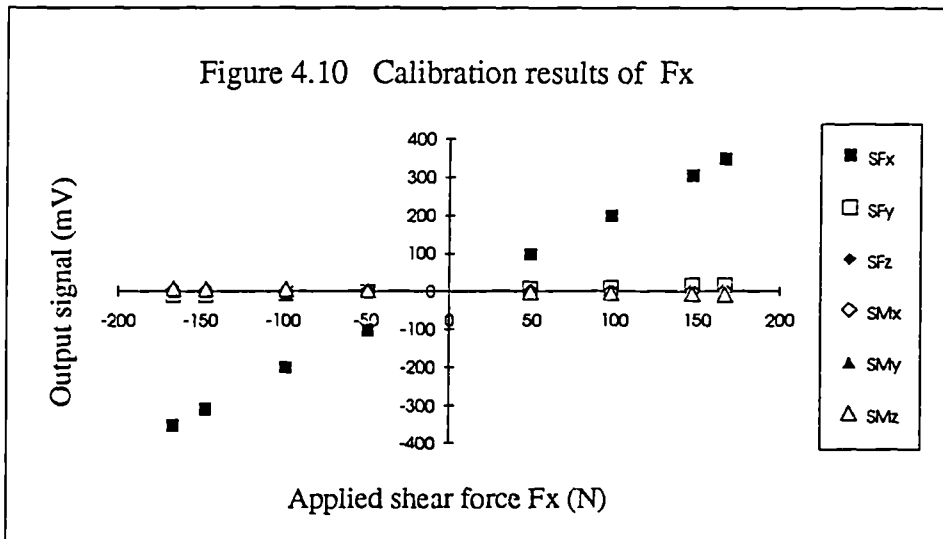


Figure 4.12 Calibration results of Mz

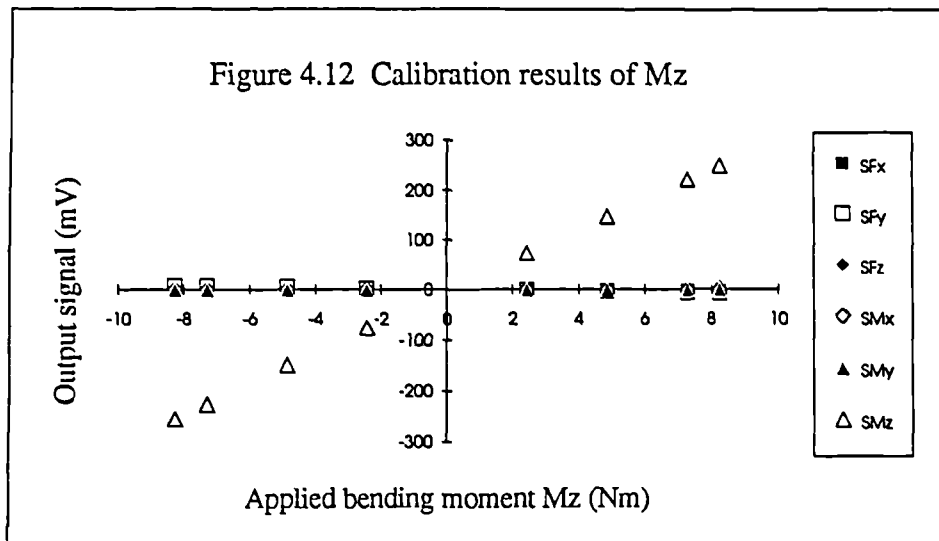
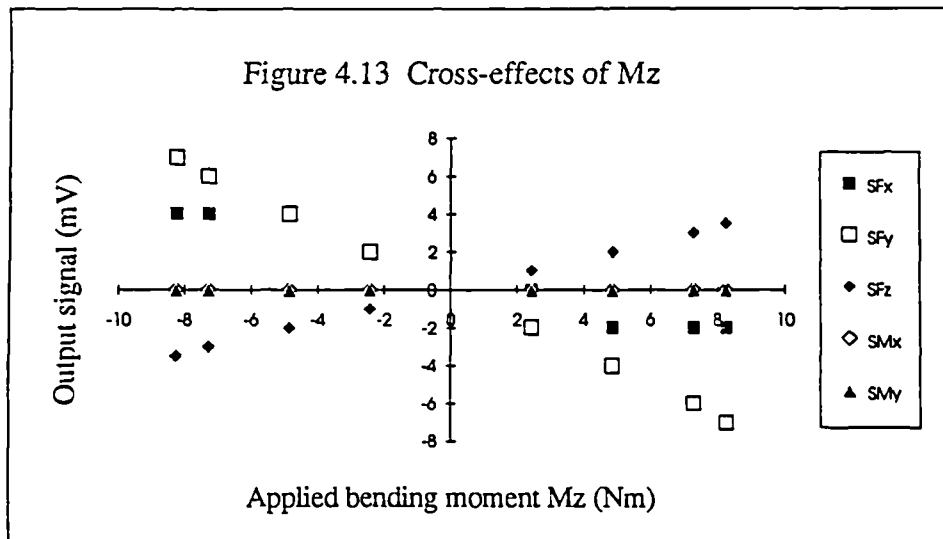


Figure 4.13 Cross-effects of Mz



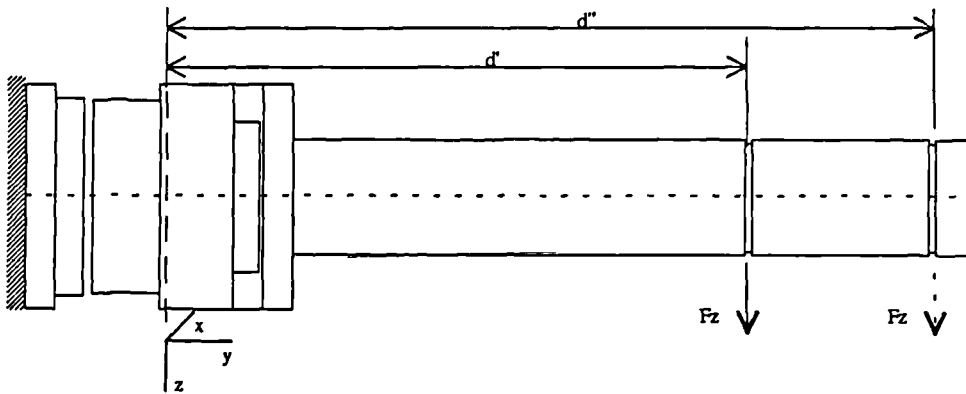


Figure 4.14 The set-up of Fz - Mx calibration

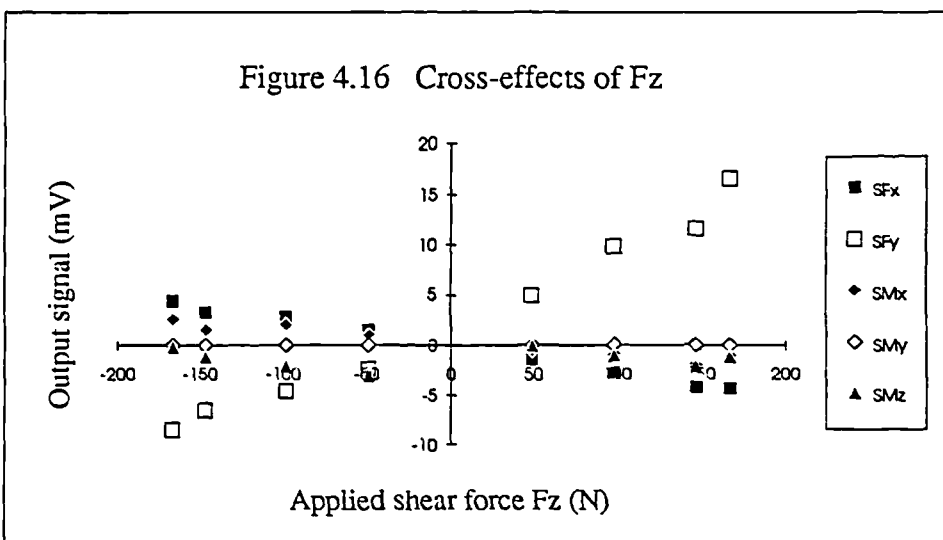
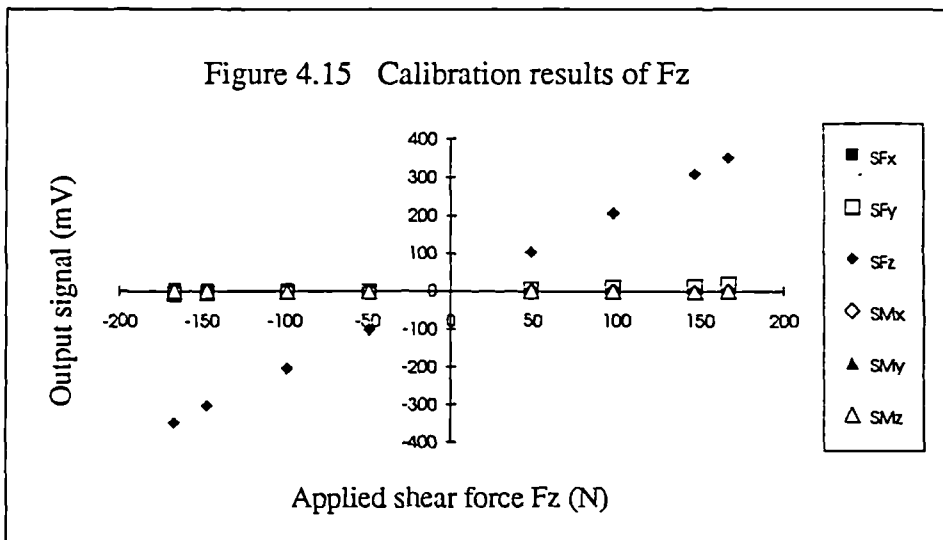


Figure 4.17 Calibration results of Mx

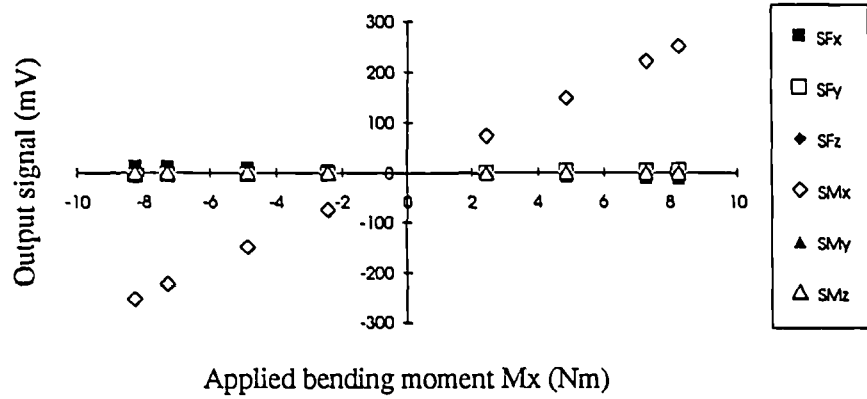


Figure 4.18 Cross-effects of Mx

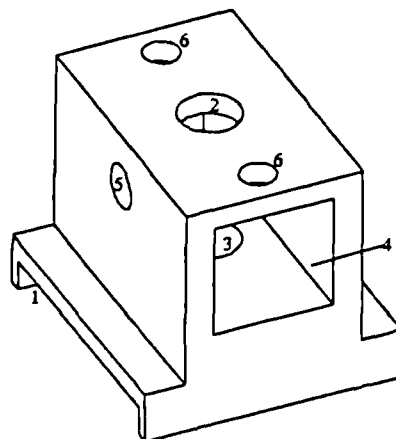
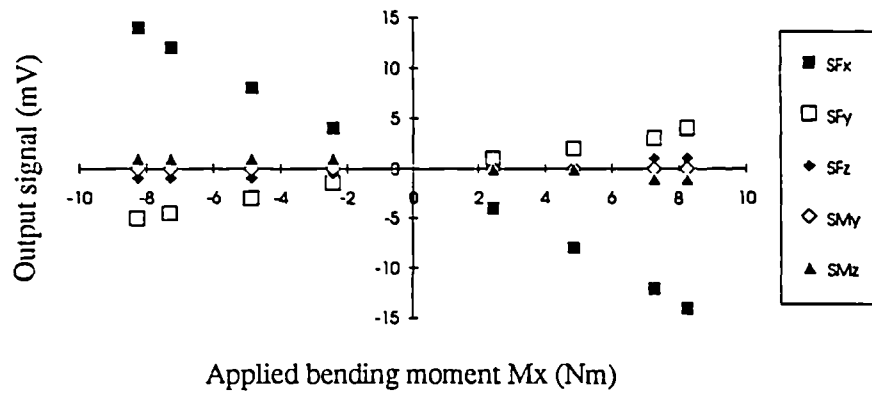


Figure 4.19 End adapter

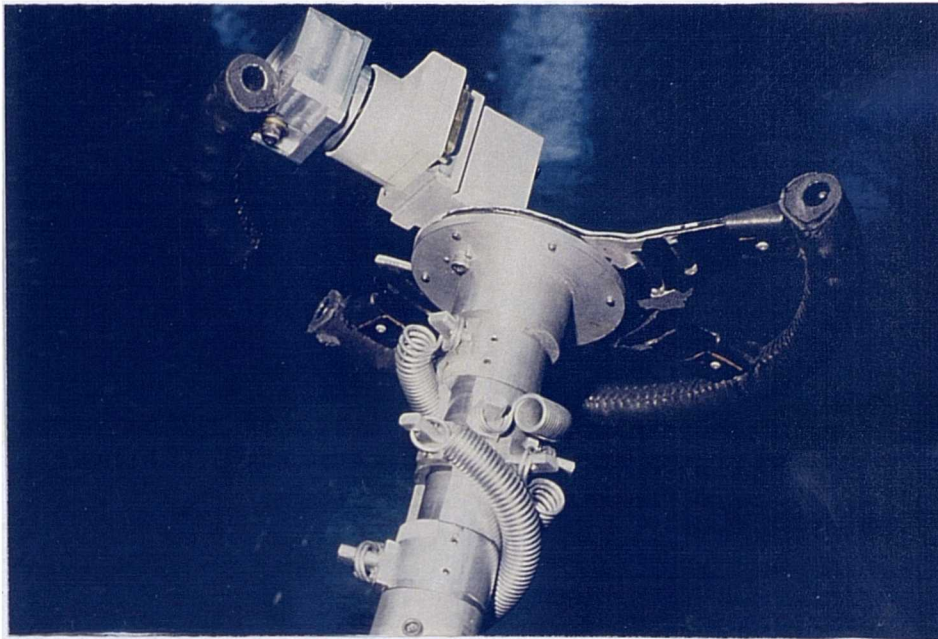


Figure 4.22 Four extension springs were wound up on the surface of the resistance unit to provide a resistive torque

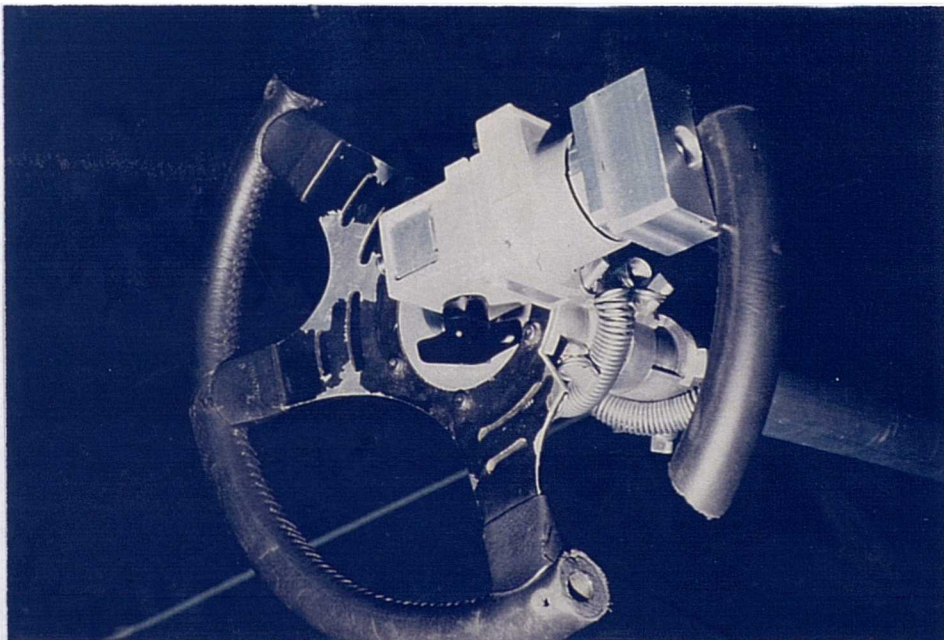


Figure 4.23 The set-up of the steering wheel system

The parameters of matrix [M] are in units of mV/N or mV/Nm, and the parameters of matrix [C] are in units of N/mV or Nm/mV.

4.2.3 The End Adapter Design

In order to fit the transducer into the driving wheel, door and cutting table, a common intermediate part, *end adapter*, between the transducer and the driving wheel, door and cutting table was designed as shown in Figure 4.19. The concave-downward bottom (1) is mounted on the square endplate of the transducer and fixed by a bolt through hole 2 and 3. The square hole (4) is used for connecting with a square bar onto other objects. The adapter and square bar are fixed together by three bolts at hole 5 and 6.

4.3 Instrumentation

In this section, the design of the laboratory used driving wheel, door and cutting plate, which were instrumented with the force transducer, are given.

4.3.1 Instrumented Driving Wheel

To design a simulating steering wheel system, a number of fundamental points should be considered. The simulating system should be able to provide a resistive torque which simulates the real driving conditions, should be able to measure the three dimensional forces and moments on the hand for holding the steering wheel, should be easily fitted within the environment of a motion analysis laboratory, and finally should be of reasonable cost.

4.3.1.1 Torque resistance unit

The first problem of providing a resistive torque to the steering wheel is to decide which type of resistance to use. Generally, there are four primary types of resistance, *static and Coulomb friction, viscous damping, inertia, and elastic resistance*. Each type of resistance has its own characteristics, advantages and disadvantages. *Static Coulomb friction* is a static resistance. The resistance is maximal at the start of movement, but drops sharply, Coulomb (sliding) friction continues as a resistance to movement, but this friction force is not related to either velocity or displacement, and has little precision control once the control has begun to move. *Viscous damping* resistance is proportional to the velocity of the control movement.

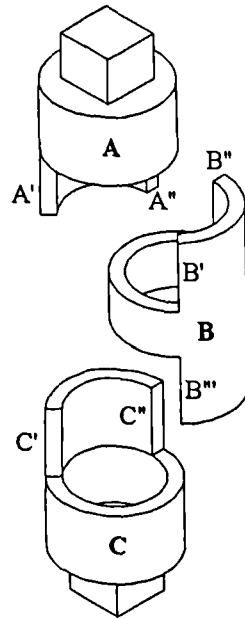
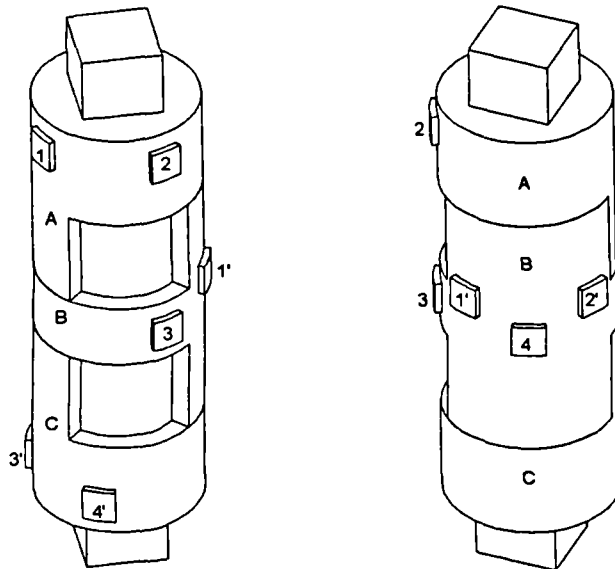


Figure 4.20 Three components of the torque resistance unit



Front View

Right side view

Fig 4.21 Torque resistance Unit

The advantage of the viscous damping resistance is good control, particularly the rate of movement. However, good control is in the engineering sense, for human activities it is difficult to control the speed of the movement of the human body. *Inertial resistance* is the resistance to the movement caused by acceleration of the mass of the mechanism involved. A force exerted on an inertial control will have little effect at first because it produces only an acceleration of the control (the greater the force, the greater the acceleration). Because the acceleration is also related to the displacement and velocity of the movement, it is more difficult to control a precise movement. *Elastic resistance* varies with displacement of a control device. The relationship may be linear or non-linear. The major advantage of elastic resistance is that it can serve as useful feedback, combining both force and displacement in a redundant manner. For human upper limb activities, the elastic resistance allows the arm to be moved at any speed. For the above reasons it was decided to use an elastic resistance to simulate the resistance of the steering wheel.

It was desired that the simulating steering wheel could be turned in either clockwise or counter-clockwise directions and that there would be a linearly increasing resistive torque during the turning of the wheel in each direction. For this purpose an individual part, called the *torque resistance unit*, was designed.

The torque resistance unit consists of three tubular components A, B, C as shown in Figure 4.20 and Figure 4.21. The lower component C is a stationary component and is fixed on an aluminium tube mounted at a convenient location in the laboratory (see section 4.3.1.3). The middle component B can rotate 90 degrees in a clockwise direction from point B''' to point C'. The upper component A can rotate 90 degrees in either a clockwise or counter-clockwise direction. When it rotates 90 degrees in the counter-clockwise direction from A' to B', the middle component B will remain stationary. When it rotates clockwise, it will push the middle component B at points A'' and B'', so that A and B can rotate together from point B''' to C' (90 degrees). The steering wheel is fitted on top of the upper component A. Therefore it can be rotated 90 degrees in either counter-clockwise or clockwise direction. The limited ± 90 degrees displacement of the steering wheel was designed so that the subjects would not have to remove their hands from the wheel during turning (Woodsom 1970).

The resistive torque is provided by four extension springs (as shown in Figure 4.22) which were wound over the surface of the resistance unit between point 1-1', 2-2', 3-3', and

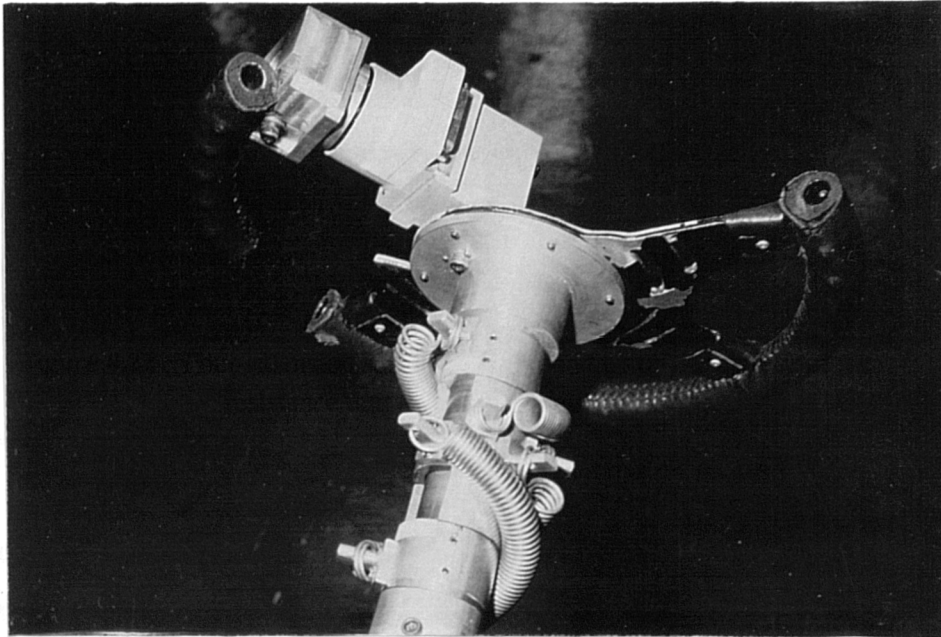


Figure 4.22 Four extension springs were wound up on the surface of the resistance unit to provide a resistive torque

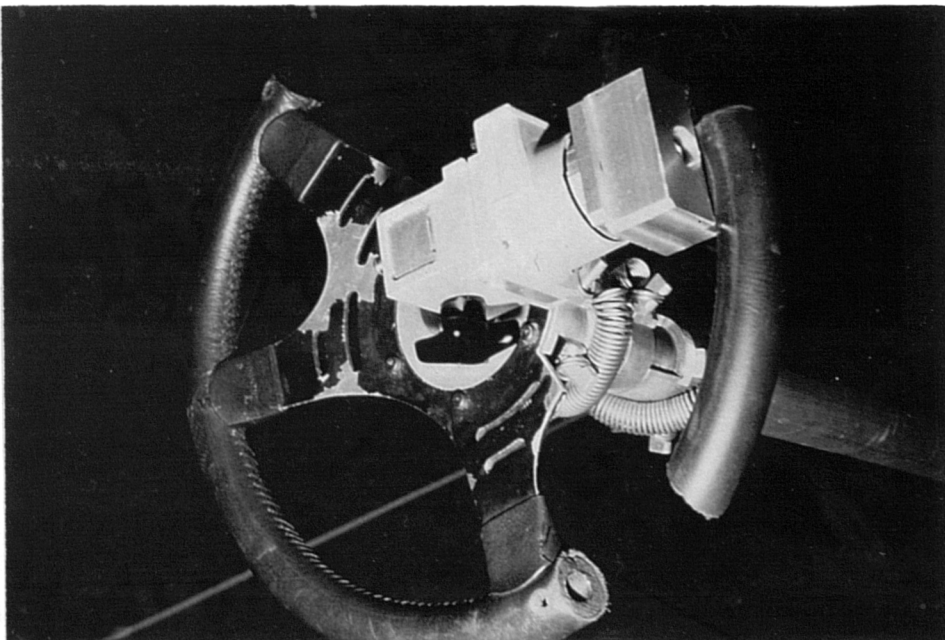


Figure 4.23 The set-up of the steering wheel system

4-4' (Figure 4.21). If the steering wheel is turned counter-clockwise, the two springs between points 1-1' and 2-2' will be extended to produce an approximately linear resistive torque. The other two springs between points 3-3' and 4-4' will produce a resistive torque to the clockwise turning of the steering wheel.

After the torque resistance unit was fitted on the steering wheel, the complete steering wheel system was calibrated to find the torque-angle relationship and the maximum resistive torque. During the calibration, a set of step-increased dead weights were suspended at the rim of the steering wheel (Figure 4.24), and the turning angle corresponding to each suspended weight was recorded. The torques applied to the steering wheel were then calculated from the suspended weights and the recorded angles. The results show a good linear relationship, with a linear correlation coefficient of 0.99789, between the resistive torque and the angle of turn (Figure 4.25). The maximum resistive torque is 19 Nm for 90 degrees of turning of the steering wheel.

4.3.1.2 Implementation of force transducer into the steering wheel

In order to measure the hand forces during turning the steering wheel, the force transducer was fitted between the hub and the rim of the steering wheel. The rim of the steering wheel was cut into two parts, one part was connected with the transducer and the hub, the other part was connected with the hub only (Figure 4.23 and 4.26). This arrangement enables the steering wheel to be driven by two hands, while the forces on only one hand (right hand in this study) is measured. The diameter of the steering wheel is 0.36m and the diameter of the rim is 0.03m.

4.3.1.3 Positioning of the steering wheel system

The top end of the torque resistance unit was fixed on the steering wheel and the lower end of the torque resistance unit was fixed on an aluminium tube constructing a complete steering wheel system (Figure 4.23). By using a specially designed clamp, the aluminium tube can be easily mounted on the wall of the laboratory forming an angle of 60 degrees between the steering wheel plane and the vertical axis. The height of the centre of the steering wheel was 0.83m from the floor. This position of the steering wheel falls into a set of recommended

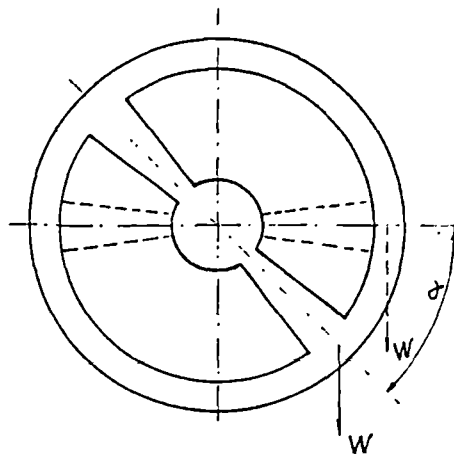


Figure 4.24 Calibration of the torque-angle relationship of the steering wheel system. A weight W was suspended at the rim of the steering wheel and the turning angle α was measured.

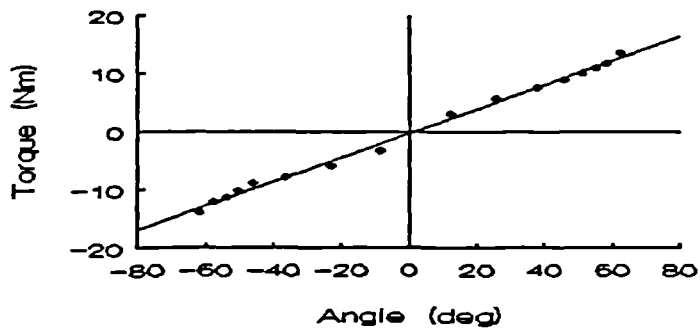


Figure 4.25 Torque-angle relationship of the steering wheel

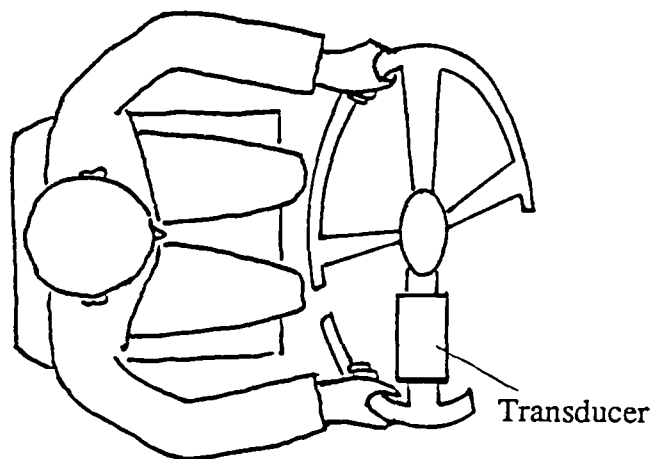


Figure 4.26 Fitting the force transducer into the steering wheel for measuring the forces on one hand during two hand driving.

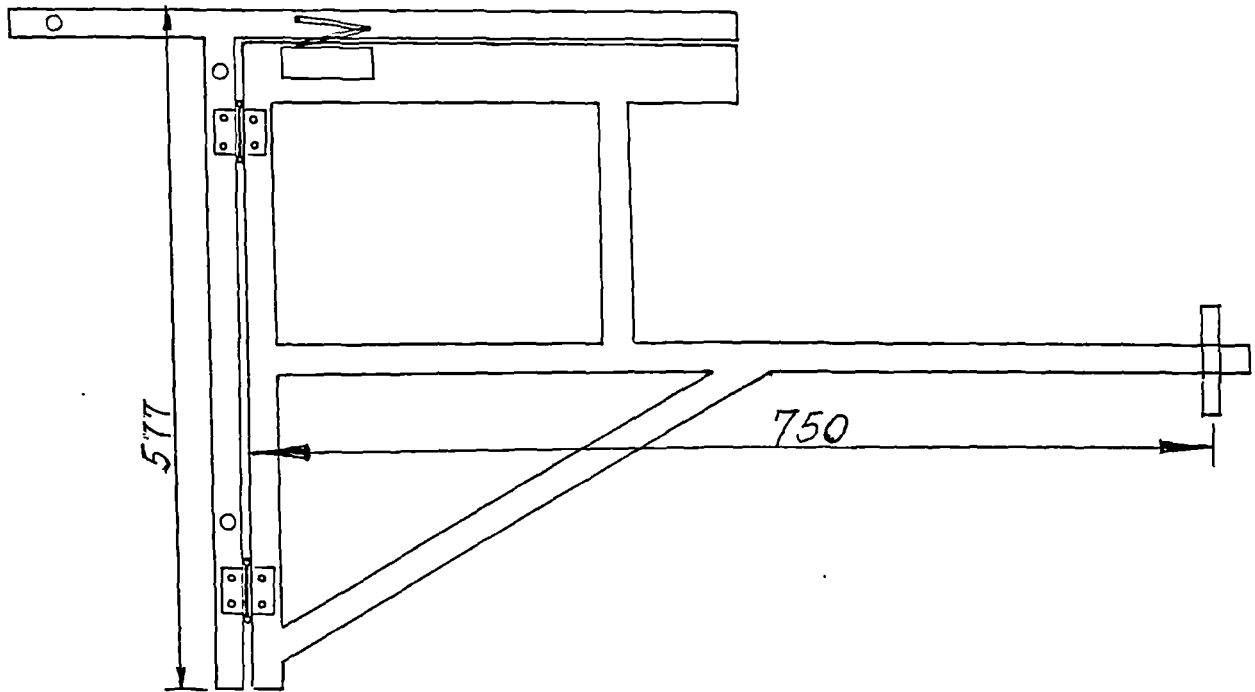


Figure 4.27 The design of a door used in this study

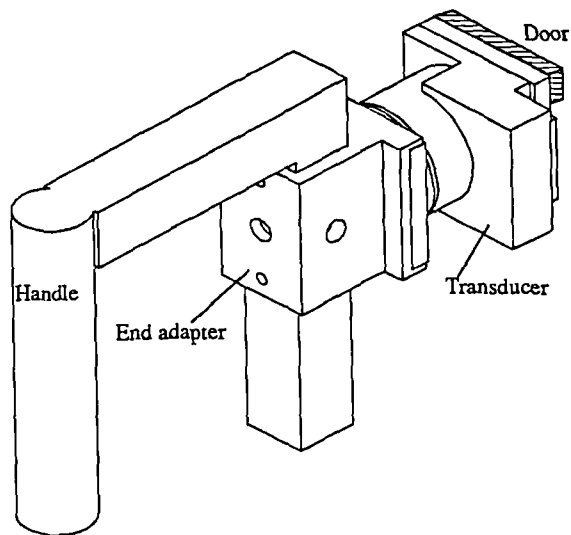


Figure 4.28 The force transducer was fitted between the handle and door

design features for a vehicle cab (Sanders et al. 1987). After the experiment, the steering wheel system can be easily dis-mounted from the wall.

4.3.2 Instrumented Door

To analyse the loads on the upper limb joints during the door opening/closing activity, the forces applied on the door handle and the movements of arm must be recorded. However, in the motion analysis laboratory, a real door will obscure the cameras from the markers on the body of subjects. Therefore a simplified door was designed for use in the motion analysis laboratory in this study (Figure 4.27), which is a steel frame hinged at one side with a T-type steel bar. The T-type bar can be easily mounted on the wall of the laboratory during experiments and dis-mounted from the wall after use. A viscous design of door closer was used. The main part of the door closer was fixed on the door and the another end was connected with the T-type bar (Figure 4.27). Considering that the simplified door will weigh less than a real door, a 10kg weight was placed at the centre of the simplified door (Figure 4.27). The weight of the door will obviously influence forces on the hand. However, the weight of the doors varies greatly and the investigation of the influence of door weight on the opening forces is beyond the purpose of this study. Therefore only one weight setting of the door was used in this study.

For measuring the hand loads during the door opening/closing activity, the force transducer was fitted between the door and a cylindrical handle of diameter of 0.031m (Figure 4.28 and 4.29). Therefore, during the opening/closing of the door the loads acting on the handle by the hand can be transmitted to the transducer to be recorded. This type and size of handle was recommended as being most comfortable for power grip (Pheasant 1986, Cushman & Rosenbery 1991).

The handle position (the horizontal distance from the handle to the hinged side and the height of handle) is another influencing factor to the hand loads of opening/closing a door, and the handle position can be varied greatly from one door to another depending on the width of the door. After measuring the handle positions of a number of doors in the University library, Bioengineering Unit building, and other buildings, one setting of horizontal position of 0.75m from the hinge was chosen to be used in this study. This handle position is often seen on the doors of 80-85cm width. The vertical holding position of the handle ranged from 0.9m to 1.3m

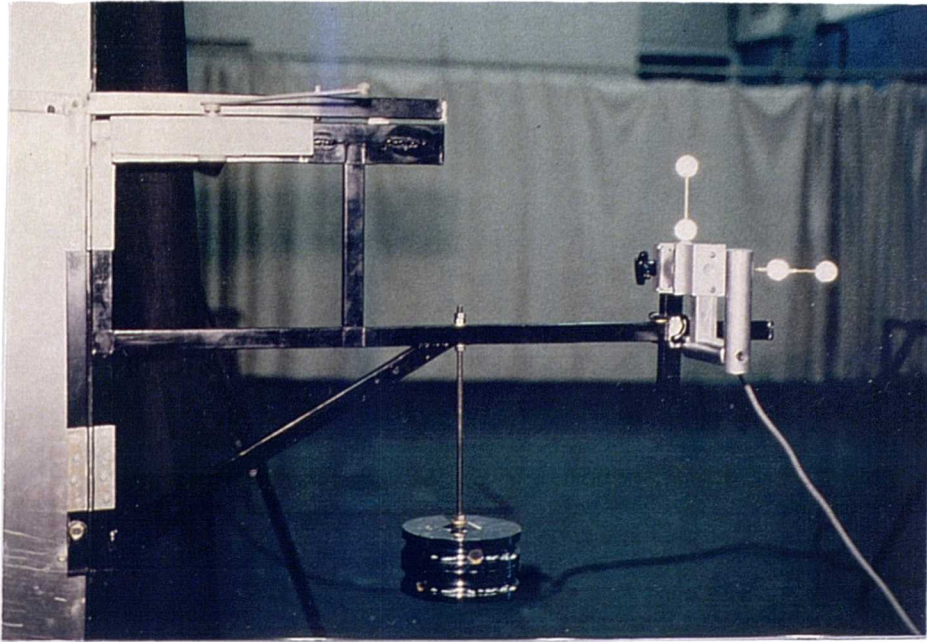


Figure 4.29 The simplified door used in this study

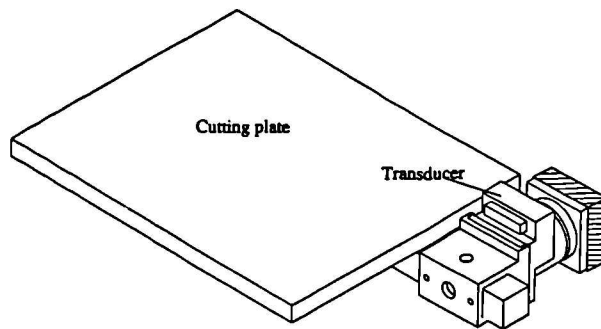
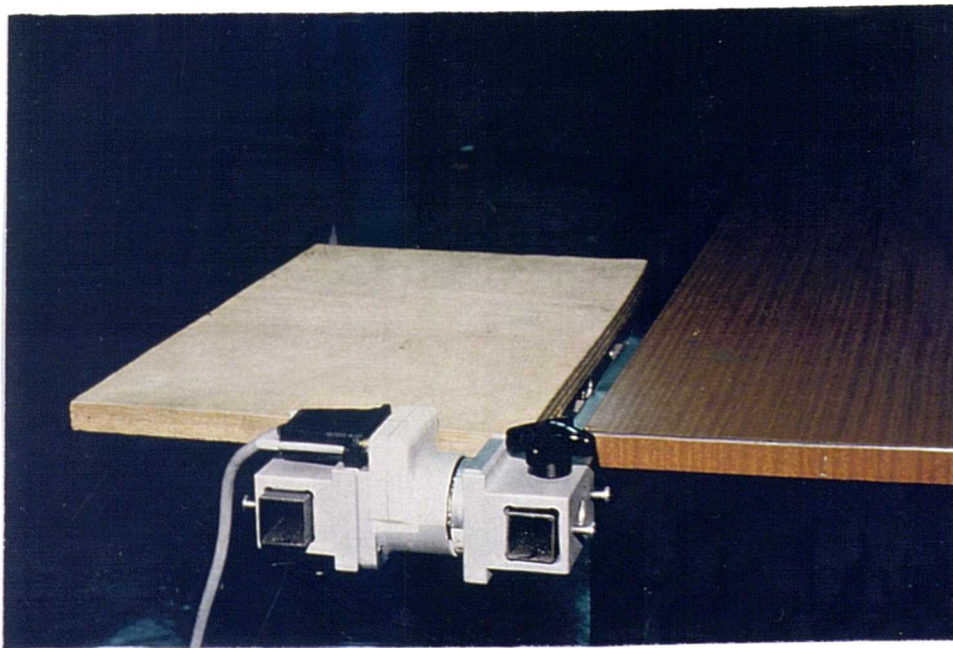


Figure 4.30 Cutting plate instrumented with force transducer

from the floor. Therefore the subjects can hold the handle at a self-determined comfortable height.

4.3.3 Instrumented Cutting Plate

For measuring the hand forces during the cutting activity, a cutting plate instrumented with the force transducer was designed. The force transducer was fitted between a table and a cutting plate forming a cantilever system (Figure 4.30). During a cutting activity, the cutting forces acting on the cutting plate could be transmitted to the transducer to be recorded. Since the three dimensional position of the transducer, the hand and arm can be measured by a VICON motion analysis system, the forces and moments on the upper limb joints can then be calculated from the transducer's signals, the positions of the transducer, and arm. The cutting plate was 0.4m long, 0.27m wide, and positioned at a height of 0.74m. The height of the cutting plate was designed for a sitting subject to conduct the cutting activity.

4.3.4 The Books Used for Lifting Activities

The non-instrumented objects used in this study were two books of mass 1kg and 2kg which were used as the weights to be lifted in the study of lifting activities. The books of A4 paper size (210mm×297mm) were made of wood and paper with thicknesses of 24mm and 40mm, respectively. It was considered that these thicknesses can be held comfortably by the subjects. The masses of the books were chosen to be lifted by one hand-arm without assistance from other parts of the body.

4.4 Test Procedures

4.4.1 Setting Up of the Measuring System

The setting up of the measuring system included the calibration of the Vicon motion analysis system and connection of the force transducer to the amplifier and Vicon system.

Before the test, the Vicon motion analysis system was calibrated. The relative positions between each camera and four calibration poles were determined by the calibration. During the calibration, the coordinates of 20 calibration markers on the four calibration poles were measured by the system and compared with their known positions in the laboratory coordinate system. The average residuals between measured and real positions of the calibration markers

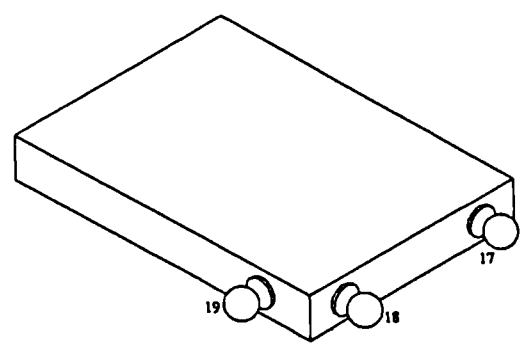
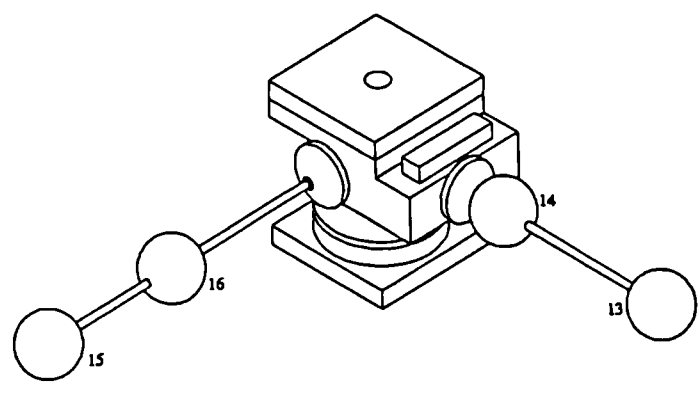
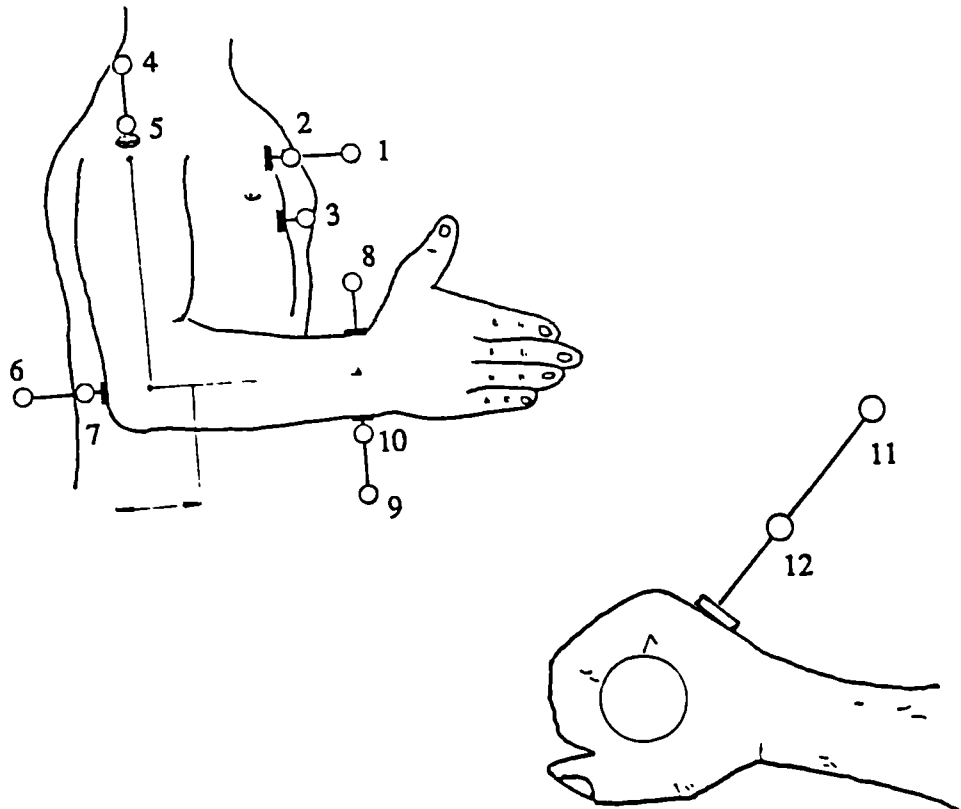


Figure 4.31 The marker system

were given corresponding to each camera. The calibration residuals are the important parameters indicating the accuracy of the measuring system. The accuracy of the calibration results and subsequent measurements depends mainly on the relative positions of the cameras and the calibration poles. In this study, all calibration residuals were below 3mm which is the allowed maximum error of the calibration of the video cameras. When some of the residuals were greater than 3mm, the camera positions were adjusted and the system calibrated again until the desired results were obtained.

Before tests, the force transducer was connected to the amplifier, the output of amplifier was connected to the Vicon system through an A-D converter. The setting of the bridge voltage and the gain of the amplifier were the same as that used in the calibration of the force transducer (Table 4.1). The output signals were adjusted to zero before testing. Because the test lasted about one to two hours, the drifting effects can not be avoided. To eliminate the drifting effects a function of initial value reduction was written in the analysis software.

4.4.2 The Landmark System

The markers used in this study are made from light plastic balls of 25.4mm in diameter covered by retro-reflective paper. These balls were affixed to bars of different lengths which had plastic bases of 25.4mm diameter.

In order to determine the joint centre positions, the origins and orientations of the trunk, transducer and book coordinate systems, at least three markers were attached on each body segment, the force transducer and the book. The determinations of the joint centres and orientations of each coordinate system from these landmarks are given in section 5.1. In determining these landmark positions the following considerations were involved:

- 1) minimal movement between marker and underlying bones;
- 2) maximal distance between markers;
- 3) visible by at least two cameras during the test at any instant of time.

The Figure 4.31 shows a diagrammatic representation of the full marker system, as well as the numbering system of the markers which indicates the order of labelling in the Vicon motion program. A total of 19 markers were used in this study, the descriptions of their location are listed in Table 4.5.

Table 4.5 Marker number, labels and description

Marker number	Marker labels	Marker description
1	THF	Higher trunk marker far from skin
2	THN	Higher trunk marker near to skin
3	TL	Lower Trunk marker
4	SHH	Higher marker of shoulder joint
5	SHL	Lower marker of shoulder joint
6	ELBF	Elbow marker far from skin
7	EBBN	Elbow marker near to skin
8	WR	Right marker of wrist (radial side)
9	WLF	Left marker of wrist far from skin (ulnar side)
10	WLN	Left marker of wrist near to skin (ulnar side)
11	HAF	Hand marker far from skin
12	HAN	Hand marker near to skin
13	PLX1	Marker 1 on x-axis of transducer
14	PLX2	Marker 2 on x-axis of transducer
15	PLZ1	Marker 1 on z-axis of transducer
16	PLZ2	Marker 2 on z-axis of transducer
17	BK1	Marker 1 of book
18	BK2	Marker 2 of book
19	BK3	Marker 3 of book

4.4.3 Measurement of Body Parameters

The body parameters required in this study are the mass, mass centre position and mass moment of inertia of upper arm, forearm, and hand. The mass and mass centre position were determined by using the data developed by Drillis & Contini (1966) (see Section 2.3 for details). The mass moments of inertia were calculated by using the non-linear regression equations (Equation 2.8 and 2.9) developed by Yeadon & Morlock (1989) (see Section 2.3 for details). Some basic parameters of the subjects were required for calculating these body parameters which will be used in the kinematic and kinetic analysis. These basic parameters, listed in Table 4.6, were manually measured directly on the subjects by using tape and caliper. In Table 4.6, parameters 12 to 15 were used with body markers for determining the joint centre positions (described in Section 5.1), other parameters were used for determining the mass, mass centre and moment of inertia of each segment. The radius of curvature of the hand was measured, when the subject was holding a bar of 30mm of diameter, as the distance between the back of hand and the centre of the cylinder bar. This information was used for determining the centre of the hand (Section 5.1). The radius of curvature of the shoulder joint

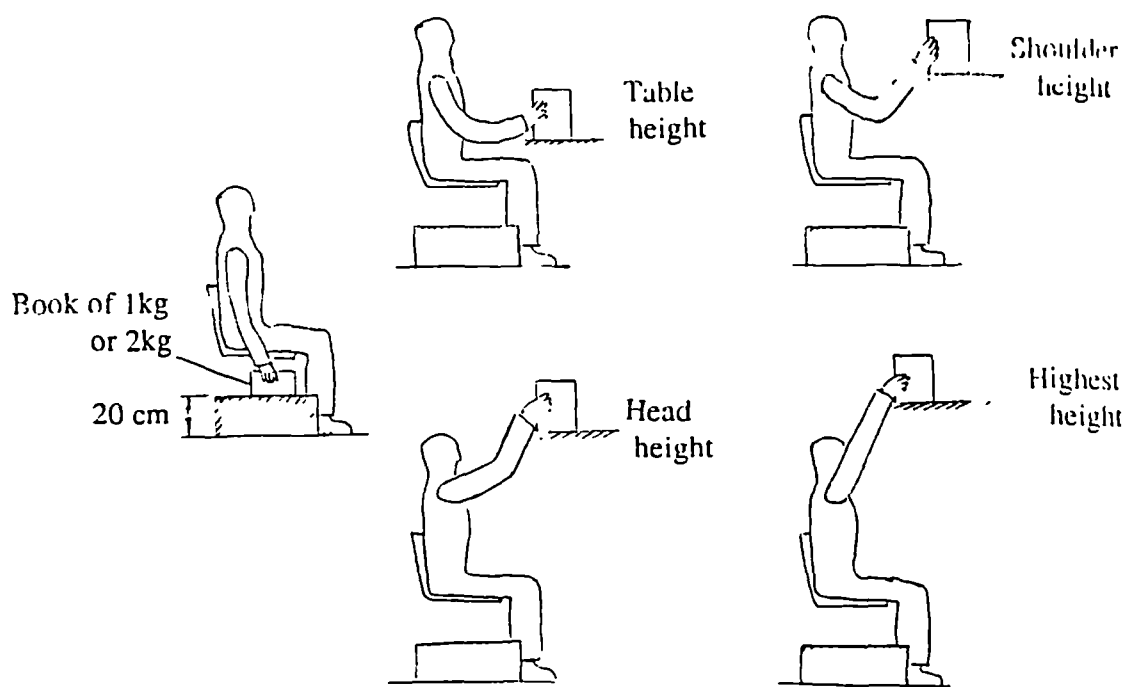


Figure 4.32 Lifting activities investigated in this study.

ball was measured as the distance from the acromial process to the estimated centre of the glenohumeral joint.

Table 4.6 Body parameters directly measured on the subject

1 Name	2 Age	3 Male/Female	4 Height	5 Mass
6 Length of upper arm (UAL)	7 Length of forearm (FAL)	8 Length of hand -- (HL)		
9 perimeter of upper arm:	P ₁	perimeter - below axilla	-----	(PU1)
		-		
	P ₂	perimeter - maximum	-----	(PU2)
	P ₃	perimeter - elbow	-----	(PU3)
10 Perimeters of forearm:	P ₁	perimeter - elbow	-----	(PF1)
	P ₂	perimeter - maximum	-----	(PF2)
	P ₃	perimeter -wrist	-----	(PF3)
11 Perimeters of hand:	P ₁	perimeter - wrist	-----	(PH1)
	P ₂	perimeter - metacarpal - phalangeal	-----	(PH2)
12 Radius of shoulder joint ball (ROS)	13 Thickness of elbow		-----	(TOE)
14 Breadth of wrist (BOW)	15 Radius of hand (ROH)			

4.4.4 Lifting a Book

The activity of lifting a light weight to several heights by one hand at the sitting position were tested in this study. The weights lifted in this test were two books of mass 1kg and 2kg (see Section 4.3.4). The whole set of lifting activities involved lifting each book to four different heights, table, shoulder, head, and highest height, respectively (Figure 4.32). Altogether 8 modes were investigated in the study of lifting activities. The table height was 0.74m high from ground, the shoulder height was the height of acromial process when the subject sat straight up on a 0.43m high chair, the head height was measured at the top of the head when the subject sat upright on the same chair. The highest height was determined by each subject as the highest height they could lift the book onto, when the subject's arm was fully stretched with little forward inclination. Each height was indicated by a horizontally placed wooden platform attached to a vertical bar. The wooden platform could be moved along the vertical bar to a specified height. The horizontal distance between the subject and the wooden platform was determined by the subject as the preferred distance after two or three practice sessions.

The subject sat on a 0.43m high chair for conducting the lifting activities. During the test, subjects were asked to lift a book from a 20cm height to each of the four heights. When



Figure 4.33 A subject in the lifting test

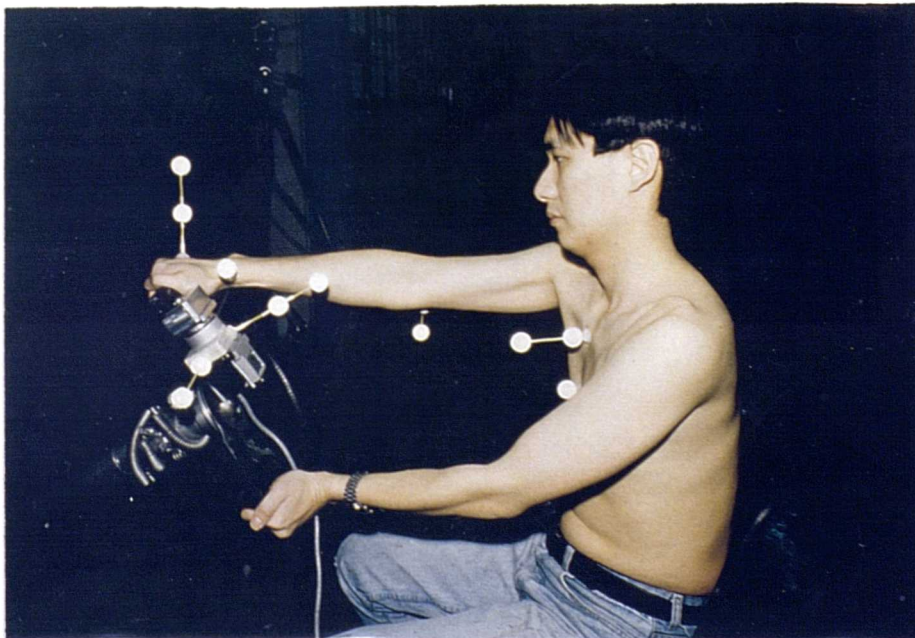


Figure 4.34 A subject in the driving test

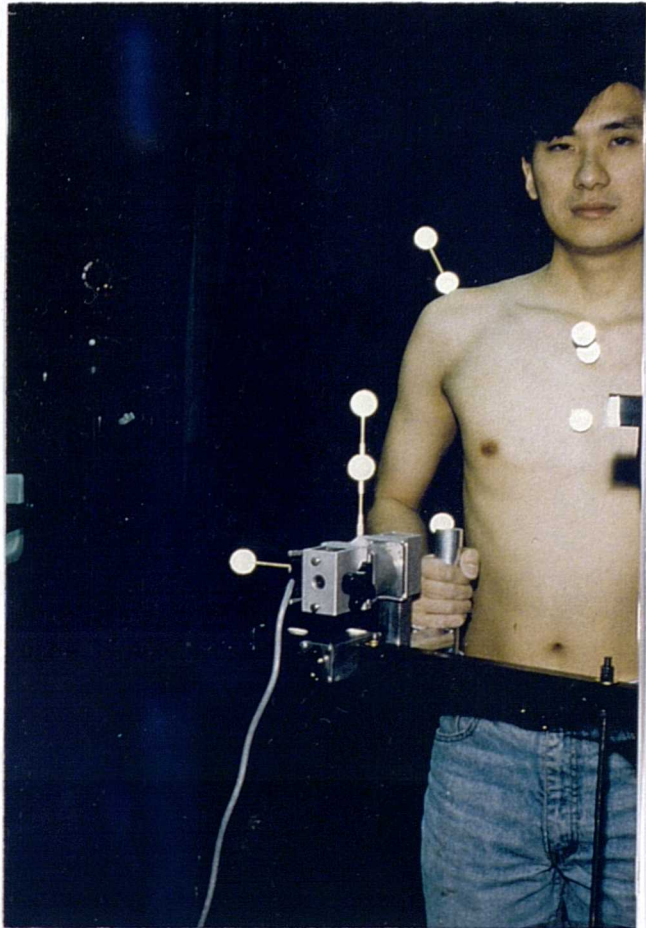


Figure 4.35 A subject in the opening/closing door test

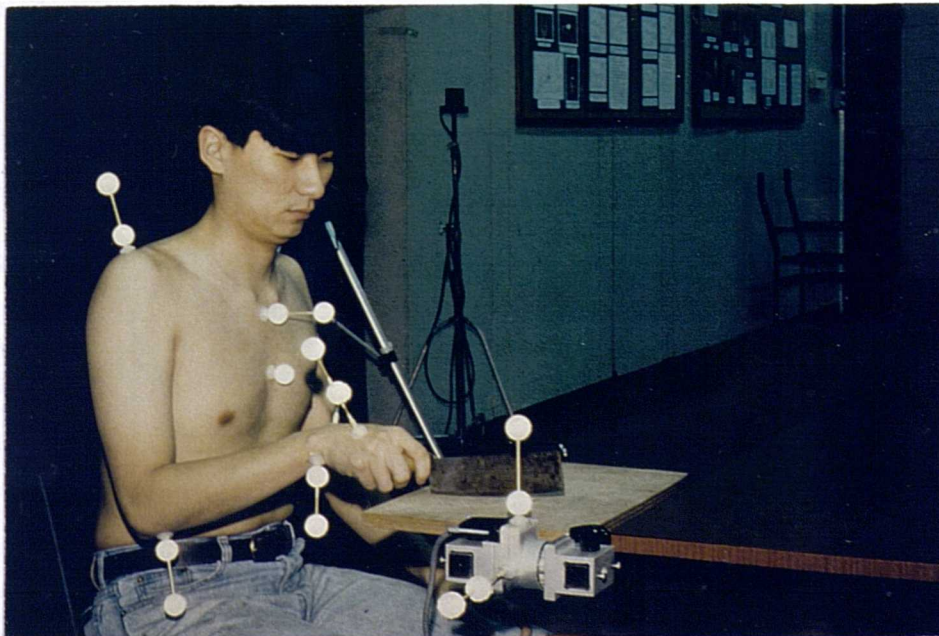


Figure 4.36 A subject in the cutting test

the book was lifted onto the wooden platform it was then lowered back to the original height without stopping between the lifting and lowering process. No instruction on any specified speed of lifting and lowering was given to the subjects, therefore the lifting actions were performed by the subjects at their own preferred speed. Only the Vicon motion analysis system was used for recording the movements of these activities. All markers were affixed at the appropriate sites described above. Six male subjects, all right hand dominant, were tested, and the lifting activities were all performed by the right arm. Each mode was measured three times for each subject. In pre-testing, each lifting was finished in 5 seconds by all subjects. Therefore, 5 seconds of data were collected for each measurement. Figure 4.33 shows a subject during the lifting test.

4.4.5 Driving the Steering Wheel

The test started after the setting up of the measuring system and affixing all markers to the appropriate positions. The subjects sat on a 0.43m high chair, the distance between the chair and steering wheel was chosen by the subject to feel comfortable for conducting the driving activity. The activity involved rotating the steering wheel counterclockwise from the zero degree position to 90 degrees position and then rotating clockwise from the 90 degree position to -90 degrees, then rotating counterclockwise again back to the zero degree position. When the steering wheel reached the 90 and -90 degrees positions the rotation was stopped by a block on the resistance unit (Figure 4.20 and 4.21), the subject could feel the resistance and then reverse direction of rotation. Before the beginning of the test, the subjects were asked to practise the activity several times to get familiar with the system. No instruction on the speed of rotation was given to the subjects who rotated the steering wheel at their self-determined preferred speed. Six male subjects (all right handed) were tested and three sequences of this activity were measured for each subject. In pre-testing each subject could finish the driving activity within 6 seconds. Therefore 6 seconds of data from both Vicon and force transducer were collected for each test. Figure 4.31 shows a subject during the driving test.

4.4.6 Door Opening and Closing

The door opening and closing activity was performed from a standing position. The subjects did not move their foot during the test. The hinge of the door was on the left side of

the subject, and the subjects used their right hand to perform the activity. The subject stood at a distance away from the door where the arm was fully stretched. The frontal plane of the subject's body and the door formed an angle of 30 to 45 degrees. This enabled the subject to open the door to the largest opening without trunk movement. The whole activity involved pulling the door to the largest opening and then pushing it back to the original (closed) position. After the set-up of the measuring system and finding the appropriate standing position by two or three practice sessions, the subject started performing the activity. Six male subjects (all right handed) were tested, each subject was measured three times. Five seconds (determined in pre-testing) of data were collected for each measurement. Figure 4.35 shows a subject performing the door opening and closing test.

4.4.7 Cutting

The cutting activity was performed in the sitting position. The subject sat on a 0.43m high chair in front of the cutting plate performing the activity with a 0.13kg knife. The knife had a cylinder handle of 0.03m diameter. The handle can be easily and firmly held by subjects for efficient transmission of hand force to the knife and cutting plate and then recorded by the force transducer instrumented with the cutting plate. Six male subjects (all right handed) were tested. Five cutting movements were continuously performed for each test. In order to continuously transfer the cutting force to the transducer at least one part of the knife was kept in contact with the cutting plate during the activity, while other parts of the knife moved up or down. Three tests were measured for each subject. Five seconds of data were collected for each test and Figure 4.36 shows a subject in the cutting test.

4.5 Data Acquisition and Pre-processing

Excepting the data acquisition period given above, a number of parameters were specified during the data acquisitions of this study. These parameters are listed in Table 4.7.

Table 4.7 Data acquisition parameters

<i>Frame intervals between samples:</i>	1
<i>Channels used by cameras:</i>	6
<i>Maximum capture time (s):</i>	6 for driving activity, 5 for other activities
<i>Maximum TVD file (blocks):</i>	100
<i>Run automatically:</i>	Yes
<i>TV frame rate (50 60 or 200 Hz):</i>	50
<i>Maximum analogue channels:</i>	0 for lifting activity, 6 for other activities
<i>Analogue data rate:</i>	1
<i>Analogue gain:</i>	1

The collected data during the tests needs to be pre-processed for generating the data in a format that could be used in the analysis program. Three steps were involved in the pre-processing, reconstruction, identification, and .A3D file generation.

The acquired data can be easily reconstructed by the program built in the Vicon system, only a command is required for doing the reconstruction. The most time consuming work in the data pre-processing is the identification. Each marker must be identified manually using the traces of markers displayed on screen. When one marker was identified on the screen, its name (Table 4.5) is given to the computer. In the case of a marker which was not viewed by at least two cameras for some frames the position information of this marker was lost for these frames and the trace was broken. When the marker was viewed again by two or more cameras, it was known as a new marker in which case the two traces were identified as one marker. The lost data in some frames can be interpolated by the Vicon system. In this study, the maximum number of interpolated frames is 20. The data files with more than 20 lost frames of data were not used for further analysis. The .C3D files were generated after the identification. However the .C3D files are not in ASCII format. In the final pre-processing of data, the .C3D files were converted into the .A3D files with ASCII format using a program ASCONV2 modified by S Nicol (1993). The .A3D files can then be analysed on the computer centre main frame by the developed program.

Chapter Five

Theoretical Aspects of the Research

The theoretical aspects of this study are given in five sections. The first section describes the methods used for data processing and normalisation. The method of determining the joint centres and segment coordinate systems from measured marker positions is given in the second section. The kinematic and kinetic analysis methods are given in the third and fourth sections, respectively. Details of a new method of determining the axial rotation angle of limb segments is given in the final section (section 5).

5.1 Data Processing

The data collected by the Vicon motion analysis system contain additive noise from many sources, such as electronic noise in optoelectric devices, spatial precision of TV scan system, and marker vibration. All these will result in random errors in the coordinates of markers and the data from the transducer. Usually the random error occurs as high frequency components and it is of considerable importance when considering the problem of calculating velocities and accelerations. During the differentiation of the data, the amplitude of each of the harmonics increases with its harmonic number; for velocities they increase linearly, and for accelerations the increase is proportional to the square of the harmonic number. Therefore the raw data have to be processed to attenuate the higher frequency noise before being analysed. This process is usually called data smoothing. A number of techniques have been used for this purpose, such as polynomial, cubic spline function, Fourier series, and more advanced digital filtering. A number of excellent reviews have appeared on the topic of the smoothing and differentiation of data obtained from noisy measurements (Vaughan 1982, Wood 1982, Woltring 1985). Recently, the most often used digital filter is the Butterworth filter which is a recursive filter and has an infinite impulse response (IIR). The great advantage of the IIR filter is computational economy. A filter characteristic requiring (say) 100 or more coefficients in a nonrecursive realisation can often be obtained using just a few recursive coefficients. However, there are two potential disadvantages (Lynn & Fuerst 1989). First, a recursive filter may become unstable if its feedback coefficients are chosen badly. Secondly, recursive designs can not generally provide the linear-phase responses so readily

achieved by nonrecursive methods. In practical applications, the data require to be filtered twice by a second order Butterworth filter, once in the forward direction of time, and once in the reverse direction of time (Winter et al. 1974), to eliminate the phase distortion. As a result, the data were filtered by a fourth order filter, and the real cut-off frequency was changed from the original cut-off frequency. Therefore this effect has to be taken into account when specifying cut-off frequency for the original filter.

5.1.1 FIR Filter Design

In this study, a low pass, nonrecursive linear-phase finite impulse response (FIR) filter with Hamming Window was used for smoothing the raw data. The advantages of the FIR filter over an IIR filter can be summarised as: (1) the nonrecursive filter is inherently stable. Its transfer function is specified in terms of z-plane zero only, so there is no danger that inaccuracies in the coefficients may lead to instability. (2) Since a nonrecursive filter has a finite impulse response (FIR), the latter can be made symmetrical in form. This produces an ideal linear-phase characteristic equivalent to a pure time-delay of all frequency components passing through the filter. This is said to be no phase distortion. The format of the FIR filter used in this study is as follows:

$$y_n = \sum_{k=-M}^M b_k x_{n-k} \quad (5.1)$$

where y_n and x_n are the output and input sequences, respectively, b_k are the filter coefficients which are simply equal to successive terms in its impulse response. The impulse response of an ideal, zero-phase low-pass filter is derived by Fourier Transform method as:

$$h'_k = \frac{1}{k\pi} \sin\left(\frac{2\pi k f_c}{f_s}\right) \quad |k| = 1, 2, \dots, M$$

$$h'_k \rightarrow 2f_c / f_s \quad \text{as } k \rightarrow 0$$

$$h'_k = h'_{-k} \quad (5.2)$$

where h'_k is the k th coefficient of the impulse response, f_c is the cut-off frequency, f_s is the sampling frequency, M is the number of terms of h'_k on each side of $k = 0$, and the total number of terms of h'_k (the filter length) is $2M+1$. In order to reduce the Gibbs oscillation in the above filter, the impulse response is multiplied by a widely used Hamming Window which is defined as:

$$\begin{aligned}
 w_k &= 0.54 + 0.46\cos(k\pi/M) & -M \leq k \leq M \\
 &= 0 \text{ elsewhere} &
 \end{aligned}
 \tag{5.3}$$

The resulting coefficients of impulse response are then written as:

$$h_k = h'_k w_k \tag{5.4}$$

This impulse response has a total of $2M+1$ terms, M terms on each side of h_0 , and it is a zero-phase filter. To make the filter with a linear-phase, h_k was shifted to the right and began at $k = 0$.

A FORTRAN program was written for calculating the coefficients of this filter and using the filter to process the coordinate and transducer data. Two parameters of this filter had to be determined, M and f_c in this program. The value M represents the length of the filter and it has been stated (Lynn 1989) that *the goodness of fit clearly improves with increasing M* . Because the length of data files collected in this study were in a range from 150-300 frames after identifications, the filter lengths ($2M+1$) were selected to be equal to the number of frames (or number of frames-1) of each data file. The determination of the second parameter, cut-off frequency is given in the following section.

5.1.2 Choice of Cut-off Frequency --- Frequency and Residual Analysis

Filtering of any signal is aimed at the selective rejection, or attenuation of certain frequencies. This can be done by adequate choice of the cut-off frequency. Two things should be noted in the selection of cut-off frequency. First, the higher frequency noise will be severely reduced but not completely rejected. Second, the signal, especially in the region where the signal and noise overlap will be slightly attenuated. This results in a slight distortion of the signal. Thus a compromise has to be made in the selection of the cut-off frequency. If f_c is set too high, less signal distortion occurs, but too much noise is allowed to pass. Conversely, if f_c is set too low, the noise is reduced drastically, but at the expense of increased signal distortion.

There are several ways to choose the best cut-off frequency. The first is to carry out a harmonic analysis. By analysing the frequency spectrum and power spectrum, a decision can be made as to how much power to accept and how much to reject. This has been done in gait analysis to find out the frequency distribution for the movement of the lower limb (Winter et al. 1974). However, this information for the upper limb activities is still unknown. Therefore

frequency and power analyses were performed on the coordinate and transducer data of the activities investigated in this study by using the Fast Fourier Transform (FFT) method. A FORTRAN program was written for this purpose, and a FFT subroutine in the NAG package installed in the computer centre VAX machine was used.

As an example, the frequency spectra of displacements of three markers in three axes during lifting a 2kg book to shoulder height are given in Figure 5.1 and the frequency spectra of transducer signals of the driving activity are given in Figure 5.2. The differences of the frequency spectra for the different data sequences can be easily observed from the two figures. It can be seen that the distinct signals disappear over a number of harmonics or continue to higher frequency components. In Figure 5.1(7) and 5.1(8), there is no distinct signal above the 7th harmonic, while this point is the 15th harmonic for the data in Figure 5.1(4), (5) and (6). However, for some data sequences, the signals with small amplitude may last to over the 30th harmonic (Figure 5.1(1), (2), and (3)) and even higher frequency components (Figure 5.2) for transducer signals. This phenomenon can be caused by the alignment of cameras, range of movement of marker in different directions, and signal to noise ratios. As a result, it is difficult to choose a cut-off frequency for a data file or a set of data files without distorting some data sequences or retaining some noise components in the filtered signals. Therefore, it can be concluded that to get the best filtering result, a different cut-off frequency is required for each data sequence. However, to choose an adequate cut-off frequency for each data sequence, it is required to inspect the frequency spectrum of each data sequence which is a tedious task for a large number of tests and markers.

Inspection of the averaged frequency and power spectra or the frequency and power spectra of some representative data sequences is an easier way. This is often accompanied by an illustration of how much signal power was included below the cut-off frequency. Winter et al. (1974) analysed frequency spectra of the vertical displacement of the toe marker for eight subjects and found that 99.7 percent of the power was contained in the 7th harmonic and lower, the corresponding frequency was 6Hz. The question is whether this quantity or other value of power content can be used as a unique criterion when choosing cut-off frequency for the data sequences of markers on other parts of body and other activities. If this criterion exists, then it can be implemented into the computer program for automatically detecting the cut-off frequency for each data sequence.

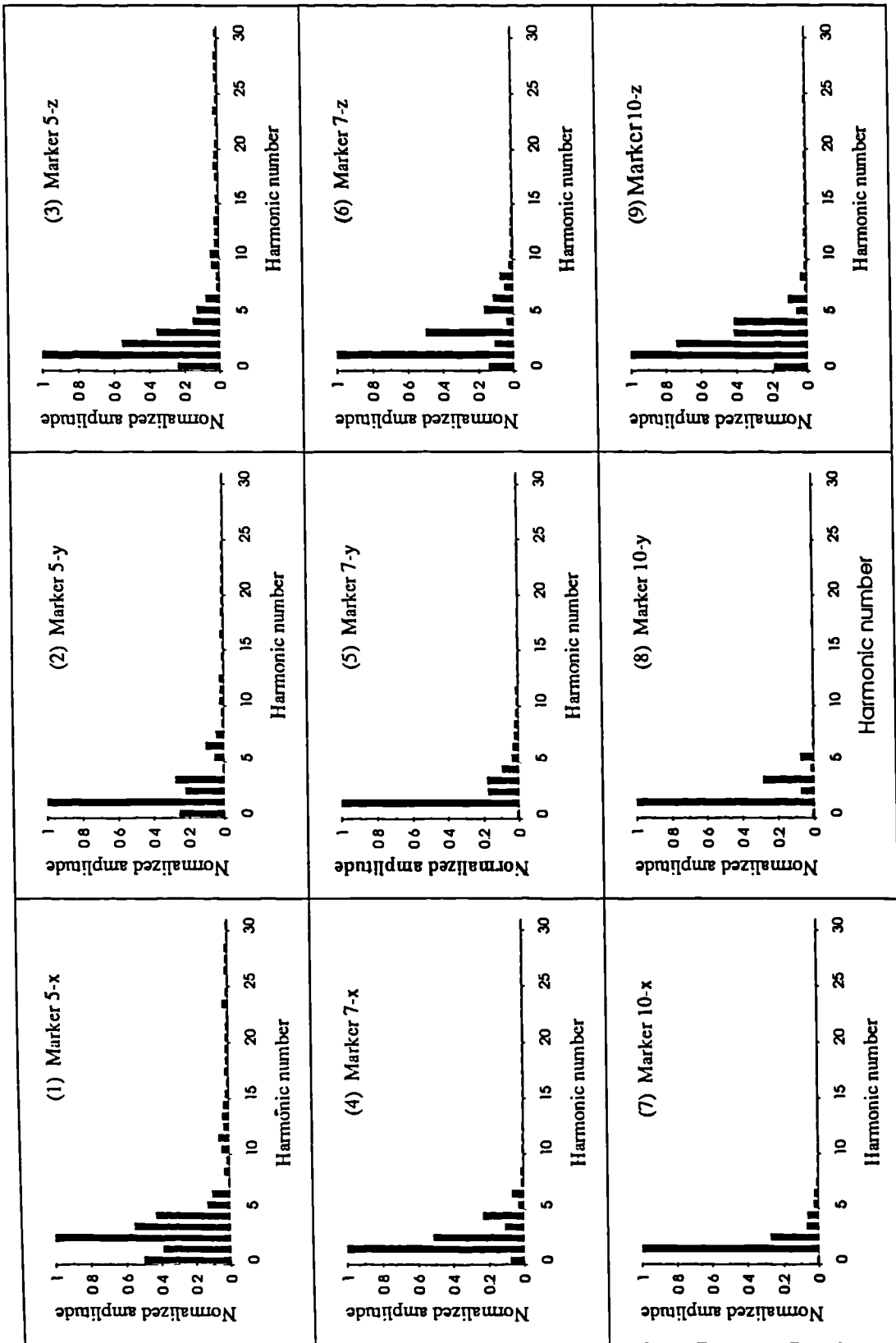


Figure 5.1 Frequency spectra of Vicon data; file yy1007; lifting 2kg to shoulder height

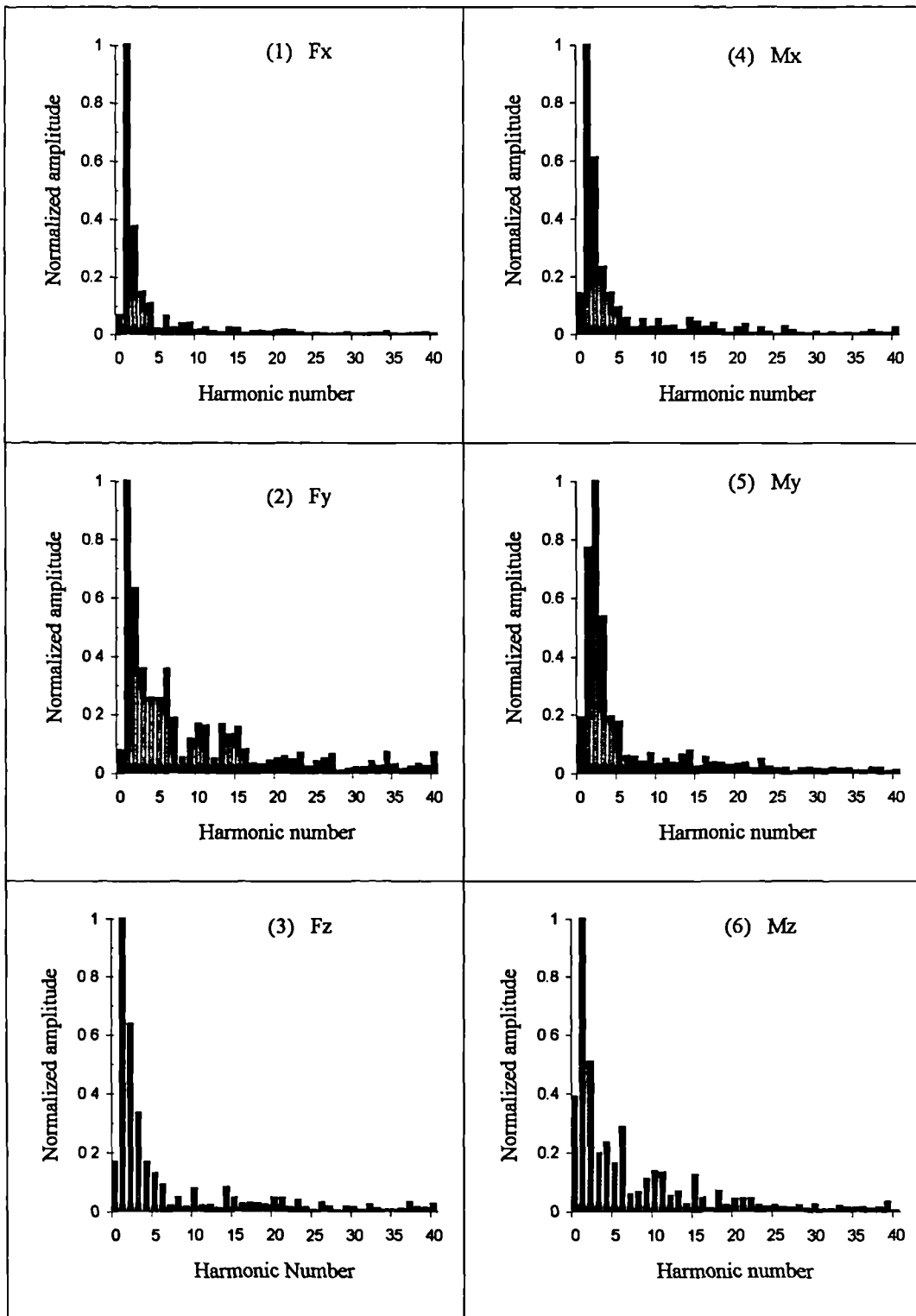


Figure 5.2 Frequency spectra of transducer signals; file: ly2009, Driving

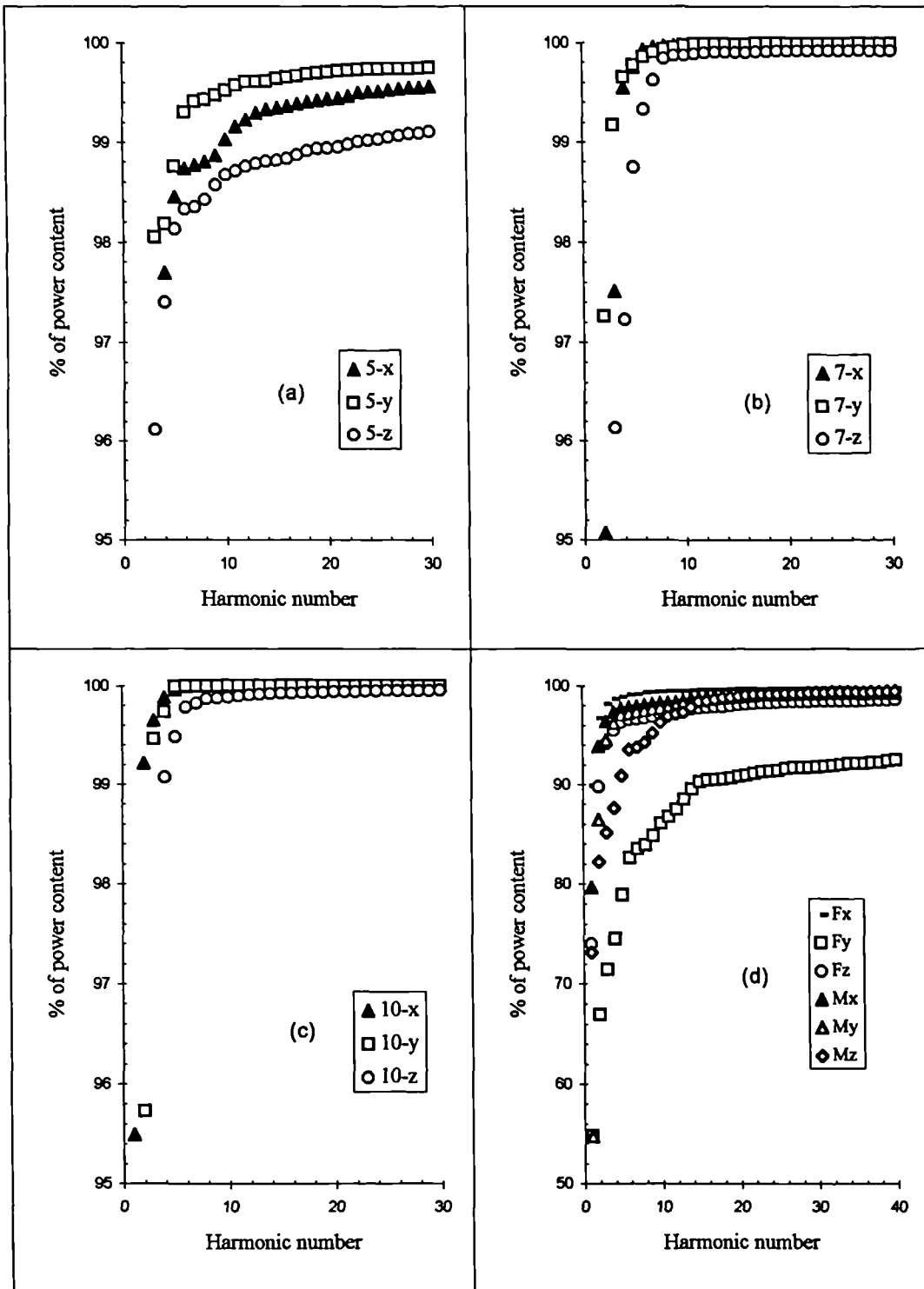


Figure 5.3 Power content below each harmonic frequency; the data are the same as those used in Figure 5.1 and 5.2.

Power contents below each harmonic number were calculated in this study. The power content of the same data in Figure 5.1 and Figure 5.2 are presented in Figure 5.3. It can be found that 99.7% of signal power is contained below the 8th harmonic for some displacement data (Figure 5.3(b) and 5.3(c)) but the power content of the displacement data of 5-z in Figure 5.3(a) is only 99.1% at the 30th harmonic. Although the difference in power content is just about 0.7% for these data, the harmonic number varied greatly by 20 harmonics. The differences are even greater for the transducer signals (Figure 5.3(d)), where 98% of the power is contained below the 8th harmonic for the Fx signal, and only 92.5% of power was contained until the 40th harmonic for the Fy signal.

The differences of power content between each data sequence result from the amount of small magnitude signals which exist in the low and middle frequency range. These small magnitude signals may be either real signals or noise. It is difficult to separate the real signals from noise in this region, because they are often overlapped. Because of this effect, it is evident that the same value of power content, such as 99.7% or 99% of total power below a certain frequency can not be used as a unique criterion for choosing a cut-off frequency for a data file including a number of data sequences or a set of data files. Therefore other methods should be considered.

An optimal method (Wood 1982) uses a residual analysis (Winter 1990) of the difference between filtered and unfiltered signals over a wide range of cut-off frequencies. In this way the characteristics of the filter in the transition region are reflected in the decision process. The residual at any cut-off frequency is calculated as follows for a signal of N sample points in time:

$$R(f_c) = \sqrt{\frac{1}{N} \sum_{i=1}^N (X_i - \hat{X}_i)^2} \quad (5.5)$$

where X_i = raw data at i th sample, \hat{X}_i = filtered data at i th sample.

A theoretical plot of residual versus frequency is given in Figure 5.4. A full description of this plot can be found in Winter's book (Winter 1990). Briefly, the line de represents the best estimate of the noise residual. The intercept oa on the ordinate (at 0Hz) is nothing more than the rms value of the noise because \hat{X}_i for a 0Hz filter is nothing more than the mean of the noise over the N samples. When the data consist of true signal plus noise, the residual will be seen to rise above the straight (dashed) line as the cut-off frequency is reduced. This rise above the dashed line represents the signal distortion that is taking place as the cut-off is

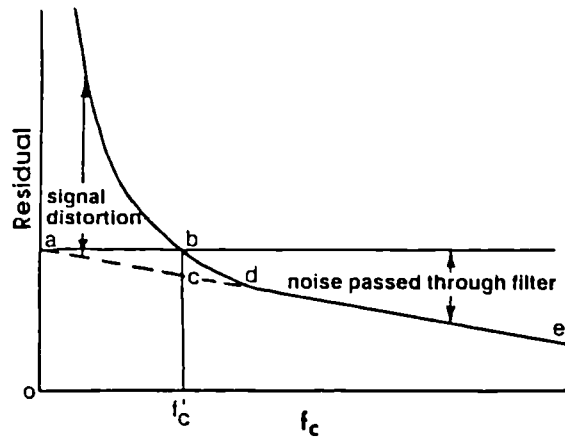


Figure 5.4 Plot of the residual between the filtered and an unfiltered signal as a function of the filter cut-off frequency (Winter 1990).

reduced more and more. The final decision of where the cut-off frequency should be chosen is the compromise of a balance between the amount of signal distortion versus the amount of noise allowed through. This can be done by simply projecting a line horizontally from a to intersect the residual line at b , the corresponding point on the abscissa could then be chosen as the cut-off frequency.

In this study, a FORTRAN subroutine was written for calculating the residuals. For displacement data the residuals were calculated at each of the first 20th harmonics and each of the even harmonics from the 20th to 30th harmonic. For transducer signals the residuals were calculated at each of the first 20 harmonics and each of the even harmonics from the 20th to 40th harmonic. As an example, the residuals of the data in Figure 5.1 and Figure 5.2 are plotted in Figure 5.5. It can be seen that all the residual curves become flat after the 15th harmonic. Therefore the straight line de and intercept point a in Figure 5.4 can be found by regressing the residuals above the 15th harmonics against the corresponding harmonic numbers. This function has been written in the program for automatically selecting the cut-off frequency for each data sequence. A regression subroutine in the NAG package was used to do the regression analysis, and the regression constant (output of regression analysis) was compared with each residual to find out the nearest residual and its corresponding harmonic number. The cut-off frequency was then calculated from the selected harmonic number. After finding the cut-off frequency, the data sequence was then filtered again to get the best filtering result. For the displacement data, the regression analysis was made on the residuals from 15th to 30th harmonics, for the transducer signals the regression were made on the residuals from 20th to 40th harmonics.

As an example, the auto-selected cut-off harmonic number and corresponding cut-off frequency for the sequences in Figure 5.1 and 5.2 are given in Table 5.1. It can be seen that a different cut-off frequency has been selected for each data sequence. Generally, the cut-off frequency for displacement data is about 2.2 Hz, which is in agreement with the fact that the movement of the lifting activity investigated in this study is slower than walking, where the cut-off frequency from 5 to 8 Hz was used (Winter et. al 1974, Schear 1992, Yang 1988, Li 1993). For transducer signals, the auto-selected cut-off frequency is about 3 Hz.

The intercept values oa of the regression line on the ordinate (Figure 5.4) are also given in Table 5.1, which indicate the noise content. It can be seen that the rms. of noise level

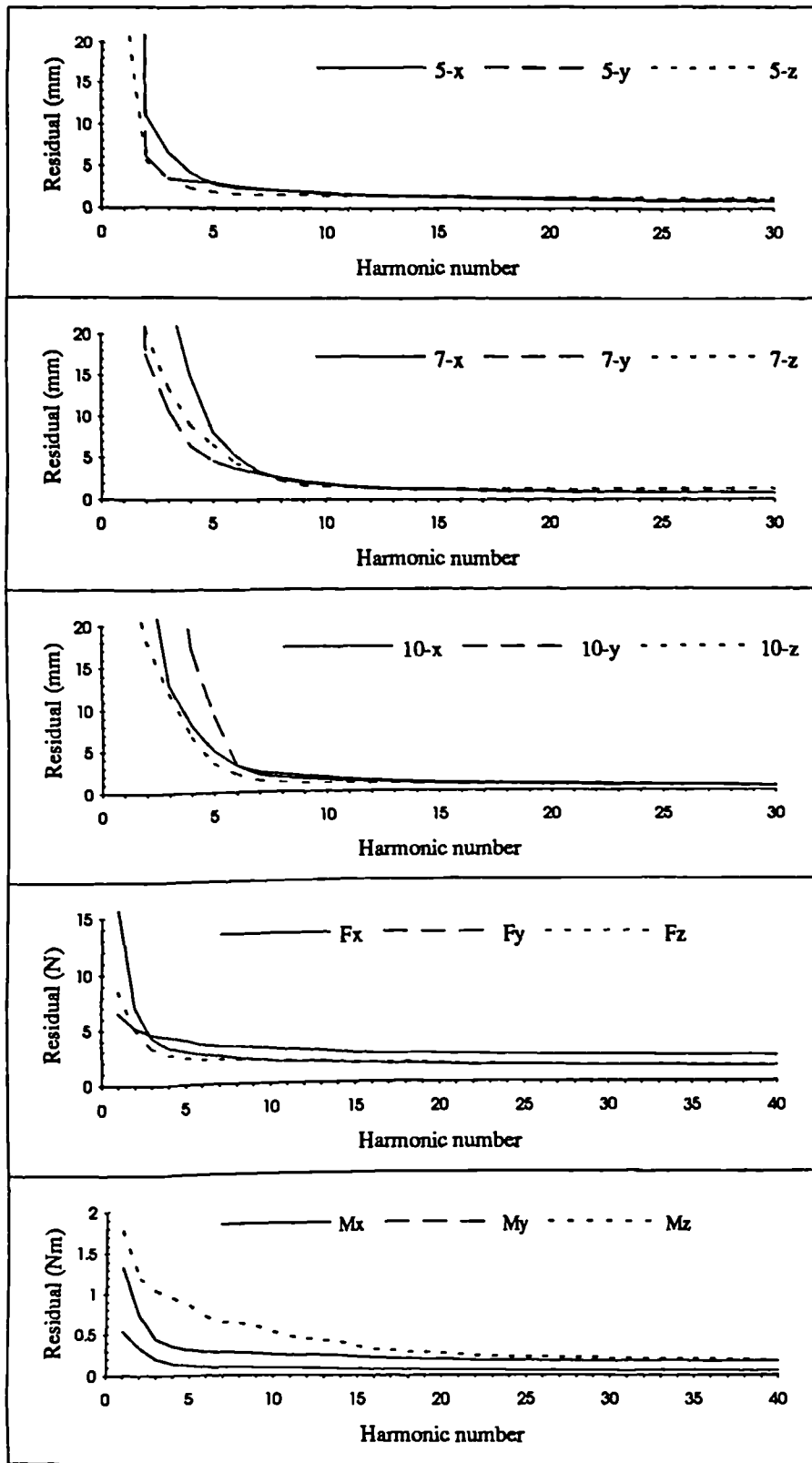


Figure 5.5 Residual analysis of the data in Figure 5.1 and 5.2

is below 1.74 mm for the displacement data. This value is very close to the result of 1.8 mm reported by Winter (1990). In Table 5.1, the noise level for the force and moment signals of the transducer are below 2.71 N and 0.3 Nm, respectively.

It should be noted that a number of data files and data sequences have been investigated and the above results are the representative example for illustrating the effectiveness of the auto selecting cut-off frequency method by using the residual analysis technique. Since the purpose is to select a cut-off frequency for each data sequence, the variation between selected cut-off frequency is evident.

Table 5.1 Auto-selected cut-off frequency for some data sequences

data sequence	harmonic number	cut-off frequency (Hz)	oa (rms)
5-x	11	2.2	1.74 mm
5-y	11	2.2	1.73 mm
5-z	9	1.8	1.59 mm
7-x	11	2.2	1.67 mm
7-y	11	2.2	1.46 mm
7-z	11	2.2	1.46 mm
10-x	12	2.4	1.15 mm
10-y	11	2.2	1.45 mm
10-z	11	2.2	0.96 mm
Fx	16	3.17	1.69 N
Fy	14	2.77	2.71 N
Fz	15	2.98	1.81 N
Mx	16	3.17	0.2 Nm
My	15	2.98	0.07 Nm
Mz	17	3.37	0.3 Nm

5.1.3 Time Normalisation

In this study, up to three tests were analysed for each subject and each activity. Due to the speed variability for each test and each subject, the period (from start to stop) of each test included different numbers of frames of data. As a result, it was not possible to average the analysed results by a simple addition process without distorting the picture. Therefore, the full period of each test was time normalised to a common time base. The full period of each test is defined as from start to stop points in time. The start and stop points were detected in a subroutine of the analysis program when the resultant velocity of a specified marker was zero in the beginning and end regions of each data file. The beginning and end regions were

determined after inspecting the velocity diagrams of the specified marker for a number of data files. Marker 17 on the book and marker 13 (Figure 4.31) on the transducer were used in this process for lifting and other activities, respectively. After defining the period of each test, a three point interpolating method was used to normalise data between start and stop points. The formula of three point interpolating is given as:

$$f(t) = \frac{(t-t_{k+1})(t-t_{k+2})}{(t_k-t_{k+1})(t_k-t_{k+2})}x_k + \frac{(t-t_k)(t-t_{k+2})}{(t_{k+1}-t_k)(t_{k+1}-t_{k+2})}x_{k+1} + \frac{(t-t_k)(t-t_{k+1})}{(t_{k+2}-t_k)(t_{k+2}-t_{k+1})}x_{k+2} \quad (5.6)$$

Where t_k ($k=1, 2, \dots, n$) are the distinct numbers in the time axis, x_k is the function value at the instance t_k , $f(t)$ is the approximation of function value at interpolating point t . In order to present the results in a percentage of a full cycle, first, 101 interpolating points t_i ($i=0,100$) were found by dividing the full period into 100 intervals. Next, the three nearest original time points (t_k, t_{k+1}, t_{k+2}) and corresponding function values (x_k, x_{k+1}, x_{k+2}) to each t_i were located by the program. The normalised function value at each interpolating point t_i could then be calculated from Equation 5.6.

5.2 Determination of Joint Centres and Segment Coordinate Systems

In this section, the determination of joint centre positions and segment coordinate systems from measured landmark positions is described. This information is required for the kinematic and kinetic analysis of the activities investigated in this study.

5.2.1 Joint Centres

In order to calculate the forces and moments at the different joints, the positions of each joint centre, the force transducer centre and the book centre during the activities must be determined. These centres were calculated from the positions of markers affixed at each joint, force transducer and the book. Since the marker positions were measured in the laboratory coordinate system, these centre positions will be described in the laboratory coordinate system.

(1) Shoulder joint centre

A double marker method developed by Nicol (1977) was used to determine the shoulder joint centre. The double marker was placed on the acromial process. Extrapolation of the line

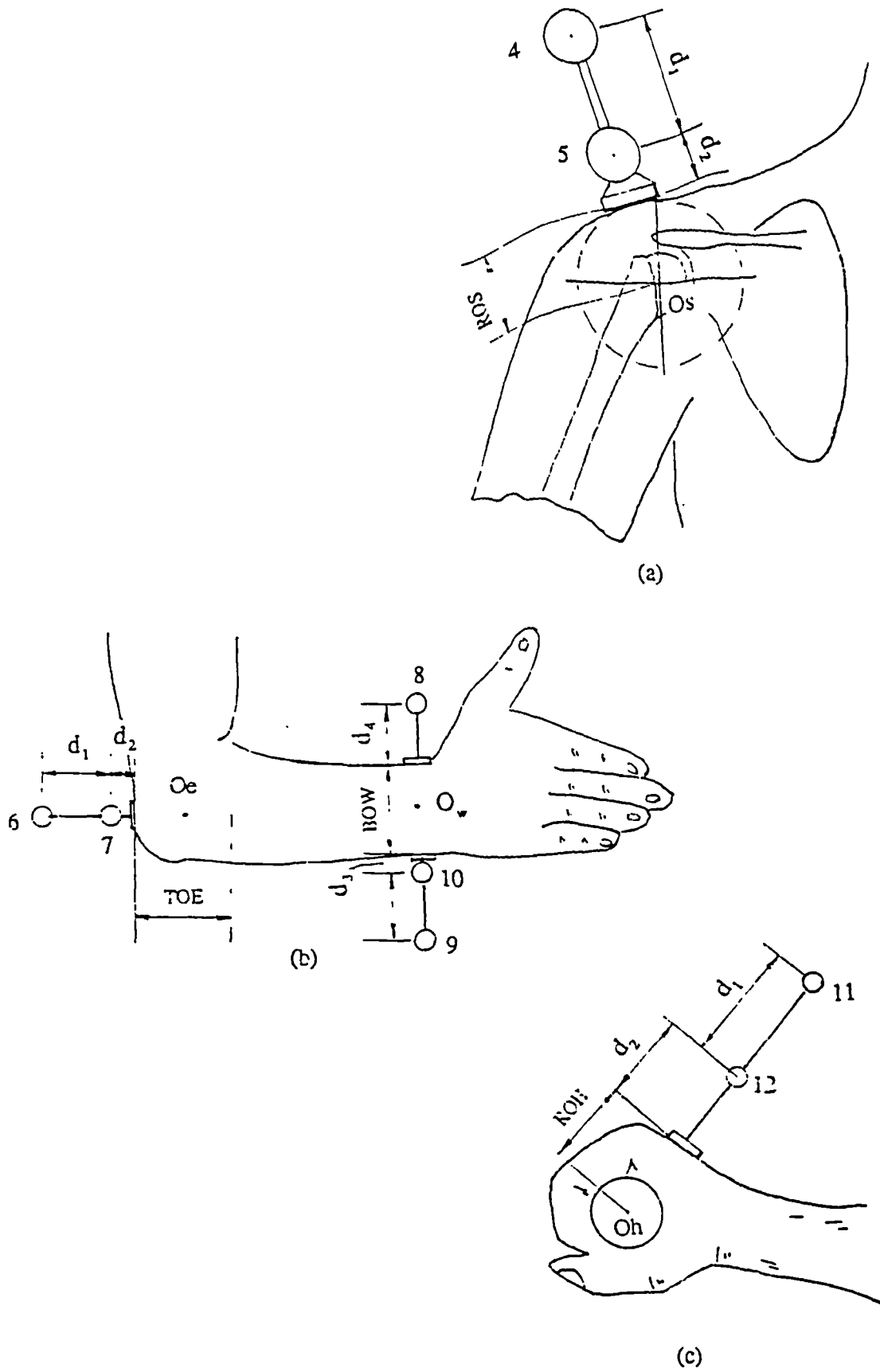


Figure 5.6 Determination of the shoulder, elbow, wrist joints and hand centre

joining the balls gives the position of such anatomical points (Figure 5.6(a)). Assuming zero bone/skin displacement, the shoulder joint centre is calculated as:

$$\begin{aligned} x_{O_s} &= x_4 + (x_5 - x_4) * (d_1 + d_2 + ROS) / d_1 \\ y_{O_s} &= y_4 + (y_5 - y_4) * (d_1 + d_2 + ROS) / d_1 \\ z_{O_s} &= z_4 + (z_5 - z_4) * (d_1 + d_2 + ROS) / d_1 \end{aligned} \quad (5.7)$$

where x_{O_s} , y_{O_s} , z_{O_s} are the three coordinates of shoulder joint centre position in the laboratory coordinate system, x_4 , y_4 , z_4 , x_5 , y_5 , and z_5 are the positions of marker 4 and 5 in the laboratory coordinate system measured by the Vicon system. The dimensions d_1 , d_2 (Figure 5.6(a)) were known from the details of marker construction, the ROS (radius of shoulder ball) was directly measured on the subject (Section 4.4.3).

(2) Elbow joint centre

The method of determining the elbow joint centre is similar to the method for the shoulder joint. A double marker affixed on the elbow joint are marker 6 and 7 (Figure 5.6(b)).

The formulae used for calculating the elbow joint centre can be written as:

$$\begin{aligned} x_{O_e} &= x_6 + (x_7 - x_6) * (d_1 + d_2 + 0.5 * TOE) / d_1 \\ y_{O_e} &= y_6 + (y_7 - y_6) * (d_1 + d_2 + 0.5 * TOE) / d_1 \\ z_{O_e} &= z_6 + (z_7 - z_6) * (d_1 + d_2 + 0.5 * TOE) / d_1 \end{aligned} \quad (5.8)$$

where the x_{O_e} , y_{O_e} , z_{O_e} , are the three coordinates of the elbow joint centre position in the laboratory coordinate system, x_6 , y_6 , z_6 , x_7 , y_7 , and z_7 are the positions of markers 6 and 7. The dimensions d_1 , d_2 and TOE (thickness of elbow) are shown in Figure 5.6(b).

(3) Wrist joint centre

At the beginning, two single markers were placed at the radial and ulnar side of the wrist joint, but in pre-testing they could not be identified for some frames because of the short distance between the two markers and inappropriate camera positions. As a modification, three markers were affixed at the wrist joint (Figure 5.6(b)), a double marker on the ulnar side and one marker on the radial side of the wrist, so that if one marker could not be identified the other two markers could be used. Due to the use of the modified marker system and increased experience in positioning cameras and techniques of identification, all three markers were identified during the pre-processing of data. Therefore only two markers (marker 8 and 10) were used for determining the wrist joint centre. The formulae used for this purpose are given as:

$$\begin{aligned}
x_{Ow} &= x_{10} + (x_8 - x_{10}) * (d_3 + 0.5 * BOW) / (d_3 + d_4 + BOW) \\
y_{Ow} &= y_{10} + (y_8 - y_{10}) * (d_3 + 0.5 * BOW) / (d_3 + d_4 + BOW) \\
z_{Ow} &= z_{10} + (z_8 - z_{10}) * (d_3 + 0.5 * BOW) / (d_3 + d_4 + BOW)
\end{aligned}
\tag{5.9}$$

where x_{Ow} , y_{Ow} , z_{Ow} , are the three coordinates of the wrist joint centre position in the laboratory coordinate system, x_8 , y_8 , z_8 , x_{10} , y_{10} , and z_{10} were the positions of markers 8 and 10. The dimensions d_3 , d_4 and BOW are shown in Figure 5.6(b).

(4) Hand centre

It was defined that the hand centre is located on the longitudinal axis of a 3cm diameter cylindrical bar when the bar is gripped by the hand. A double marker (Marker 11 and 12) was affixed at the middle of the hand back. The hand centre can be found by:

$$\begin{aligned}
x_{Oh} &= x_{11} + (x_{12} - x_{11}) * (d_1 + d_2 + ROH) / d_1 \\
y_{Oh} &= y_{11} + (y_{12} - y_{11}) * (d_1 + d_2 + ROH) / d_1 \\
z_{Oh} &= z_{11} + (z_{12} - z_{11}) * (d_1 + d_2 + ROH) / d_1
\end{aligned}
\tag{5.10}$$

where x_{Oh} , y_{Oh} , z_{Oh} , are the three coordinates of the hand centre position in the laboratory coordinate system, x_{11} , y_{11} , z_{11} , x_{12} , y_{12} , and z_{12} are the positions of markers 11 and 12. The dimensions d_1 , d_2 and ROH are shown in Figure 5.6(c).

(5) The book and force transducer centre

The book centre is defined at its mass centre which is also the origin of the book coordinate system. Its position can be found after the book coordinate system has been established as shown in section 5.2.2(5). The centre of the force transducer is determined following the determination of the force transducer coordinate system in section 5.2.2(6).

5.2.2 Segment Coordinate Systems

In the biomechanical analysis, it is convenient to describe the kinematic and kinetic parameters in the segment reference frame. In this section the trunk, upper arm, forearm, and hand coordinate system are defined according to the anatomical structures of these segments. The book and force transducer coordinate systems are also defined in this section. The dynamic positions and orientations of these coordinate systems are determined by the marker

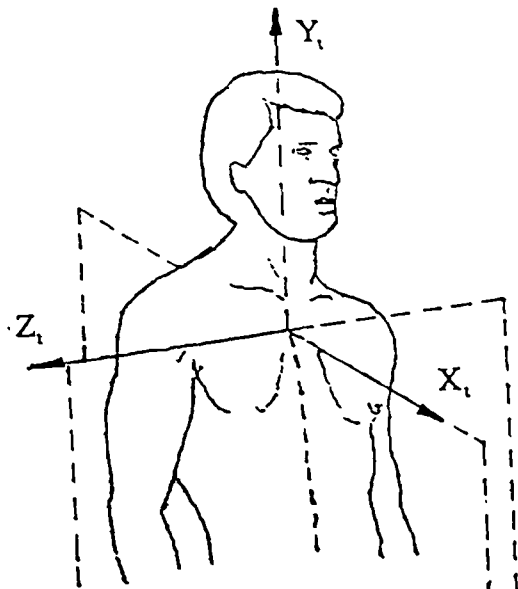


Figure 5.7 Trunk coordinate system

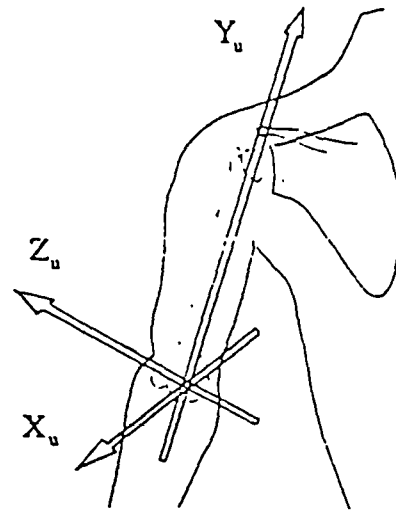


Figure 5.8 Upper arm coordinate system

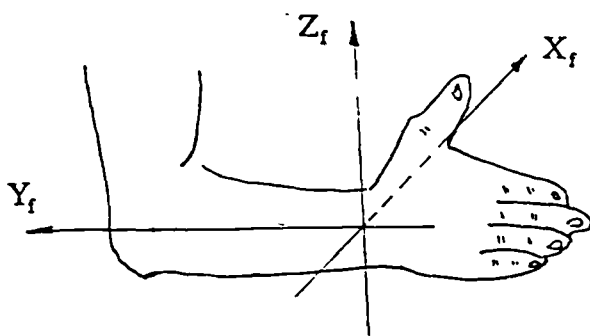


Figure 5.9 Forearm coordinate system

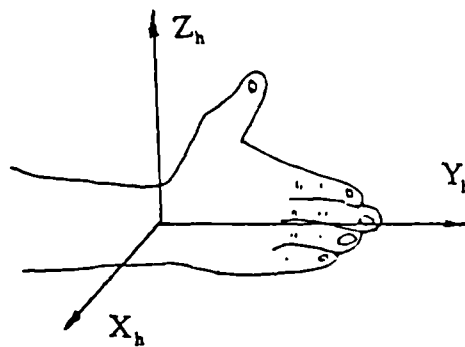


Figure 5.10 Hand coordinate system

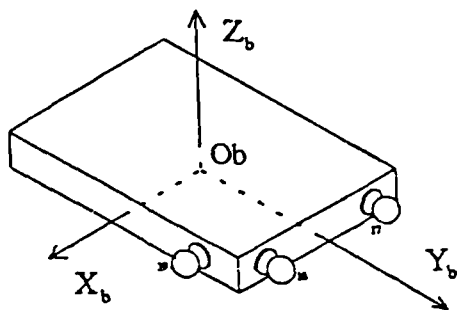


Figure 5.11 Book coordinate system

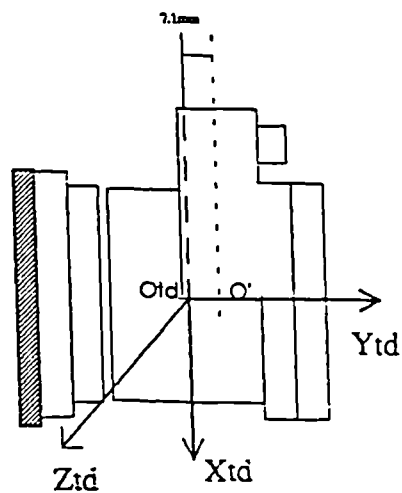


Figure 5.12 Transducer coordinate system

positions and the orientations are expressed as a direction cosine matrix with respect to the laboratory frame of reference.

(1) Trunk

The origin of the trunk coordinate system is located at the manubrium sterni where the double marker (marker 1 and 2 in Figure 4.28) was affixed. This position is determined from the positions of marker 1 and 2 as:

$$\begin{aligned} x_{O_t} &= x_1 + (x_2 - x_1) * (d_1 + d_2) / d_1 \\ y_{O_t} &= y_1 + (y_2 - y_1) * (d_1 + d_2) / d_1 \\ z_{O_t} &= z_1 + (z_2 - z_1) * (d_1 + d_2) / d_1 \end{aligned} \quad (5.11)$$

where x_{O_t} , y_{O_t} , z_{O_t} , are the three coordinates of origin of trunk coordinate system in the laboratory system, x_1 , y_1 , z_1 , x_2 , y_2 , z_2 are the positions of marker 1 and 2. The dimension d_1 is the distance between marker 1 and marker 2, and d_2 is the distance between marker 2 and skin. The orientations of the trunk system are shown in Figure 5.7, and are defined as:

- Xt: directing forward.
- Yt: directing upward.
- Zt: directing from left to right.

The three orthogonal unit vectors of the trunk coordinate system are calculated as:

$$\begin{aligned} \mathbf{e}_1^t &= (\mathbf{R}_1 - \mathbf{R}_2) / |\mathbf{R}_1 - \mathbf{R}_2| \\ \mathbf{e}_2^t &= (\mathbf{R}_2 - \mathbf{R}_3) / |\mathbf{R}_2 - \mathbf{R}_3| \\ \mathbf{e}_3^t &= \mathbf{e}_1^t \times \mathbf{e}_2^t \\ \mathbf{e}_2^t &= \mathbf{e}_3^t \times \mathbf{e}_1^t \end{aligned} \quad (5.12)$$

where

$$\begin{aligned} \mathbf{e}_1^t &= [\mathbf{e}_{11}^t \quad \mathbf{e}_{12}^t \quad \mathbf{e}_{13}^t] \\ \mathbf{e}_2^t &= [\mathbf{e}_{21}^t \quad \mathbf{e}_{22}^t \quad \mathbf{e}_{23}^t] \\ \mathbf{e}_3^t &= [\mathbf{e}_{31}^t \quad \mathbf{e}_{32}^t \quad \mathbf{e}_{33}^t] \end{aligned} \quad (5.13)$$

represent the unit vectors of Xt, Yt, Zt axes of the trunk coordinate system in the laboratory coordinate system, respectively. \mathbf{R}_1 , \mathbf{R}_2 , \mathbf{R}_3 are the position vectors of marker 1, 2 and 3 in the laboratory coordinate system respectively. \mathbf{e}_2^t is the unit vector directed from marker 3 to marker 2. From Equations 5.12 and 5.13 the direction cosine matrix of the trunk coordinate system with respect to the laboratory system is constructed as:

$$\mathbf{D}_{T-L} = \begin{bmatrix} \mathbf{e}_{11}^t & \mathbf{e}_{12}^t & \mathbf{e}_{13}^t \\ \mathbf{e}_{21}^t & \mathbf{e}_{22}^t & \mathbf{e}_{23}^t \\ \mathbf{e}_{31}^t & \mathbf{e}_{32}^t & \mathbf{e}_{33}^t \end{bmatrix} \quad (5.14)$$

(2) Upper arm

The upper arm coordinate system is defined as (Figure 5.8):

Origin: elbow centre

Yu: from elbow centre to shoulder centre.

Zu: from elbow centre to the right, at right angles to Yu and parallel to a line joining the epicondyles.

Xu: from elbow centre forward, at right angles to Yu and Zu.

The three orthogonal unit vectors of the upper arm coordinate system are calculated as:

$$\begin{aligned} \mathbf{e}_2^u &= (\mathbf{R}_{Os} - \mathbf{R}_{Oe}) / |\mathbf{R}_{Os} - \mathbf{R}_{Oe}| \\ \mathbf{e}_1^u &= (\mathbf{R}_7 - \mathbf{R}_6) / |\mathbf{R}_7 - \mathbf{R}_6| \\ \mathbf{e}_3^u &= \mathbf{e}_1^u \times \mathbf{e}_2^u \\ \mathbf{e}_1^u &= \mathbf{e}_2^u \times \mathbf{e}_3^u \end{aligned} \quad (5.15)$$

where

$$\begin{aligned} \mathbf{e}_1^u &= [\mathbf{e}_{11}^u \quad \mathbf{e}_{12}^u \quad \mathbf{e}_{13}^u] \\ \mathbf{e}_2^u &= [\mathbf{e}_{21}^u \quad \mathbf{e}_{22}^u \quad \mathbf{e}_{23}^u] \\ \mathbf{e}_3^u &= [\mathbf{e}_{31}^u \quad \mathbf{e}_{32}^u \quad \mathbf{e}_{33}^u] \end{aligned} \quad (5.16)$$

represent the unit vectors of Xu, Yu, Zu axes of the upper arm coordinate system in the laboratory coordinate system, respectively. \mathbf{R}_{Os} , \mathbf{R}_{Oe} , \mathbf{R}_6 , \mathbf{R}_7 are the position vectors of shoulder centre, elbow centre, marker 6 and 7 in the laboratory coordinate system, respectively. \mathbf{e}_1^u is the unit vector directed from marker 6 to marker 7. From Equations 5.15 and 5.16 the direction cosine matrix of the upper arm coordinate system with respect to the laboratory system is constructed as:

$$\mathbf{D}_{U-L} = \begin{bmatrix} \mathbf{e}_{11}^u & \mathbf{e}_{12}^u & \mathbf{e}_{13}^u \\ \mathbf{e}_{21}^u & \mathbf{e}_{22}^u & \mathbf{e}_{23}^u \\ \mathbf{e}_{31}^u & \mathbf{e}_{32}^u & \mathbf{e}_{33}^u \end{bmatrix} \quad (5.17)$$

(3) Forearm

The forearm coordinate system (Figure 5.9) is defined as:

Origin: wrist centre

Yf: from wrist centre to elbow centre.

Xf: at right angles to Yf, pointing forward.

Zf: at right angles to Yf and Xf.

The three orthogonal unit vectors of the forearm coordinate system are calculated as:

$$\begin{aligned}
 \mathbf{e}_2^f &= (\mathbf{R}_{Oe} - \mathbf{R}_{Ow}) / |\mathbf{R}_{Oe} - \mathbf{R}_{Ow}| \\
 \mathbf{e}_3^f &= (\mathbf{R}_8 - \mathbf{R}_{10}) / |\mathbf{R}_8 - \mathbf{R}_{10}| \\
 \mathbf{e}_1^f &= \mathbf{e}_2^f \times \mathbf{e}_3^f \\
 \mathbf{e}_3^f &= \mathbf{e}_1^f \times \mathbf{e}_2^f
 \end{aligned} \tag{5.18}$$

where

$$\begin{aligned}
 \mathbf{e}_1^f &= [\mathbf{e}_{11}^f \quad \mathbf{e}_{12}^f \quad \mathbf{e}_{13}^f] \\
 \mathbf{e}_2^f &= [\mathbf{e}_{21}^f \quad \mathbf{e}_{22}^f \quad \mathbf{e}_{23}^f] \\
 \mathbf{e}_3^f &= [\mathbf{e}_{31}^f \quad \mathbf{e}_{32}^f \quad \mathbf{e}_{33}^f]
 \end{aligned} \tag{5.19}$$

represent the unit vectors of Xf, Yf, Zf axes of the forearm coordinate system in the laboratory coordinate system, respectively. \mathbf{R}_{Ow} , \mathbf{R}_{Oe} , \mathbf{R}_8 , \mathbf{R}_{10} are the position vectors of wrist centre, elbow centre, marker 8 and 10 in the laboratory coordinate system, respectively. \mathbf{e}_3^f is the unit vector directed from marker 10 to marker 8. From Equations 5.18 and 5.19 the direction cosine matrix of the forearm coordinate system with respect to the laboratory system is constructed as:

$$\mathbf{D}_{F-L} = \begin{bmatrix} \mathbf{e}_{11}^f & \mathbf{e}_{12}^f & \mathbf{e}_{13}^f \\ \mathbf{e}_{21}^f & \mathbf{e}_{22}^f & \mathbf{e}_{23}^f \\ \mathbf{e}_{31}^f & \mathbf{e}_{32}^f & \mathbf{e}_{33}^f \end{bmatrix} \tag{5.20}$$

(4) Hand

The hand coordinate system is defined as (Figure 5.10):

Origin: Wrist centre

Xh: perpendicular to the palm, directed from the palm to the back of the hand.

Zh: in the plane of palm, at right angles to Xh and directed from the small finger to the index finger.

Yh: at right angles to Xh and Zh, directed from the wrist centre to the tip of the

middle finger.

The three orthogonal unit vectors of the hand coordinate system are calculated as:

$$\begin{aligned}
 \mathbf{e}_1^h &= (\mathbf{R}_{11} - \mathbf{R}_{12}) / |\mathbf{R}_{11} - \mathbf{R}_{12}| \\
 \mathbf{e}_{2'}^h &= (\mathbf{R}_{12} - \mathbf{R}_{Ow}) / |\mathbf{R}_{12} - \mathbf{R}_{Ow}| \\
 \mathbf{e}_3^h &= \mathbf{e}_1^h \times \mathbf{e}_{2'}^h \\
 \mathbf{e}_2^h &= \mathbf{e}_3^h \times \mathbf{e}_1^h
 \end{aligned} \tag{5.21}$$

where

$$\begin{aligned}
 \mathbf{e}_1^h &= [\mathbf{e}_{11}^h \quad \mathbf{e}_{12}^h \quad \mathbf{e}_{13}^h] \\
 \mathbf{e}_2^h &= [\mathbf{e}_{21}^h \quad \mathbf{e}_{22}^h \quad \mathbf{e}_{23}^h] \\
 \mathbf{e}_3^h &= [\mathbf{e}_{31}^h \quad \mathbf{e}_{32}^h \quad \mathbf{e}_{33}^h]
 \end{aligned} \tag{5.22}$$

represent the unit vectors of Xh, Yh, Zh axes of the forearm coordinate system in the laboratory coordinate system, respectively. \mathbf{R}_{Ow} , \mathbf{R}_{11} , \mathbf{R}_{12} are the position vectors of wrist centre, marker 11 and 12 in the laboratory coordinate system, respectively. $\mathbf{e}_{2'}^h$ is the unit vector directed from the wrist centre to marker 12. From Equations 5.21 and 5.22 the direction cosine matrix of the hand coordinate system with respect to the laboratory system is constructed as:

$$\mathbf{D}_{H-L} = \begin{bmatrix} \mathbf{e}_{11}^h & \mathbf{e}_{12}^h & \mathbf{e}_{13}^h \\ \mathbf{e}_{21}^h & \mathbf{e}_{22}^h & \mathbf{e}_{23}^h \\ \mathbf{e}_{31}^h & \mathbf{e}_{32}^h & \mathbf{e}_{33}^h \end{bmatrix} \tag{5.23}$$

(5) Book

The origin of the book coordinate system is at the mass centre. The orientation of each axis is shown in Figure 5.11, and three unit vectors are determined as:

$$\begin{aligned}
 \mathbf{e}_1^b &= (\mathbf{R}_{18} - \mathbf{R}_{17}) / |\mathbf{R}_{18} - \mathbf{R}_{17}| \\
 \mathbf{e}_{2'}^b &= (\mathbf{R}_{19} - \mathbf{R}_{18}) / |\mathbf{R}_{19} - \mathbf{R}_{18}| \\
 \mathbf{e}_3^b &= \mathbf{e}_{2'}^b \times \mathbf{e}_1^b \\
 \mathbf{e}_2^b &= \mathbf{e}_3^b \times \mathbf{e}_1^b
 \end{aligned} \tag{5.24}$$

where

$$\begin{aligned}
 \mathbf{e}_1^b &= [\mathbf{e}_{11}^b \quad \mathbf{e}_{12}^b \quad \mathbf{e}_{13}^b] \\
 \mathbf{e}_2^b &= [\mathbf{e}_{21}^b \quad \mathbf{e}_{22}^b \quad \mathbf{e}_{23}^b] \\
 \mathbf{e}_3^b &= [\mathbf{e}_{31}^b \quad \mathbf{e}_{32}^b \quad \mathbf{e}_{33}^b]
 \end{aligned} \tag{5.25}$$

represent the unit vectors of Xb, Yb, Zb axes of the book coordinate system in the laboratory

coordinate system, respectively. \mathbf{R}_{17} , \mathbf{R}_{18} , \mathbf{R}_{19} are the position vectors of marker 17, 18 and 19 in the laboratory coordinate system respectively. \mathbf{e}_2^b is the unit vector directed from marker 18 to marker 19. From Equations 5.24 and 5.25 the direction cosine matrix of the book coordinate system with respect to the laboratory system is constructed as:

$$\mathbf{D}_{B-L} = \begin{bmatrix} \mathbf{e}_{11}^b & \mathbf{e}_{12}^b & \mathbf{e}_{13}^b \\ \mathbf{e}_{21}^b & \mathbf{e}_{22}^b & \mathbf{e}_{23}^b \\ \mathbf{e}_{31}^b & \mathbf{e}_{32}^b & \mathbf{e}_{33}^b \end{bmatrix} \quad (5.26)$$

From the position vectors of marker 17 (or marker 18, 19) in the laboratory and book frame, and the direction cosines given in Equation 5.26, the position of the origin of the book coordinate system in the laboratory coordinate system can be found as:

$$\mathbf{R}_{Ob} = \mathbf{R}_{17} - (\mathbf{D}_{B-L})^T \cdot \mathbf{r}_{17} \quad (5.27)$$

where \mathbf{R}_{Ob} and \mathbf{R}_{17} are the position vectors of the origin of the book coordinate system and marker 17 in the laboratory coordinate system, $(\mathbf{D}_{B-L})^T$ is the transpose of the direction cosine matrix of book frame with respect to laboratory frame, and \mathbf{r}_{17} is the position vector of marker 17 in the book coordinate system which is known from the size of the book and the arrangement of markers.

(6) Force transducer

At the beginning, three markers were placed on the transducer, but it was difficult to fully identify these markers for some frames in the pre-testing. As a modification, four markers were affixed on the force transducer during the tests (Figure 4.31): two markers were on a line parallel to the x-axis and the other two markers were on a line parallel to the z-axis of the transducer. Therefore the orientations of the transducer coordinate system (Figure 5.12) can be determined as:

$$\begin{aligned} \mathbf{e}_1^{td} &= (\mathbf{R}_{14} - \mathbf{R}_{13}) / |\mathbf{R}_{14} - \mathbf{R}_{13}| \\ \mathbf{e}_3^{td} &= (\mathbf{R}_{16} - \mathbf{R}_{15}) / |\mathbf{R}_{16} - \mathbf{R}_{15}| \\ \mathbf{e}_2^{td} &= \mathbf{e}_3^{td} \times \mathbf{e}_1^{td} \end{aligned} \quad (5.28)$$

where

$$\begin{aligned}
\mathbf{e}_1^{td} &= \begin{bmatrix} e_{11}^{td} & e_{12}^{td} & e_{13}^{td} \end{bmatrix} \\
\mathbf{e}_2^{td} &= \begin{bmatrix} e_{21}^{td} & e_{22}^{td} & e_{23}^{td} \end{bmatrix} \\
\mathbf{e}_3^{td} &= \begin{bmatrix} e_{31}^{td} & e_{32}^{td} & e_{33}^{td} \end{bmatrix}
\end{aligned} \tag{5.29}$$

represent the unit vectors of Xtd, Ytd, Ztd axes of the force transducer coordinate system in the laboratory coordinate system, respectively. \mathbf{R}_{13} , \mathbf{R}_{14} , \mathbf{R}_{15} , \mathbf{R}_{16} are the position vectors of marker 13, 14, 15 and 16 in the laboratory coordinate system respectively. From Equations 5.28 and 5.29 the direction cosine matrix of the force transducer coordinate system with respect to the laboratory system is constructed as:

$$\mathbf{D}_{Td-L} = \begin{bmatrix} e_{11}^{td} & e_{12}^{td} & e_{13}^{td} \\ e_{21}^{td} & e_{22}^{td} & e_{23}^{td} \\ e_{31}^{td} & e_{32}^{td} & e_{33}^{td} \end{bmatrix} \tag{5.30}$$

The position of the origin of the transducer coordinate system in the laboratory frame is found as:

$$\mathbf{R}_{Otd} = \mathbf{R}_{14} - (\mathbf{D}_{Td-L})^T \cdot \mathbf{r}_{14} \tag{5.31}$$

where the \mathbf{R}_{Otd} and \mathbf{R}_{14} are the position vectors of the origin of the transducer coordinate system and marker 14 in the laboratory coordinate system, \mathbf{r}_{14} is the position vector of marker 14 with respect to the transducer coordinate system and is known from the construction of the force transducer and positioning of markers. $(\mathbf{D}_{Td-L})^T$ is the transpose of the direction cosine matrix of the transducer frame with respect to the laboratory frame. During positioning of the markers, the lines passing through markers 13, 14 and the line passing through markers 15, 16 were designed to join the Ytd axis of the transducer frame at a point O', 7.1mm from the origin of transducer frame (Figure 5.12).

5.3 Kinematic Analysis

The methods used in the kinematic analysis of arm movements are given in this section, which involve the determination of joint positions in the trunk coordinate system, numerical differentiation of displacement data, calculation of angular velocities and accelerations of limb segments, and the determination of upper arm orientations in the trunk coordinate system and variation of elbow angle.

5.3.1 Joint Motion

Since the activities investigated in this study were all performed with little trunk movement, it is easier to understand the patterns of the arm movements if the joint movements are represented with respect to the trunk frame of reference. Having found the joint centre positions in the laboratory frame of reference and the direction cosine matrix of the trunk frame with respect to the laboratory frame (Section 5.2), the joint centre or other representative marker positions in the trunk system can be calculated as:

$$\mathbf{R}_{JT} = \mathbf{D}_{T-L} (\mathbf{R}_{JL} - \mathbf{R}_{OT}) \quad (5.32)$$

where

\mathbf{D}_{T-L} = direction cosine matrix of trunk system with respect to the laboratory system

\mathbf{R}_{OT} = position vector of the origin of trunk frame in laboratory frame

$\mathbf{R}_{JT}, \mathbf{R}_{JL}$ = position vectors of the joint centres or some representative markers in trunk and laboratory frame, respectively.

The linear velocities and accelerations of these points can be calculated by numerical differentiation techniques described in the following section.

5.3.2 Numerical Differentiation

In this study, a Newtonian numerical differentiator derived from a 4th order polynomial was used for differentiating the coordinate data and obtaining the velocities and accelerations. This method is known as the simplest and has been used by a number of authors (Nicol 1977, Winter 1983, Yang 1988 and Gagnon & Smyth 1991) on digitally filtered data. The formula for calculating the first and second order derivatives of the coordinate data are given as:

$$\dot{x}_i = \frac{1}{12T} (x_{i-2} - 8x_{i-1} + 8x_{i+1} - x_{i+2}) \quad (5.33)$$

$$\ddot{x}_i = \frac{1}{12T^2} (-x_{i-2} + 16x_{i-1} - 30x_i + 16x_{i+1} - x_{i+2}) \quad (5.34)$$

where x_i is the data point under consideration, T is the time interval between two adjacent points. In this study, T=0.02 second corresponds to the sampling frequency of 50 Hz.

5.3.3 Angular Velocity and Acceleration

Except for the linear velocity and acceleration, other important kinematic parameters are the angular velocities and angular accelerations of segments. This information is also

required in the kinetic analysis to calculate the inertial moments of a segment. Having established the direction cosine matrix of each segment, the angular velocity of the segment can be found using Poisson's equation described in Equation 3.12 as:

$$(\dot{\mathbf{D}}_{S-L})(\mathbf{D}_{S-L})^{-1} = - \begin{bmatrix} 0 & -\omega_z & \omega_y \\ \omega_z & 0 & -\omega_x \\ -\omega_y & \omega_x & 0 \end{bmatrix} \quad (5.35)$$

where \mathbf{D}_{S-L} is the direction cosine matrix of the segment frame of reference with respect to laboratory frame of reference, and $\dot{\mathbf{D}}_{S-L}$ is its time derivative, ω_i ($i= x, y, z$) are the angular velocities of the segment with respect to the laboratory frame are expressed in the segment frame, i.e. the x, y, z are the axes of the segment coordinate system. The Equation 5.35 can be rewritten as:

$$\begin{bmatrix} \dot{d}_{11} & \dot{d}_{12} & \dot{d}_{13} \\ \dot{d}_{21} & \dot{d}_{22} & \dot{d}_{23} \\ \dot{d}_{31} & \dot{d}_{32} & \dot{d}_{33} \end{bmatrix} \begin{bmatrix} d_{11} & d_{21} & d_{31} \\ d_{12} & d_{22} & d_{32} \\ d_{13} & d_{23} & d_{33} \end{bmatrix} = - \begin{bmatrix} 0 & -\omega_z & \omega_y \\ \omega_z & 0 & -\omega_x \\ -\omega_y & \omega_x & 0 \end{bmatrix} \quad (5.36)$$

Therefore, explicitly, we have

$$\begin{aligned} \omega_x &= -(d_{21}\dot{d}_{31} + d_{22}\dot{d}_{32} + d_{23}\dot{d}_{33}) \\ \omega_y &= -(d_{31}\dot{d}_{11} + d_{32}\dot{d}_{12} + d_{33}\dot{d}_{13}) \\ \omega_z &= -(d_{11}\dot{d}_{21} + d_{12}\dot{d}_{22} + d_{13}\dot{d}_{23}) \end{aligned} \quad (5.37)$$

The angular acceleration of the segment with respect to the laboratory frame of reference can then be obtained using the numerical differentiator in Equation 5.33 as:

$$\begin{aligned} \varepsilon_x &= d\omega_x / dt \\ \varepsilon_y &= d\omega_y / dt \\ \varepsilon_z &= d\omega_z / dt \end{aligned} \quad (5.38)$$

where, the angular accelerations are expressed in the segment coordinate system.

5.3.4 Angular Orientation of the Upper Arm and Elbow Angle

The orientation of the upper arm in the trunk frame are represented by the line connecting the shoulder joint and elbow joint (y -axis of upper arm coordinate system). The three angles about each axis of the trunk frame are calculated as:

$$\begin{aligned}
\alpha_{xt} &= \arctan\left(\frac{y_{et} - y_{st}}{z_{et} - z_{st}}\right) \\
\alpha_{yt} &= \arctan\left(\frac{x_{et} - x_{st}}{z_{et} - z_{st}}\right) \\
\alpha_{zt} &= \arctan\left(\frac{y_{et} - y_{st}}{x_{et} - x_{st}}\right)
\end{aligned} \tag{5.39}$$

where α_{xt} , α_{yt} , α_{zt} = upper arm angles in the trunk frame.

x_{et} , y_{et} , z_{et} = coordinates of the elbow joint in the trunk frame.

x_{st} , y_{st} , z_{st} = coordinates of the shoulder joint in the trunk frame.

For the forearm, only the flexion angle relative to the upper arm is calculated. This angle is called the elbow angle and is defined as the angle between the two y-axes of the upper arm and forearm coordinate systems, and is calculated as:

$$\alpha_{f-u} = 180^\circ - \arccos(\mathbf{e}_2^f \cdot \mathbf{e}_2^u) \tag{5.40}$$

5.4 Kinetic Analysis

The purpose of the kinetic analysis is to find the intersegment forces and moments acting on the upper limb joints during the activities investigated in this study. The forces and moments arise from three sources, gravitational effects, inertial effects, and hand loads measured by the force transducer. The determination of gravitational forces, the inertial forces and moments, and the forces and moments measured on force transducer are given in three separate parts. The calculations of joint intersegment forces and moments from the three effects are presented in the final part of this section.

5.4.1 Gravitational Force

The gravitational force of a segment is due to the weight of the segment and acts downward (along the -y direction of the laboratory reference frame) on the centre of gravity (mass centre) of the segment. Since the joint centre location is described in the laboratory coordinate system (section 5.2.1), the calculation of joint intersegment forces and moments due to gravity requires that the gravitational force and mass centre of the segment are described in the laboratory reference frame. The mass of each segment is calculated as a ratio of the body weight based on the investigation of Drillis & Contini (1966), which is given in Table 2.6. The centre of gravity of a segment is assumed to be fixed on the segment, and its

location relative to the origin of the segment coordinate system is determined as a ratio of segment length given by Drillis and Contini (1966). These ratios are shown in Table 2.7. Therefore the centre of gravity can be described by a constant vector \mathbf{r}_c in the segment coordinate system. Knowing the location of the origin of the segment coordinate system and the direction cosine matrix of the segment, the location of centre of gravity of the segment in laboratory frame can be found as:

$$\mathbf{R}_{\text{COG}} = \mathbf{R}_{s_0} + \mathbf{D}_{s-L}^T \mathbf{r}_{\text{COG}} \quad (5.41)$$

where:

\mathbf{R}_{COG} is the position vector of the centre of gravity of the segment in the laboratory frame.

\mathbf{R}_{s_0} is the position vector of the origin of the segment frame in the laboratory frame.

\mathbf{D}_{s-L}^T is the transpose of the direction cosine matrix of the segment frame with respect to the laboratory frame.

Therefore the gravitational force can be applied at the centre of gravity of the segment in the laboratory reference frame as:

$$\mathbf{F}_y = (0, -mg, 0) \quad (5.42)$$

and where the m is the mass of segment, g is the acceleration due to gravity.

5.4.2 Inertial Forces and Moments

The inertial force of a segment is related to the linear acceleration of the segment. It may be considered to act at the mass centre (centre of gravity) of the segment, and is computed as the product of the mass of the segment and the linear acceleration of the mass. By D'Alembert's principle, this action is along the direction opposite to the linear acceleration of the mass centre and can be expressed as:

$$\mathbf{F}_{\text{inertial}} = -m \mathbf{a}_{\text{COG}} \quad (5.43)$$

where, m is the mass of segment, \mathbf{a}_{COG} is the linear acceleration vector of the mass centre. Having found the mass centre position in the laboratory frame (Equation 5.41), the acceleration can be obtained using the numerical differentiator in Equation 5.34 as:

$$\mathbf{a}_{\text{COG}} = d^2 \mathbf{R}_{\text{COG}} / dt^2 \quad (5.44)$$

Since the linear acceleration is derived in the laboratory coordinate system, the inertial force (Equation 5.43) is also expressed in the laboratory frame.

The inertial moments of the segment are related with the moments of inertia and the angular velocities and accelerations of the segment. For each segment, there are three principal moments of inertia corresponding to the three mutually orthogonal coordinate axes known as the principal axes. As mentioned in Section 5.2.2, the axes of each segment coordinate system were defined to coincide with their principal axes. The moments of inertia of each segment are calculated using the non-linear equations derived by Yeadon & Morlock (1989). These equations have been detailed in Section 2.3.4 (Equations 2.2 and 2.3). Having found the moments of inertia and angular velocities and angular accelerations (Section 5.3.3), the inertial moments of the segment can be calculated by the D'Alembert's principle as:

$$\begin{aligned} M_{ix}^s &= -[I_x \dot{\omega}_x + (I_z - I_y) \omega_y \omega_z] \\ M_{iy}^s &= -[I_y \dot{\omega}_y + (I_x - I_z) \omega_x \omega_z] \\ M_{iz}^s &= -[I_z \dot{\omega}_z + (I_y - I_x) \omega_y \omega_x] \end{aligned} \quad (5.45)$$

where M_{ix}^s , M_{iy}^s , M_{iz}^s are the three components of inertial moment expressed in the segment coordinate system; I_x , I_y , I_z are the three principal moments of inertia corresponding to the three principal axes, x, y, z, of the segment coordinate system; ω_x , ω_y , ω_z are the three components of angular velocity of the segment derived by Equation 5.37; $\dot{\omega}_x$, $\dot{\omega}_y$, $\dot{\omega}_z$ are the three components of angular acceleration of the segment derived by Equation 5.38.

The calculation of inter-segment forces and moments requires that these inertial moments are expressed in the laboratory system. Therefore the inertial moments calculated by Equation 5.45 are transformed to the laboratory coordinate system using the direction cosine matrix of the segment as:

$$\mathbf{M}_i^L = \mathbf{D}_{S-L}^{-1} \mathbf{M}_i^S \quad (5.46)$$

where $\mathbf{M}_i^L = [M_{ix}^L \quad M_{iy}^L \quad M_{iz}^L]^T$ is the inertial moment vector expressed in the laboratory frame of reference; $\mathbf{M}_i^S = [M_{ix}^S \quad M_{iy}^S \quad M_{iz}^S]^T$ is the inertial moment vector expressed in the segment frame of reference; \mathbf{D}_{S-L}^{-1} is the inverse of direction cosine matrix of the segment with respect to the laboratory frame of reference.

5.4.3 Forces and Moments Measured by Transducer

The output of transducer signals measured through the Vicon system were given as a number (1 - 4098) in the A-D converter unit. Therefore to convert the A-D units to the equivalent voltage signal, all analogue data were reduced by 2048 (zero signal), and then

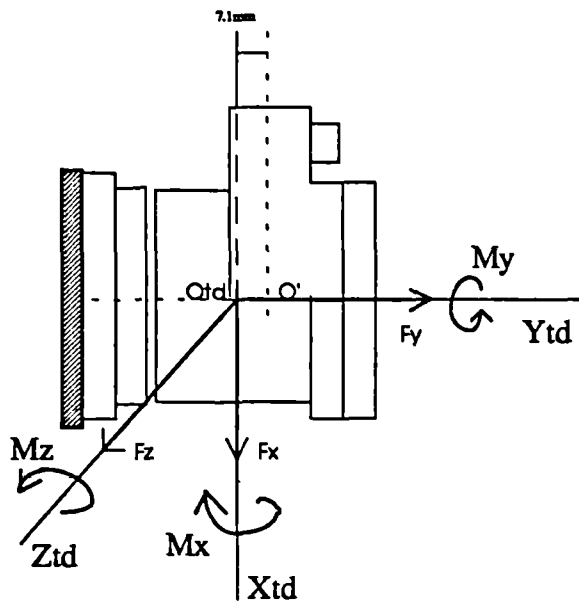


Figure 5.13 Forces and moments on the transducer

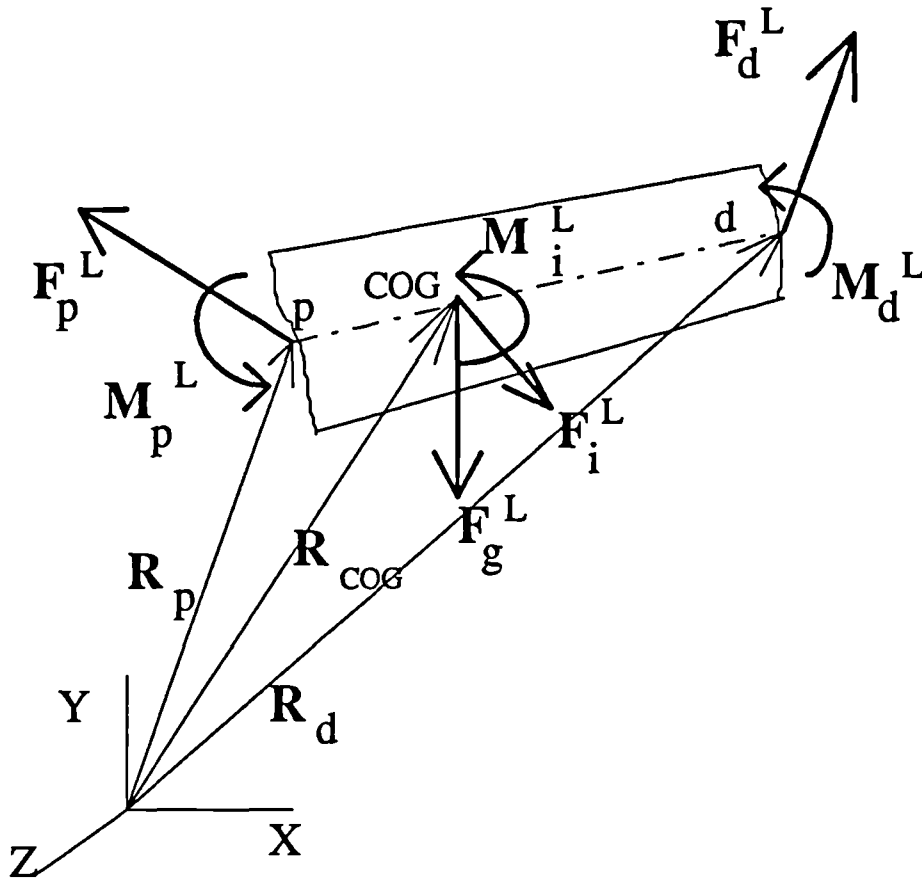


Figure 5.14 A standard link-segment model

XYZ: the laboratory coordinate system; p: the proximal joint; d: the distal joint; COG: centre of gravity of the segment; R_p , R_d , R_{COG} are the positional vectors.

multiplied by a factor p ($p=4.88$ mv/A-D converter unit) which is related to the set-up of the analogue gain during the data acquisition. To find the force and moment information, the voltage signals are multiplied by the calibration matrix of the force transducer obtained in section 4.4.2. The calculation is expressed as:

$$\begin{bmatrix} F_{Tdx}^{Td} \\ F_{Tdy}^{Td} \\ F_{Tdz}^{Td} \\ M_{Tdx}^{Td} \\ M_{Tdy}^{Td} \\ M_{Tdz}^{Td} \end{bmatrix} = p[C] \begin{bmatrix} S_{Fx} \\ S_{Fy} \\ S_{Fz} \\ S_{Mx} \\ S_{My} \\ S_{Mz} \end{bmatrix} \quad (5.47)$$

where $S_{Fx} \dots M_{Mz}$ are the signals of six transducer channels in the A-D converter unit after subtracting a number of 2048, $[C]$ is the calibration matrix of the force the transducer shown in Table 4.3, p is the factor mentioned above. F_{Tdx}^{Td} , F_{Tdy}^{Td} , F_{Tdz}^{Td} and M_{Tdx}^{Td} , M_{Tdy}^{Td} , M_{Tdz}^{Td} are the three force and moment components corresponding to the three axes of the transducer frame of reference, respectively. The forces and moments in Equation 5.47 are in units of N and Nm respectively, and they act at the force transducer centre. The directions of the forces and moments are shown in Figure 5.13. For the requirement of calculating the joint intersegment forces and moments, the forces and moments in Equation 5.47 are transformed to the laboratory frame of reference using the direction cosine matrix of the transducer frame as:

$$\begin{bmatrix} F_{Tdx}^L \\ F_{Tdy}^L \\ F_{Tdz}^L \end{bmatrix} = \mathbf{D}_{Td-L}^{-1} \begin{bmatrix} F_{Tdx}^{Td} \\ F_{Tdy}^{Td} \\ F_{Tdz}^{Td} \end{bmatrix} \quad (5.48)$$

and

$$\begin{bmatrix} M_{Tdx}^L \\ M_{Tdy}^L \\ M_{Tdz}^L \end{bmatrix} = \mathbf{D}_{Td-L}^{-1} \begin{bmatrix} M_{Tdx}^{Td} \\ M_{Tdy}^{Td} \\ M_{Tdz}^{Td} \end{bmatrix} \quad (5.49)$$

where the F_{Tdx}^L , F_{Tdy}^L , F_{Tdz}^L and M_{Tdx}^L , M_{Tdy}^L , M_{Tdz}^L are the forces and moments at the transducer centre expressed in the laboratory frame of reference, \mathbf{D}_{Td-L}^{-1} is the inverse of the direction cosine matrix of the transducer frame with respect to the laboratory frame.

5.4.4 Joint Intersegment Forces and Moments

Having expressed the gravitational forces, inertial forces and moments and transducer forces and moments in the laboratory coordinate system the joint intersegment forces and moments can be found using the standard link-segment model as shown in Figure 5.14. According to D'Alembert's principle, the equilibrium equation of the forces is written as:

$$\mathbf{F}_d^L + \mathbf{F}_p^L + \mathbf{F}_i^L + \mathbf{F}_g^L = 0 \quad (5.50)$$

where, \mathbf{F}_p^L = intersegment force vector acting at the proximal joint is resolved for.

\mathbf{F}_i^L = inertial force vector acting at the centre of gravity (Equation 5.43).

\mathbf{F}_d^L = intersegment force vector acting at the distal joint (known).

\mathbf{F}_g^L = gravitational force vector acting at the mass centre of the segment.

If the segment under consideration is the hand, \mathbf{F}_d^L denotes the force vector acting at the centre of the force transducer. Therefore the force acting at the proximal joint can be found as

$$\mathbf{F}_p^L = -\mathbf{F}_d^L - \mathbf{F}_i^L - \mathbf{F}_g^L \quad (5.51)$$

Similarly, the equilibrium equation of moments about the proximal joint for the system can be written as:

$$\mathbf{M}_d^L + \mathbf{M}_p^L + \mathbf{M}_i^L + (\mathbf{R}_d - \mathbf{R}_p) \times \mathbf{F}_d^L + (\mathbf{R}_{COG} - \mathbf{R}_p) \times (\mathbf{F}_i^L - \mathbf{F}_g^L) = 0 \quad (5.52)$$

where, \mathbf{M}_p^L = intersegment moment vector acting at the proximal joint.

\mathbf{M}_i^L = inertial moment vector acting at the centre of gravity (Equation 5.43).

\mathbf{M}_d^L = intersegment moment vector acting at the distal joint (known).

Therefore the intersegment moment at the proximal joint is

$$\mathbf{M}_p^L = -\mathbf{M}_d^L - \mathbf{M}_i^L - (\mathbf{R}_d - \mathbf{R}_p) \times \mathbf{F}_d^L - (\mathbf{R}_{COG} - \mathbf{R}_p) \times (\mathbf{F}_i^L - \mathbf{F}_g^L) \quad (5.53)$$

For the lifting activities, only gravitational forces and inertial forces and moments are considered, for other activities the gravitational forces, the inertial forces and moments, and the forces and moments measured on the transducer are all considered in the above calculations. The inter-segment loads obtained above are with respect to the laboratory frame of reference. To refer them to the segment frame of reference, the direction cosine matrix is used:

$$\begin{aligned} \mathbf{F}_p^S &= \mathbf{D}_{S-L} \mathbf{F}_p^L \\ \mathbf{M}_p^S &= \mathbf{D}_{S-L} \mathbf{M}_p^L \end{aligned} \quad (5.54)$$

The results of the above analysis are presented in the next chapter.

5.5 Determination of Axial Rotation Angles of Limb Segments

One of the frequently discussed problems in biomechanics of human movement analysis is how to properly describe angular rotation of a limb segment. A number of methods have been proposed and used for this purpose which have been reviewed in detail in Chapter Three. Briefly, previous methods can be divided into two categories, sequence dependent methods and sequence independent methods. The Euler/Cardan angles belong to the first category; this method describes the rotation of the limb segment from one attitude to another by three ordered rotations about three orthogonal axes of the body fixed coordinate system. The problems of this method can be summarised as follows. First it is difficult to imagine how the rotations of the limb segment follow the sequences defined by Euler/Cardan angles in real activities. Second, different rotation angles can be obtained by changing the sequence of rotation, especially for finite rotations. Third there is no confident evidence to prove that the limb segment rotates in a way described by the sequenced rotations and there is lack of evidence to show which sequence is the best to describe the rotations of the limb segment, because rotation patterns of the limb segment may vary with various activities.

The instantaneous screw or helical axis (Kinzel et. al 1972) is a sequence independent method. It describes the displacement and rotation of a limb segment by using an instantaneous axis in a three-dimensional reference frame. The movement of the segment from one attitude to another can be expressed as a rotation about and a translation along an instantaneous axis in a three-dimensional reference frame. In general, the direction of the instantaneous helical axis varies with time and therefore it is difficult to visualise it in three-dimensional space. Perhaps the major problem of this method is that 'this description of motion is not readily understood by clinicians' (Grood and Suntay 1983) because it lacks proper physical interpretations.

Because neither of above methods can produce fully satisfactory information on the rotations of the limb segment, especially for axial rotation which is clinically described as the rotation about longitudinal axis of the limb segment, to search for a new method is of interest to most biomechanists. Chao (1980) and Grood & Suntay (1983) proposed a coordinate system with three non orthogonal unit base vectors in which two axes are embedded in two adjacent segments and the third axis is not fixed to any segment, the so called *floating axis*. This coordinate system has been used in the study of knee joint kinematics (Grood and Suntay

1983), where nonsequenced rotations of the knee joint were described in the clinical convention as flexion-extension, adduction-abduction and internal-external rotations. However the movement information of two segments must be known in the use of this method. The usefulness of this method in complex joints such as the shoulder joint has been questioned (Woltering 1994, Miyazaki & Ishida 1991).

Miyazaki & Ishida (1991) proposed a mathematical definition of axial rotation, in which the axial rotation was calculated by integration of the component of the angular velocity vector projected onto the long axis of the body segment, but this method is Euler angles based.

In clinical practice, the movements of limb segments are always described as flexion-extension, adduction-abduction and internal-external rotations, in which the flexion-extension, adduction-abduction can occur in two different planes (Kapandji 1970, Shipman et. al 1985). Physicians and physical therapists also prefer to identify the segment in terms of the angular formula of the long axis of the segment in three orthogonal planes, such as sagittal, coronal and transverse planes of a reference frame, such as the trunk coordinate system (Braune & Fischer 1987). In this way, the position of the long axis of the segment can be fully determined by two such angles, unfortunately leaving the axial rotation angle unknown. In this section a new method is developed to determine the axial rotation angle from the known positional information of the long axis and a known direction cosine matrix.

Method

In rigid body dynamics, the motion of a body can be described by two simple motions, translation and rotation. In this section, the three-dimensional movement of a limb segment is considered to be composed as a translation of and a rotation about its proximal joint. Because the translation and rotation can be treated separately (Goldstein 1960), only rotation is considered in the following and it is assumed that the translations of the proximal joint of the segment are known.

Instead of describing the movement of the limb segment from one attitude to another by a three-step rotation (Euler/Cardan angles), a one-step rotation (screw/helical axis), or a non-step rotation (Floating axis method), this method assumes that the movement of the limb segment from one attitude to another can be described by a two-step rotation, one is the rotation of the long axis of the limb segment about a specific axis passing through the

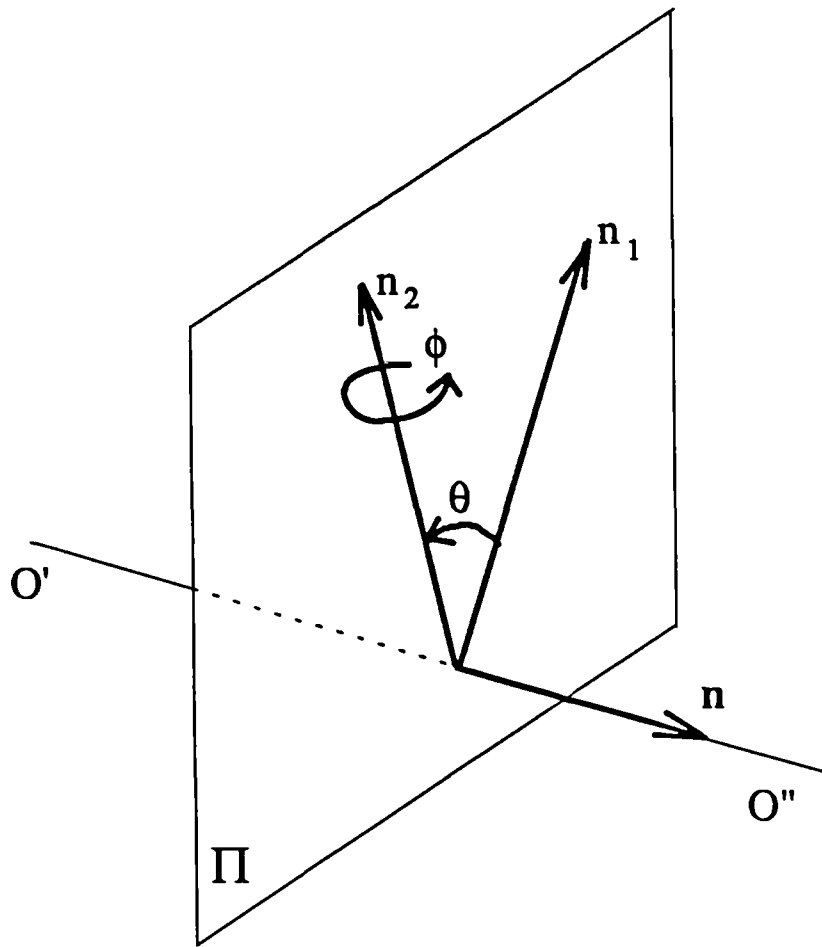


Figure 5.15 The rotation of a limb segment can be described as a long axis rotation θ about axis $O'O''$ and an axial rotation ϕ about the long axis of limb segment. Where \mathbf{n}_1 and \mathbf{n}_2 are the unit vectors of the long axis of limb segment before and after the long axis rotation, \mathbf{n} is the unit vector of rotation axis $O'O''$.

proximal joint and perpendicular to the long axis of the limb segment, and the other is an axial rotation about the long axis (Figure 5.15). The direction of the rotation axis of the first rotation may vary in three-dimensional space relative to the long axis rotation from time to time. If the second rotation (axial rotation) is zero, the rotation axis of the long axis rotation becomes the instantaneous rotation axis of the limb segment. In the general case, the second rotation is not zero and the first rotation axis is not the real instantaneous axis. For this reason and convenience of illustration the rotation axis of the long axis rotation is called the semi-instantaneous rotation axis in the following.

In clinical or physical descriptions of limb segment rotation, the flexion/extension and adduction/abduction are originally used to describe the rotation of the long axis of the limb segment in specified planes such as flexion/extension in the sagittal plane and abduction/adduction in the frontal or horizontal plane (Kirby & Roberts 1985). Therefore they are two dimensional definitions and are referred to as primary rotations (Kapandji 1970). For three-dimensional rotation of a limb segment, the position of the long axis of the segment can be fully determined by a set of flexion/extension and adduction/abduction angles. However it is necessary to illustrate that the flexion/extension and adduction/abduction angles used in the three-dimensional case must not be misunderstood as rotation angles because these words are defined as planar rotations, and can only be used to determine the position of the long axis of the limb segment in a three-dimensional space or describe an equivalent three-dimensional rotation. Although the three-dimensional rotation of the long axis of the limb segment from one position to another can be simulated by two primary rotations such as a flexion/extension followed by an adduction/abduction or reverse, it is not the real movement route performed by the long axis of the limb segment. In fact, in real activities, the rotation of the long axis of the limb segment goes a direct route from one position to another which can be stated in other words as that the long axis of the limb segment rotates about a semi-instantaneous rotation axis passing through the proximal joint of the limb segment from one position to another in the physiological reachable range. In contrast with this, if the rotation of the long axis of the limb segment did not go a direct way from one position to another, it may imply some functional abnormalities.

Combining the one-step rotation of the long axis of the limb segment and the axial rotation about the long axis, the three-dimensional rotation of the limb segment from one

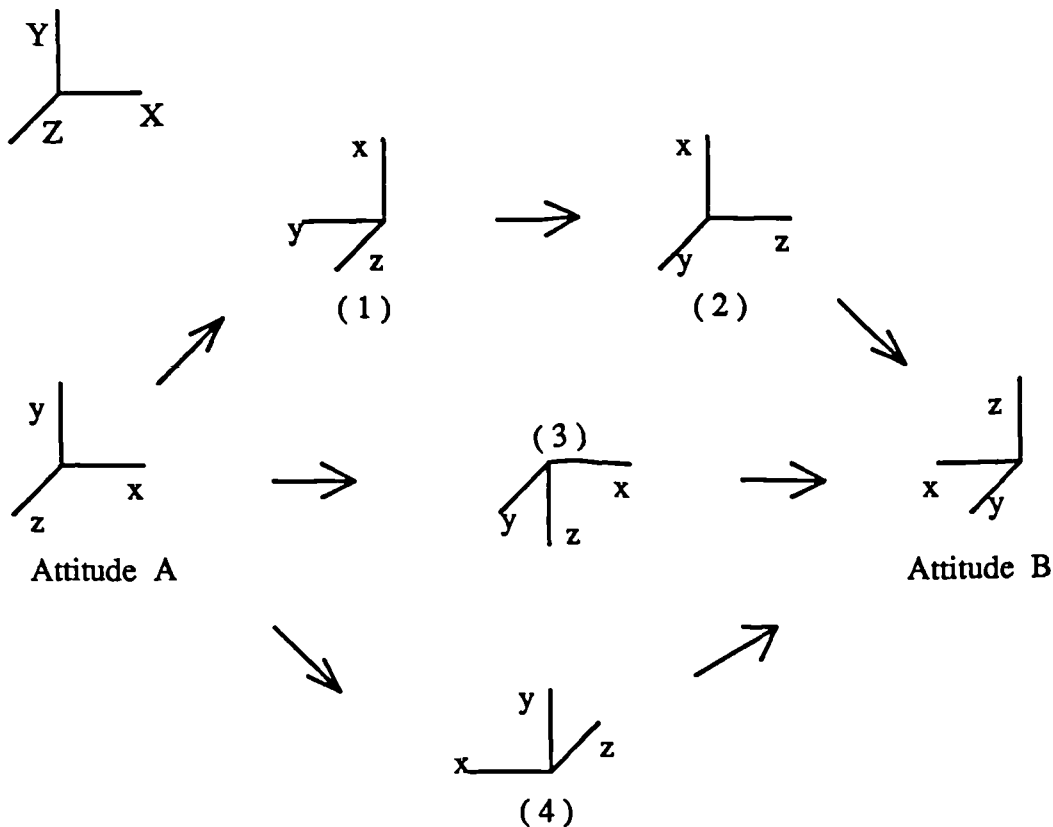


Figure 5.16 Example of the two-step rotation compared with 3-1-2 sequence Cardan angles.

XYZ is a reference Cartesian coordinate system.

xyz is a segment fixed coordinate system, y-axis represents the long axis of the segment.

Rotation 1: Attitude A \Rightarrow (1) \Rightarrow (2) \Rightarrow Attitude B is the 312 sequence rotation.

- Attitude A \Rightarrow (1) : 90 degrees of rotation about z-axis
- (1) \Rightarrow (2) : 90 degrees of rotation about x-axis
- (2) \Rightarrow Attitude B : 90 degrees rotation about y-axis

Rotation 2: Attitude A \Rightarrow (3) \Rightarrow Attitude B is the rotation of long axis + the axial rotation

- Attitude A \Rightarrow (3) : long axis (y-axis) rotate 90° about X-axis of the reference frame
- (3) \Rightarrow Attitude B : 180° axial rotation about long axis of the segment

Rotation 3: Attitude A \Rightarrow (4) \Rightarrow Attitude B is the axial rotation + the rotation of long axis

- Attitude A \Rightarrow (4) : 180° axial rotation about long axis of the segment
- (4) \Rightarrow Attitude B : long axis (y-axis) rotate 90° about X-axis of the reference frame

attitude to another in the physiological reachable range can be fully determined. The reader can support his/her elbow on a table and move the forearm/hand around to touch or take up and put down something in the surroundings. During this simple test, it will be found that the two-step rotation is the real way in which this is done in daily activities. It can also be easily found that the same result can be reached by changing the order of the two rotations (i.e. rotation of long axis followed by axial rotation, or axial rotation followed by rotation of long axis) or performing the two rotations simultaneously. Therefore the two-step rotation is sequence independent. To show this, an example is given below and compared with the rotations described by Euler/Cardan angles in 3-1-2 sequences.

Example

In Figure 5.16, XYZ is a reference Cartesian coordinate system, xyz denotes a segment fixed Cartesian coordinate system and the y-axis represents the long axis of the segment. For simplicity, the segment fixed coordinate system xyz is assumed to be parallel to the reference coordinate system XYZ before rotation, and it is denoted as attitude A.

In order to create a comparable attitude, first let the segment (xyz frame) rotate from attitude A to attitude B by three ordered rotations, +90 degrees each, following the 3-1-2 sequence used by Tupling & Pierrynowski (1987) as shown in the top of Figure 5.16. The two-step rotation from attitude A to attitude B by this method is shown in the middle and bottom of the figure. First, in the middle of Figure 5.16, the long axis (y-axis) of the segment rotates 90 degrees about the X-axis of the reference frame, then the segment axially rotates 180 degrees about the long axis (y-axis) of itself. If we change the order of the two rotations as shown in the bottom of Figure 5.16, i.e. first let the segment rotate 180 degrees about its long axis, then let the long axis rotate 90 degrees about X-axis of the reference frame, the same result can be obtained. More examples corresponding to other ordered rotations can be carried out by readers, therefore they are not repeated here.

The above example shows that the movement of a segment between any two attitudes can be described by two rotations, a rotation of the long axis of a limb segment and a rotation about the long axis (axial rotation). It also shows that the two rotations are sequence independent, and that the rotation of the long axis can be uniquely determined by its initial and final positions in the reference frame, therefore the movement of the segment between any two

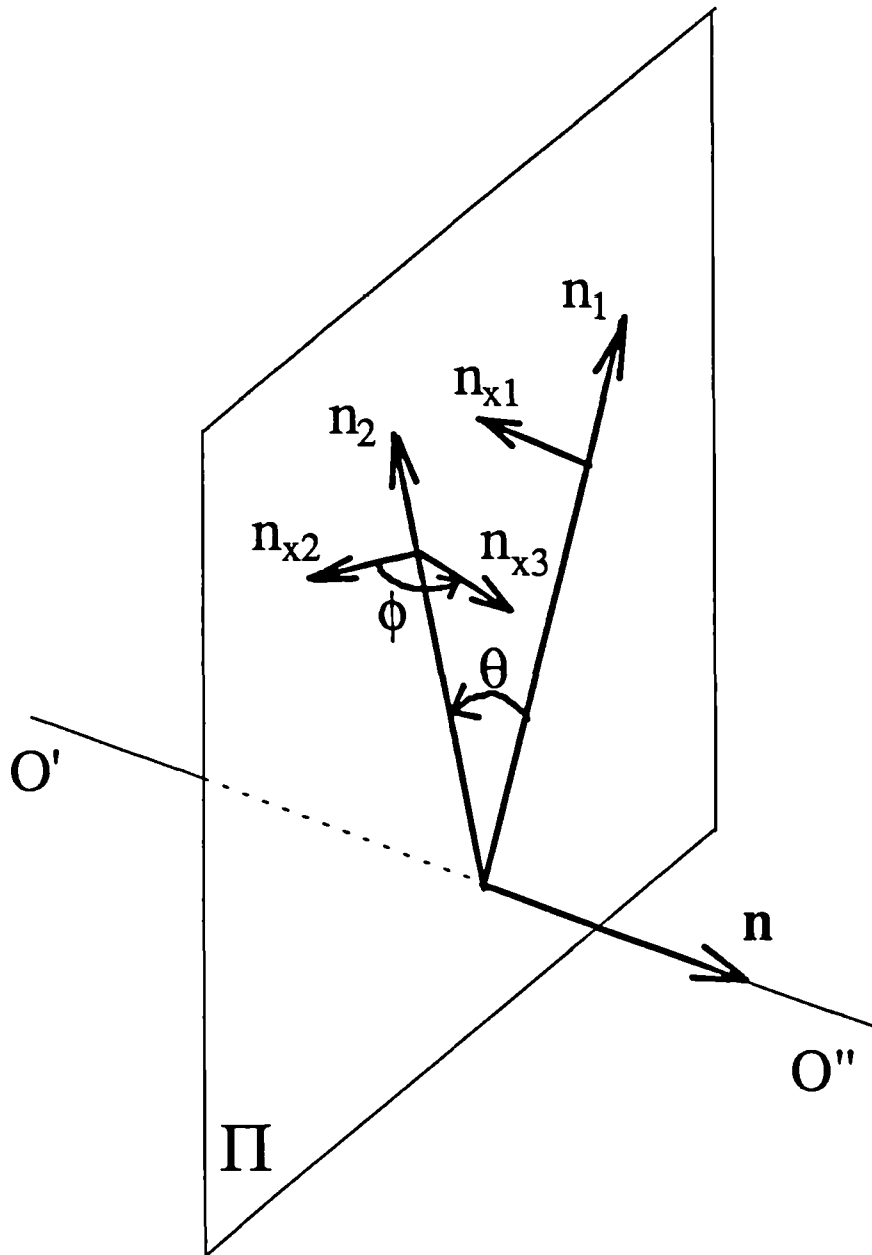


Figure 5.17 The unit vector n_{x1} of x-axis, which is one of the axes of the segment fixed coordinate system and is perpendicular to the long axis n_1 , rotates to n_{x2} with the long axis rotating to n_2 , then it rotates (axial rotation) about the long axis n_2 to position n_{x3} . Knowing the unit vector n_{x2} , the axial rotation angle ϕ can be determined from the scalar product of the unit vectors n_{x2} and n_{x3} . The unit vectors n_1 , n_{x1} and n_2 , n_{x3} represent the two known attitudes of the limb segment.

attitudes can be uniquely described by the two sequence independent rotations. The problem is how to determine the two rotations from two known attitudes in general three-dimensional conditions. Details of the solution are given below.

Determination of rotation of long axis of segment

In modern human movement analysis, the three-dimensional movement of limb segments can be measured by using various techniques reviewed in Chapter Three, therefore in this section it is assumed that the three-dimensional attitudes of the limb segment have been found. Because the rotation of the long axis can be uniquely determined by its initial and final positions in the reference frame, we begin the analysis with the rotation of the long axis. As shown in Figure 5.17, the positions of the long axis of the limb segment in the three-dimensional reference frame are represented by its unit vectors \mathbf{n}_1 and \mathbf{n}_2 for its initial and final positions, respectively. The unit vectors \mathbf{n}_1 and \mathbf{n}_2 form a plane Π , in which the rotation from \mathbf{n}_1 to \mathbf{n}_2 occurs. The rotation axis, designated the semi-instantaneous rotation axis, is perpendicular to vector \mathbf{n}_1 and \mathbf{n}_2 and plane Π , and it is denoted as $O'O''$ with a unit vector \mathbf{n} . The rotation angle from \mathbf{n}_1 to \mathbf{n}_2 is θ . Knowing the unit vector \mathbf{n}_1 and \mathbf{n}_2 , the rotation angle θ can be calculated as:

$$\theta = \arccos(\mathbf{n}_1 \cdot \mathbf{n}_2) \quad (5.55)$$

Because the rotation axis is perpendicular to both \mathbf{n}_1 and \mathbf{n}_2 , its direction can be determined by the cross product of unit vector \mathbf{n}_1 and \mathbf{n}_2 as:

$$\mathbf{n} = \mathbf{n}_1 \times \mathbf{n}_2 / |\mathbf{n}_1 \times \mathbf{n}_2| \quad (5.56)$$

Determination of axial rotation

In rigid body kinematics, the distance between any two points in the body is assumed to be constant. Therefore the positional vector between any two points in the body with respect to the body-fixed coordinate system remains unchanged during movement, and the rotation of the body can be represented by the orientation of a body-fixed coordinate system. For this reason, we now examine the movement of the x-axis, one of three axes of the segment fixed Cartesian coordinate system, in the three-dimensional reference frame. The x-axis is perpendicular to the long axis (y-axis) of the segment, and is represented by its unit vectors \mathbf{n}_{x1} , \mathbf{n}_{x2} and \mathbf{n}_{x3} in Figure 5.17. The term \mathbf{n}_{x1} represents the initial position of the x-axis before rotation;

following the rotation of the long axis it moves to a position denoted as \mathbf{n}_{x2} , then it rotates about the long axis \mathbf{n}_2 to the final position \mathbf{n}_{x3} . Because the initial and final attitudes of the segment are known, the unit vectors \mathbf{n}_{x1} and \mathbf{n}_{x3} being a component of the attitude of the segment, are known too. Therefore, if the unit vector \mathbf{n}_{x2} is found, the axial rotation from \mathbf{n}_{x2} to \mathbf{n}_{x3} can be determined by the scalar product of \mathbf{n}_{x2} and \mathbf{n}_{x3} . The relationship between \mathbf{n}_{x1} and \mathbf{n}_{x2} can be described as:

$$\mathbf{n}_{x2} = \mathbf{R}(\theta, \mathbf{n})\mathbf{n}_{x1} \quad (5.57)$$

where \mathbf{R} is called the transformation or rotation matrix, \mathbf{n} is the unit vector of the semi-instantaneous rotation axis, and θ is the rotation angle about the semi-instantaneous rotation axis. The Equation 5.57 describes an orientational change of the x-axis with the long axis rotation from \mathbf{n}_{x1} to \mathbf{n}_{x2} . The transformation matrix has been derived (see Appendix) as:

$$\mathbf{R}(\theta, \mathbf{n}) = \cos(\theta)\mathbf{I} + (1-\cos(\theta)) \mathbf{nn}^T + \sin(\theta) [\tilde{\mathbf{n}}] \quad (5.58)$$

where \mathbf{I} is a 3x3 unit matrix, $[\tilde{\mathbf{n}}]$ is a skew-symmetric matrix. Explicitly, \mathbf{n} , \mathbf{nn}^T , and $[\tilde{\mathbf{n}}]$ can be written in matrix form as:

$$\begin{aligned} \mathbf{n} &= [l_1 \ l_2 \ l_3]^T \\ \mathbf{nn}^T &= \begin{bmatrix} l_1^2 & l_1l_2 & l_1l_3 \\ l_2l_1 & l_2^2 & l_2l_3 \\ l_3l_1 & l_3l_2 & l_3^2 \end{bmatrix} \\ [\tilde{\mathbf{n}}] &= \begin{bmatrix} 0 & -l_3 & l_2 \\ l_3 & 0 & -l_1 \\ -l_2 & l_1 & 0 \end{bmatrix} \end{aligned} \quad (5.59)$$

where l_1, l_2, l_3 are the three components of the unit vector of the rotation axis on each axis of the reference frame. As shown in Appendix A, \mathbf{n} is a unit vector of an arbitrary rotation axis in a three-dimensional reference Cartesian coordinate system and $\mathbf{R}(\theta, \mathbf{n})$ can be used to transform any body-fixed unit vector from one orientation to another following the rotation (with angle θ) about \mathbf{n} . Therefore, knowing the unit vector \mathbf{n} of the semi-instantaneous rotation axis, and rotation angle θ of the long axis about \mathbf{n} by Equation 5.55 and 5.56, the rotation matrix \mathbf{R} and unit vector \mathbf{n}_{x2} can be determined from equation 5.58 and 5.57. The axial rotation angle can then be found from \mathbf{n}_{x2} and \mathbf{n}_{x3} as:

$$\phi = \arccos(\mathbf{n}_{x2} \cdot \mathbf{n}_{x3}) \quad (5.60)$$

The sign of axial rotation angle ϕ is defined by the right hand rule, and determined as follows. Assuming the vector \mathbf{n}' is the cross product of vector \mathbf{n}_{x2} and \mathbf{n}_{x3}

$$\mathbf{n}' = \mathbf{n}_{x2} \times \mathbf{n}_{x3} / |\mathbf{n}_{x2} \times \mathbf{n}_{x3}| \quad (5.61)$$

If \mathbf{n}' is in the direction of long axis \mathbf{n}_2 , the axial rotation angle is positive and the scalar product of \mathbf{n}' and \mathbf{n}_2 equals 1. If \mathbf{n}' is in the opposite direction of \mathbf{n}_2 , the axial rotation angle is negative and the scalar product of \mathbf{n}' and \mathbf{n}_2 equals -1. Therefore the value of +1 or -1 of the scalar product of \mathbf{n}' and \mathbf{n}_2 can be theoretically used to decide the signs of axial rotation angle. However, due to the errors in measurement, \mathbf{n}' may not exactly coincide with \mathbf{n}_2 , and the scalar product is not exactly equal to +1 or -1, but may be a little smaller than 1.0 or slightly bigger than -1.0. Fortunately the sign of the scalar product will be unaffected in this case. Therefore, in practice, the sign of the scalar product of \mathbf{n}' and \mathbf{n}_2 can also be used to show whether the axial rotation angle ϕ is positive or negative. Mathematically, the sign of axial rotation angle can be expressed as:

$$\phi > 0 \quad \text{if } 0 < \mathbf{n}' \cdot \mathbf{n}_2 \leq 1 \quad (5.62)$$

$$\phi < 0 \quad \text{if } -1 \leq \mathbf{n}' \cdot \mathbf{n}_2 < 0 \quad (5.63)$$

In clinical terms, the sign of the axial rotation angle indicates whether the axial rotation is an internal rotation or an external rotation. For example, if the long axis of the upper arm is defined in the direction from the elbow joint to the shoulder joint, positive ϕ by the right hand rule will represent internal rotation and negative ϕ will represent external rotation.

Numerical solution of the above example

To show the effectiveness of the method, the axial rotation angle pictorially presented in the above example (Figure 5.16) is calculated using Equation 5.55 to 5.60. Details of the calculation are given as follows.

$$\begin{aligned} \text{Known variables: } \mathbf{n}_1 &= [0 \ 1 \ 0]^T, & \mathbf{n}_2 &= [0 \ 0 \ 1]^T \\ \mathbf{n}_{x1} &= [1 \ 0 \ 0]^T, & \mathbf{n}_{x3} &= [-1 \ 0 \ 0]^T \end{aligned}$$

calculated results:

$$\theta = \arccos(\mathbf{n}_1 \cdot \mathbf{n}_2) = \arccos(0.0) = 90^\circ$$

$$\mathbf{n} = \mathbf{n}_1 \times \mathbf{n}_2 / |\mathbf{n}_1 \times \mathbf{n}_2| = [1 \ 0 \ 0], \text{ where } l_1 = 1.0; l_2 = 0.0; l_3 = 0.0$$

$$\mathbf{R} = \begin{bmatrix} 1 & 0 & 0 \\ 0 & 0 & -1 \\ 0 & 1 & 0 \end{bmatrix}$$

$$\mathbf{n}_{x2} = \mathbf{R}\mathbf{n}_{x1} = \begin{bmatrix} 1 & 0 & 0 \\ 0 & 0 & -1 \\ 0 & 1 & 0 \end{bmatrix} \begin{bmatrix} 1 \\ 0 \\ 0 \end{bmatrix} = \begin{bmatrix} 1 \\ 0 \\ 0 \end{bmatrix}$$

$$\phi = \arccos(\mathbf{n}_{x2} \cdot \mathbf{n}_{x3}) = \arccos(-1.0) = 180^\circ$$

The example proves the validity of the method. It is believed that the method can be easily understood by clinicians and physiotherapists for its clear physical description of limb segment rotation in nearly the same way as seen in various activities. Since no restrictive conditions were imposed on the two known attitudes, the method can be used to describe a finite rotation of the limb segment between any two attitudes.

Gimbal-lock problem

The only problem of the method seems that when the second unit vector \mathbf{n}_2 of the long axis is in the same or opposite direction of the first unit vector \mathbf{n}_1 of the long axis (here we denote the \mathbf{n}_1 as the initial position of long axis), i.e. $\mathbf{n}_2 = \mathbf{n}_1$ or $\mathbf{n}_2 = -\mathbf{n}_1$, the direction of the semi-instantaneous axis determined by Equation 5.56 becomes undefined, consequently it makes the calculation of the axial rotation angle impossible because the transformation matrix (Equation 5.58 to 5.59) and unit vector \mathbf{n}_{x2} in Figure 5.17 can not be found. In the first case, $\mathbf{n}_2 = \mathbf{n}_1$ indicates that no rotation occurs of the long axis, and in the second case $\mathbf{n}_2 = -\mathbf{n}_1$ indicates that the long axis of limb segment rotates 180 degrees from its initial position \mathbf{n}_1 . The phenomenon is a well-known problem called *gimbal-lock* in the literature (Chao 1980, Woltring 1994), but the situation is rarely met in most activities of daily living, and it can only occur in a limited number of limb segment or joints, such as the upper arm and the shoulder joint. If the problem occurs in some activities to be investigated it can be solved in two ways when using the method. First the *gimbal-lock* points can be easily detected in the computation. If $\mathbf{n}_2 = \mathbf{n}_1$ were detected, it means no long axis rotation occurred, therefore it is not necessary to calculate the transformation matrix and to look for \mathbf{n}_{x2} , because $\mathbf{n}_{x2} = \mathbf{n}_{x1}$ in this case, and the axial rotation angle can be calculated from Equation 5.60 by substituting \mathbf{n}_{x2} with \mathbf{n}_{x1} . If $\mathbf{n}_{x1} = \mathbf{n}_{x3}$ were also detected, it indicates that no movement occurred and the calculation can be jumped over to the next data point. Second if the investigated activity

involves the long axis of the limb segment exceeding 180 degrees rotation, it is recommended to choose an attitude at any point in the mid period of the activity as a second initial attitude and the unit vector of long axis at this attitude is denoted as n_i ; thus dividing the full period of the activity into two sections. In the second section the rotation of the long axis is with respect to the second initial attitude n_i . If both sections involve less than 180 degrees rotations of the long axis of the limb segment (which can be easily reached), the *gimbal-lock* problem can be avoided. Since the direction of the semi-instantaneous axis varies with time, it may be argued that the choice of a second initial attitude may make the interpretation of long axis rotation difficult. However the problem can be disregarded for the reason that the position of the long axis of the limb segment can be fully determined with proper physical descriptions such as flexion/extension and adduction/abduction by the projections of the long axis in three orthogonal planes of reference frame. The definition of axial rotation given in this method is the rotation about the long axis of the limb segment and no restriction was given to where the long axis is. Therefore the determination of axial rotation can be considered as a one dimensional problem and the additive law holds. If the axial rotation angle from the first initial attitude n_1 to the second initial attitude n_i is ϕ_1 , and from the second initial attitude to any attitude in the second section is ϕ_i , then the axial rotation angle from the first initial attitude to any attitude in the second section can be calculated as:

$$\phi_2 = \phi_1 + \phi_i \quad (5.64)$$

In fact, more than one initial attitude can be used for this purpose. If n initial attitudes were selected, the full period would be divided into n sections, and the axial rotation angle from the first attitude to any attitude in the final section can be expressed as:

$$\phi_n = \phi_1 + \phi_2 + \phi_3 + \cdots + \phi_i + \cdots + \phi_n \quad (5.65)$$

where the ϕ_i is the axial rotation angle from the i th initial attitude to the $i+1$ th initial attitude, and ϕ_n is the axial rotation angle from the n th initial attitude to any attitude in the final section. It is believed that the selection of one to three initial attitudes of this kind will be enough to deal with most activities involving over 180 degrees of long axis rotation. It should be noted that the number of initial attitudes can not be too many, if the number of initial attitude equals nearly the number of data points, the rotation will become an infinitesimal rotation and the errors due to noise of measurement will become a crucial problem such as Woltring et al. (1985) indicated *the direction and position of helical axis and centroid are*

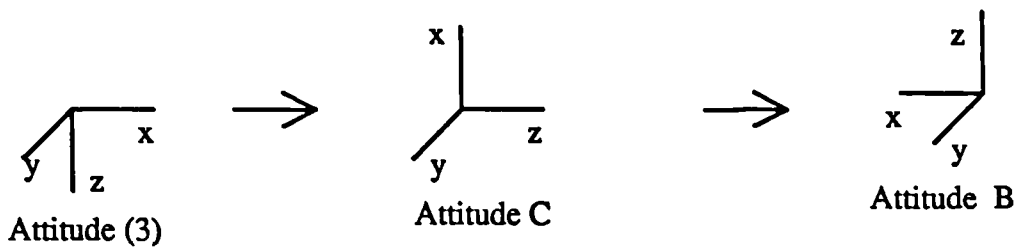


Figure 5.18 Rotation from attitude (3) to attitude B was divided into two sections by attitude C. The positive 180 degrees rotations about the long axis (y-axis) of the limb segment from attitude (3) to attitude B can be obtained by the sum of two positive 90 degrees rotations about the same axis from Attitude (3) to attitude C and from attitude C to attitude B. Therefore the *gimbal-lock* problem is avoided.

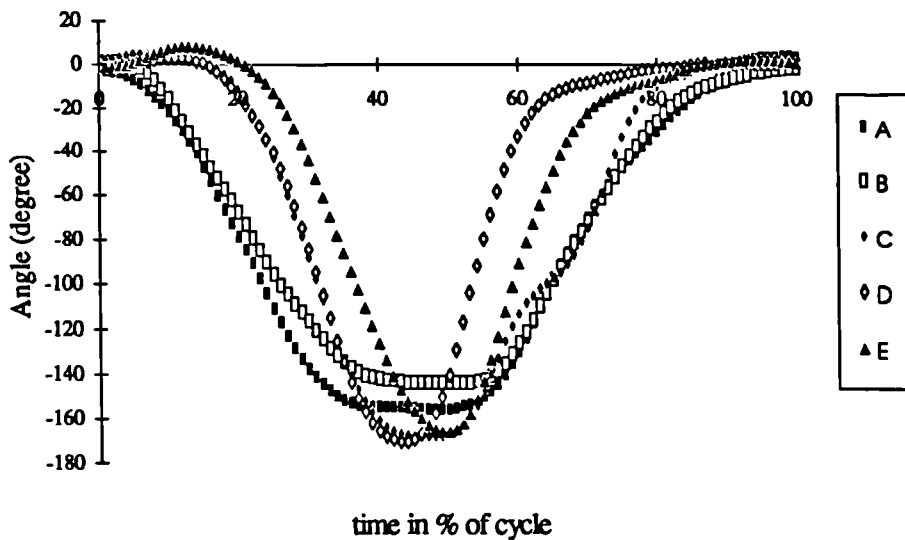


Figure 5.19 Axial rotation angles of forearm during forearm flexion/extension + axial rotation, curves A and B from subject 1, and curves C, D, and E from subject 2.

very sensitive to landmark measurement errors, particularly in the cases of small rotations. Unless some error reduction procedure is applied, the results will become unpredictable. However using this method, not only the *gimbal-lock* but also the noise problem can be avoided by filtering the raw data and dividing the full cycle of activity into a limited number of sections, because the method describes a real finite rotation.

The *gimbal-lock* problem may also occur in the determination of axial rotation angles. When the unit vectors \mathbf{n}_{x3} and \mathbf{n}_{x2} are in opposite directions i.e. $\mathbf{n}_{x2} = -\mathbf{n}_{x3}$, an absolute axial rotation angle of 180 degrees can be obtained from Equation 5.60, but the sign of the angle can not be determined from Equation 5.61 to 5.63 because the unit vector \mathbf{n}' in Equation 5.61 is undefined in this case. However the problem can also be resolved by dividing the full cycle of activity into a limited number of sections described above. It is believed that if the full cycle of activity is divided into a limited number of sections, the *gimbal-lock* problems in both long axis rotation and axial rotation can be avoided at the same time.

Readers may have found that in the above graphic example (Figure 5.16), the axial rotation from attitude (3) to attitude B and from attitude A to attitude (4) can be reached by either a 180 degrees rotation or a -180 degrees rotation about the long axis (y-axis) of the segment. However the above calculation example can only give an absolute rotation angle without the sign. This is an example of the *gimbal-lock* problem occurring in axial rotation. In what follows the problem is solved by dividing the full cycle into a number of sections.

Further example

In order to show how to solve the *gimbal-lock* problem occurring in axial rotation of the above example, the rotation from attitude (3) to attitude B in Figure 16 is used in this example. As shown in Figure 5.16 the rotation from attitude (3) to attitude B is a purely axial rotation about the long axis (y-axis) of the limb segment without long axis rotation. As stated above the axial rotation (rotation angle and its sign) can not be fully determined from the two attitudes due to the *gimbal-lock* problem. Therefore we assume that there is a number of attitudes which have been measured between the two attitudes (attitude (3) and attitude B). For simplicity, a special attitude C among these measured attitudes is selected as a second initial attitude as shown in Figure 5.18, and it can be reached by a positive 90 degrees rotation about the y-axis from attitude (3). It can be seen that the rotation from attitude C to attitude B

can also be reached by a positive 90 degrees rotation about the y-axis. Therefore a positive 180 degrees rotation about the y-axis from attitude (3) to attitude B can be obtained by summing the two 90 degrees rotations together. Because the two rotations, (3) to C and C to B are all less than 180 degrees, there is no *gimbal-lock* problem in the two sections. The example shows that although there is a *gimbal-lock* problem for the rotation from attitude (3) to attitude B, the problem has been easily resolved by dividing the full rotation into two less than 180 degrees rotations. The same numerical result can also be obtained by using the equations given above, which can be carried out by readers. In fact in order to solve the *gimbal-lock* problem between two attitudes, the second initial attitude can be selected at anywhere between the two attitudes in case the *gimbal-lock* point is not involved in either of the two sections divided by it.

Experimental study

The purpose of the experiment is to show the validity of the method in analysing real kinematics data collected by the motion analysis system. An activity involving forearm flexion/extension and internal/external rotations was tested in the experiment. Two subjects were tested performing the activity in the standing position with the upper arm unmoved. At the beginning of the activity, the forearm is at the free hanging position with palm facing backward. During the activity the forearm flexed about 90 degrees from the free hanging position, meanwhile the forearm externally rotated to a position of palm facing up, then extended and internally rotated back to the free hanging position. Four retro-reflective markers were used to define the elbow, wrist joint centres and the forearm coordinate system, in which two markers were affixed at the medial and lateral epicondyles of the elbow joint and two markers were affixed at the radius and ulna sides of the wrist joint. The forearm coordinate system is defined as: y-axis (long axis) directed from wrist joint centre to elbow joint centre, z-axis directed from ulna side to radius side of wrist joint, and x-axis was perpendicular to both y and z axes and is determined by the cross product of unit vectors of y, z axes.

The three-dimensional positions of these markers were measured by a six camera VICON motion analysis system. The collected data were filtered at auto-selected cut-off frequencies for each data sequence using the residual analysis technique (Winter 1990). Three measurements were made for each subject, five of the six measurements were analysed, and

the calculated axial rotation angles were normalised to a time scale of 100% of the cycle and are given in Figure 5.19.

As shown in Figure 5.19, the axial rotation angles of the forearm are successfully determined. The negative angles indicate that the axial rotation is external rotation (supination). The curves denoted as A, B are from the first subject, and the curves C, D, and E are from the second subject. It can be seen that the supination of the forearm from the first subject starts early and stops later than the second subject, while the maximum supination angles from the second subject are bigger than from the first. It can also be seen that the maximum supination angles are below 180 degrees. The results indicate that the forearm is not fully supinated during the test, the reason may be that the subjects were instructed only to flex and supinate the forearm to a comfortable palm facing up position. It can be predicted that bigger maximum supination angles can be measured if the subjects were instructed to supinate the forearm to the maximum range.

Discussion

Although the emphasis of this section is the determination of axial rotation of limb segments, the method describes a new way of determining the three-dimensional rotation of the limb segment. The advantage of the two-step rotation method is that it describes the three-dimensional rotation of the limb segment in the natural way as it is seen in daily activities. As proved in the first example and direct observations of limb segment rotations, the two-step rotation is sequence independent. However the determination of the two rotations from kinematic data measured by a motion analysis system should begin with the determination of long axis rotation, because the long axis rotation is uniquely determined by the orientations of the long axis at the initial and final attitudes of the limb segment. Finally the gimbal-lock problem can be easily solved when using the method. It is believed that the method can be used not only in the biomechanics of human movement analysis for describing the three-dimensional rotation of limb segments, but also in other fields for describing the three-dimensional rotation of any moving object with a long axis.

Chapter Six

Results and Discussions

A computer program was written using the principles given in the previous chapter, and the results calculated by the program are presented in this chapter. Six normal subjects were tested for each of the four activities. The particulars of the subjects are given in Table 6.1. Each activity was tested three times for each subject. Different numbers of trials were analysed for each activity for the reasons given in chapter four. All the results were normalised in time, and the mean values are presented. The following results are grouped by the activities, and given in four separate sections. Each section involves the results of one activity.

Table 6.1 Subject Characteristics

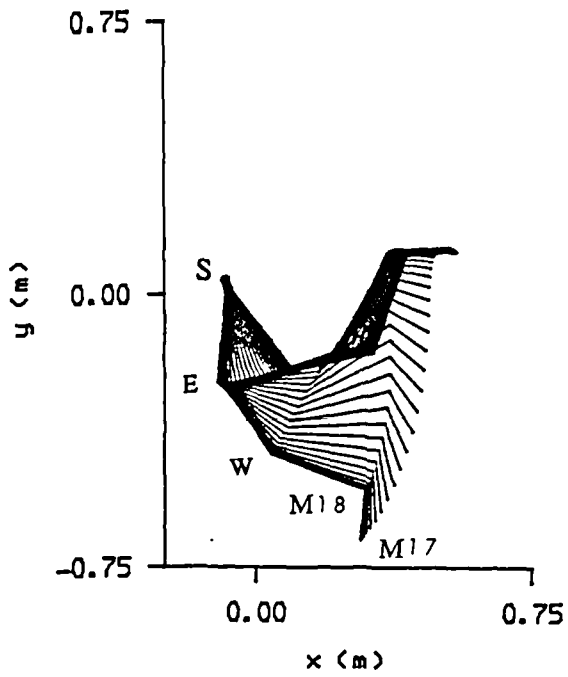
Subject	Age (years)	Height (cm)	Mass (kg)
No.1	32	175	68
No.2	35	185	70
No.3	36	174	63
No.4	38	160	60
No.5	30	174	58
No.6	27	172	60
Average (SD)	33 (4.1)	173.3 (8)	63.2 (4.8)

6.1 Lifting Activity

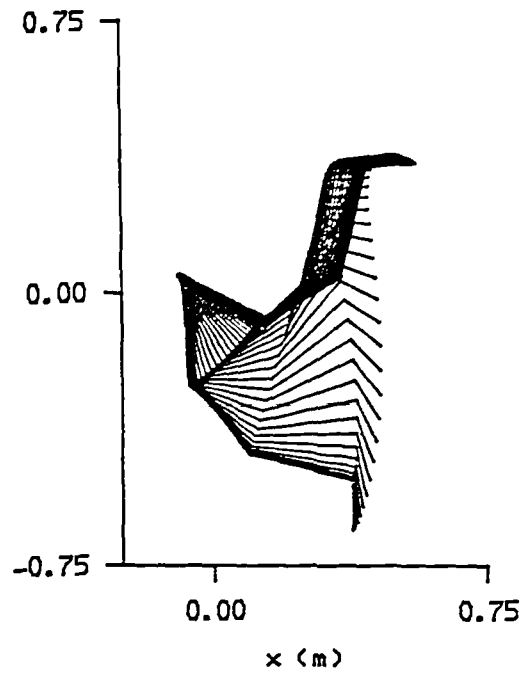
As mentioned in chapter four, the lifting activity involved eight modes, lifting a book of 1kg and 2kg to table, shoulder, head, and the highest heights. The number of trials analysed for each case is given in Table 6.2. At least 1 trial for each subject and each mode are included in the mean results. The results are given and discussed by the sequence from the kinematic parameters to kinetic parameters. Effort has been made to put the results of each parameter from the eight modes together for easier comparison.

Table 6.2 Number of trials analysed for lifting activities.

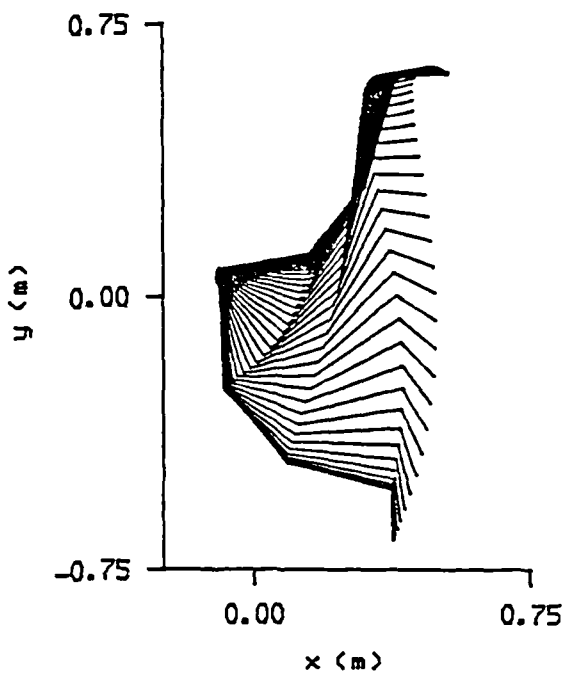
	Table height	shoulder height	head height	highest height
1kg	15	14	15	15
2kg	15	16	16	15



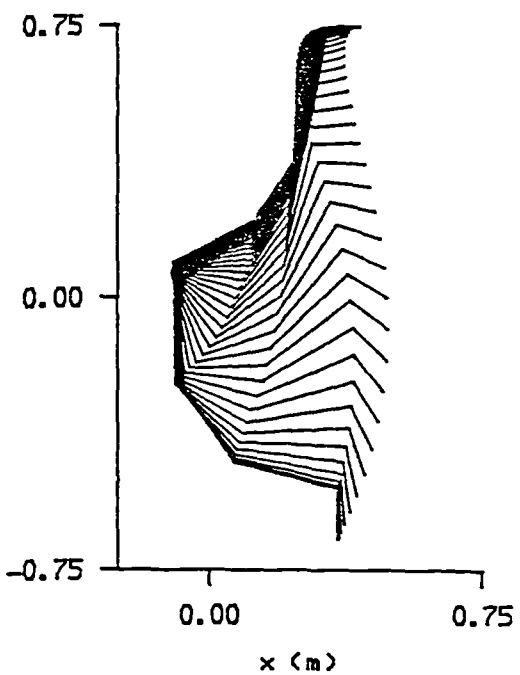
(1) Table height



(2) Shoulder height

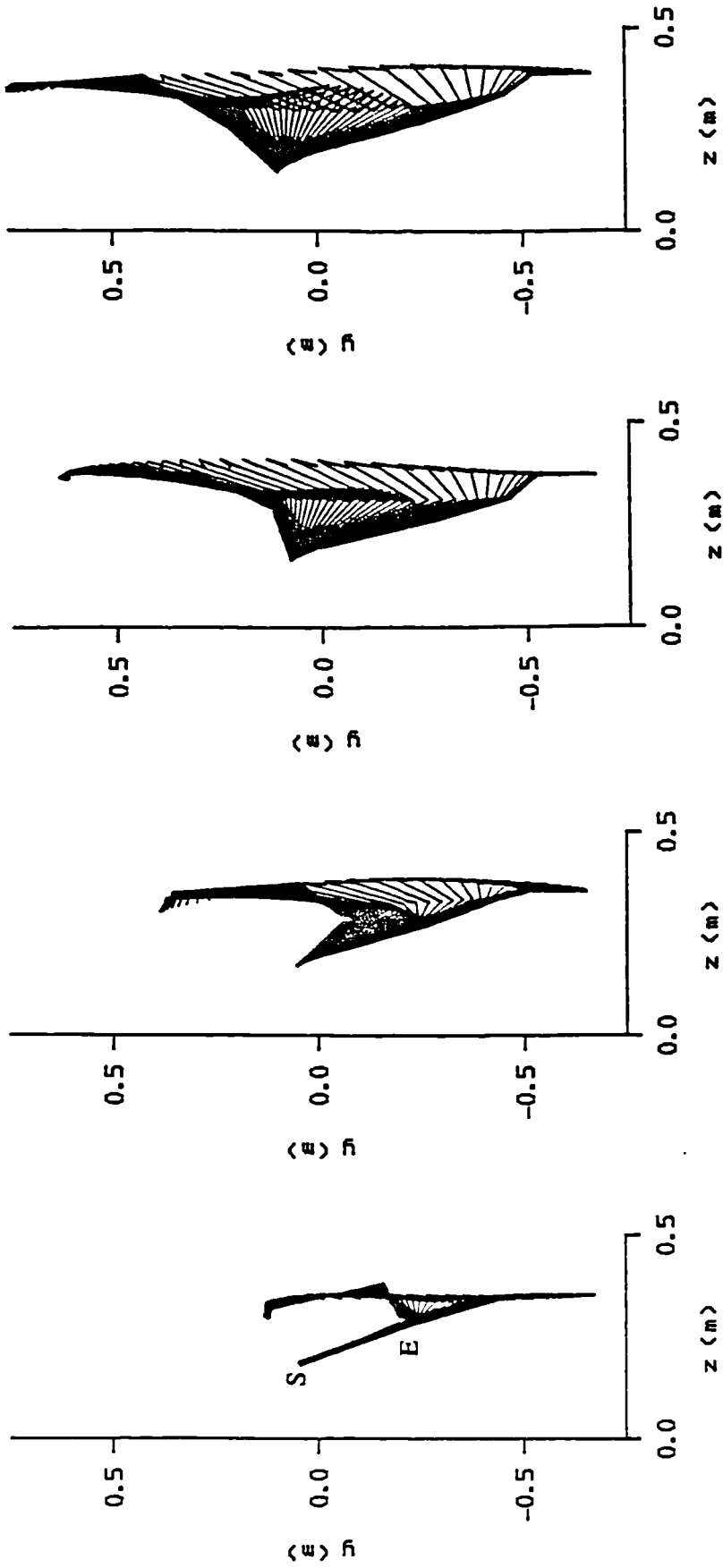


(3) Head height



(4) Highest height

Figure 6.1 Sagittal plane view of arm and book movement for lifting a 1kg book from 20cm height to four different heights. S, E, W, M18, M17 refer to the shoulder, elbow, wrist joints, marker 18, and marker 17 on the book, respectively.



(1) Table height (2) Shoulder height (3) Head height (4) Highest height

Figure 6.2 Frontal plane view of arm and book movements for lifting a 1kg book.

6.1.1 Kinematic Results and Discussions

The kinematic results presented in this section include the regeneration of arm and book movements by stick diagrams, the rotation angles of the upper arm about the three axes of the trunk coordinate system, the elbow angles, the axial rotation angles of upper arm and forearm, and the velocities and accelerations of the book mass centre in the trunk coordinate system.

6.1.1.1 Regeneration of arm movement for lifting activities

The motion of the arm during lifting activities is regenerated by a stick diagram which is a group of straight lines connecting the shoulder, elbow, wrist joint centres, markers 18 and 17 on the book at each instant of time. The positions of these joints and markers are given in the trunk coordinate system. The stick diagrams are presented in three anatomical planes, namely sagittal, coronal, and transverse plane. This arrangement allows the 3-D movements of arm and book relative to the trunk to be observed. Only the lifting phase of the lifting activities is presented by the stick diagrams.

Sagittal plane view

The major arm movement of the lifting activity occurs in the sagittal plane which is shown in Figure 6.1, where the x-axis is forward, y-axis is upward, and the dimensions of x, y axes are given in the same scale. It can be seen that the shoulder joint has very little movement in the trunk coordinate system during lifting to four different heights.

The movements of the upper arm are composed of translation of the shoulder joint and rotation around the shoulder joint. In the sagittal plane the rotation is about the transverse axis (z-axis) of the trunk coordinate system, and is referred to as flexion and extension (Kapandji 1970). The flexion angles of the upper arm can be directly observed from Figure 6.1 and it can be seen that the flexion angle increases with the height of lifting. Results of the other rotation angles of the upper arm are given in section 6.1.1.2.

The variations of the angle between the upper arm and forearm can also be found in Figure 6.1. The changes of this angle represent the relative movements of the forearm with respect to the upper arm. The decrease and increase of the angle indicate the flexion and extension of the elbow respectively. During the lifting phase the forearm experienced both

flexion and extension movements. The details of variations of the forearm/upper arm angle (elbow angle) with time will be given in section 6.1.1.3.

The movements of the book are presented by the straight lines connecting marker 18 and 17 on the book. It can be seen that this line varies from a vertical line at the beginning of lifting to a horizontal line at the end of the lifting phase. This result shows that the book was rotated 90 degrees during lifting in order to be vertically (long side of the book in the vertical direction) placed at the proposed height, which is indicated by a shelf. This rotation is required because the book was held by the subject in a horizontal position before the lifting (Figure 4.32). It is noticed that the rotation of the book in the sagittal plane (Figure 6.1) was completed by nearly half way through the lifting phase and was then moved forward during lifting to table height. During lifting to shoulder, head, and highest height, the book moved upward continually to the destination height after rotating 90 degrees and before moving forward to the target. This phenomenon is more obvious for lifting to head and highest height. By careful observation of Figure 6.1, it can be found that the angle between the line from the wrist joint to marker 18 and the line from marker 18 to marker 17 is nearly unchanged during the first half of the lifting phase when the book rotated 90 degrees. This result shows that the rotation of the book is not due to the angular movements at the wrist joint, but is a result of forearm movements, mostly the flexion of the forearm which is discussed in section 6.1.1.3.

From the stick diagrams of lifting to head and highest heights in Figure 6.1, it can be found that the book moved towards the body slightly (decrease of the x dimension) when it was lifted to above the shoulder height, and the moving forward action occurs after the book reached the chosen height. The movement towards the body is required to avoid touching the shelf, and the movement forward is for the book to be placed onto the shelf. In addition, the action of moving towards the body reduces the distance between the book and the shoulder joint, therefore it can reduce the moment acting on the shoulder during the lifting phase.

Frontal plane view

The frontal plane view of arm and book motions of lifting a 1kg book are presented in Figure 6.2 which shows the rotations of the upper arm about the posterior-anterior axis (x-axis) of the trunk coordinate system. This rotation is called abduction-adduction (Kapandji

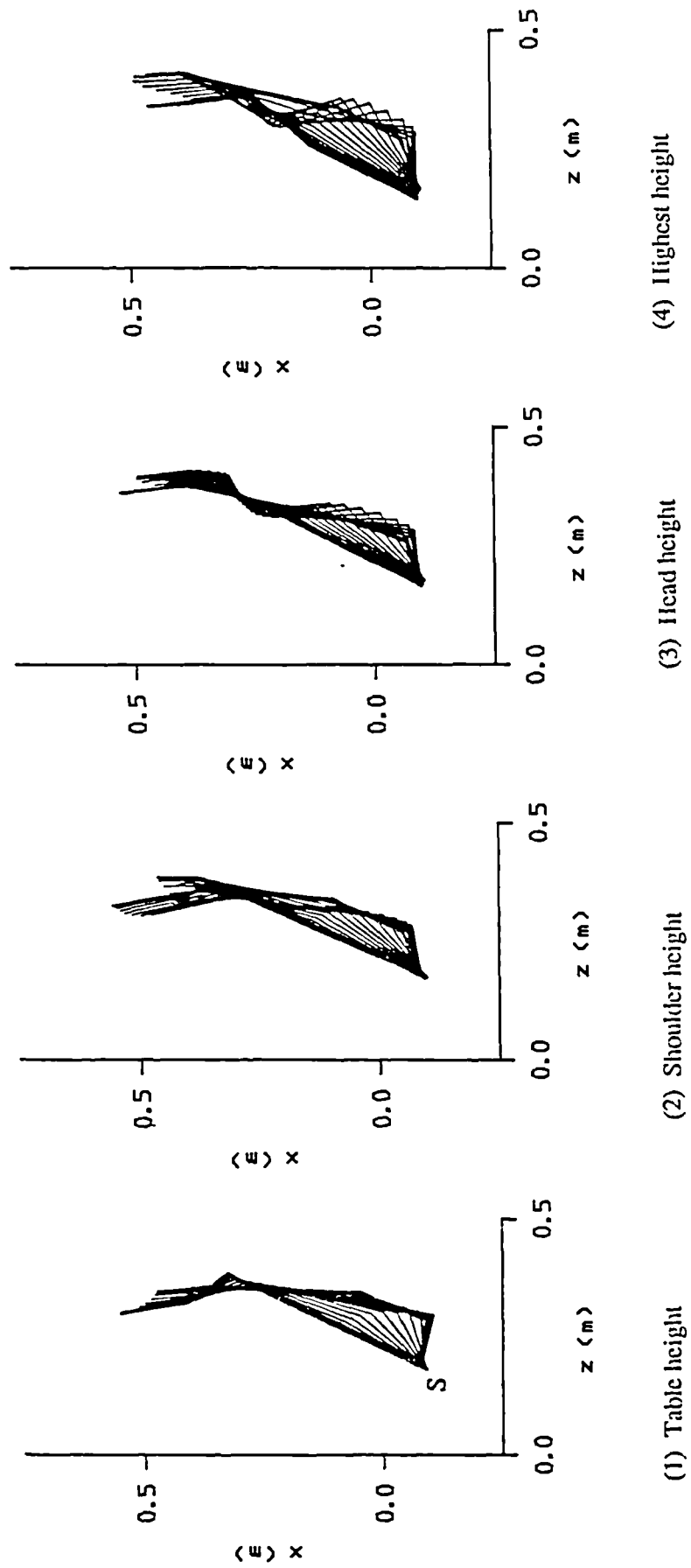


Figure 6.3 Horizontal plane view of arm and book movement for lifting a 1kg book.

1970). From Figure 6.2 very little abduction of the upper arm can be found for lifting to table height, and obvious abduction can be seen for lifting to above table height. The abduction angles increase with the height of lifting.

The book followed a nearly vertical straight line in the frontal plane as it was lifted to table height. When the book was lifted to a height above table height its trace in the frontal plane describes a curve. The curve is the combination of upward movement and slight unintended medial-lateral displacement. A small rotation of the book can also be found in the frontal plane view.

Horizontal plane view

The projections of the arm and book movement on the horizontal plane are presented in Figure 6.3. The position of the upper arm in the horizontal plane can be reached by the combination of flexion+abduction or extension+adduction movement according to the definition of Kapandji (1970). Alternatively, the rotation angles of the upper arm about the vertical axis (y-axis) of the trunk coordinate system can also be observed from its projection in the horizontal plane. From Figure 6.3 it can be seen that the upper arm rotated approximately the same angles during the four heights of lifting.

It should be noted that only the movements of arm and book for lifting of the 1kg book are presented in the form of stick diagrams in Figure 6.1 to 6.3. Similar results for lifting a 2kg book have been found. For this reason they are not given here.

6.1.1.2 Upper arm rotation angles about the axes of trunk coordinate system

The above results give a general view of the pattern and range of arm movement during the lifting activity. The details of the rotation angles of the upper arm about the three axes of the trunk frame are given in Figure 6.4 for lifting a 1kg book, where the flexion and abduction angles are measured from the position of the upper arm free hanging vertically, and the inward rotation angles are measured from the positive direction of the transverse axis (z-axis) of the trunk coordinate system.

It is interesting to find that during lifting to table and shoulder heights the flexion angles of the upper arm about the transverse axis (from left to right) of the trunk system are higher

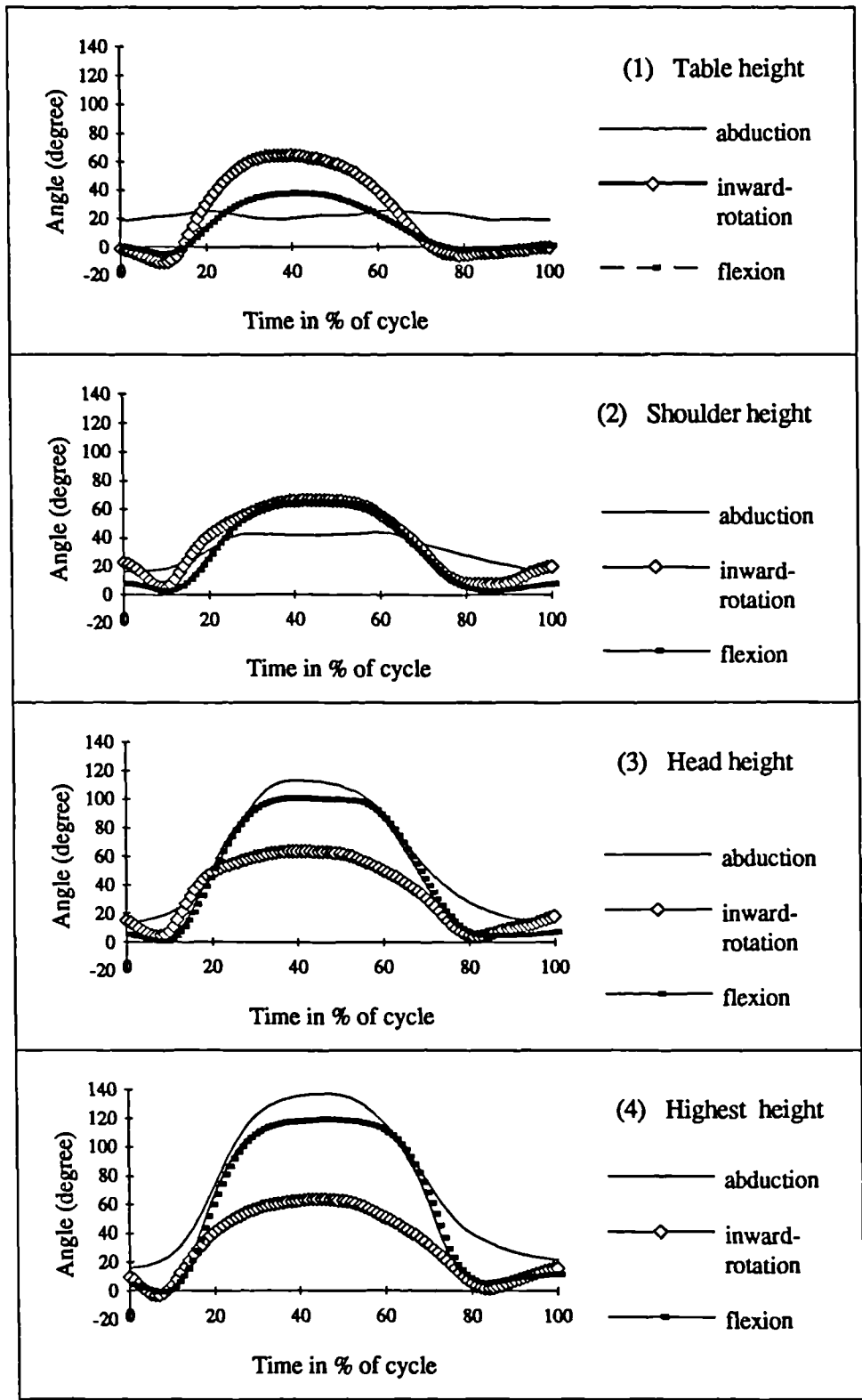


Figure 6.4 Upper arm rotation angle about the axes of trunk frame for lifting a 1kg book

than the abduction angles about the posterior-anterior axis, however during lifting to head and highest heights the abduction angles are higher than the flexion angles.

It can be found that the inward rotation angles have nearly the same pattern and values for the four heights of lifting. The inward rotation angle may be related to the target position in the transverse axis (from left to right). From Figures 6.2 and 6.3 it is known that the book was lifted to the position at the right side of the right shoulder joint. If the book were to be lifted to just in front of the body or toward the left side of the body more inward rotations may be observed.

In the study of upper arm movement, the flexion and abduction angles have been divided into a number of phases (Kapandji 1970). For flexion there are three phases, 0 to 60 degrees, 60 to 120 degrees, and 120 to 180 degrees. For abduction there are also three phases, 0 to 90 degrees, 90 to 150 degrees, and 150 to 180 degrees. Inman (1944) found that approximately 30 degrees of abduction or 60 degrees of flexion could occur at the glenohumeral joint before any upward rotation of the scapula was required, but from those respective positions 1 degree of upward scapular movement accompanied 2 degrees of humeral movement. Kapandji (1970) indicated that the first phase of abduction ends at 90 degrees, when the shoulder '*locks*' as a result of the greater tuberosity hitting the superior margin of the glenoid. In the third phase of flexion and abduction, movement of the spinal column becomes necessary (Kapandji 1970). Comparing with the results in Figure 6.4 it can be assumed that no scapular movement occurred for lifting to table height. According to Inman (1944), Kapandji (1970), and the results in Figure 6.4, a little rotation of the scapula may occur during lifting to shoulder height. If the lifting height is a little lower than the shoulder, scapular rotation may be avoided. Lifting to the shoulder height may be, therefore, at the limit of whether scapular movement is involved or not. For safety, it can be suggested that the lifting height should be designed a little lower than shoulder height if possible.

From Figure 6.4 it can be seen that the upper arm movement during lifting to head and highest height falls in the second abduction and flexion phases. It is evident that not only scapular movement but also rotations of the sterno-clavicular and acromio-clavicular joints were involved in the lifting to the two latter heights. It can also be noticed that the maximum flexion and abduction angles for lifting to the highest height are a little lower than the upper limits of the second flexion and abduction phases. These results indicate that there is probably

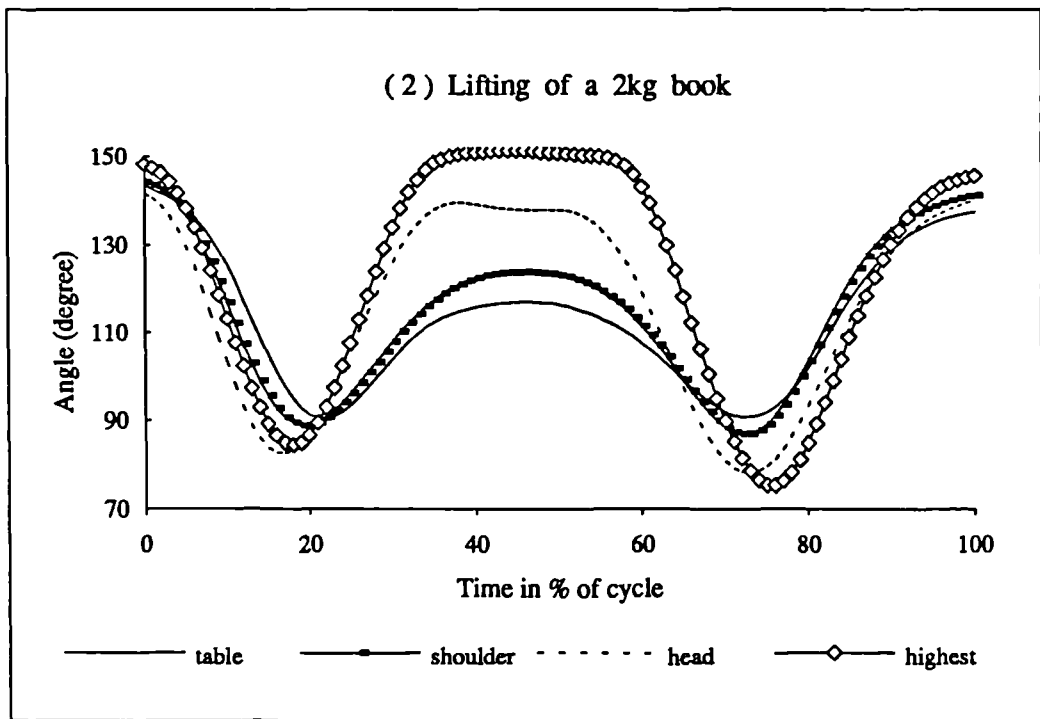
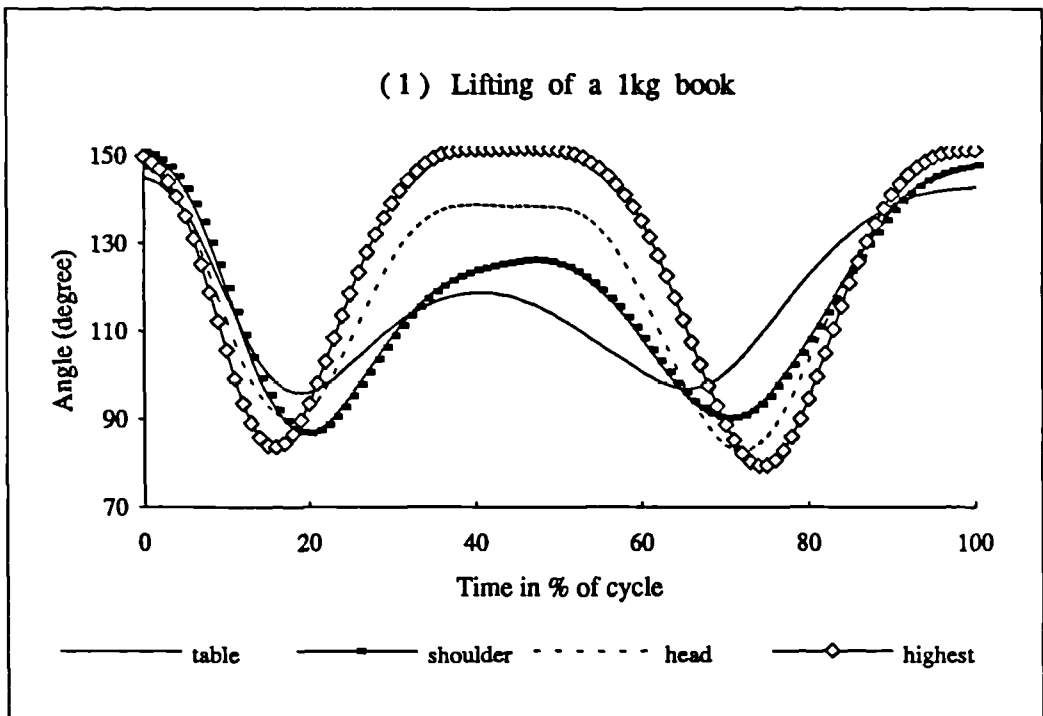


Figure 6.5 Elbow angles of lifting activities

no movement of the spinal column during lifting to the highest height, and is in agreement with the experimental design.

It is worth mentioning that the highest height of this study was determined by the subjects as the highest height that could be lifted comfortably without assistance of other parts of the body. It is suggested that any design of lifting to over this height should be carefully considered because it will cause movement of the spinal column. Although the movement of the spinal column may provide a great assistance to the lifting activity in some situations, the lower back of the spinal column is the most easily injured site during manual material handling.

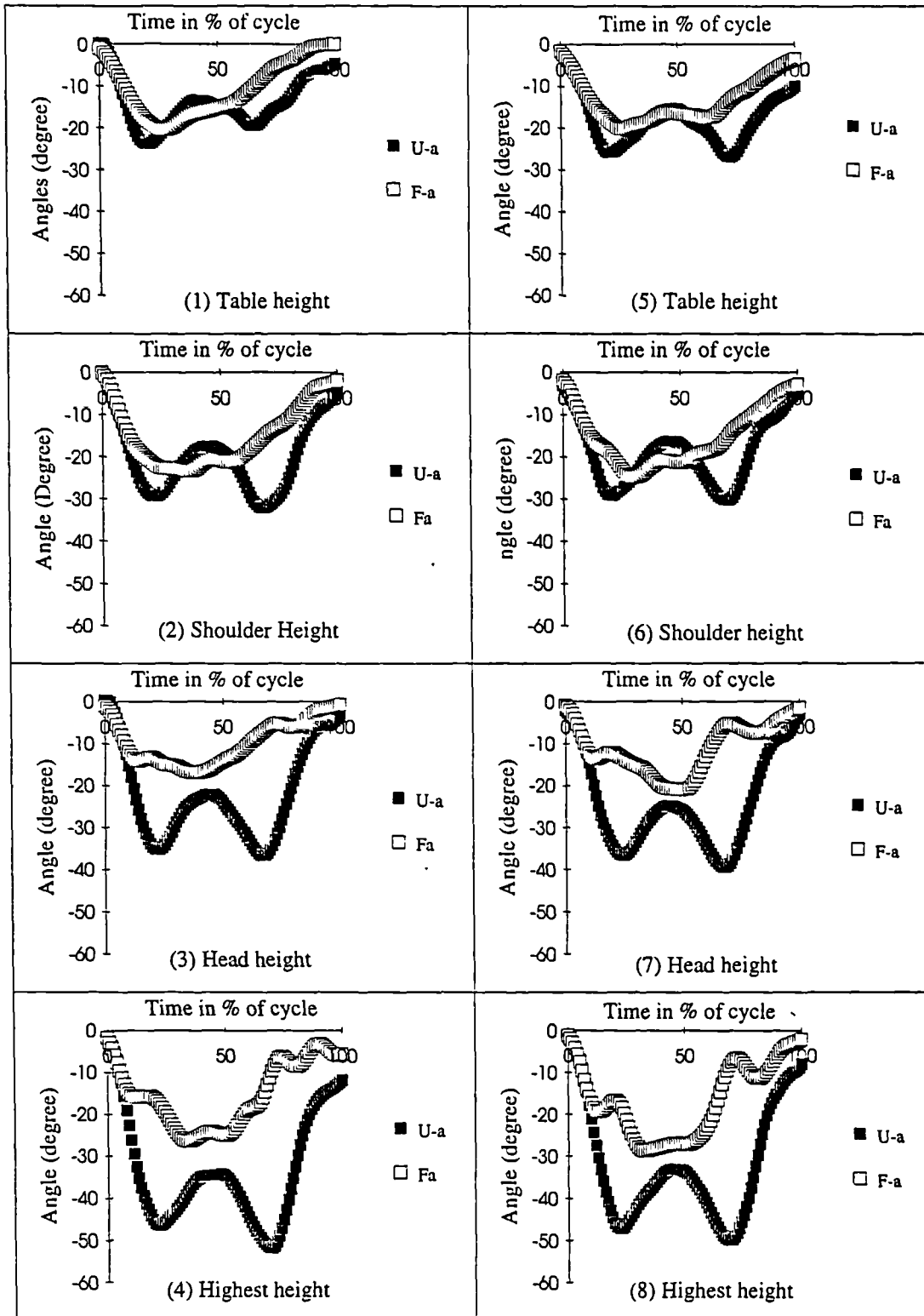
The mean and standard deviations of the maximum rotation angles of the upper arm for the lifting of a 1kg book are given in Table 6.3. Because the results are obtained from normal subjects it gives a general range of upper arm movements for the lifting activities. It is expected that these results can form a data base for clinical reference when assessment of the functional movement of the upper arm and the ability of doing activities of daily living is required.

Table 6.3 Mean and standard deviation of Maximum rotation angles (in degrees) of upper arm for lifting a 1kg book to four different heights.

	Table (Sd)	Shoulder(Sd)	Head (Sd)	Highest (Sd)
Flexion	37.3° (8.0)	65.2° (5.3)	100.7° (8.2)	118.7° (6.7)
Abduction	25.6° (10.3)	44.2° (11.6)	113.1° (6.6)	137.0° (7.2)
Rotation	64.6° (14.9)	66.6° (8.5)	63.6° (8.3)	63.3° (4.1)

6.1.1.3 Elbow angle

One of the important parameters describing forearm movements is the elbow angle which is the angle between the longitudinal axes of upper arm and forearm. The calculated elbow angles for the lifting activities are given in Figure 6.5. It can be seen that the lifting phase can be marked from 0 to 44% ($\pm 3.4\%$) of the full cycle, and the lowering phase marked the rest of the full cycle. The results show that the variation of the elbow angle is a little quicker during the lifting phase than the lowering phase. To achieve the quicker elbow angular movement, larger joint moments and greater muscle activity are required. The lifting phase and lowering phase can be further divided into two sub-phases, elbow flexion phase and elbow



Lifting a 1kg book

Lifting a 2kg book

Figure 6.6 Axial rotation angles of upper arm and forearm during lifting activities

U-a: Upper arm

F-a: Forearm

extension phase. In the elbow flexion phase the elbow angle decreases and in the elbow extension phase the elbow angle increases. During the lifting phase the forearm first flexed to the smallest elbow angle, then extended to the end of the lifting phase reaching a peak elbow angle at the target height. It is evident that the peak elbow angle at the end of the lifting phase increases with the height of lifting. During the lowering phase, the forearm first flexed to the smallest elbow angle of the lowering phase and then extended to the end of the full cycle.

It is interesting to find that the smallest elbow angle in the lowering phase decreases with the increase of the height of lifting. The result may be explained as follows. As the book is lifted higher, greater extension of the forearm is required during the lifting phase, which will increase the moment lever arm between the book and the elbow and shoulder joints, and consequently increases the moments on the elbow and shoulder joints and the muscle tensions. Therefore, the elbow flexes more during the lowering phase and reduces the lever arm and consequently reduces the elbow and shoulder joint moment and the tension of muscles. The results also indicate the important effects of functional movement of the forearm in manipulating the joint loads during the lifting activity.

6.1.1.4 Axial rotation angles of upper arm and forearm

Using the new method described in Section 5.5, the axial rotation angles of the upper arm and forearm about their longitudinal axes were calculated and are given in Figure 6.6, where the positive and negative values denote internal and external rotations respectively with respect to the initial arm position at the beginning of the tests.

It can be found that the axial rotations of the upper arm and forearm have nearly the same patterns for lifting a 1kg book and a 2kg book. For this reason, only variations of axial rotation angles with respect to the different heights of lifting are discussed.

The axial rotation angles of the upper arm are all negative during the full cycle of the lifting activity, which means that the axial rotations are external rotations. In each case of lifting, the upper arm rotated externally from the beginning to the middle of the lifting phase then rotated internally to the end of the lifting phase. In the lowering phase, the upper arm first rotates externally to the middle of the lowering phase then rotated internally to the original position at the end of activity. The maximum external rotation angles in the middle of the

lifting phase or the middle of the lowering phase increase with the height of lifting and the maximum values for each height of lifting are given in Table 6.4 with standard deviations.

Table 6.4 Maximum external rotation angles (degrees) of upper arm during lifting activity.

	Table (Sd)	Shoulder (Sd)	Head (Sd)	Highest (Sd)
Lifting a 1kg book	23.8 (9.9)	32.0 (17.2)	36.6 (14.2)	51.7 (21.1)
Lifting a 2kg book	26.8 (12.0)	30.2 (15.2)	39.4 (17.6)	49.8 (19.3)

From Figure 6.1 to 6.5, it can be found that the increase of the maximum external rotation angle of the upper arm is due to the increase of flexion and abduction of the upper arm. The internal rotation angle of the upper arm in the lifting phase is due to the extension of the forearm.

Figure 6.6 shows that the forearm axial rotation angles are all negative during lifting to the different heights. The mean values of maximum external rotation angles of each height of lifting are given in Table 6.5 with the standard deviations. It can be seen that the maximum external rotation angles do not change significantly with the lifting height except for the highest height. The results indicate that the axial rotation of the forearm has no direct relationship with the height of lifting, which is in agreement with the fact that the forearm can be more freely axially rotated than the upper arm.

Table 6.5 Maximum external axial rotation angles (degree) of forearm during lifting activities.

	Table (Sd)	Shoulder (Sd)	Head (Sd)	Highest (Sd)
Lifting a 1kg book	20.4 (9.3)	23.3 (12.2)	17.0 (10.3)	26.5 (11.6)
Lifting a 2kg book	20.1 (15.7)	24.8 (16.1)	21.0 (13.8)	28.8 (16.1)

6.1.1.5 Book centre velocity and acceleration

The purpose of the lifting activity is to move the book to several heights. The effects of the lifting can be presented by the velocities and accelerations of the book mass centre in three dimensional space. In this section, the velocities and accelerations of the book mass centre in the trunk reference frame are presented. Instead of giving the velocities and accelerations in a time series, the variations of accelerations with velocities are given in phase planes in Figure 6.7a for the lifting of a 1kg book, in which both lifting and lowering phases are included.

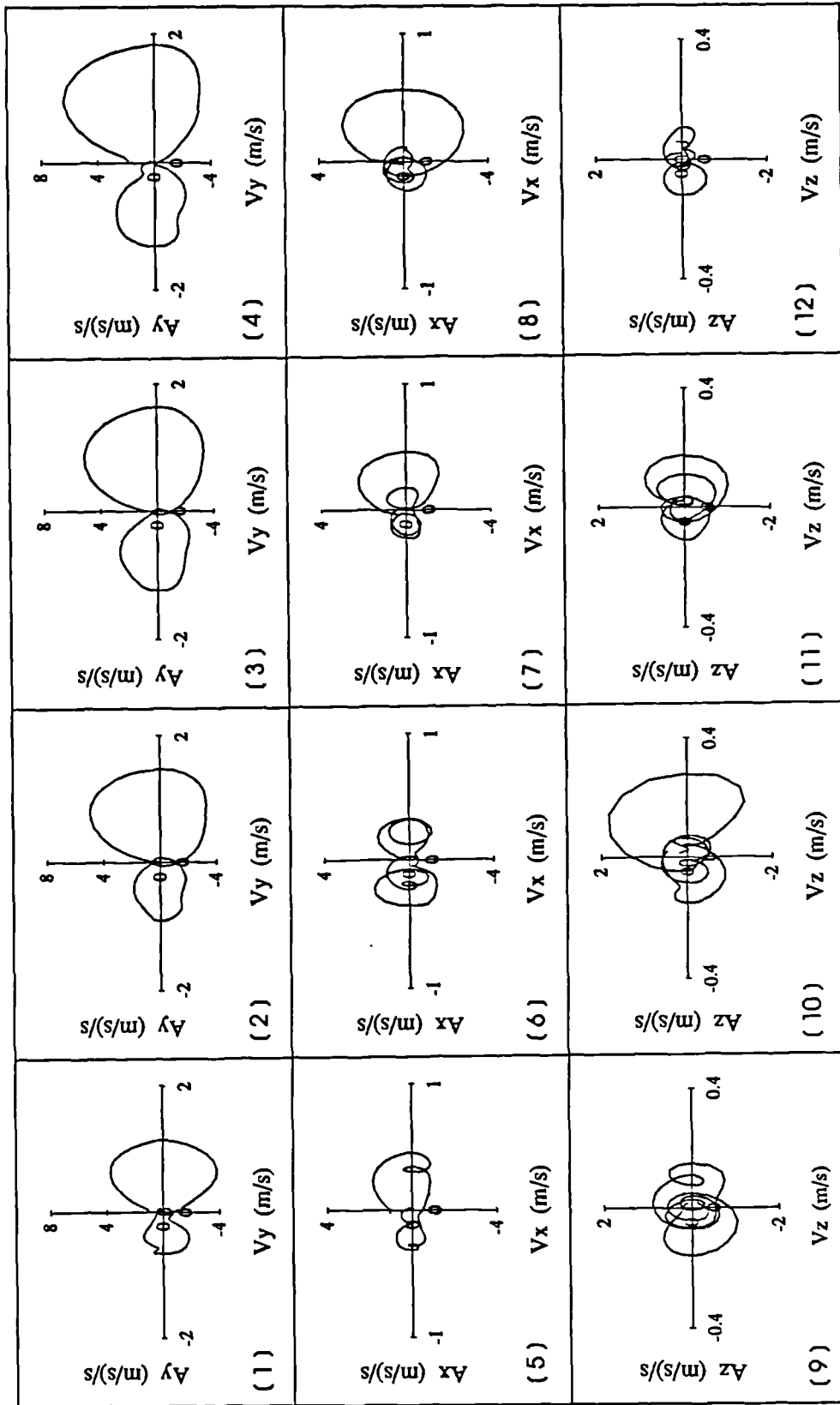


Table height Shoulder height Head height Highest height

Figure 6.7a Phase plane view of book centre velocities and accelerations for the lifting of a 1kg book

The major movement of the book during the lifting activity is along the vertical axis (y-axis). The vertical velocity and acceleration in V_y - A_y plane describes two loops (Figure 6.7a [1]-[4]), one on the right side of each figure and another on the left side. The right loop represents the lifting phase, and the left loop represents the lowering phase. It can be seen that the right loop is bigger than the left loop which indicates that the book moves at a greater velocity and acceleration in the lifting phase than in the lowering phase. Each vertical velocity and acceleration loop can be further divided into two phases, the velocity increase phase on the upper part of the loop and the velocity decrease phase on the lower part of the loop. Comparing with Figure 6.5, it can be seen that the increase and decrease phases of vertical velocity of the book correspond to the forearm flexion and extension phases, respectively. Therefore, the increase of vertical velocity of the book is related to flexion of the forearm, and the decrease of vertical velocity of the book is related to extension of the forearm.

In each increase and decrease phase of vertical velocity of the book, the acceleration changes its direction once. From the beginning of the lifting phase, the book is accelerated to the maximum value of acceleration at nearly the middle point of the velocity increase phase, and from that point the book is decelerated to zero acceleration at the end of the velocity increase phase (with maximum value of velocity). In the decrease phase of vertical velocity, the book is accelerated in the downward direction ($-A_y$) to maximum negative acceleration at the middle point of the decrease phase of vertical velocity, then decelerated to nearly zero velocity and acceleration at the target.

Another point which can be observed from Figure 6.7a [1]-[4] is that the absolute value of acceleration in the vertical velocity increase phase is greater than the corresponding value in the vertical velocity decrease phase for the lifting to shoulder, head, and highest height. It is interesting to find that the maximum acceleration in the vertical velocity increase phase increases with the height of lifting, while in the decrease vertical velocity phase, the maximum acceleration has nearly the same values for the four different height of lifting. Comparing with the results of elbow angles in Figure 6.5, it can be concluded that the forearm flexion phase is a much more accelerated process than the forearm extension phase, especially when the lifting height is increased. Also, flexion of the forearm results in greater vertical acceleration on the book mass centre than the extension of the forearm. The exception to this result occurred during the lifting to table height, where the accelerations in both increase and

decrease phases of vertical velocity have nearly the same values, which may be related to the small flexion angles during the lifting to table height.

In the lowering phase, the book vertical velocities and accelerations have the same patterns as in the lifting phase, except smaller values and opposite direction. The smaller velocities and accelerations in the lowering phase are in agreement with the finding in section 6.1.13 that the lifting phase is shorter than the lowering phase. The results indicate that in order to overcome the gravity of arm and book in the lifting phase, more muscle tension is required to accelerate the book for reducing the duration of the gravitational force and moment which acted on the elbow and shoulder joints. It has been found that the lifting phase is shorter than the lowering phase in section 6.1.1.3 (Figure 6.5).

The velocities and accelerations in the posterior-anterior direction are given in the V_x - A_x plane (Figure 6.7a [5]-[8]), where the right side of the A_x axis represents the lifting phase, and the left side represents the lowering phase. Two major differences can be found by comparing the Figure 6.7a [5]-[8] with the Figures 6.7a [1]-[4]. First the posterior-anterior velocities and accelerations are smaller than the vertical velocities and accelerations. Second, there are two loops (generally) in each lifting and lowering phase, respectively.

The double loops in each lifting and lowering phase in V_x - A_x plane imply that the book mass centre changed its direction of displacement in the posterior-anterior direction. This result is in agreement with the observations from the stick diagram of Figure 6.1. The changes of the direction of displacement are observed as the backward movement in the lifting phase and the forward movement in the lowering phase. The backward and forward movement of the book seem to contradict the purpose of lifting and lowering, because the purpose of lifting is to move the book upward and forward to the target, while the lowering is to move the book downward and backward to the starting position. However, the backward and forward movements of the book are required. If it is assumed that any human movement is performed in an optimum way as it is performed most comfortably, then according to the above results the optimum idea can not be understood as an optimum route of the displacement. The optimum route should be the nearest route from the starting to the end position. In the lifting and lowering phases this route should involve the straight forward and straight backward movements, respectively. In the study of human walking, Inman (1981) stated: *the human body will integrate the motions of the various segments and control the activity of muscles*

so that the metabolic energy required for a given distance walked is minimised. For lifting, the backward and forward displacement in the lifting and lowering phases can be assumed to be controlling the joint moments and muscle activity in order to minimise the energy consumption.

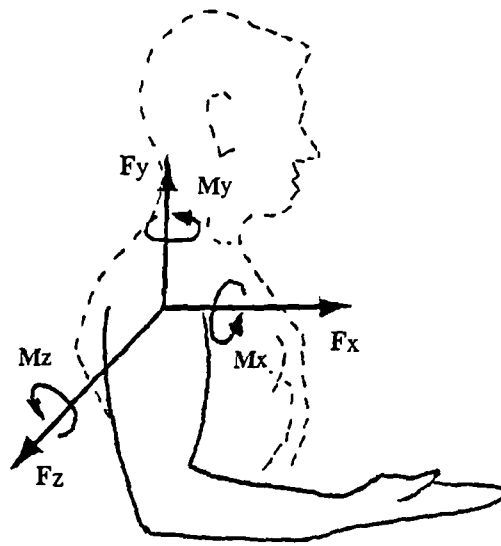
As is seen in Figure 6.7a [9]-[12] the transverse velocities and accelerations in the Vz-Az plane have the most complex shapes. Generally a number of loops with very small magnitude describe the variation of transverse velocity and acceleration. This result indicates that the book experienced a number of changes of acceleration and deceleration in the transverse direction. Because the transverse displacement of the book is not the major movement of the lifting activity, the oscillation of velocity and acceleration of the book centre in the transverse direction can be explained as an adjustment of the transverse movement for keeping a stable and smooth movement of the book in the major directions.

The Vy-Ay and Vx-Ax loops for the lifting a 2kg book in Figure 6.7b [1]-[8] are smaller than the corresponding loops in Figure 6.7a [1]-[8]. The result indicates that the 2kg book is lifted at smaller velocity and acceleration than the 1kg book in the two major directions of movement for lifting to the same height. Other characteristics of the results in Figure 6.7b are similar with that in Figure 6.7a, therefore they are not discussed again.

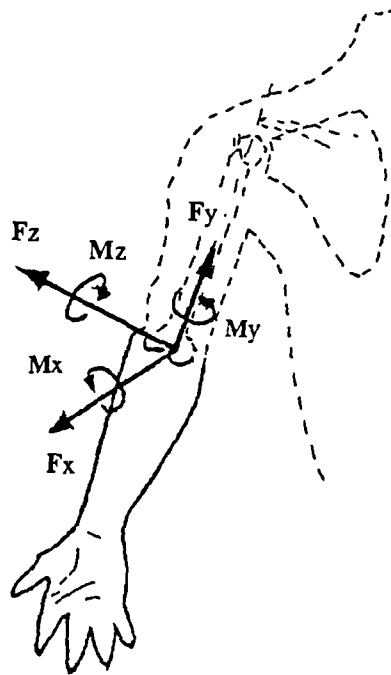
6.1.2 Kinetic Results and Discussions I - Shoulder Forces and Moments

The kinetic results given in this section are the shoulder forces and moments which are considered to act on the proximal end of the upper arm segment and are expressed in the trunk coordinate system defined in Section 5.2.2.

The contributions to the shoulder forces and moments during the lifting activities can be divided into the inertial and gravitational effects or the arm and book (the weight) effects. In order to investigate how the different factors influence the shoulder loads, not only the total shoulder forces and moments but also the shoulder forces and moments due to each factor are given and discussed in this section by the following arrangements: three-dimensional shoulder forces; inertial and gravitational effects on the shoulder forces; the three-dimensional shoulder moments; three-dimensional inertial moments on shoulder; inertial to total shoulder moment ratios; arm and book effects on shoulder moments.

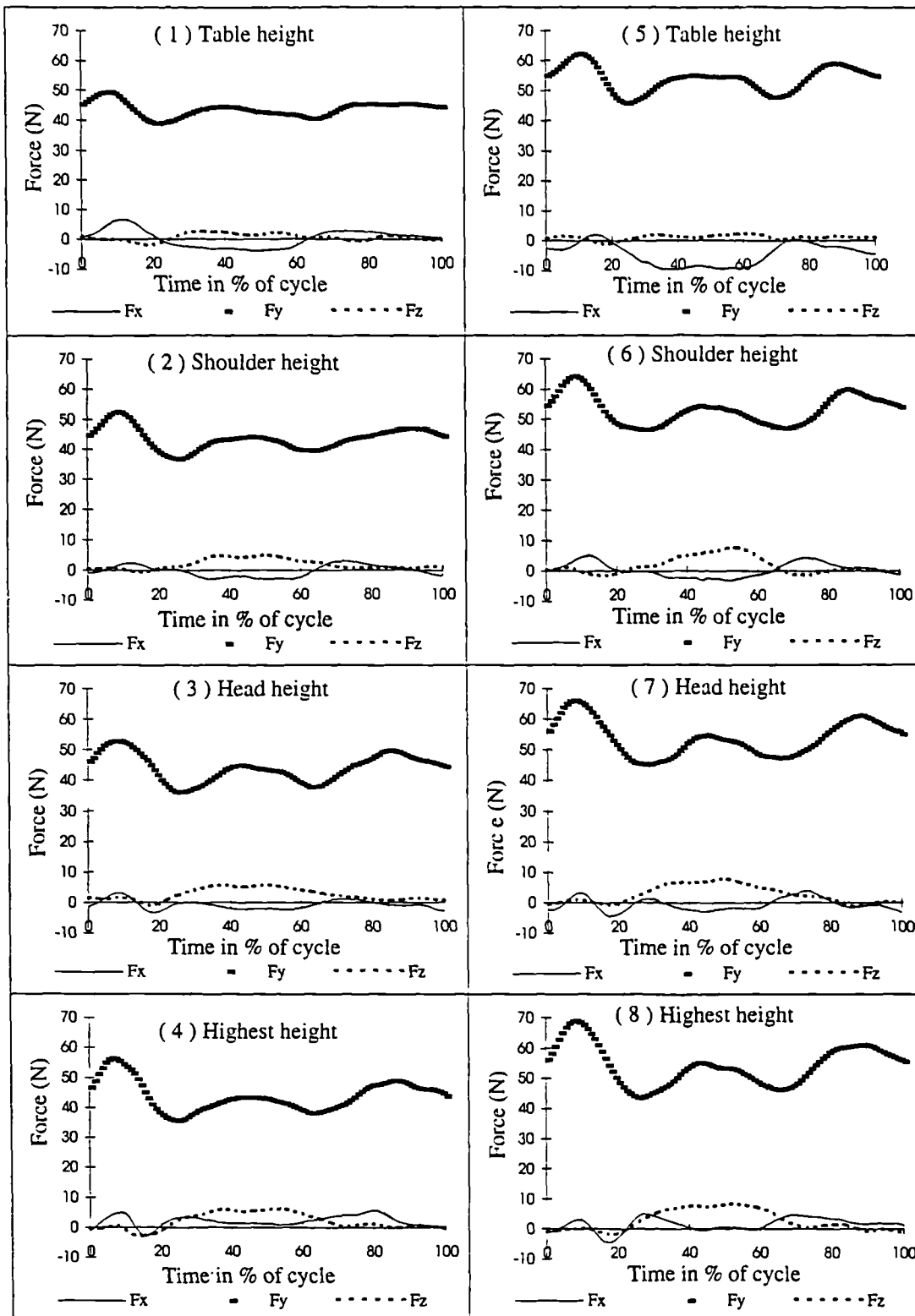


(a)



(b)

Figure 6.8 Forces and moments on the shoulder and elbow joints
 (a) The shoulder forces and moments at the proximal end of the upper arm are given in the trunk coordinate system
 (b) The elbow forces and moments at the proximal end of the forearm are given in the upper arm coordinate system



Lifting a 1kg bok

Lifting a 2kg book

Figure 6.9 3-D shoulder forces during lifting activities

Fx, Fy, Fz are expressed in the trunk coordinate system

6.1.2.1 Three-dimensional shoulder forces

The three-dimensional shoulder forces during the lifting activities are given in Figure 6.9, where positive F_x , F_y , and F_z direct forward, upward and from left to right, respectively (Figure 6.8a).

The results show that the vertical force F_y is dominant and positive during the full period of the lifting activity primarily due to gravity. The wave form of F_y is due to the vertical inertial forces on the arm and book, because the directions of vertical inertial forces vary with time. It can be seen that the maximum F_y increases with the height of lifting.

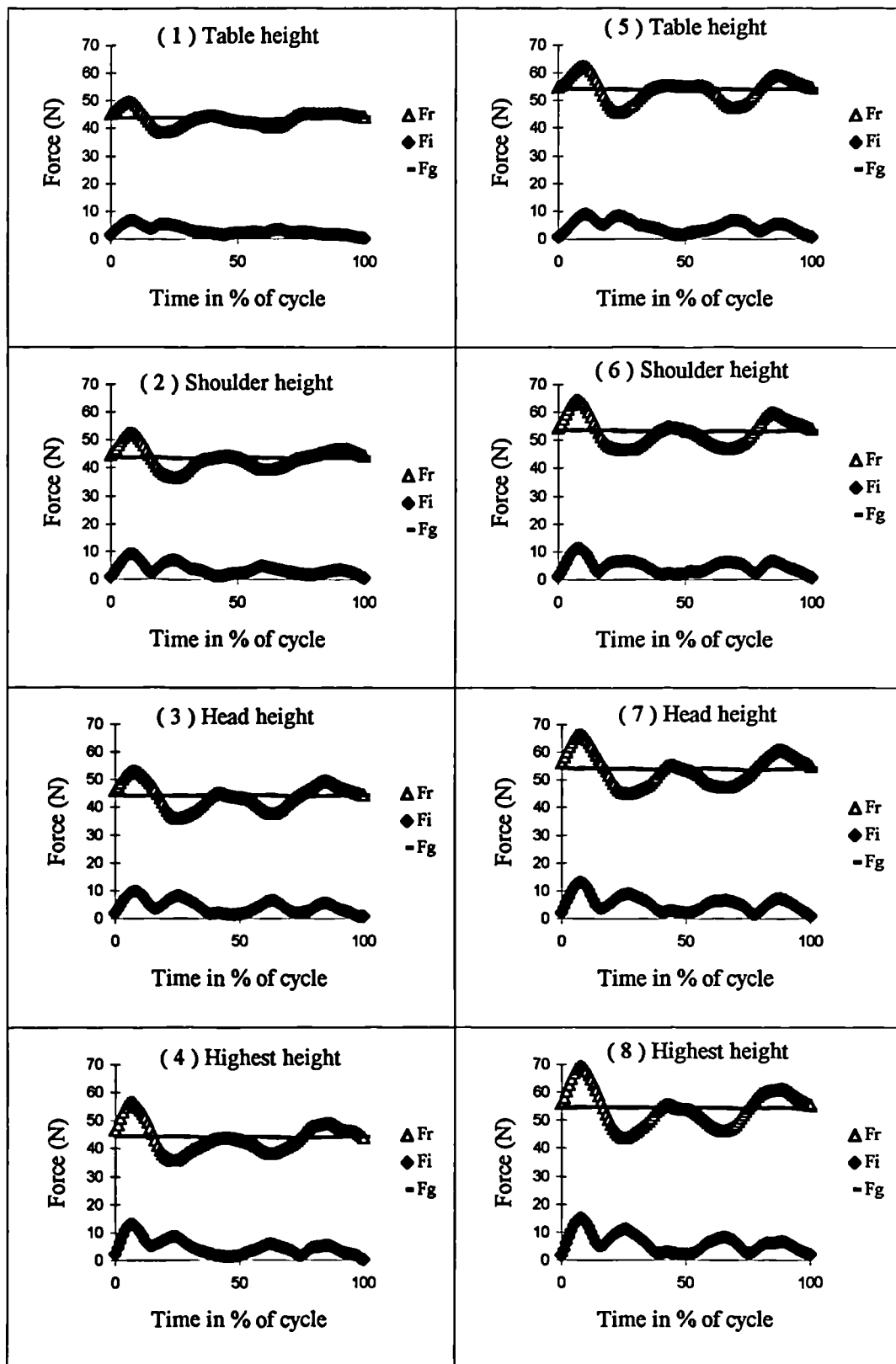
It can also be found that the anterior-posterior and left-right forces (F_x and F_z) are of low magnitude and change their signs during the activity. Only the inertial forces of the arm and book act in the anterior-posterior and left-right directions, therefore the result is in agreement with the low accelerations in the two directions. Quantitative results show that the maximum magnitude of F_x and F_z are all below 15% and 12%, respectively, of maximum F_y during the lifting activities.

6.1.2.2 Gravitational and inertial effects on shoulder forces

The resultant inertial and gravitational forces (F_i and F_g) on the shoulder are given in Figure 6.10 with the resultant total shoulder force (F_r). It can be seen that gravitational forces are dominant for each case of lifting and the gravitational forces do not vary with time and lifting height.

The magnitude of the resultant inertial force F_i on the shoulder is much lower than the magnitude of the resultant gravitational force. The maximum magnitude of inertial force occurs during the lifting to the highest height and values as 29% and 27% of the gravitational force for the lifting of a 1kg and a 2kg book, respectively.

It is seen that the resultant total shoulder forces are combined by the inertial and gravitational forces. Since the gravitational force does not vary with time and lifting height, the maximum total shoulder force coincides in time with the maximum inertial force, and increases with the height of lifting. The ratios of the maximum inertial force to the maximum total force are given in Table 6.6. The results indicate that the inertial shoulder force can reach between 14% to 23% of the total shoulder force for the lifting of a 1kg or 2kg weight.

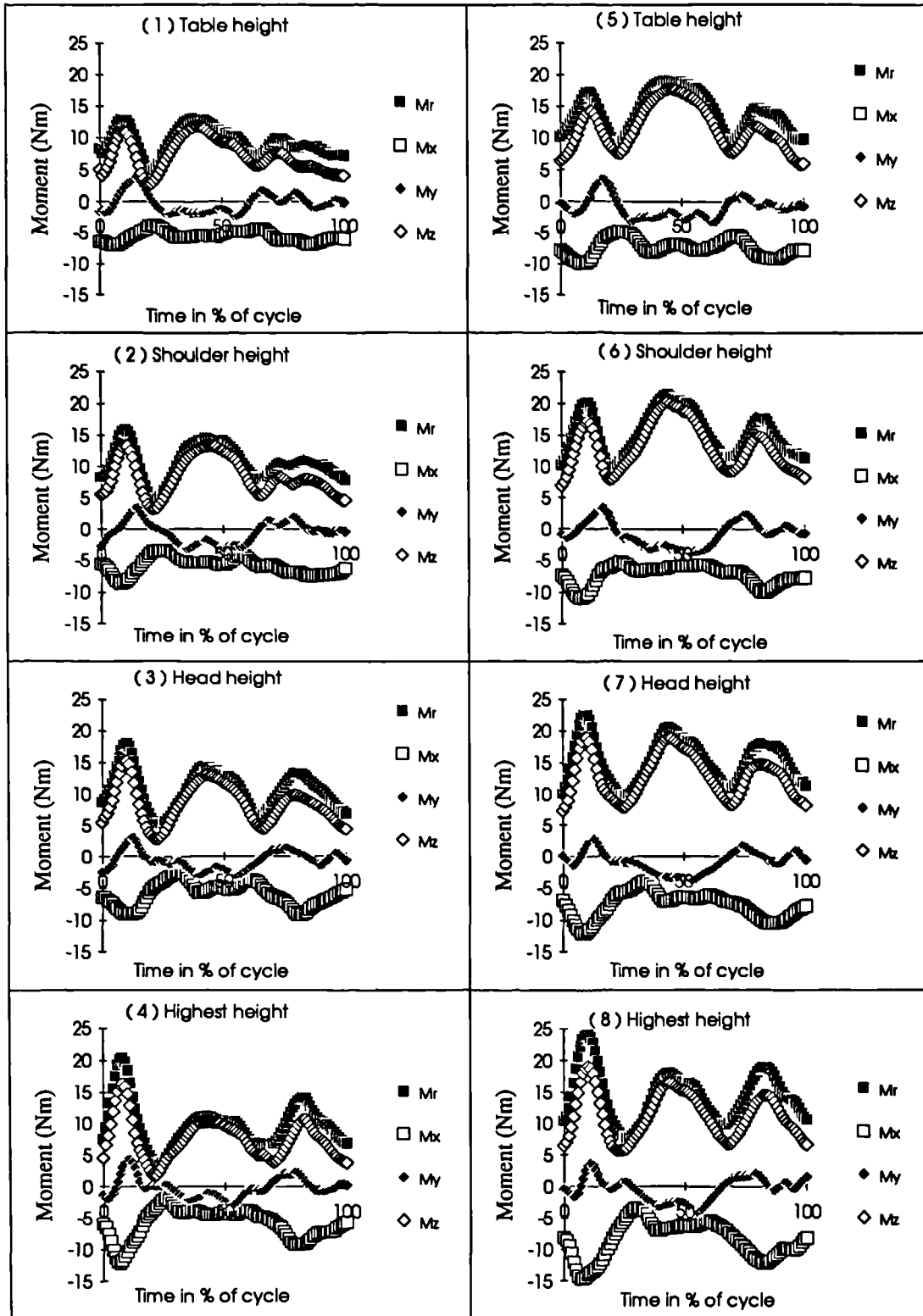


Lifting a 1kg book

Lifting a 2kg book

Figure 6.10 Inertial and gravitational forces on shoulder

Fr: resultant total force; Fi: resultant inertial force; Fg: resultant gravitational force.



Lifting a 1kg book

Lifting a 2kg book

Figure 6.11 3-D Shoulder moments of lifting activities.

Mr: resultant; Mx: adduction/abduction; My: internal/external; Mz: flexion/extension

Table 6.6 The maximum resultant inertial shoulder force to the maximum resultant total shoulder force ratios.

	Table height	Shoulder height	Head height	Highest height
Lifting a 1kg book	0.135	0.172	0.186	0.228
Lifting a 2kg book	0.144	0.174	0.196	0.217

6.1.2.3 Three-dimensional shoulder moments

The resultant shoulder moments and their components about the three axes of the trunk coordinate system for the lifting of a 1kg and 2kg book are given in the Figure 6.11. The positive/negative signs of M_x , M_y and M_z represent the adduction/abduction, internal/external rotation and flexion/extension moments on shoulder joint, respectively according to the movement of the upper arm it may cause (Figure 6.8a).

A number of general features can be found from these figures. The flexion-extension moment has a similar pattern with the resultant moment and its magnitude is a little lower than the magnitude of the resultant moment. The flexion-extension moments are always positive during the full cycle of the lifting, which illustrates that only a flexion moment acts on the shoulder joint in the sagittal plane. The results indicate that the dominant moment on the shoulder joint for lifting is the flexion moment which is in agreement with the fact that the major movement of the arm during lifting is flexion. In contrast with this, the adduction/abduction moments are always negative, which indicates that only an abduction moment acts on the shoulder joint in the coronal plane. To generate the flexion and abduction moments, the activities of prime humeral elevators, deltoid and supraspinatus are required. The internal-external rotation moment on the shoulder about the vertical axis of the trunk coordinate system varies around zero.

Since the resultant and flexion moments have nearly the same patterns and values, the results of resultant and flexion moments are discussed together. The resultant and flexion moments have three peak values in the full cycle of the lifting activity. The first and third peak values occur in the lifting and lowering phases respectively, the second high peak value is in the middle of the full cycle when the book is lifted to the target height.

The second peak resultant and flexion moments on the shoulder is mainly due to gravity of the arm and book, because when the book is lifted to the target, its vertical acceleration is reduced to nearly zero (Figure 6.7a and 6.7b). Therefore the inertial effect on the shoulder moment nearly vanishes at this point.

It can be seen (Figure 6.11) that the first high peak of the resultant/flexion moment occurs at about 10% of full cycle. Looking at Figure 6.5 and 6.7a, it can be seen that this point is just within the forearm flexion and the book vertical velocity increase phases when the book is accelerated. Therefore, the first peak resultant/flexion shoulder moment is mainly due to the inertial effect of the arm and book. For the same reason the third peak resultant/flexion moment in the lowering phase is also due to the inertial effects of the arm and book.

During the lifting of a 1kg book to table height, the first and second peak resultant/flexion moments have nearly the same values, while the differences between the first and the second peak resultant/flexion moments increase with the height of lifting, which is mainly due to the increase of the first peak values. The increase of the first peak resultant/flexion moment is related to the vertical accelerations of the book and arm, which increase with the height of lifting. Therefore, it can be concluded that for the lifting to above the table height, the maximum resultant/flexion shoulder moments increase with the height of lifting due to the contributions of the inertial effect (further discussion are given Section 6.1.2.5).

When the weight is increased, such as the lifting of a 2kg book (Figure 6.11[5], [6]), the maximum resultant/flexion shoulder moments during the lifting to table and shoulder heights occur at the second peak value instead of at the first peak value in the case of lifting a 1kg book to the same heights (Figure 6.11[1], [2]). As discussed above the second peak resultant/flexion moment is mostly due to the gravitational effect of the arm and book, therefore the result indicates that the lifted mass has a significant effect on the shoulder moment for the lifting to table and shoulder height.

For the lifting of a 2kg book to the head and highest heights, the maximum resultant/flexion shoulder moment occurs at the first peak value again but the difference between the first and second peak value is smaller than the lifting of a 1kg book. This result indicates that the contribution of the inertial effect decreases with the increase of the lifted mass. This can be easily understood, for example, a light weight can be easily lifted at a higher velocity and acceleration than a heavy weight.

6.1.2.4 Three-dimensional inertial moments on the shoulder.

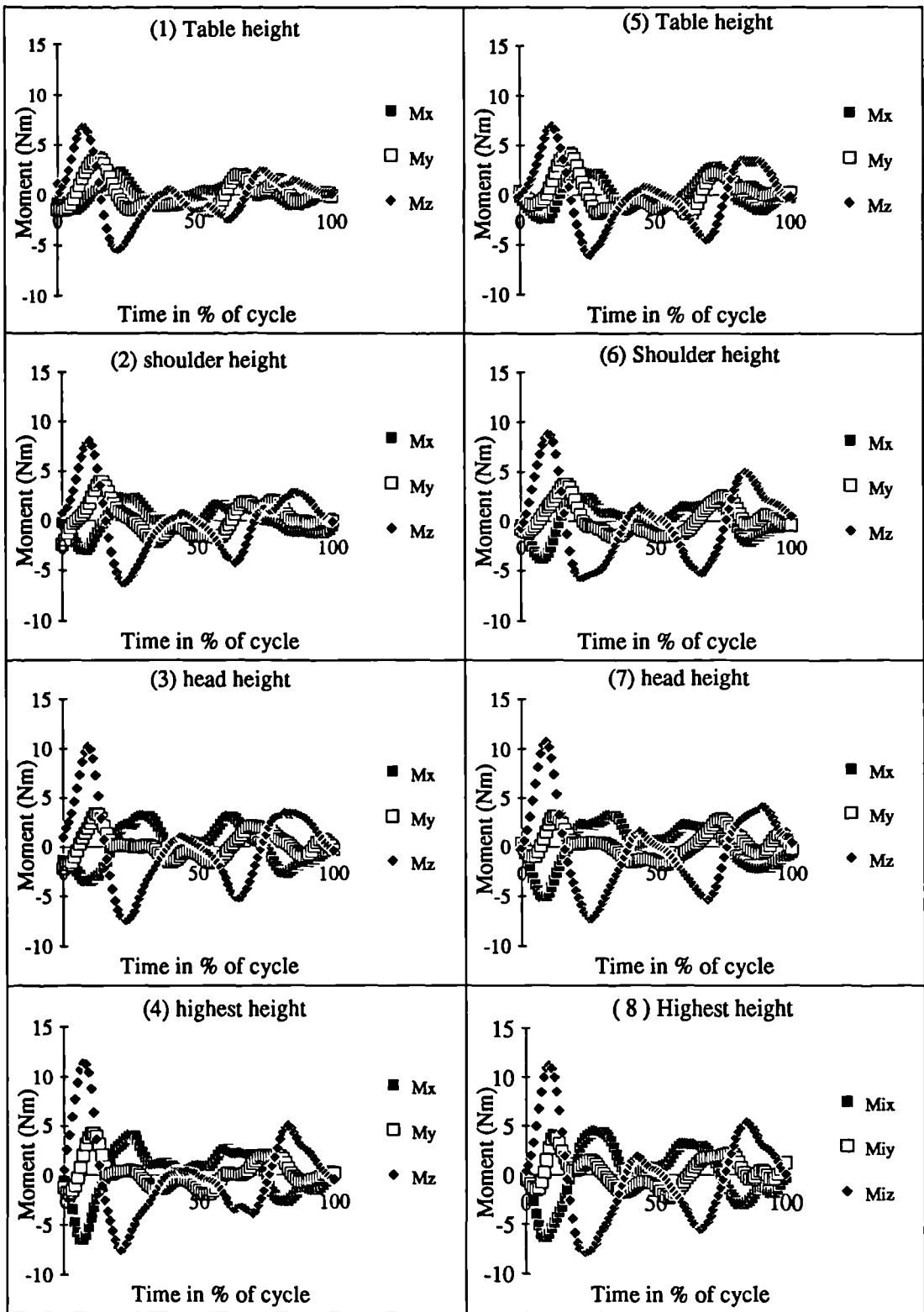
The three-dimensional inertial moments involving the combined inertial effects of arm and book on the shoulder are given in Figure 6.12. These inertial moments are expressed in the trunk coordinate system and the conventions are the same as those used in above section.

It can be seen that the dominant inertial moments on the shoulder during the lifting activities are the flexion-extension moments (+Mz) where the highest values occur in each case of the lifting. Peak inertial flexion moment (+Mz) occurs in the early lifting phase which corresponds to the vertical velocity increase phase of the book (Figure 6.7 and Figure 6.8). The peak flexion moments increase with the height of lifting. Significant increase of the peak flexion moment can be observed for lifting to the height below and above shoulder. Following the peak flexion moment, there is a peak extension moment (-Mz) in the lifting phase, which is related to the accelerations in the vertical velocity decrease phase of the book in Figure 6.7 and 6.8, and increases with the height of lifting.

In the lowering phase, there is also a peak flexion and a peak extension moment but with smaller values than the corresponding points in the lifting phase, because of the lower accelerations in the lowering phase than in the lifting phase observed in section 6.1.1.5.

It is interesting to find that there is no significant difference on the peak flexion/extension moments between lifting a 1kg and a 2kg book. This result is due to the fact that the heavier mass (2kg book) is lifted at lower accelerations than the light weight (1kg book). Because the inertial moment is proportional to the mass (and moment of inertial) and accelerations (linear and angular) of the segment and the lifted mass, the result may be further explained by an assumption that the decrease of acceleration is a trade-off with the increase of the lifted weight to keep an equivalent inertial moment. However, because only two levels of mass were tested in this study, further investigations are required on more levels of mass to testify whether the assumption is true for the general lifting activity.

The results also show that the magnitude of the inertial adduction/abduction moment (+Mx/-Mx) is lower than the inertial flexion/extension moment, and the abduction moment (-Mx) at the early lifting phase increase with the height of lifting which can be ranked as the second major inertial shoulder moment for lifting to above shoulder height. As with the flexion/extension inertial moments, there is no significant difference on the inertial



Lifting a 1kg book

Lifting a 2kg book

Figure 6.12 Inertial moments on shoulder during lifting activity

Mx: add-abduction moment; My: inward-outward moment; Mz: flexion-extension moment

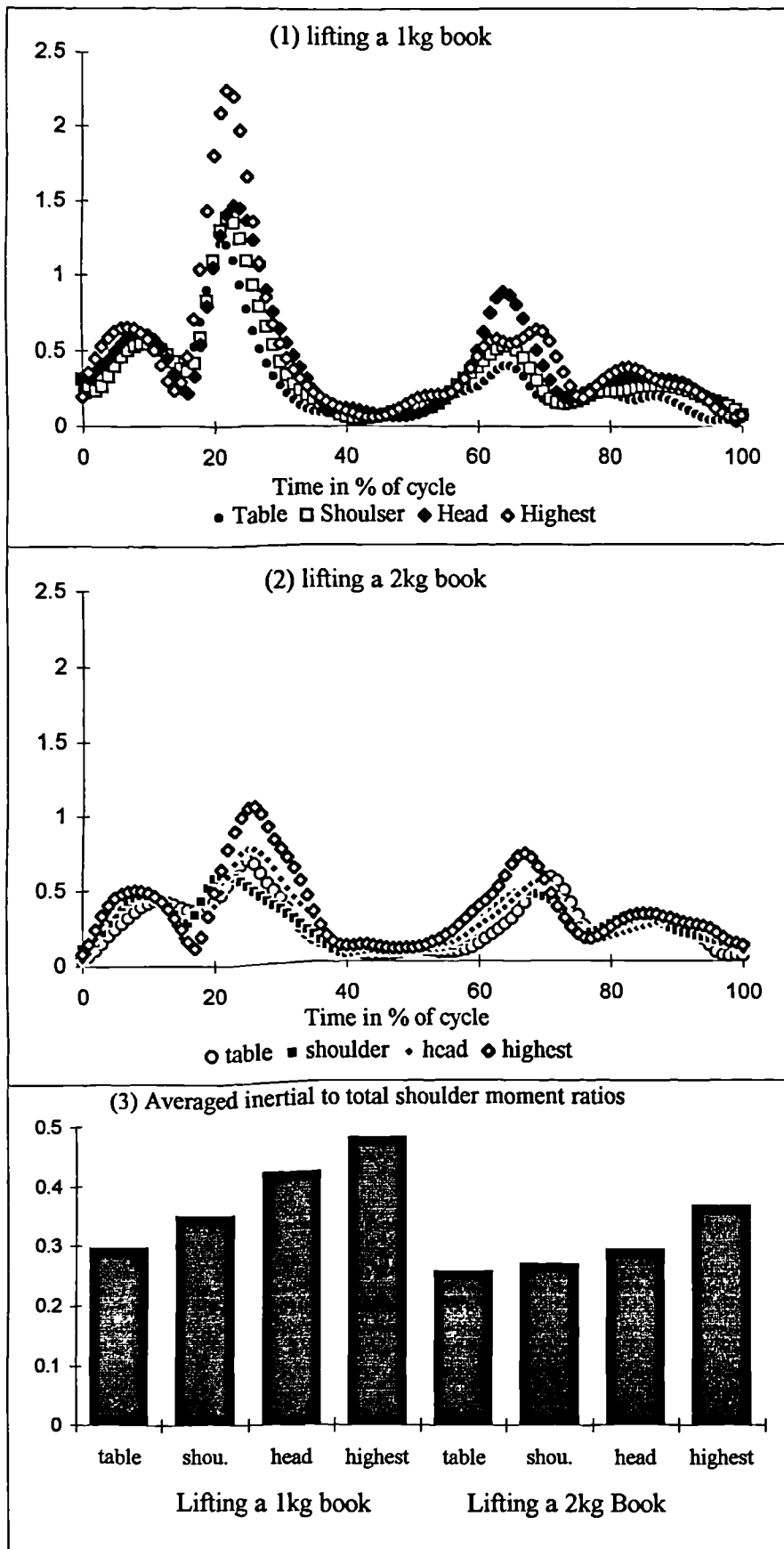


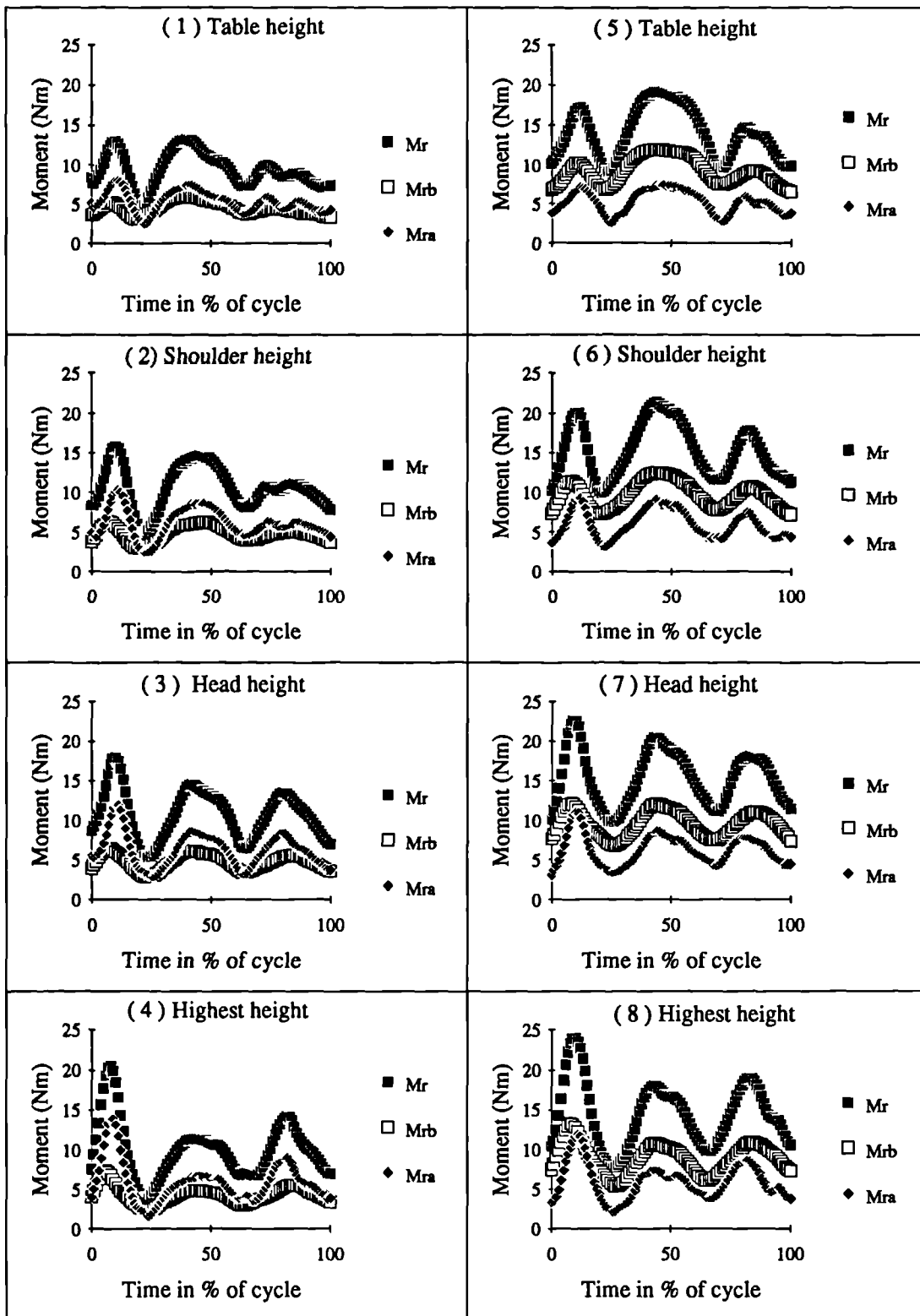
Figure 6.13 Inertial to total shoulder moment ratios

adduction/abduction moments between the lifting a 1kg book and a 2kg book, and the inertial adduction/abduction moments in the lowering phase are lower than in the lifting phase.

The inward/outward rotational moment (M_y) on the shoulder about the vertical axis of the trunk coordinate system does not seem to vary with either the mass of lifting or the height of lifting. The result is in agreement with the inward/outward rotations of the upper arm about the y-axis of trunk coordinate system, which varies little with the height of lifting (Figure 6.4). However the peak inward rotational inertial moment ($+M_y$) can be ranked as the second highest inertial moments during the lifting to below and involving shoulder height. The result reflects the important contribution of the inward/outward rotational inertial moment to the resultant inertial moment but the contribution decreases during the lifting to above shoulder height because of the increase of adduction/abduction moments.

6.1.2.5 Inertial to total shoulder moment ratios.

The resultant inertial shoulder moment to resultant total shoulder moment ratios at each instance of time are given in Figure 6.13(1) and 6.13(2), which vary greatly with time. In order to estimate the overall influence of inertial effects on the shoulder moment, the ratios in Figure 6.13(1) and 6.13(2) are averaged over time and the results are given in Figure 6.13(3). It can be seen that the averaged inertial to total shoulder moment ratio increases with the height of lifting, and the ratios are higher for lifting a 1kg book than lifting a 2kg book. The maximum ratio reaches 0.47 (47%) during the lifting of a 1kg book to the highest height, and the minimum ratio is 0.25 (25%) during the lifting of a 2kg book to the table height. The results indicate that the higher the mass to be lifted, the greater the inertial effect will contribute to the total shoulder moments, and the contributions of inertial effects to the total shoulder moment will decrease with the increase of lifted mass. Neglecting inertial effects in the biomechanical analysis of lifting activities will result in up to 47% (average) under estimating of the resultant shoulder moment for lifting a 1kg book to the highest height, and at least 30% lower (average) estimating of the resultant shoulder moment for lifting a 1kg book to table height. For the lifting of a 2kg book, the corresponding values are the 36% and 25 % respectively.



Lifting a 1 kg book

Lifting 1 2kg book

Figure 6.14 Book and arm effects on shoulder moments. Mr: resultant total moment; Mrb: resultant moment by the book; Mra: resultant moment caused by the arm.

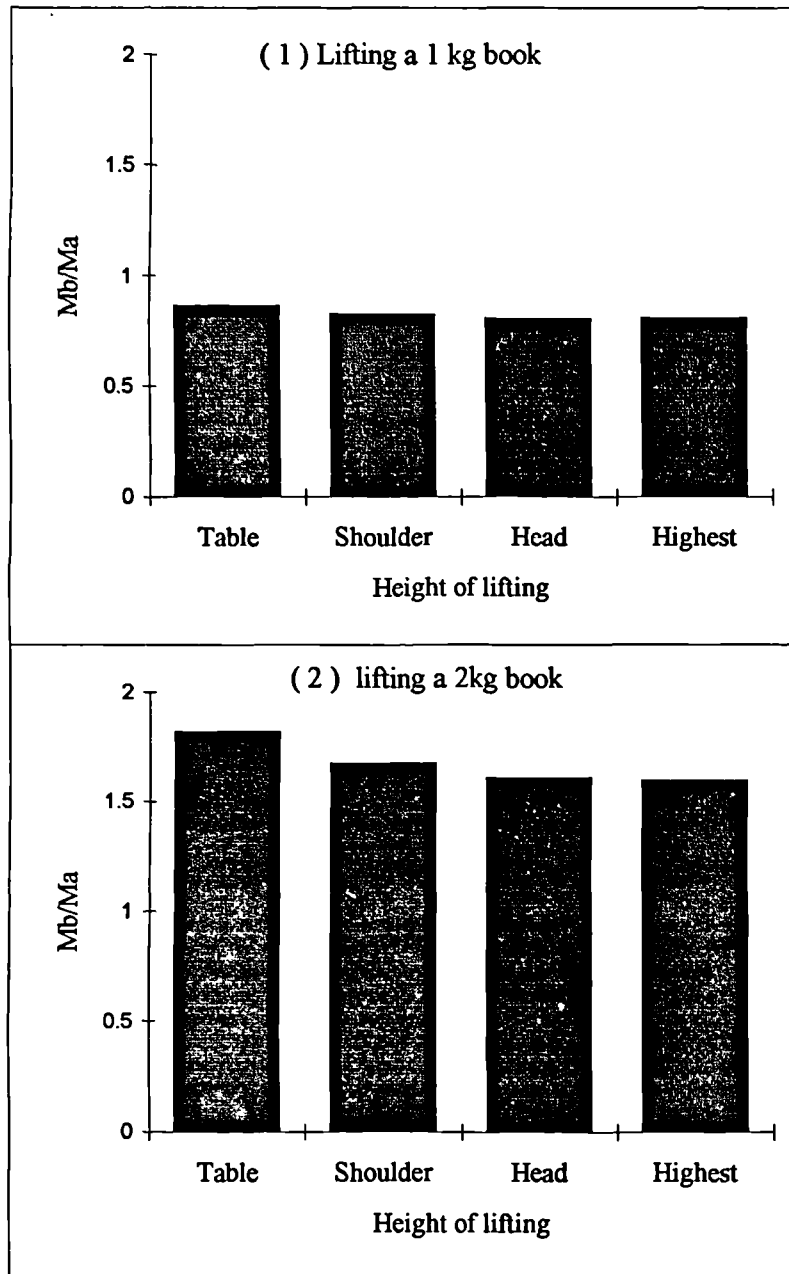


Figure 6.15 Averaged shoulder book moment to shoulder arm moment ratios

6.1.2.6 Arm and book effects on shoulder moments

In order to investigate the influence of the lifted mass on shoulder moments during the lifting activity, the resultant shoulder moments caused by arm and book effects (M_{ra} and M_{rb}) involving both inertial and gravitational effects were calculated and are given in Figure 6.14 with the resultant total shoulder moments (M_r).

It is interesting to find that the magnitude of resultant shoulder moment caused by the 1kg book is lower than that caused by the arm, while the magnitude of resultant moment caused by the 2kg book is higher than that caused by the arm. In order to quantitatively describe the effects of different mass on the shoulder moment, the ratios of resultant shoulder moment caused by the book to the resultant shoulder moment caused by the arm (M_b/M_a) were calculated at each instance of time, and the averaged ratios over the full period of time are given in Figure 6.15.

The results show that the ratios decrease with increase of lifting height, and the highest ratio occurs at lifting to table height. The 1kg book can produce a moment on the shoulder with values from at least 0.8 times to a maximum of 0.86 times the shoulder moment caused by raising the arm without any mass on the hand. The shoulder moment generated while lifting the 2kg book can increase from at least 1.6 times to a maximum of 1.8 times of the moment caused by raising the arm only.

The above results are useful information for clinicians and physiotherapists to design a training program for patients with upper limb disorders. For example, if a patient lifts a 1kg object to table height, it will cause 86% of additional shoulder moment than raising only the arm to the same height without any load. When lifting a 2kg object to table height, 181% of additional moment will act on the shoulder than raising the arm to table height without any object in the hand.

It should be noted that the arm effects on the shoulder moments may vary between subjects. For example a shorter or higher subject may cause a smaller or greater shoulder moment. However the book effects on the shoulder moment may also be varied with subject, a shorter or higher subject may have a shorter or longer lever arm from the book to shoulder joint, which can cause a smaller or greater shoulder moments. Since only six subjects and two masses were tested in this study, further investigations on more subjects and masses are required to find out how the two factors interact in a wider range of subjects.

6.1.3 Kinetic Results and Discussions II - Elbow Forces and Moments

The calculated results of elbow forces and moments are given and discussed in this section as follows: three-dimensional elbow forces; inertial and gravitational effects on elbow forces; three-dimensional elbow moments; inertial and gravitational effects on elbow moments; inertial to total elbow moment ratios; and arm and book effects on elbow moments. The 3D elbow forces and moments are considered to act at the proximal end of the forearm segment and are expressed in the upper arm coordinate system, defined in section 5.2.2.

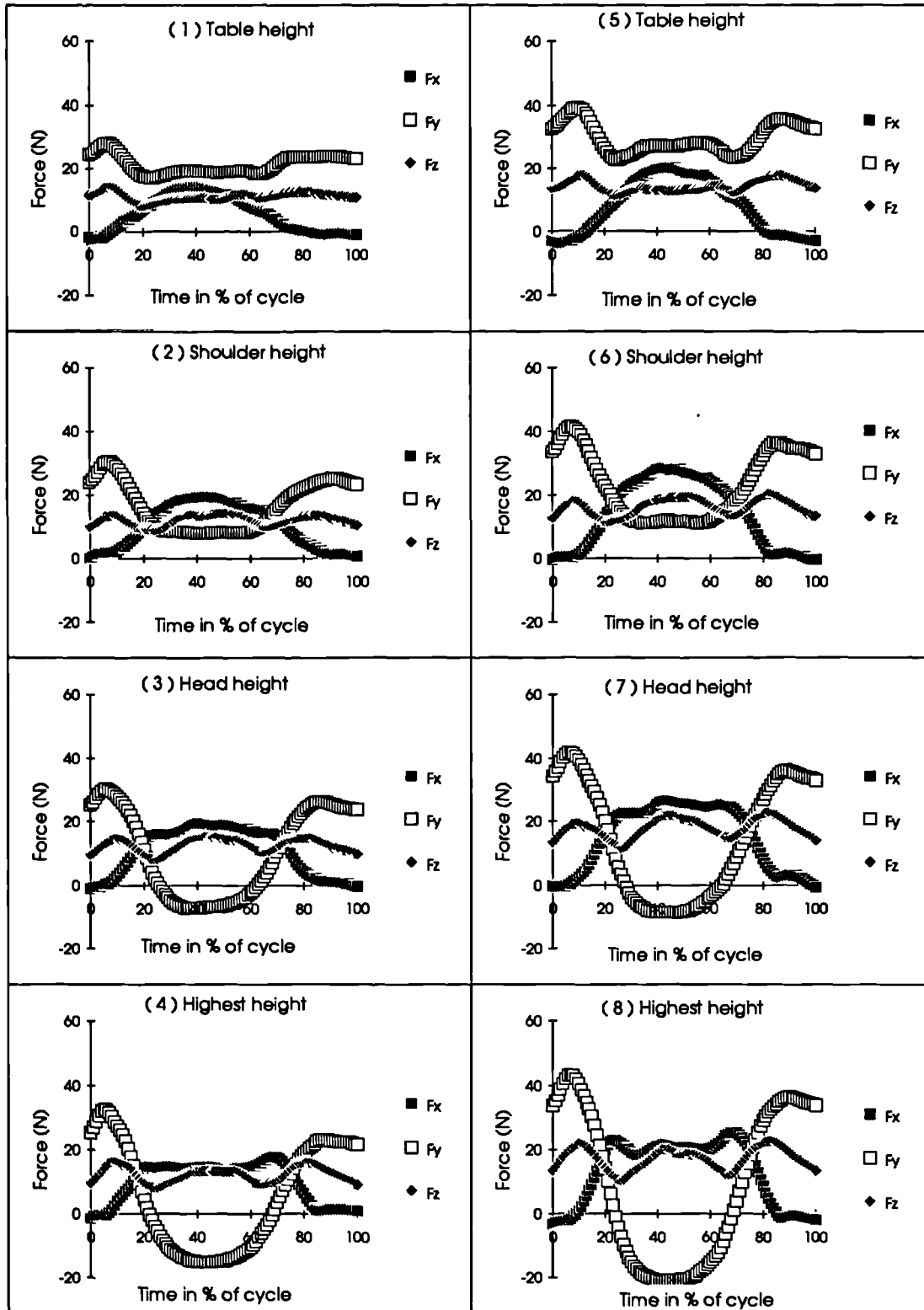
6.1.3.1 Three-dimensional elbow forces

The three-dimensional elbow forces are given in Figure 6.16, where the positive F_x directs forward when the forearm and upper arm are in the free hanging position with the palm facing forward, the positive and negative of F_y denote the tension and compression along the long axis of the upper arm, and the positive F_z directs from medial epicondyle to lateral epicondyle of the right arm (Figure 6.8b).

It can be seen that F_y increases from an initial positive value at the beginning of the activity to a maximum positive peak value in the early lifting phase, then it decreases to the minimum value at the end of the lifting phase. The maximum positive F_y increases with the height of lifting due to the inertial effects of the arm and the book. During the lifting to below shoulder height (table and shoulder heights) the minimum values are positive. However the minimum value becomes negative and increases in the negative side of zero during the lifting to above shoulder height (head and highest heights).

The F_y is generated mainly by the projections of gravitational and inertial forces of the forearm-hand and the book on the longitudinal axis of the upper arm, which changes its direction during the lifting activity. Because gravitational forces are constant in the vertical direction the changes of F_y are due to the directional variation of the long axis of the upper arm and the decrease of F_y may relate to the increase of the flexion and abduction angles of the upper arm.

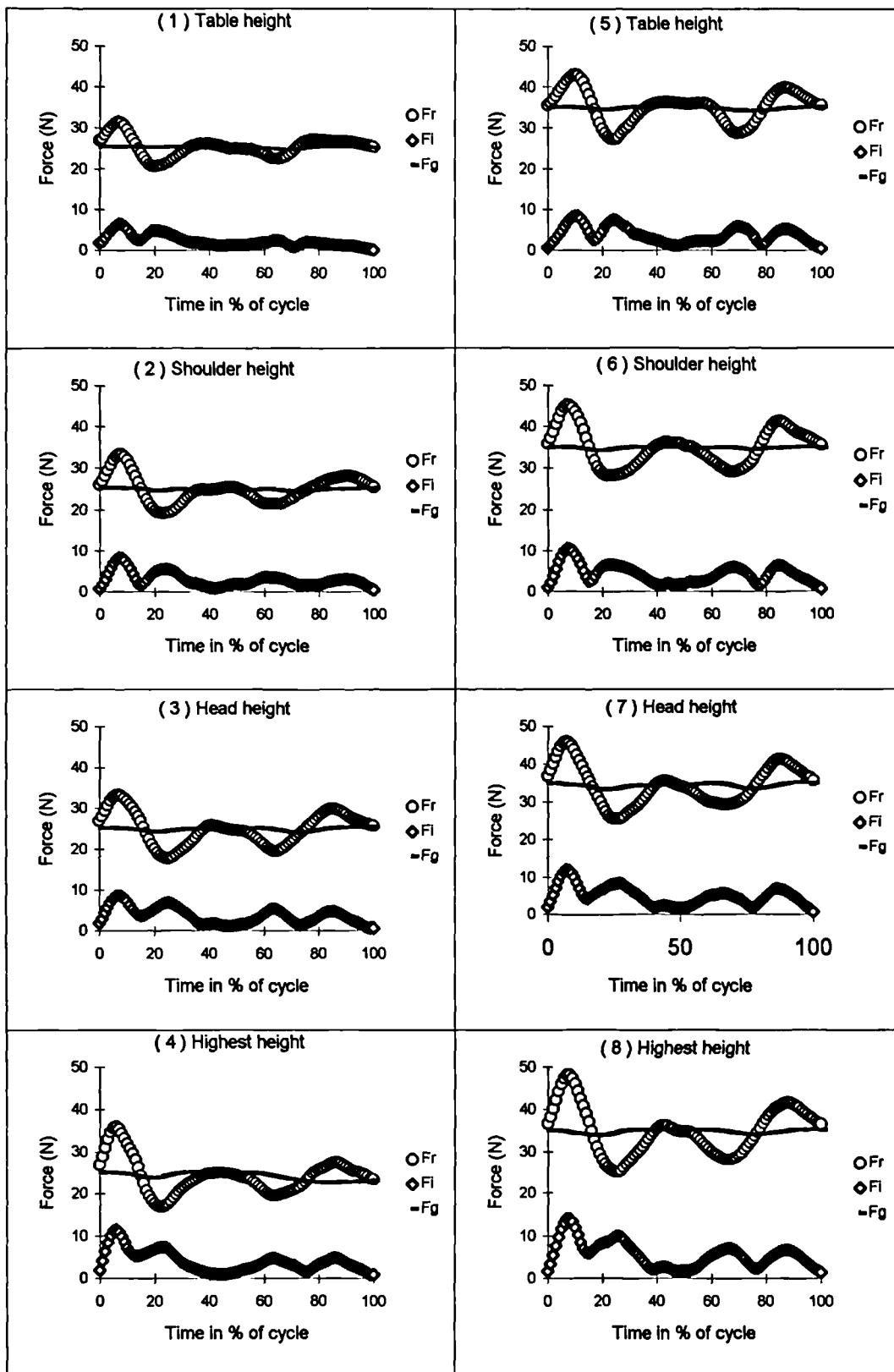
It has been found in section 6.1.1.2 that the maximum flexion and abduction angles of the upper arm are about 65 and 44 degrees during the lifting to the shoulder height, which indicates that the elbow joint is lower than the shoulder joint during the lifting to below the



Lifting a 1kg book

Lifting a 2kg book

Figure 6.16 3-D elbow forces expressed in upper arm system



Lifting a 1kg book

Lifting a 2kg book

Figure 6.17 Inertial and gravitational effects on elbow forces

Fr: resultant total force; Fi: resultant inertial force; Fg: resultant gravitational force.

shoulder heights. Therefore the minimum F_y is positive, which is an axial extension on the upper arm. When the flexion angle of the upper arm increases to over 90 degrees (lifting above shoulder height), the elbow joint is higher than the shoulder joint and the negative F_y becomes axial compression on the upper arm, which increases with the height of lifting as shown in Figure 6.16 (3), (4), (7), (8).

In contrast with the decrease of F_y in the lifting phase, F_x increases from zero at the beginning of the activity to the maximum value at the end of lifting phase, then it decreases in the lowering phase to zero at the end of activity. Because F_x also changes its magnitude with the position of the upper arm it is difficult to relate F_x to any single component of the arm movement. However the results show that the maximum F_x on the elbow occurs during the lifting to the shoulder height and it reaches 64% and 68% of the maximum F_y , the dominant component of elbow force, for the lifting of a 1kg and 2kg books, respectively. The result shows that F_x is a significant action at the elbow joint during the lifting activity.

The F_z on the elbow is positive, which directs from medial epicondyle to lateral epicondyle all the time. Although the maximum F_z is the smallest among the three components of elbow force, the action of F_z is not negligible because it varies little with time.

6.1.3.2 Inertial and gravitational effects on elbow forces

The resultant inertial and gravitational forces on the elbow are given in Figure 6.17 with the resultant total forces on the elbow.

It can be seen that the gravitational forces are dominant in each case of the lifting activities, and the gravitational forces do not vary. The maximum magnitude of inertial elbow force occurs during lifting to the highest height.

It can also be seen that the resultant elbow forces are the combined results of the inertial and the gravitational elbow forces. The maximum total elbow force coincides in time with the maximum inertial elbow force and increases with the height of lifting and the inertial effects. The ratios of the maximum resultant inertial elbow force to the maximum resultant total elbow force for each height and weight of lifting are given in Table 6.7. The results show the significance of the inertial effects on elbow forces.

Table 6.7 The maximum resultant inertial elbow force to the maximum resultant total elbow force ratios

	Table height	Shoulder height	Head height	Highest height
Lifting a 1kg book	0.202	0.249	0.255	0.316
Lifting a 2kg book	0.196	0.231	0.259	0.291

6.1.3.3 Three-dimensional elbow moments

Three components of elbow moments about the three-axes of the upper arm coordinate system for the lifting activities are given in Figure 6.18.

M_z is the dominant elbow moment for each case of the lifting. The positive M_z is a flexion moment corresponding to elbow flexion. The maximum values of M_z in the lifting phase are higher than that in the lowering phase, and increase with the height of lifting.

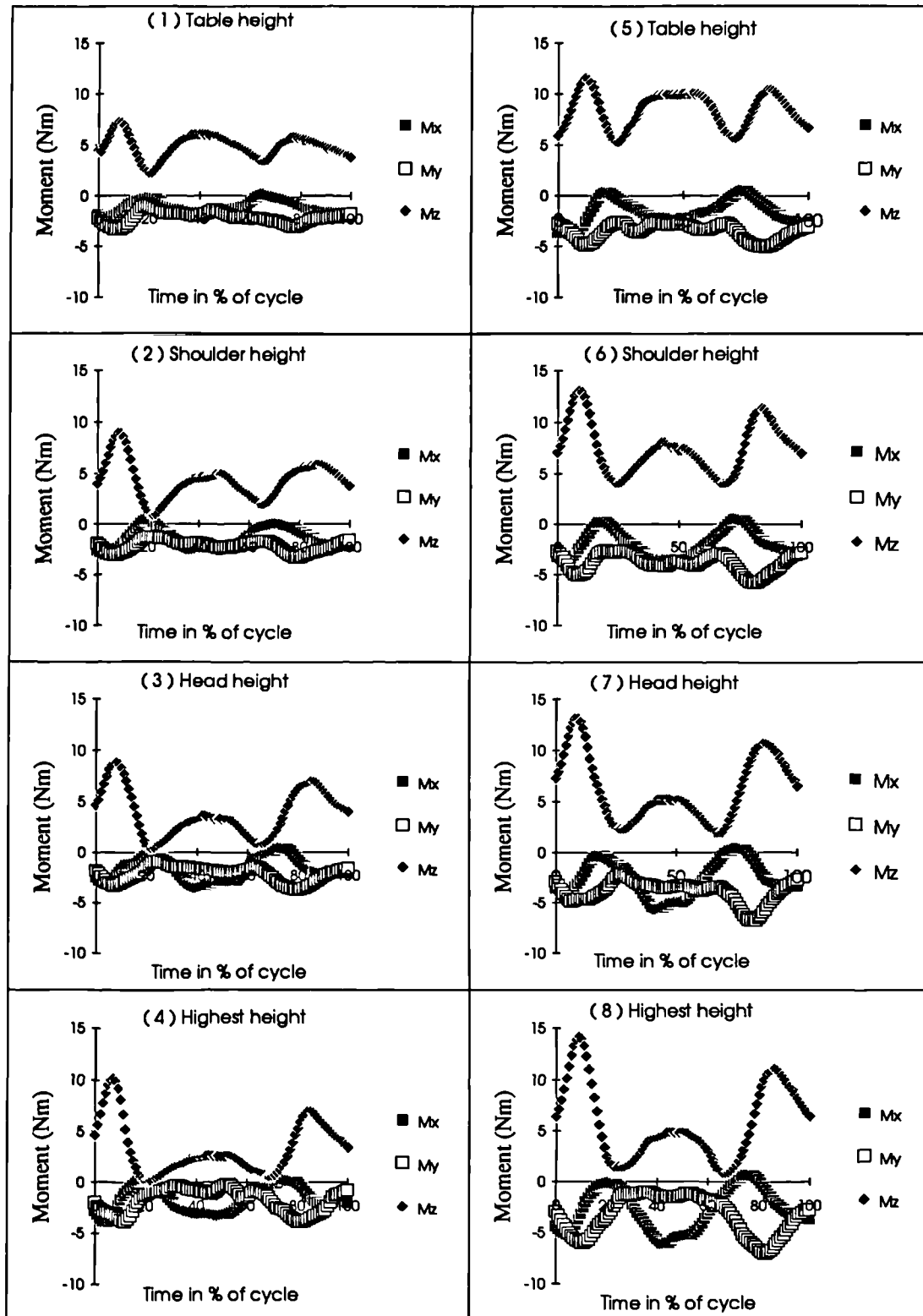
M_x and M_y are negative during the full cycle of the activity. When the forearm is fully extended with 180 degrees of elbow angle, the negative M_x and M_y correspond to the abduction and external rotation moments of the forearm, respectively. If the forearm is flexed 90 degrees, negative M_x and M_y become external axial rotation and abduction moments respectively. When the forearm moves to anywhere different with the two positions, such as that occurred in the lifting activity, it is difficult to relate the two components expressed in the upper arm coordinate system to the clinical descriptions of forearm movements.

An alternative way is to represent the elbow moment in the forearm coordinate system. The problem is that flexion of the forearm about the z-axis of the upper arm coordinate system is often accompanied by axial rotation of the forearm about its longitudinal axis. In this case, it is difficult to tell whether flexion of the forearm about the upper arm (z-axis) is a flexion-extension or adduction-abduction about the z-axis or x-axis of the forearm coordinate system.

As a recommendation, it is beneficial to express the elbow moments in both upper arm and forearm coordinate systems by two components, one is the flexion-extension moment about the upper arm (z-axis), and the other is the axial rotation moment of the forearm.

6.1.3.4 Inertial and gravitational effects on elbow moments

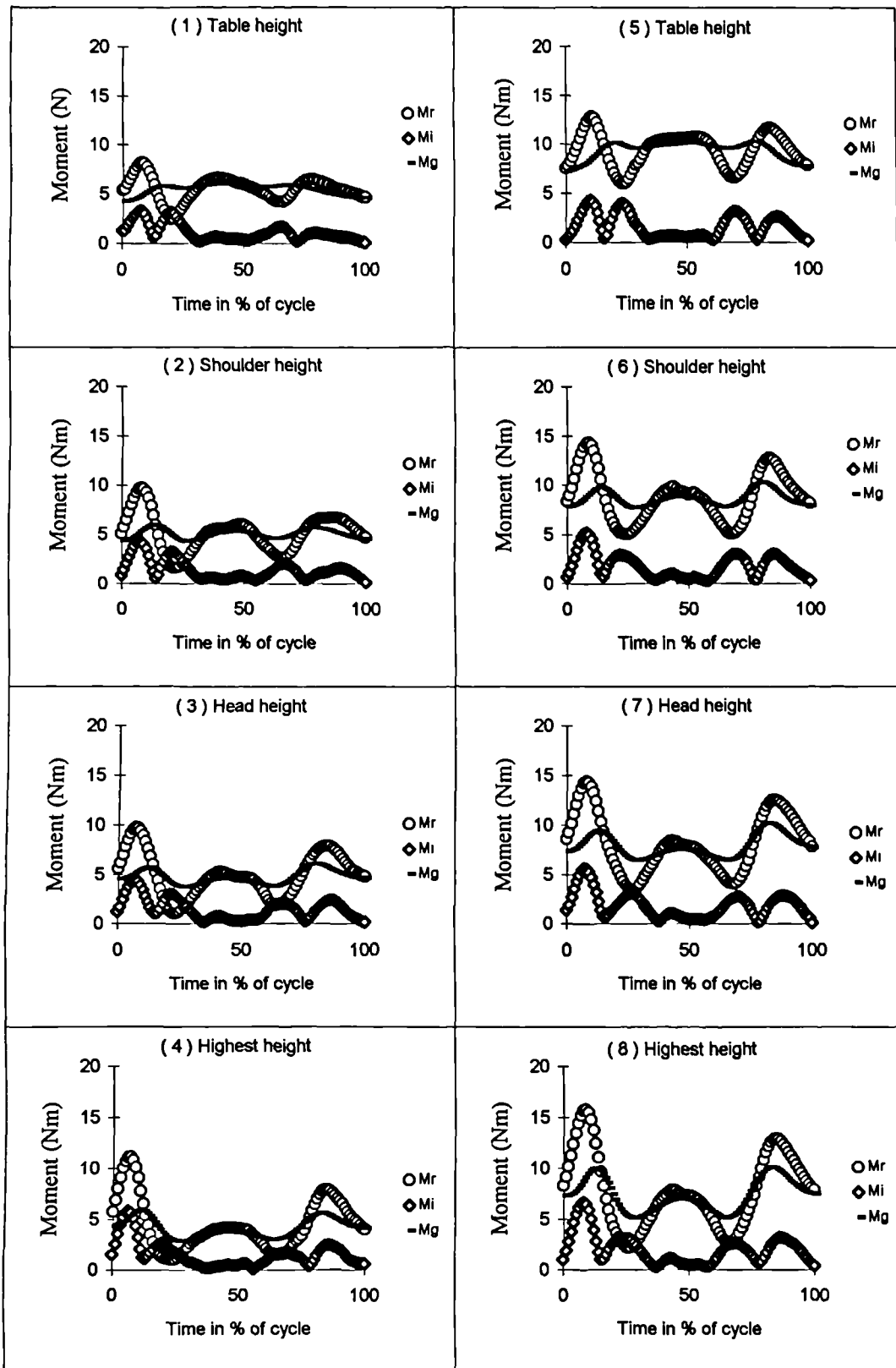
Resultant elbow moments caused by inertial and gravitational effects are given in Figure 6.19 together with the resultant total elbow moment.



Lifting a 1kg book

Lifting a 2kg book

Figure 6.18 Three-dimensional elbow moments expressed in the upper arm system



Lifting a 1kg book

Lifting a 2kg book

Figure 6.19 Inertial and gravitational effects on elbow moments

Mr: resultant total moment; Mi: resultant inertial moment; Mg: resultant gravitational moment

The elbow moment caused by gravitational effects is higher than that caused by inertial effects, and the differences are greater for lifting a 2kg book than a 1kg book. The results indicate the significant contribution of gravitational effects on the total elbow moment when the lifted mass is increased. The elbow gravitational moment varies greatly and has three peak values in the full cycle of the activity. Since the elbow joint moves greatly with the rotations of the upper arm during the lifting activities, the changes of the elbow gravitational moment is not only due to the displacements of mass centres of forearm-hand and book but also due to the movement of elbow joint.

6.1.3.5 Inertial to total elbow moment ratios

In order to quantitatively describe the inertial effects on the elbow moment, the resultant inertial elbow moment to the resultant total elbow moment ratios at each instance of time are given in Figure 6.20(1)-(2), and the averaged ratios over time are given in Figure 6.20(3).

It can be seen that the averaged inertial to total elbow moment ratio increases with the height of lifting, and the ratios are higher for lifting a 1kg book than lifting a 2kg book. The maximum ratio reaches 0.49 during the lifting of a 1kg book to the highest height and the minimum ratio is 0.19 during the lifting of a 2kg book to the table height. The results indicate that the contributions of inertial effects to the total elbow moment decrease with the increase of lifted mass and increase with the height of lifting. Neglecting inertial effects in the biomechanical analysis of lifting activities will result in up to 49% (average) lower estimating of the resultant total elbow moment for lifting a 1kg object to the highest height, and at least 24% lower (average) estimating of the resultant total elbow moment for lifting a 1kg book to table height. For lifting a 2kg book the corresponding values are 35% and 19%, respectively.

6.1.3.6 Arm and book effects on elbow moments

In order to investigate the influence of the lifted mass on the elbow moments during the lifting activity, the resultant elbow moment caused by the arm and book (M_a and M_b) involving both inertial and gravitational effects were calculated and are given in Figure 6.21 with the resultant total elbow moments (M_r).

It can be seen that the resultant elbow moments caused by the forearm-hand have nearly the same patterns during the lifting of a 1kg and 2kg book to the different heights, and the

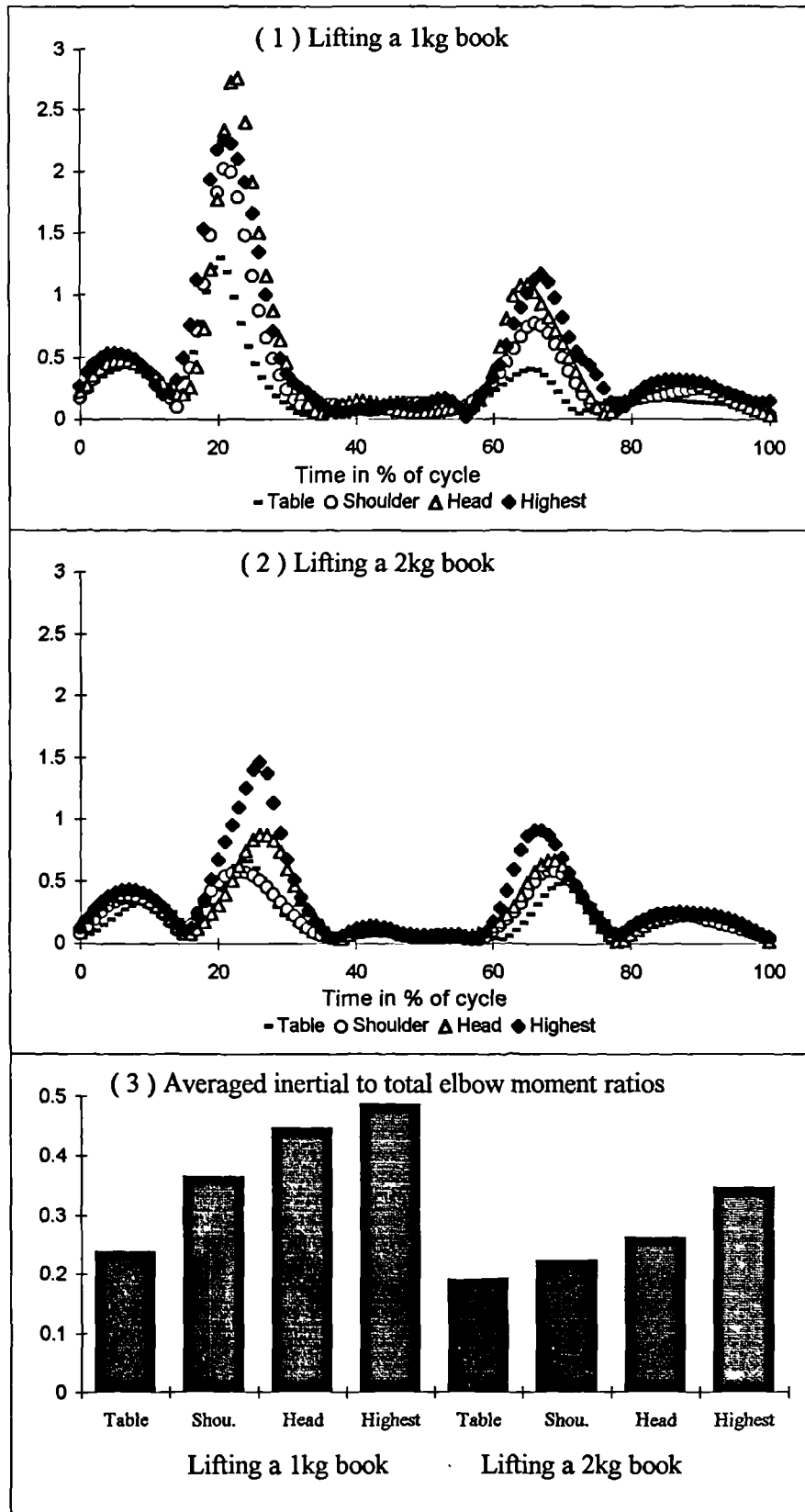
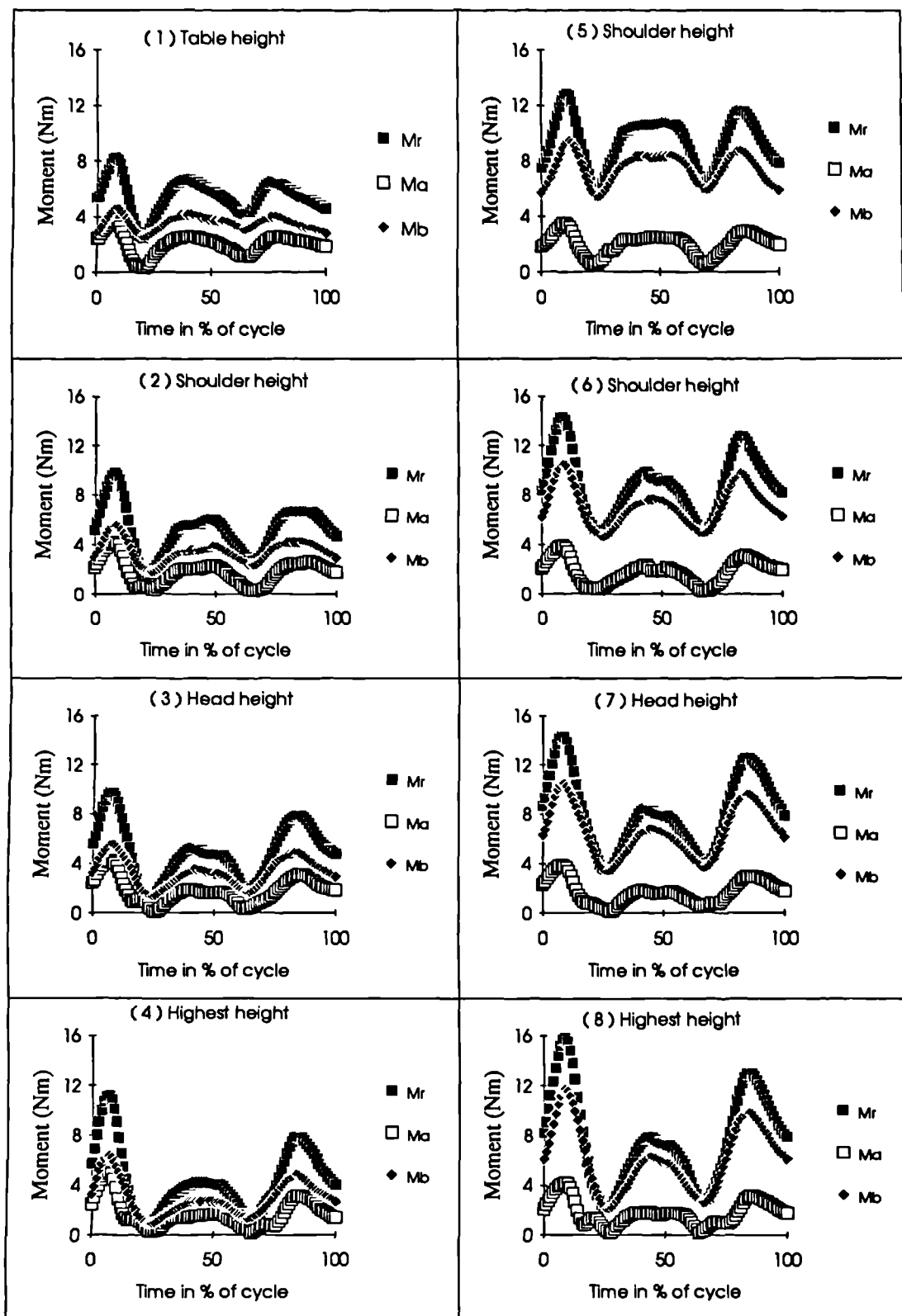


Figure 6.20 Inertial to total elbow moment ratios.



Lifting a 1kg book

Lifting a 2kg book

Figure 6.21 Arm and book effects on elbow moments

Mr: Resultant total elbow moment; Ma: Resultant elbow moment caused by the arm; Mb: Resultant elbow moment caused by the book

maximum M_a increases slightly with the lifting height. Since M_a is produced by the gravitational and inertial effects of the forearm-hand, the results indicate that the forearm-hand experiences a similar movement during the lifting activities.

It can also be seen that the resultant elbow moments caused by the book (M_b), are all higher than the corresponding M_a for the lifting of the 1kg and the 2kg book to the different heights, and the difference between M_b and M_a during the lifting of a 2kg book is bigger than that during the lifting of a 1kg book. The results are obvious because the book is at the distal end of the forearm-hand segment, and the moment lever arm from the book centre to the elbow joint is longer than that from the mass centre of forearm-hand segment to the elbow joint. Therefore, if the lifted weight is the same as (or nearly same as) the mass of forearm-hand segment, the lifted weight will produce a bigger elbow moment than the forearm-hand segment. Although M_a can be influenced by the body build (height and weight) of the subjects, M_b can also be influenced by the characteristics of the subjects because the taller subject usually has a longer forearm-hand, i.e. a longer moment lever arm from the lifted mass to the elbow joint. For these reasons, it is difficult to say how much lifted mass can produce an equivalent elbow moment as raising the arm only. From Figure 6.21 it can be found that the maximum M_b is a little higher than the maximum M_a during the lifting of a 1kg book to the four different heights. The result indicates that for the subjects of this study, the maximum resultant elbow moment caused by the 1kg book is nearly the same as the maximum resultant elbow moment caused by the forearm-hand segment without load on the hand during the lifting to the four different heights.

In order to quantitatively describe the effects of lifted mass on the elbow moment, the ratios of the resultant elbow moment caused by the lifted book to that caused by the forearm-hand were calculated at each instance of time and the averaged ratios over time are given in Figure 6.22. The results show that the highest ratio occurs at lifting to the shoulder height, while the lowest ratio occurs at lifting to the highest height. The results are different with the same ratios for the shoulder moment which decrease with the height of lifting. Also the M_b/M_a ratios of elbow moment in Figure 6.22 are much higher than the same ratios for the shoulder moment in Figure 6.15, and vary from 2.1 to 2.6 for the lifting of a 1kg book and 4.1 to 5.5 for the lifting of a 2kg book. Therefore more attention should be given to the elbow than the shoulder in this aspect. Since only two lifted masses were tested in this study further

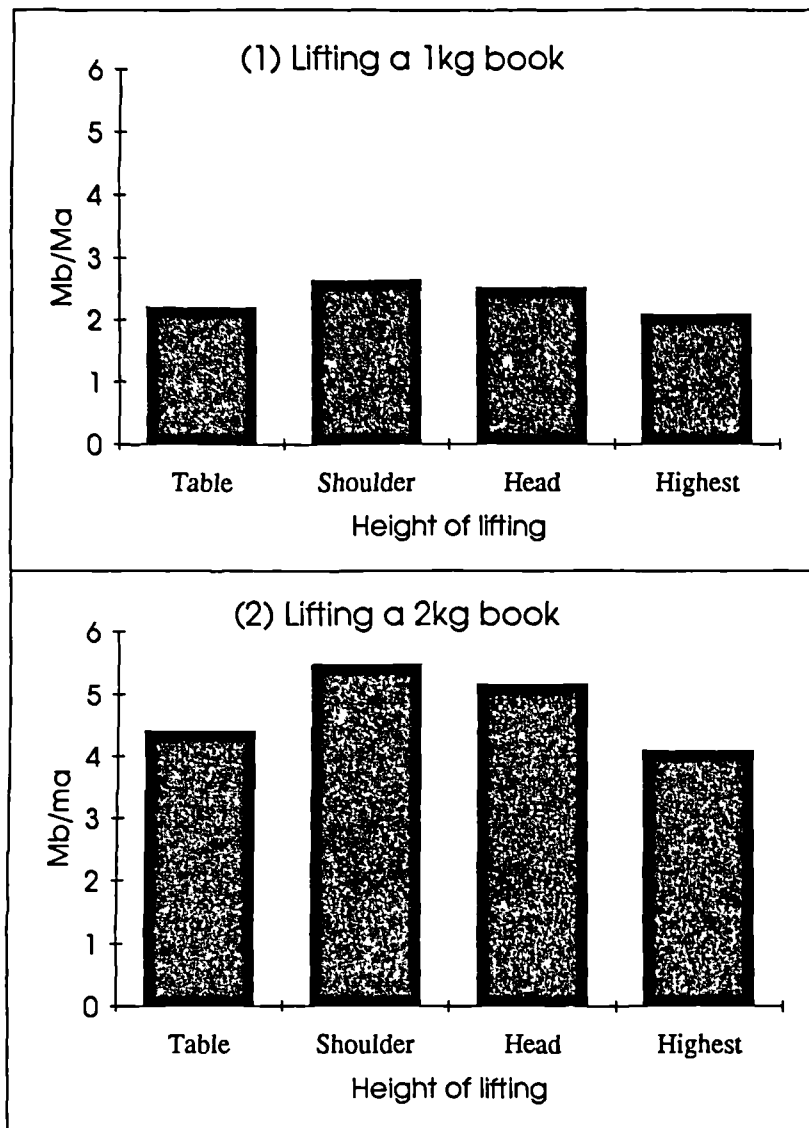


Figure 6.22 Averaged Mb/Ma ratios of lifting activity
 Mb: resultant elbow moment caused the book
 Ma: resultant elbow moment caused by forearm-hand

investigations on more masses are required in order to give a full picture of the influence of the lifted mass on the elbow moment.

6.2 Door Opening and Closing Activity

Thirteen trials were analysed for the door opening/closing activity and the mean kinematic and kinetic results are given in the following.

6.2.1 Kinematic Results and Discussions

The kinematic results given in this section involve the stick diagram presentation of arm movement (Fig. 6.23), upper arm rotation angles with respect to the axes of the trunk coordinate system (Fig. 6.24), variation of elbow angle (Fig. 6.25), axial rotation angles of upper arm and forearm (Fig. 6.26), and the 3-D velocities and accelerations of the hand centre (Fig. 6.27).

The major arm movement occurs in the sagittal plane (Fig. 6.23(1)). It was found that the flexion/extension angle of the upper arm varies from 53 degrees of flexion to 33 degrees of extension. The outward rotation angle of the upper arm changes from 16 degrees at the beginning of the activity to 142 degrees when the door is at the largest opening (Fig. 6.24), while the abduction angle is nearly unchanged.

The elbow angle decreases from 159 degrees to 67 degrees during the pulling phase (Fig. 6.25). Comparing Fig. 6.25 with Fig. 6.23(1) shows that the decrease of the elbow angle is mostly due to the extension of the upper arm, but less due to the movement of the forearm. It was also found that both upper arm and forearm rotate (axially) externally during the pulling phase when opening the door. The forearm axial rotation angle is very small with a maximum value of 6.5 degrees, which is reasonable since holding the handle by the hand limits the axial rotation of the forearm.

Similar to the lifting activity, the velocity and acceleration (V_x , A_x) of the hand centre in the major direction of movement (posterior-anterior) describe two loops, while the velocities and accelerations in the vertical and transverse directions describe more than two loops which means that the hand experienced a number of accelerations and decelerations in the two directions during the activity.

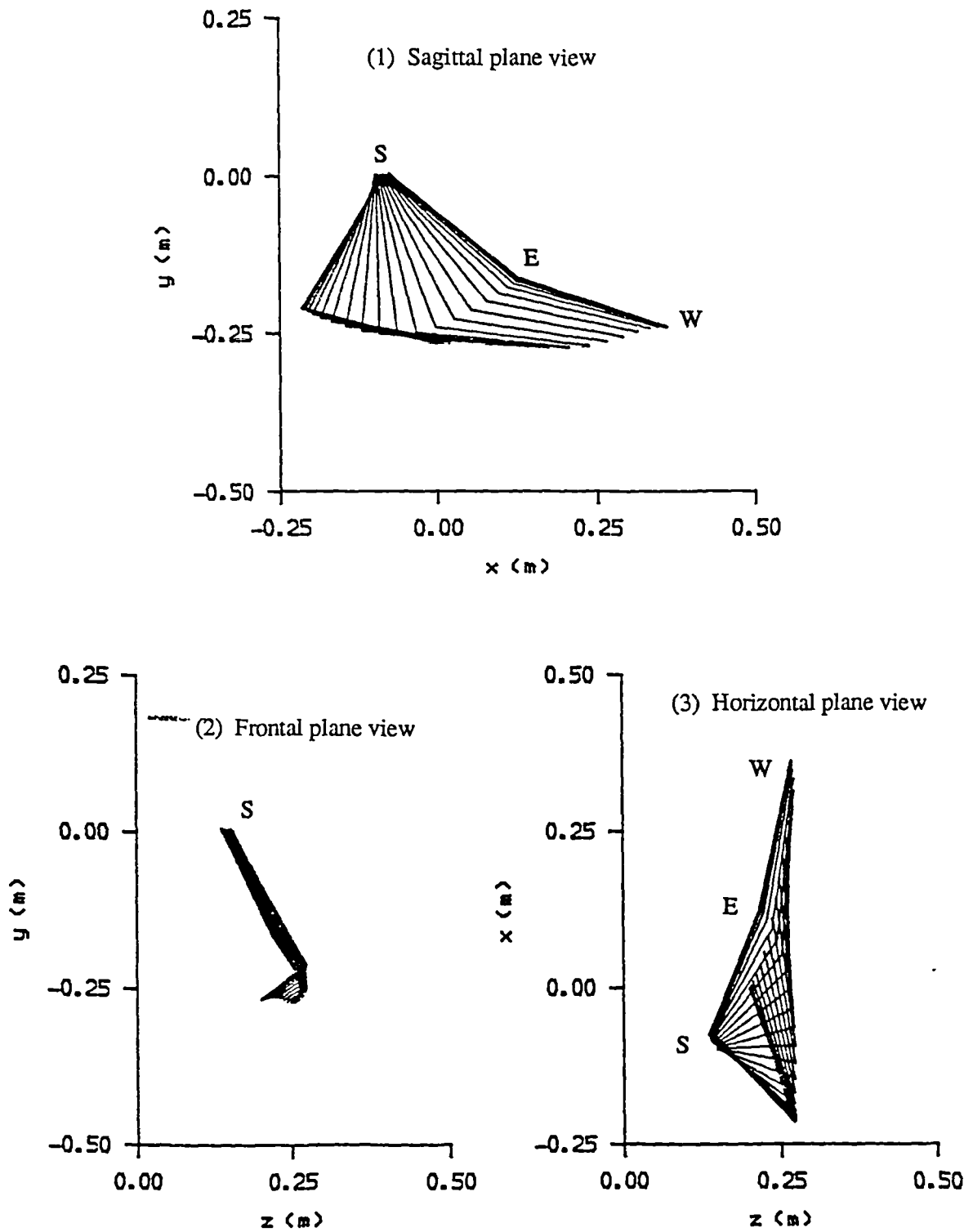


Figure 6.23 Stick diagram presentation of upper arm and forearm movement in the trunk coordinate system during door opening/closing activity. Positive x , y , z , direct forward, upward, and from left to right, respectively. S: shoulder, E: elbow, W: wrist.

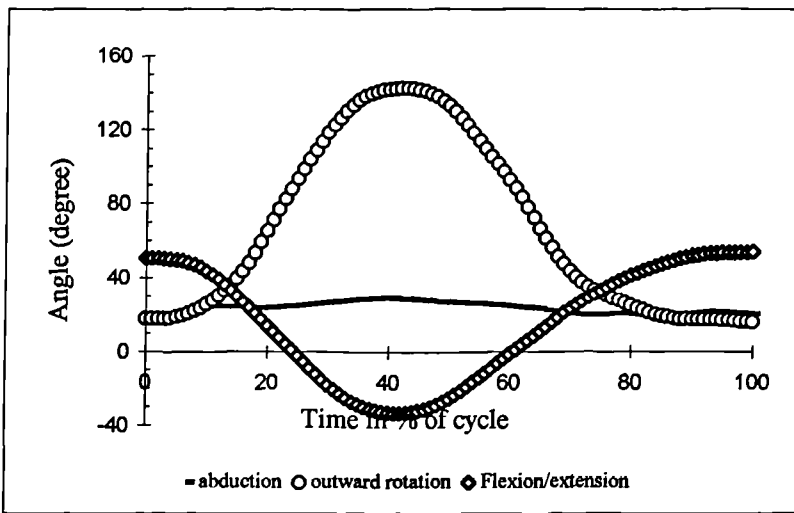


Figure 6.24 Upper arm rotation angles about the axes of trunk frame during the door opening/closing activity

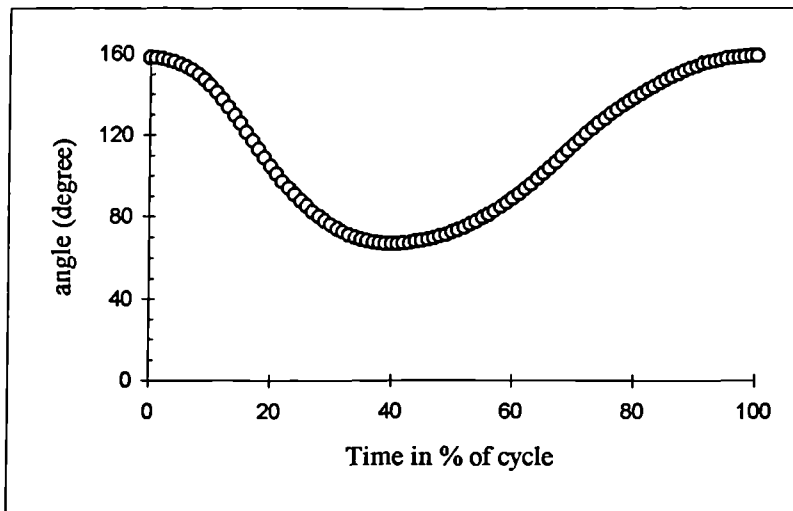


Figure 6.25 Elbow angle during door opening activity

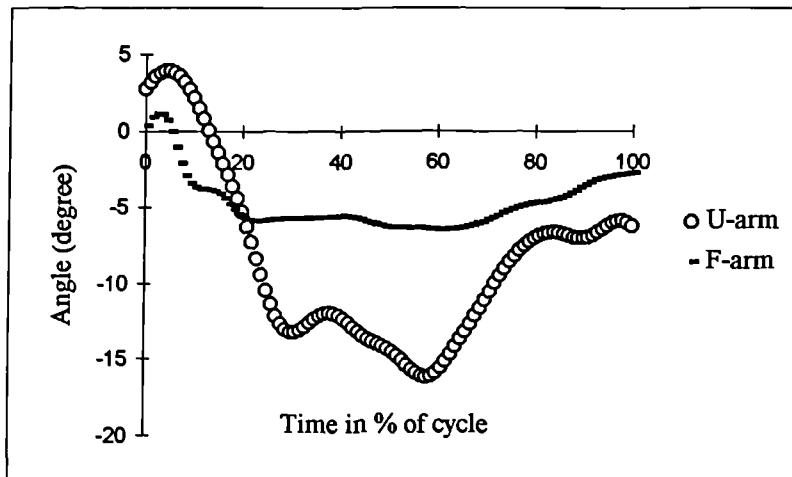


Figure 6.26 Axial rotation angles of upper arm and forearm during door opening/closing activity. Positive and negative values refer to the internal and external rotation angles, respectively.

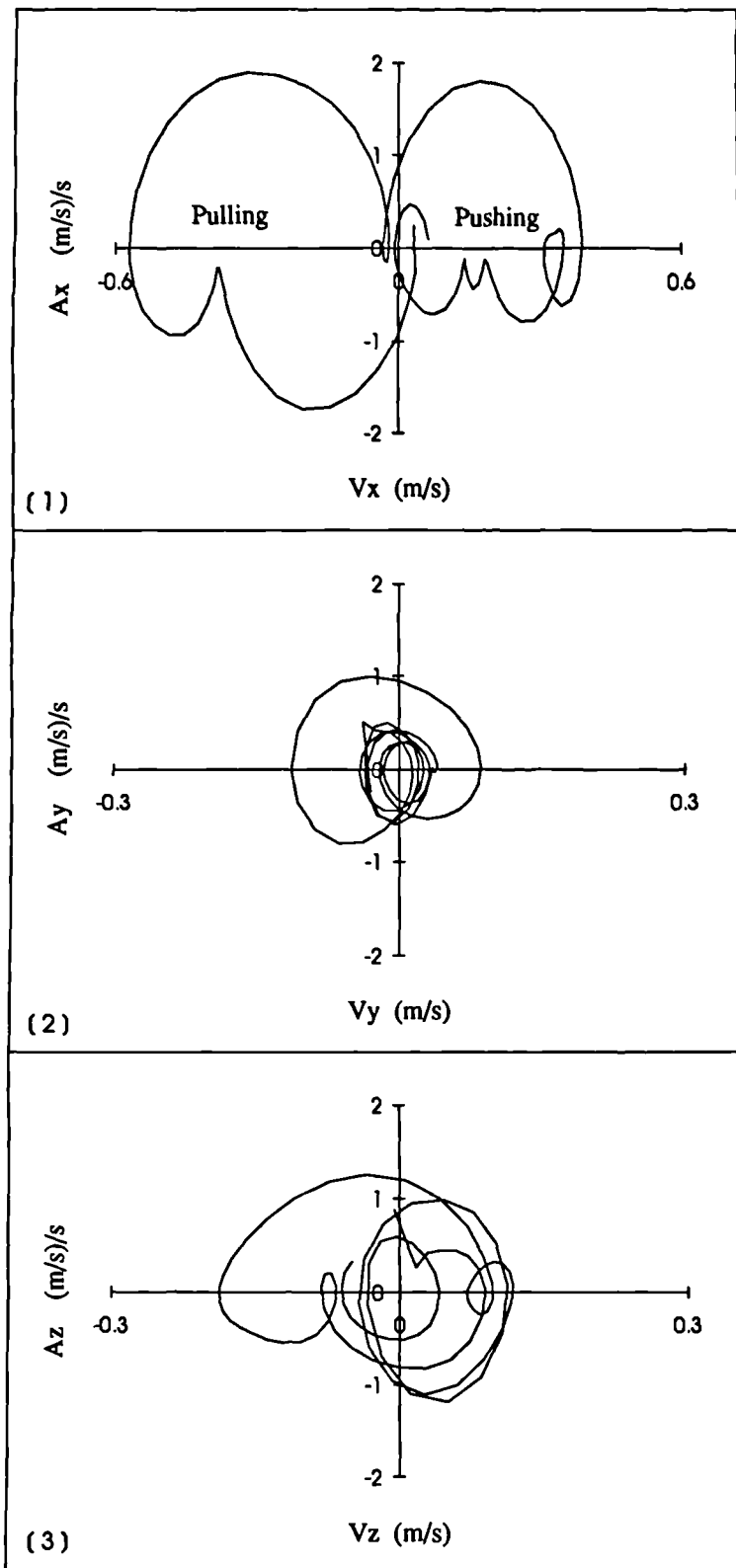


Figure 6.27 Phase plane view of hand centre velocity and acceleration during door opening and closing activity

6.2.2 Kinetic Results and Discussions

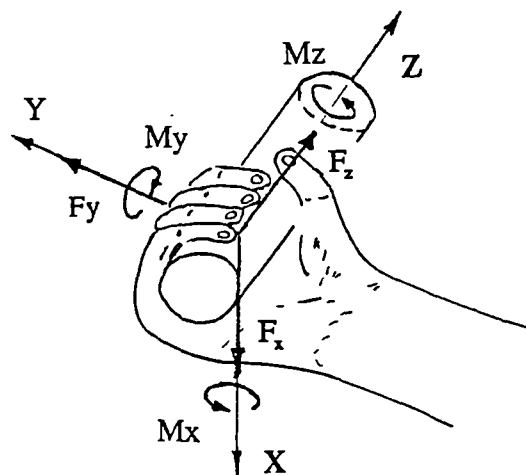
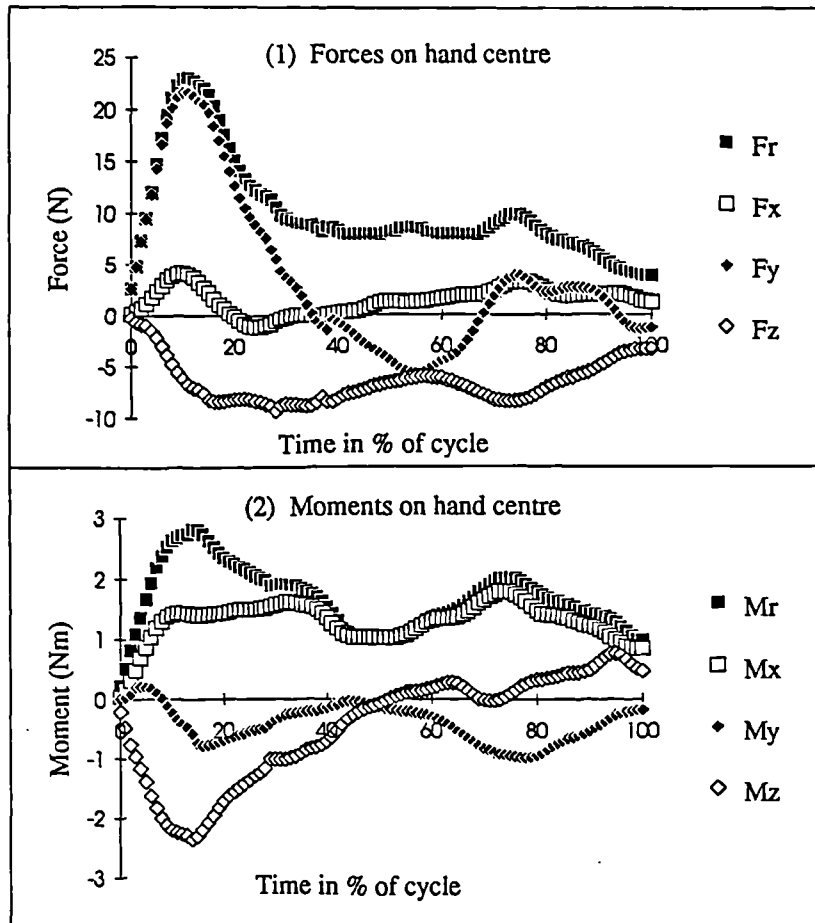
The kinetic results given in this section are the 3-D forces and moments on the hand centre, shoulder and elbow.

The three-dimensional hand forces and moments measured by the force transducer are given in Fig. 6.28. The forces and moments act on the hand centre at the distal end of the forearm-hand segment and are expressed in terms of the three-axes of the hand coordinate system (Fig. 6.28(3)). Figure 6.28(1) shows that F_y is dominant where a positive F_y is a pulling force and is related to the resistance provided by the door closer. The magnitude of F_y in the pushing phase, when the door is being pushed to close, is much lower than that in the pulling phase. The result is mainly due to the auto-close function of the door closer. At the beginning of the pushing phase, a small pushing force ($-F_y$) is required to start the process, but when the door is being closed, the function of the door closer is working, it causes a quick closing of the door in the later pushing phase. The quick closing action is even quicker than expected by the subject, and produces a pulling force ($+F_y$) on the hand of the subject. The maximum resultant hand force F_r is 23N.

The highest component of hand moment is flexion ($+M_z$)/extension ($-M_z$) moment with a maximum value of 2.4Nm. The maximum resultant hand moment is 2.8Nm.

The shoulder forces given in Fig. 6.29 show that the shoulder forces are mainly due to the gravitational force of the arm and the hand load, while the inertial effect plays a less important role.

The 3-D total shoulder moments and the 3-D shoulder moment caused by each effect are given in Fig. 6.30. It was found that the flexion moment ($+M_z$ in Fig. 6.30(1)) causing the flexion of the upper arm is the dominant shoulder moment. The flexion moment is due to the gravitational effect (Fig. 6.30(2)). It can be seen that the flexion moment ($+M_x$) decreases sharply in the early pulling phase, and increases from the later pulling phase to the maximum magnitude of 9.87Nm. The decrease of flexion moment in the early pulling phase is due to the decrease of M_{gz} caused by the gravitational effects when the arm moves backward, and the flexion moment M_{hz} (Fig. 6.30(4)) caused by the hand loads. Since the M_{gz} and M_{hz} are positive, the flexion moment M_z at the end of the activity is higher than that at the beginning of the activity. The results show that the magnitude of flexion shoulder moment depends on the posture and geometry of the upper arm relative to the door. It can be predicted that if the



(3) Hand centre and hand coordinate system

Figure 6.28 Forces and moments on hand centre in hand system during door opening activity

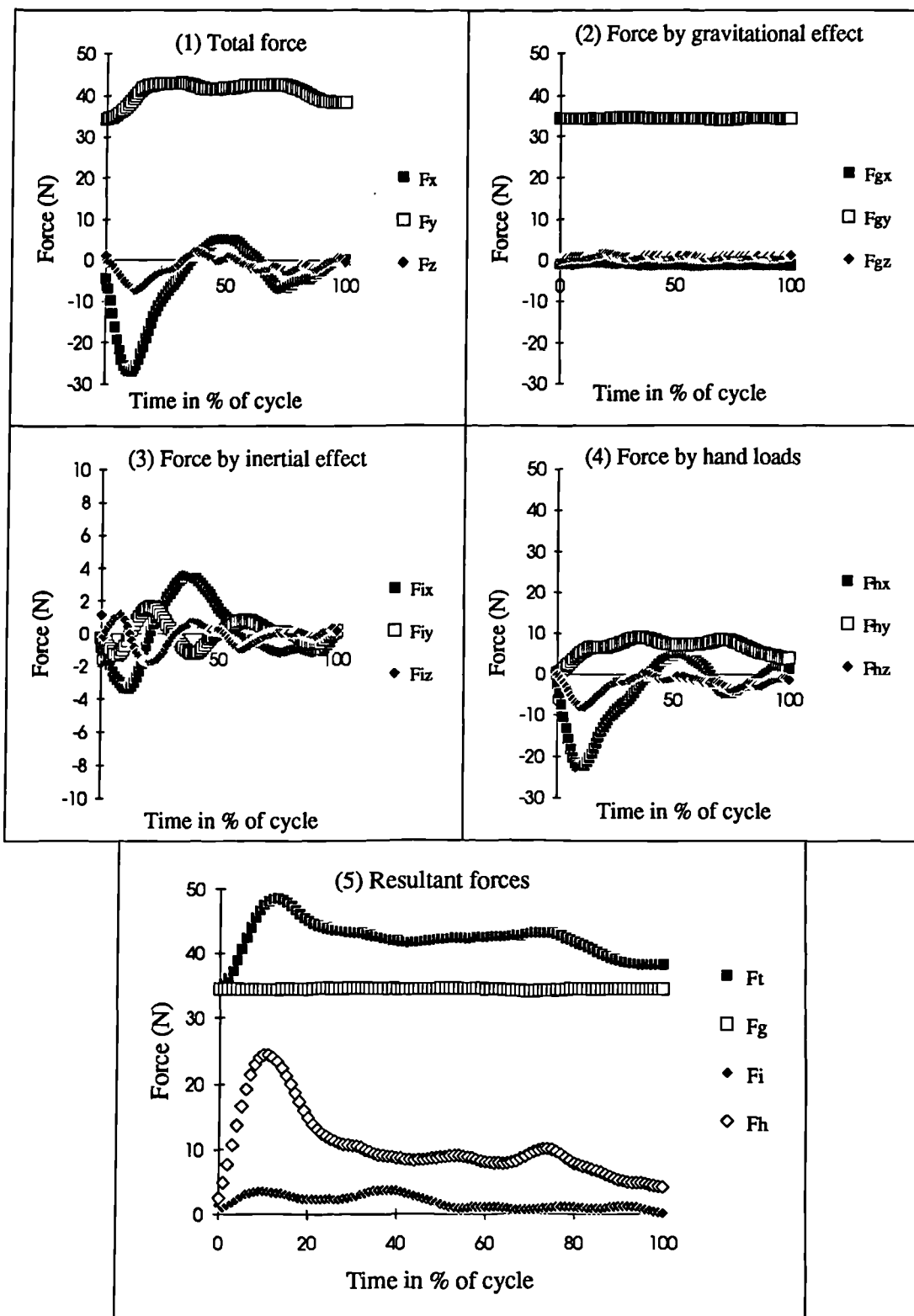


Figure 6.29 3-D shoulder forces during door opening and closing activity

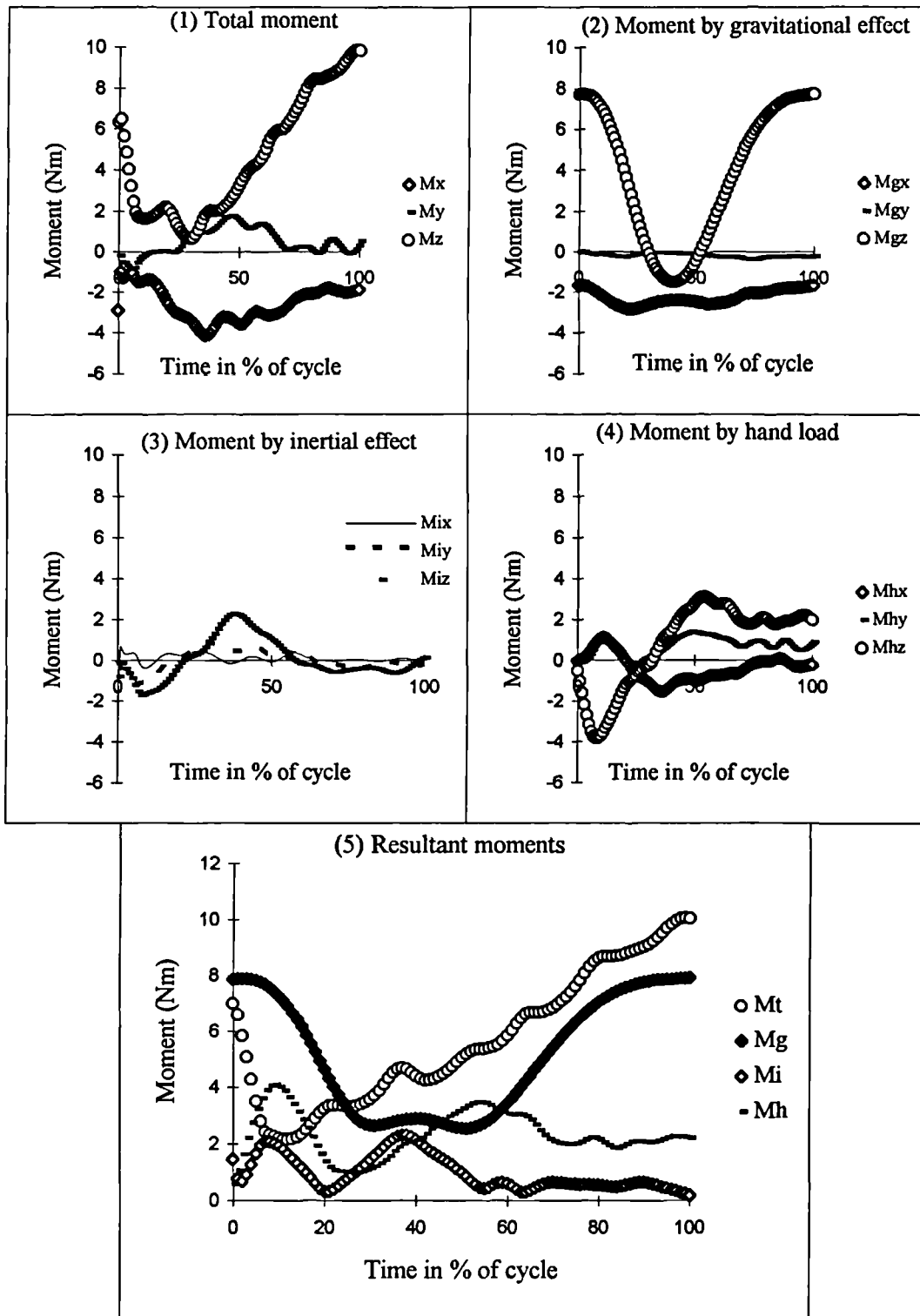


Figure 6.30 3-D shoulder moments during door opening and closing activity

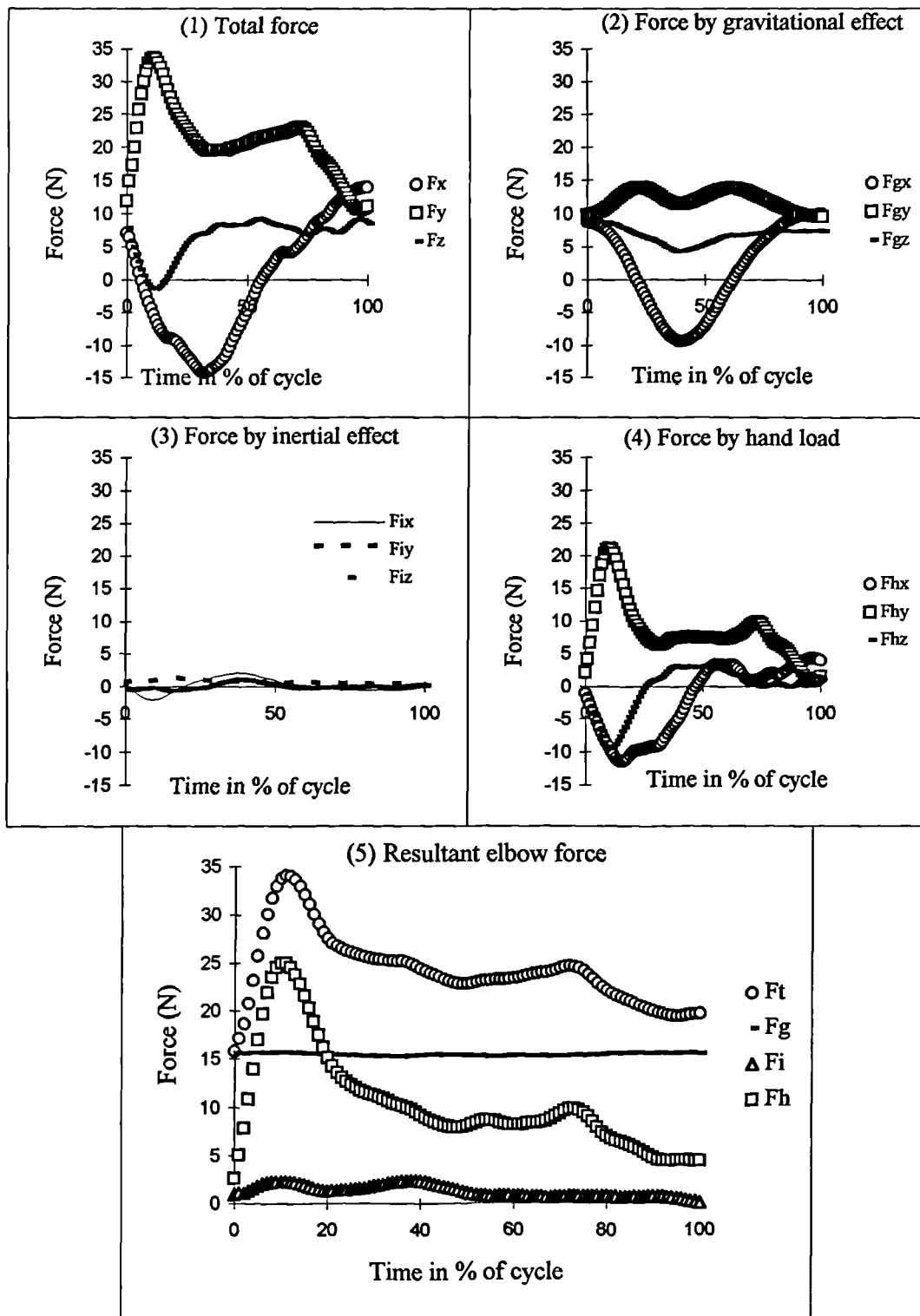


Figure 6.31 3-D elbow forces in upper arm system during door opening and closing activity

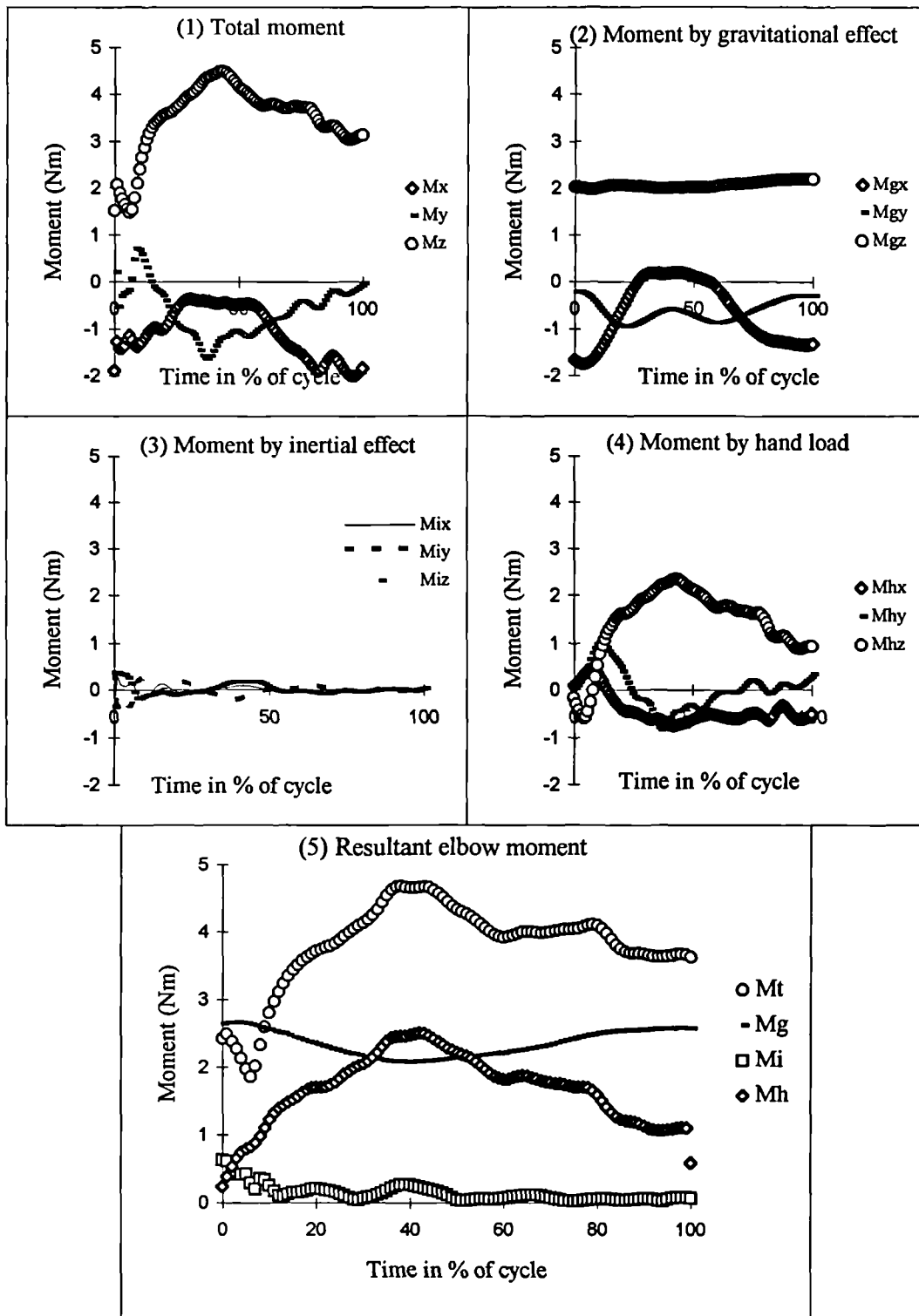


Figure 6.32 3-D elbow moment in upper arm system during door opening and closing activity

door is pushed to open, M_{hz} will become positive and the total flexion moment M_z at the beginning of the activity will be much higher than M_z in Fig. 6.30(1) when the door is pulled to open. Therefore it can be concluded that pulling to open a door is easier than pushing to open a door because less shoulder flexion moment is required in the case of the activity being conducted by the arm only without assistance of other parts of the body.

The second major shoulder moment is the abduction moment ($-M_x$ in Fig. 6.30(1)) with a maximum magnitude of 4.15Nm. The maximum M_y is only 1.76Nm, the lowest among the three components of total shoulder moment.

Figure 6.30(5) shows that the major contributor to the resultant total shoulder moment is the gravitational effect (M_g). The peak value of M_g is 7.93Nm. The second major contribution to the total shoulder moment is that caused by the hand loads M_h with a maximum value of 4.07Nm, a little higher than half of the maximum M_g . The resultant inertial shoulder moment is the lowest of the three contributions, and the maximum M_i is only 2.32Nm. The ratio of the maximum resultant inertial shoulder moment to the maximum resultant total shoulder moment is 0.23, which is much lower than the same ratios of the lifting activity. The peak resultant total shoulder moment M_r is 10.06Nm.

The elbow forces (Fig. 6.31) and moments (Fig. 6.32) are expressed in the upper arm coordinate system in the same way as for the lifting activity. The dominant component of elbow force is F_y with a maximum value of 34N. The maximum magnitude of the second major component of elbow force F_x is 14.3N, and the maximum value of F_z is only 9N. Considering the relative position of the upper arm to the door and trunk it was found that in the early part of the pulling phase the maximum elbow force is along the long axis of the upper arm, while in the later pulling phase the pulling force acting along the long axis of the forearm becomes significant.

It can be seen (Fig. 6.31(5)) that the maximum resultant elbow force due to the hand load F_h is much higher than the gravitational force F_g , and the maximum resultant total force F_t is mostly due to the hand load. Therefore it can be concluded that the action of the hand load is more important than the action of gravity on the elbow. This result is a major difference from the shoulder force where the gravitational effect is more important than the effect of the hand load in this activity. The inertial elbow force F_i is low in magnitude and the numerical results show that the maximum resultant inertial elbow force is only 6.9% of the

maximum total elbow force, which becomes the major difference between the door opening/closing (pushing/pulling) activity and the lifting activity where the inertial effect is dominant as discussed in pervious sections. The maximum resultant total elbow force is 34N which is lower than the maximum resultant total shoulder force of 48N. It can be predicated that greater muscle force is required on the shoulder than on the elbow for conducting door opening/closing activity in the way specified in this study.

The flexion moment (+Mz in Fig. 6.32(1)) is the dominant elbow moment and the maximum Mz is 4.5Nm. The resultant maximum elbow moments (Fig. 6.32(5)) caused by the gravitational effect and hand loads are of the same level. The maximum Mg is 2.06Nm and maximum Mh is 2.51Nm. The results indicate that the gravitational effect and hand load effect are equally important to the resultant total elbow moment. The resultant inertial elbow moment Mi is of very low magnitude with a maximum of 0.63Nm. The ratio of the maximum Mi to maximum Mt is only 0.13 and at the point of maximum Mt the ratio Mi/Mt is even lower. Therefore neglecting inertial effects will not cause a significant difference to the estimated maximum resultant total elbow moment for the door opening/closing activity.

6.3 Driving Activity

Six subjects were tested for the driving activity and 14 trials were analysed. The mean results are given in this section in the same way as for the door opening/closing activity.

At the beginning of the driving activity the hand is at about the 4 o'clock position as shown in Fig. 6.33. The turning angles of the steering wheel during the activity were calculated and are given in Fig. 6.34, where the increase and decrease of the steering wheel angle represent anticlockwise and clockwise rotation respectively. As shown in Fig. 6.34, the steering wheel was rotated anticlockwise from the beginning of the activity to about 90 degrees position, then rotated 180 degrees clockwise to about -90 degrees position followed by anticlockwise rotation to the original position. For simplicity, the rotation of the steering wheel is referred to as anticlockwise turning when the rotation angle of the steering wheel is positive, or clockwise turning when the rotation angle is negative in the following.

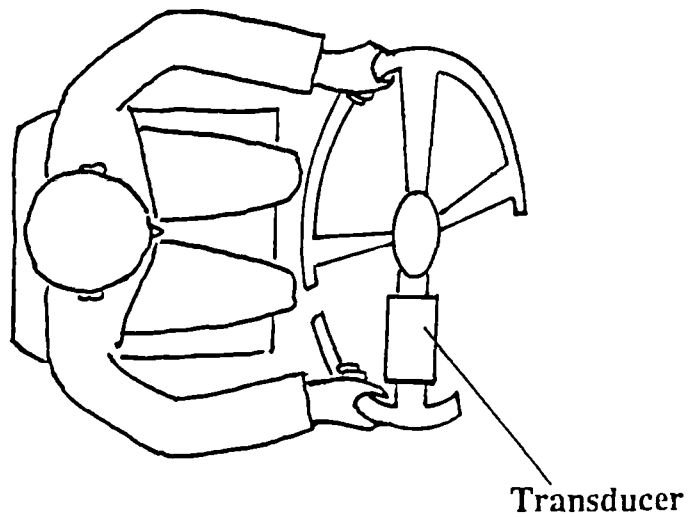


Figure 6.33 Subject holding the steering wheel at the beginning of the driving activity

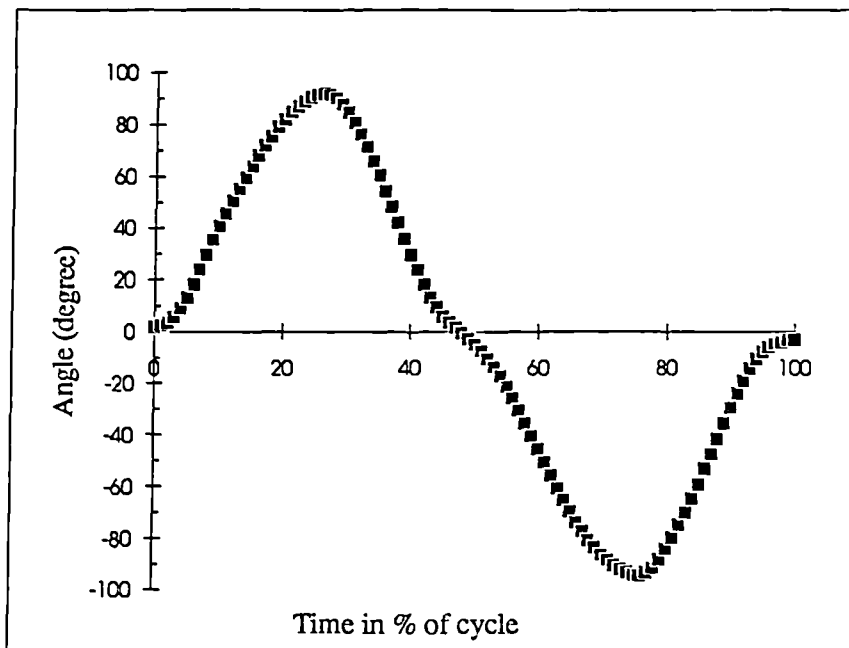
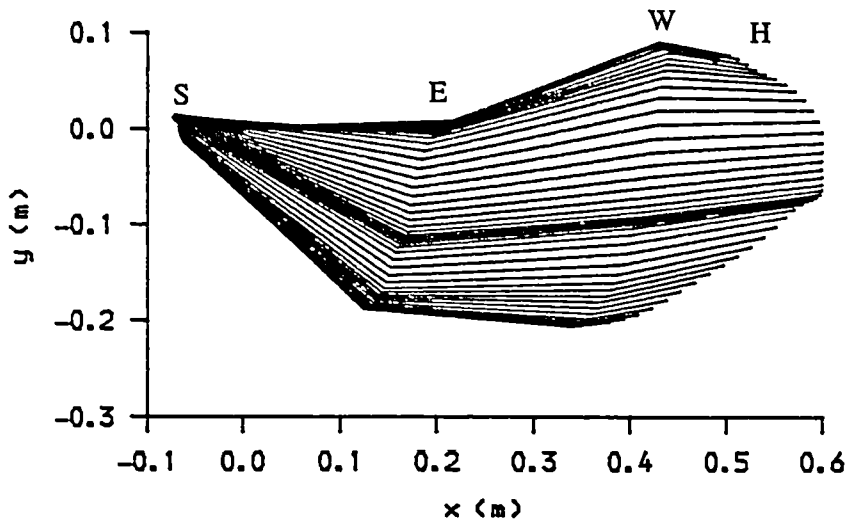
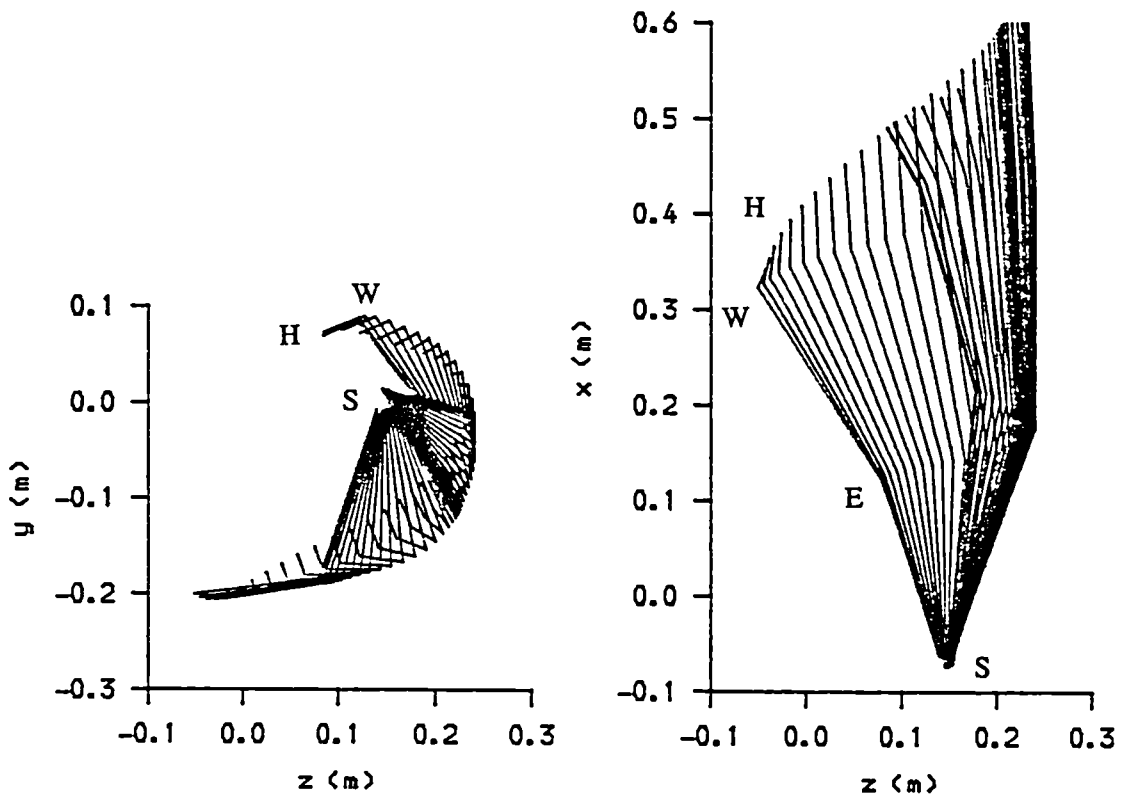


Figure 6.34 Rotation angle of steering wheel during driving activity



(1) Sagittal plane view



(2) Frontal plane view

(3) Horizontal plane view

Figure 6.35 Stick diagram presentation of arm movement in the trunk coordinate system during driving activity. Positive x, y, z , direct forward, upward, and from left to right, respectively. S: shoulder, E: elbow, W: wrist.

6.3.1 Kinematic Results and Discussions

A general view of the arm movements (represented by the line connecting shoulder, elbow, wrist joint centres and hand centre) for turning the steering wheel from 90 degrees to -90 degrees are given in Fig. 6.35. In the sagittal plane view, a decrease of flexion angle of the upper arm during clockwise turning of the steering wheel can be observed, while a small rotation of the forearm about z-axis of trunk coordinate system can also be found. In the frontal plane view, the hand centre and wrist joint describe a half circle, but the hand and wrist at the highest and lowest points (y-coordinate) are not on the same vertical line. The reason for this result is that when the steering wheel is rotated to the 90 degrees position (12 o'clock position) the hand is at about the 1 o'clock position, while when the steering wheel is at the -90 degrees position (6 o'clock position) the hand is at about the 7 o'clock position. Fig. 6.35(3) shows that the upper arm moved from an outward rotation angle about the y-axis of the trunk frame to an inward rotation angle position.

The variations of upper arm angles with respect to the axes of the trunk coordinate system are shown in Fig. 6.36, where the ab(positive)/adduction(negative) and flexion angles are measured from the upper arm at the free hanging position and the inward(negative)/outward(positive) angles are measured from a position where the arm is fully stretched out and the long axis of the upper arm is parallel with the posterior-anterior axis of the trunk coordinate system. The most significant changes among the three position angles of the upper arm is the ad/abduction angle, which varies from 80.5 degrees abduction to 23.8 degrees adduction. The maximum and minimum flexion angles are 90.5 and 43.8 degrees respectively. The inward/outward rotation angle varies between -23.8 degrees to 20.6 degrees during the driving activity. Comparing Fig. 6.36 with Fig. 6.4 and Fig. 6.24, it can be found that the adduction and inward rotation angles of the upper arm are observed only in the driving activity. The results indicate that driving is much more complicated than the lifting and door opening/closing activities in terms of upper arm movement, and that the upper arm needs to move to the medial side of the shoulder joint which is not required during the lifting and door opening/closing activities.

The maximum elbow angle is 151 degrees when the steering wheel is turned to 90 degrees anticlockwise and the minimum angle is 132 degrees when the steering wheel is turned to -90 degrees position. The elbow angle during the driving activity can be influenced by the

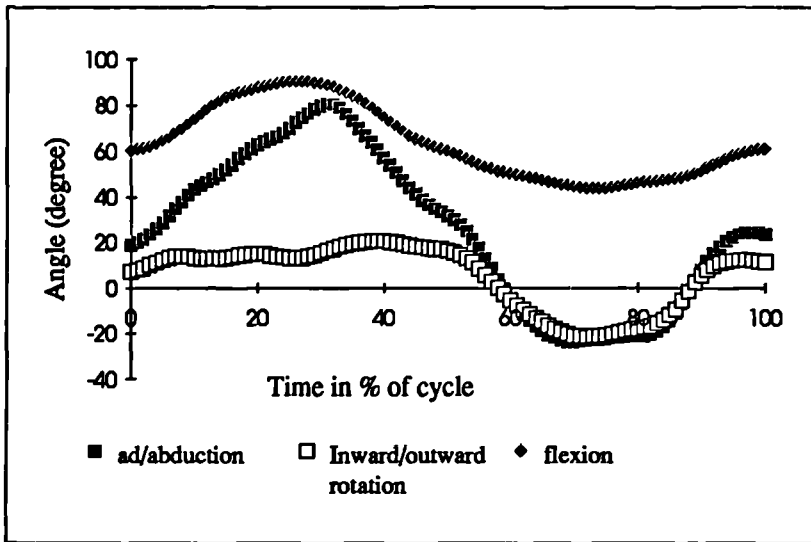


Figure 6.36 Upper arm rotation angles about the axex of trunk frame

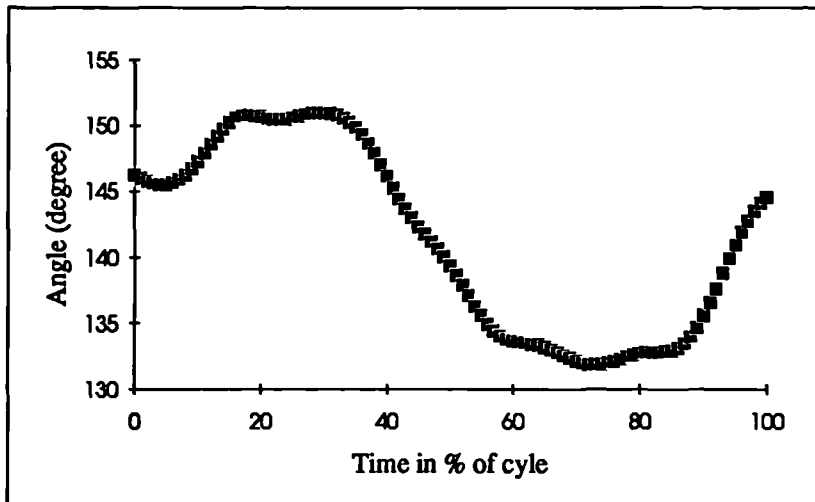


Figure 6.37 Elbow angle during driving activity

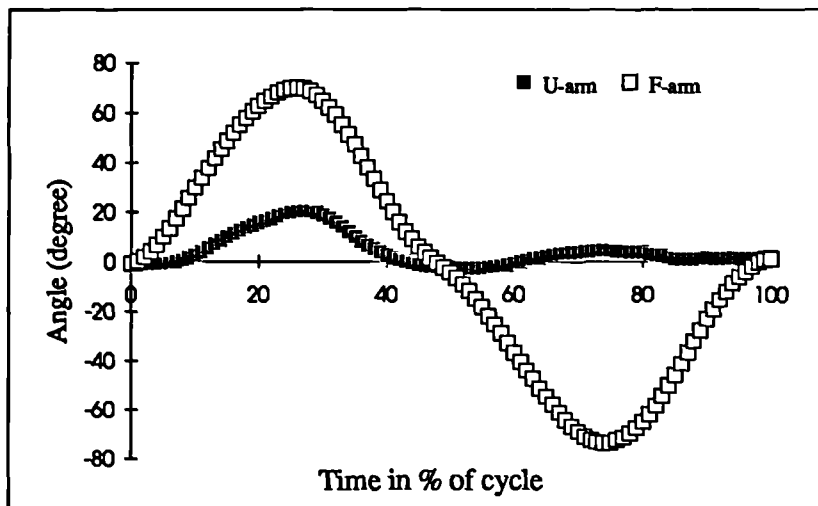


Figure 6.38 Axial rotation angles of upper arm and forearm during the driving activity

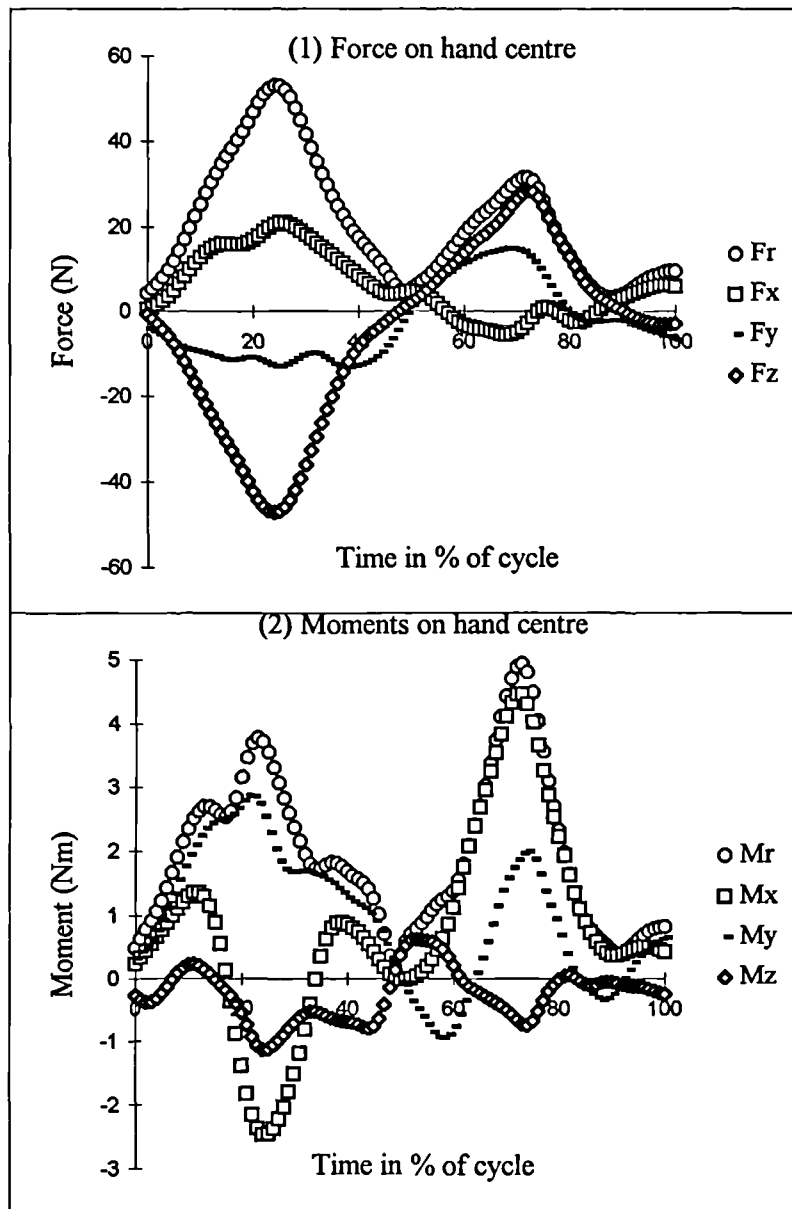


Figure 6.39 Forces and moments on hand centre in hand coordinate system during the driving activity

sitting posture of the subject (mainly the distance between subject and steering wheel). Since the distance between the steering wheel and subject was decided by the subject as the most comfortable position, the above results represent a normal range of elbow angle for the driving activity.

A maximum of 70 degrees of forearm internal (positive, pronation) rotation angle (Fig. 6.37) and maximum of 73.5 degrees of forearm external (negative, supination) rotation angle were found for the driving activity. The result is much greater than that found in the lifting and door opening/closing activities. The maximum value of upper arm axial rotation is 20.2 degrees (positive, internal rotation), which is much lower than the maximum forearm axial rotation angle. Therefore good flexibility of forearm axial rotation is required during driving.

6.3.2 Kinetic Results and Discussions

The major component of hand force (Fig. 6.39(1)) is F_z acting along the transverse direction of the hand (Fig. 6.28), which is greater during anticlockwise turning than clockwise turning of the steering wheel. The transverse force F_z on the hand can also be considered as the force acting on the rim of steering wheel along the tangential direction. The second major component of hand force is F_x acting in the direction perpendicular to the palm, and the lowest component (F_y) of hand force is on the pushing and pulling direction. As shown in Fig. 6.39(1), the resultant hand force F_r follows the pattern of F_z , which indicates the importance of the transverse hand force during the driving activity. However the transverse hand force has received little attention in the functional assessment of driving ability. Most previous assessments of driving ability were made on assessing the pushing/pulling or grip strength as reviewed in chapter 2, however according to the above results very low push/pull force is required during the driving activity, and the transverse force F_z is most important.

The resultant hand moments M_r (Fig. 6.39(2)) have similar forms with supination moment ($+M_y$) and radial deviation moment ($+M_x$) during anticlockwise and clockwise turning of the steering wheel, respectively. The maximum resultant hand moment is 4.92Nm and occurs in the clockwise turning of the steering wheel. The results show that the ability to generate a hand radial/ulna deviation moment (M_x) is more important than the pronation/supination (M_y) and flexion/extension (M_z) moments for the driving activity.

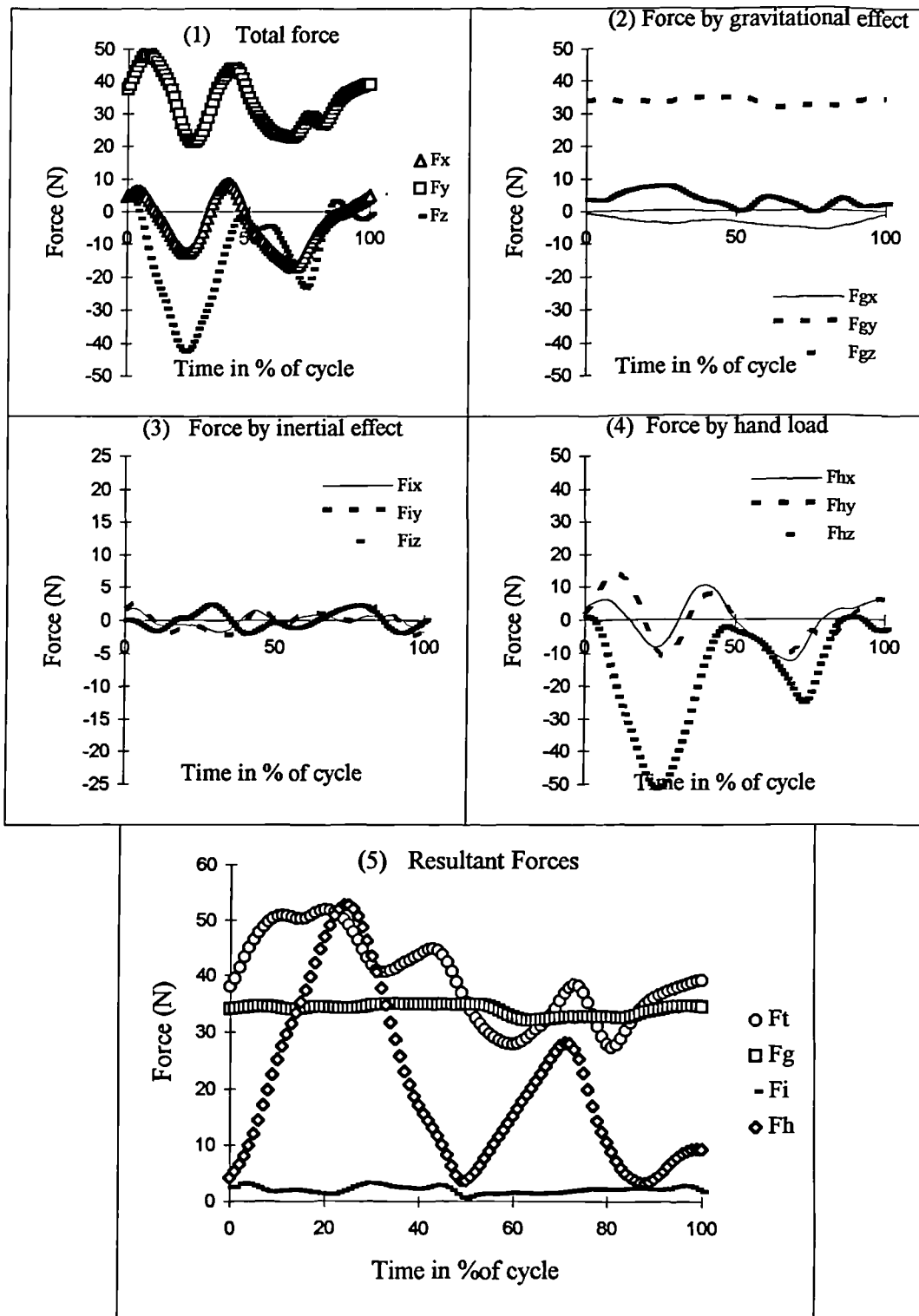


Figure 6.40 3-D shoulder forces in trunk system during driving activity

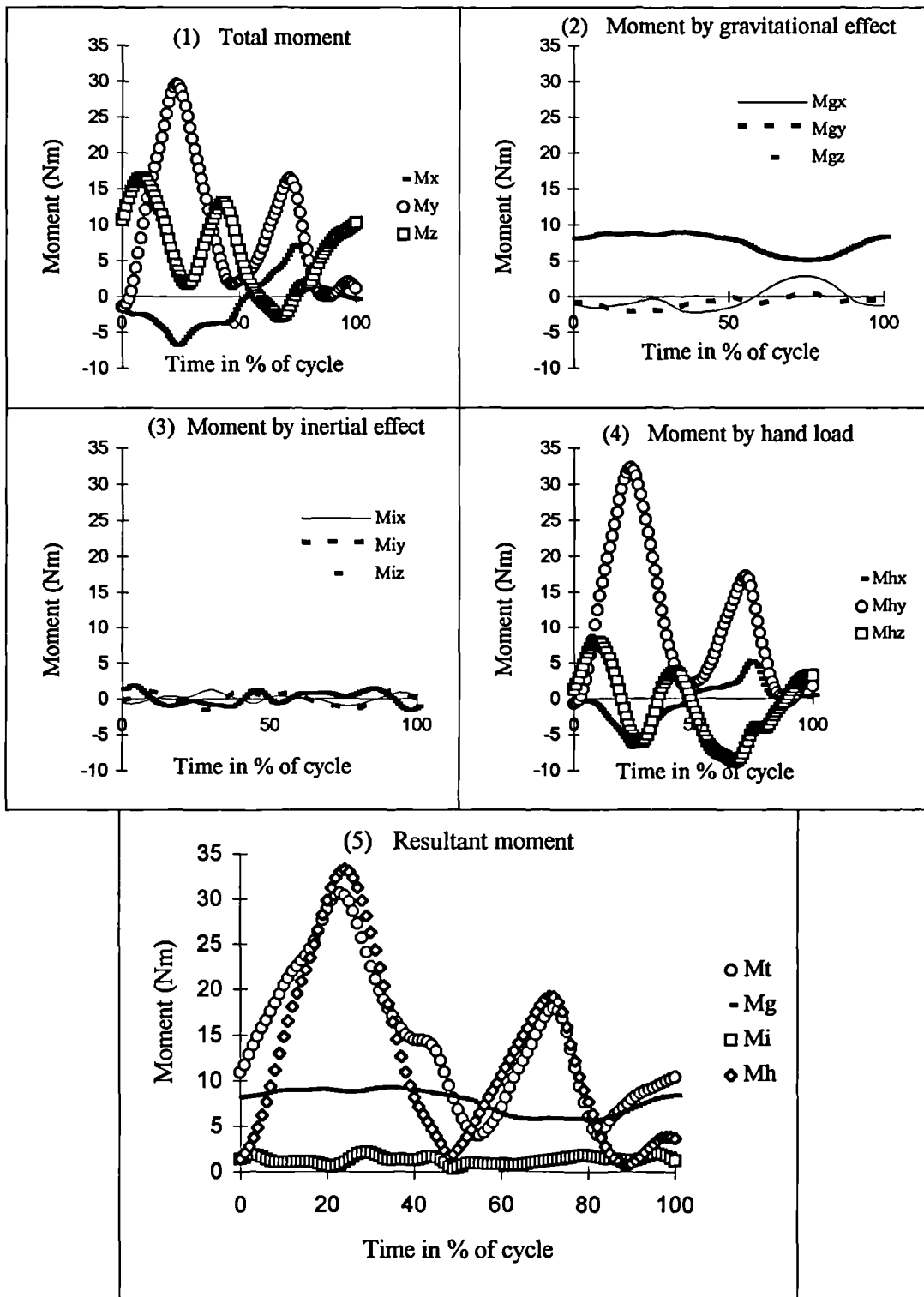


Figure 6.41 3-D shoulder moment during driving activity

Both F_y and F_z on the shoulder (Fig. 6.40(1)) are of high magnitude but they are caused by different effects, F_y mainly by the gravitational effect of the arm (F_{gy} in Fig. 6.40(2)) and F_z mainly by the hand loads (F_{hz} in Fig. 6.40(4)). Therefore the gravitational effect and hand loads are all important contributions to the total shoulder force F_t (Fig. 6.40(5)). The maximum F_h of 52.8N is slightly higher than the maximum F_t of 51.9N. The maximum F_i is 3.2N, only 6% of the maximum F_t , therefore neglecting inertial effects will not cause much difference on the estimated maximum total shoulder force of the driving activity. It is interesting to find that the resultant shoulder force F_h in Fig. 6.40(5) is greater for anticlockwise turning than for clockwise turning of the steering and its major component M_{hz} (Fig. 6.40(4)) has the same sign in each direction of turning.

In contrast to the lifting and door opening/closing activities, the major component of total shoulder moment during driving is M_y (Fig. 6.41(1)), the inward (positive) rotation moment in both turning directions of the steering wheel due to the hand load (Fig. 6.41(4)). Therefore turning a steering wheel requires a high inward rotation strength on the shoulder rather than flexion/extension strength required for lifting and door opening/closing activities. The maximum magnitude of M_x , M_y , M_z on the shoulder are 7.19Nm, 29.51Nm, and 16.45Nm, respectively. The contribution of hand load to the resultant total shoulder moment is much higher than the other effects. The maximum M_h and M_t (Fig. 6.41(5)) are 33.25Nm and 30.63Nm, respectively. The magnitude of M_g varies at a level about 1/3 of the maximum magnitude of M_h and M_t with a maximum value of 9.19Nm. The resultant inertial shoulder moment M_i is at a very low level of magnitude with a maximum value of 2.15Nm, about 7% of the maximum M_t and 6.5% of the maximum M_h .

The elbow forces and moments during driving are given in Fig. 6.42 and Fig. 6.43 where the effect on the total and resultant elbow forces and moments can be observed. Comparisons of these results with that of other activities are given in section 6.5.

6.4 Cutting Activity

Six subjects were tested for the cutting activity and 14 trials were analysed. Three cuttings in each trial were normalised to a 100% of time base, and the mean results of 14 trials are given. Since the arm has a very small range of movement during the cutting activity, only

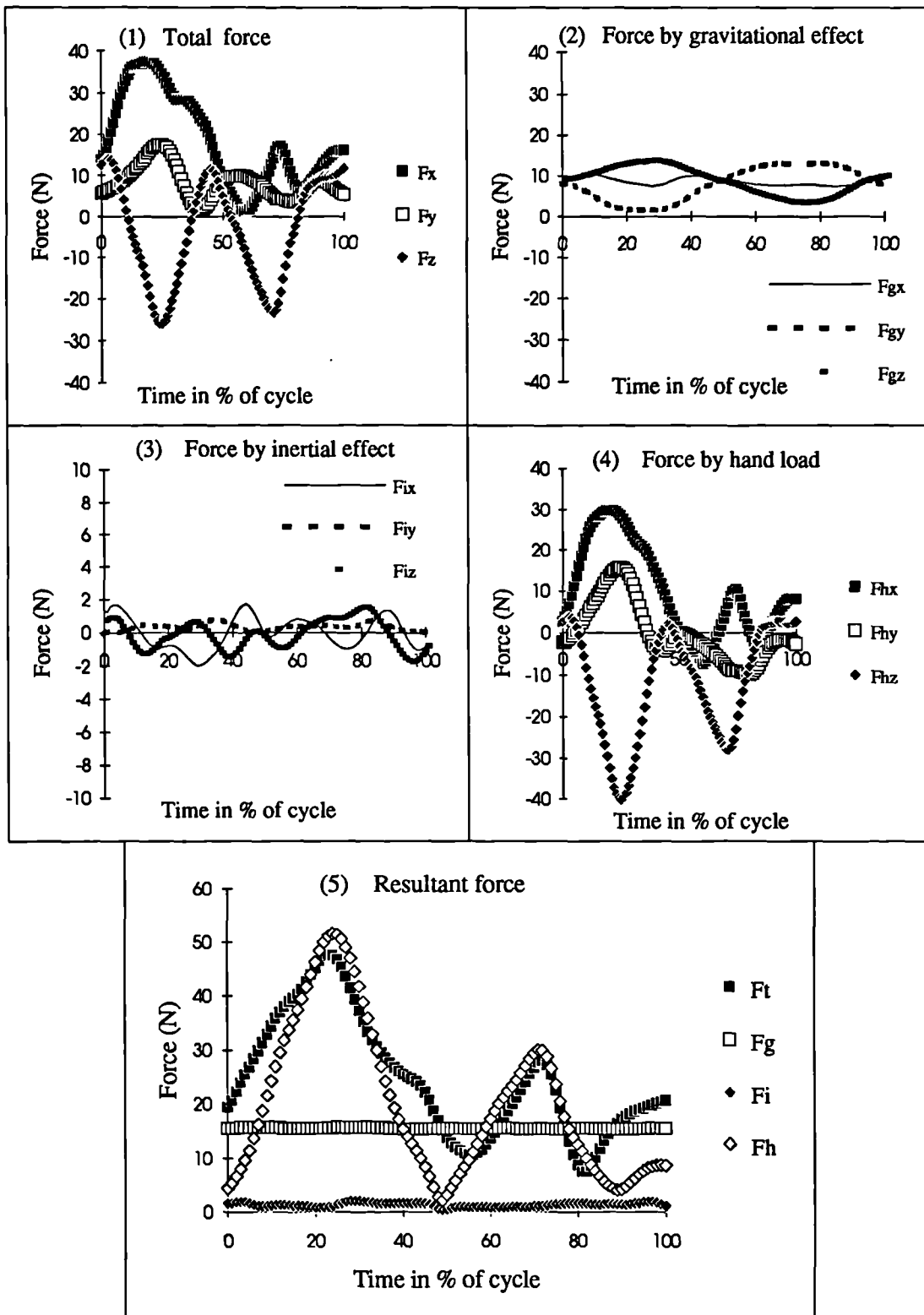


Figure 6.42 3-D elbow forces during driving activity

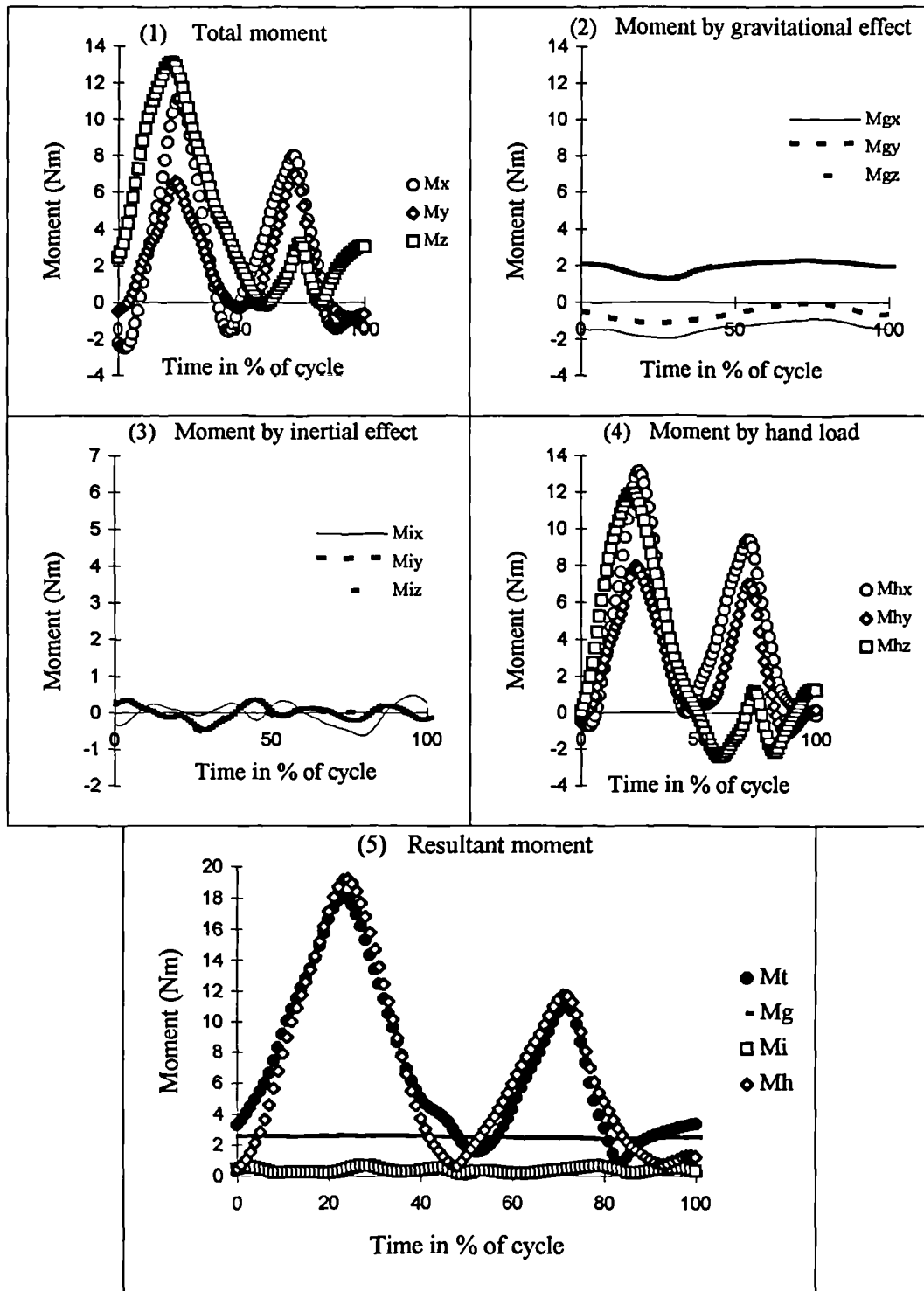


Figure 6.43 3-D elbow moment during driving activity

kinetic results are presented in the following in the same way as for the door opening/closing and driving activities.

6.4.1 Kinetic Results and Discussions

The major component of hand force (Fig. 6.44(1)) is F_x , which is perpendicular to the palm and positive F_x directs from palm to the back of hand. The maximum F_x is 9.3N, and maximum F_r , the resultant hand force, is 10.1N. The three components of hand moment (Fig. 6.44(2)) during the cutting activity are similar in level of magnitude. The maximum magnitude of M_x , M_y , M_z , and resultant hand moment M_r are 1.02Nm, 0.74Nm, 1.15Nm, and 1.56Nm, respectively.

As shown in Fig. 6.45(1), F_y is high in magnitude and is a major component of shoulder force for the cutting activity, while F_x and F_z are all of low magnitude. The maximum magnitude of F_x , F_y , and F_z are 7.1N, 35.1N, and 5.9N, respectively. It is interesting to find that the resultant total shoulder force F_t (Fig. 6.45(5)) is lower than the resultant shoulder force F_y caused by the gravitational effect at most of the data points. The reason for this can be found from Fig. 6.45(2) and Fig. 6.45(4), where all three components of shoulder force caused by the hand loads are in the opposite direction to the corresponding components of shoulder force caused by the gravitational effect. Therefore the resultant shoulder force decreases with the increase of cutting force. The maximum F_t , F_g , F_h and F_i are 35.8N, 35.5N, 10.7N, and 4.1N, respectively.

It can be seen that shoulder moments M_{gz} (Fig. 6.46(2)) and M_{hz} (Fig. 6.46(4)) are in opposite directions, which causes the flexion moment M_z (Fig. 6.46(1)) to be lower than M_{gz} , a reduction of gravitational effect on the shoulder flexion moment. If a greater cutting force were exerted, a greater reduction of gravitational effect on shoulder flexion moment would result. If the cutting force increases to a certain magnitude the gravitational effect will be fully balanced out and produce an extension moment on shoulder. Since M_{gx} and M_{hx} are also in opposite directions, the negative M_x , an adduction moment, can be stated as dominated by the gravitational effect during the cutting activity. However it should be noted that the gravitational effect on the adduction/abduction shoulder moment can be greatly changed by

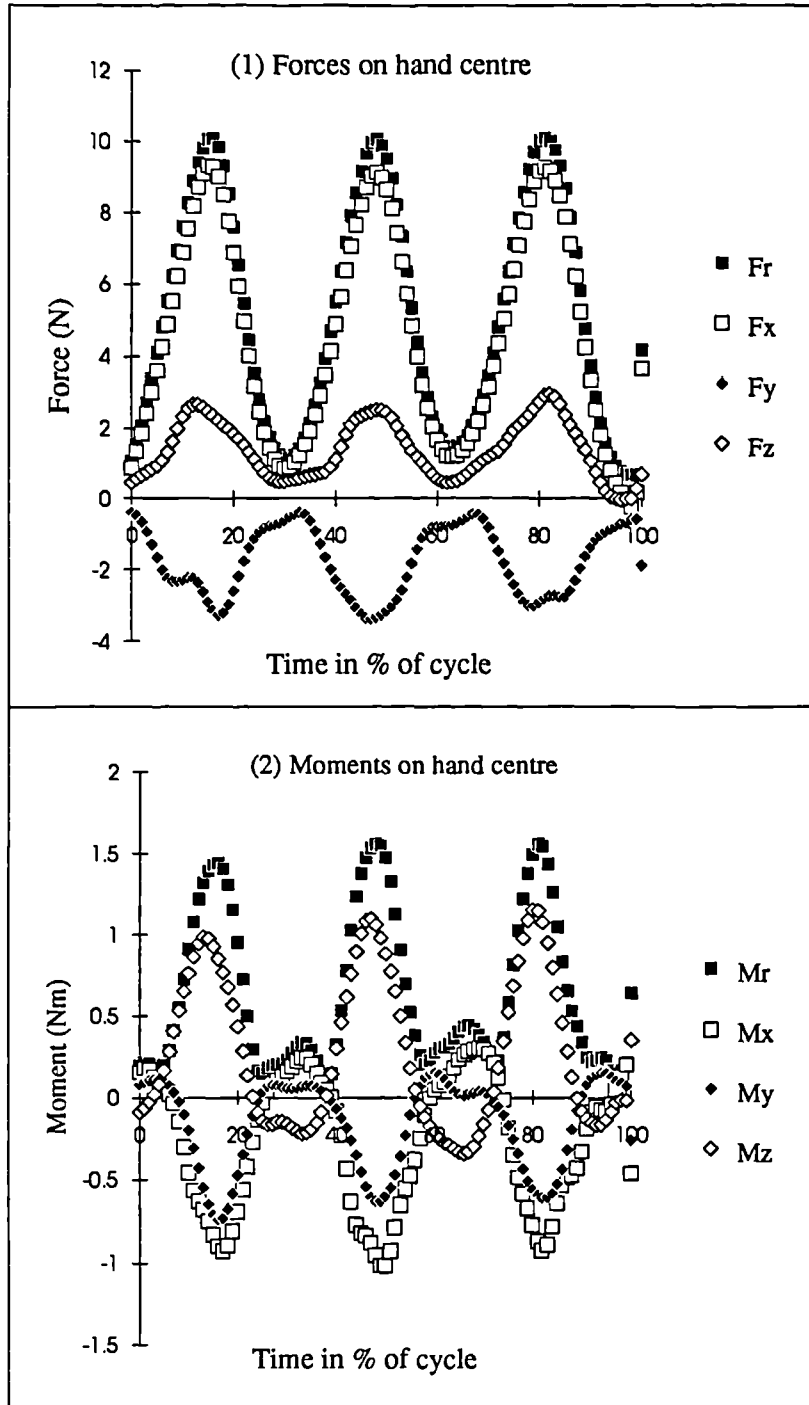


Figure 6.44 Forces and moments on hand centre in hand coordinate system during cutting activity

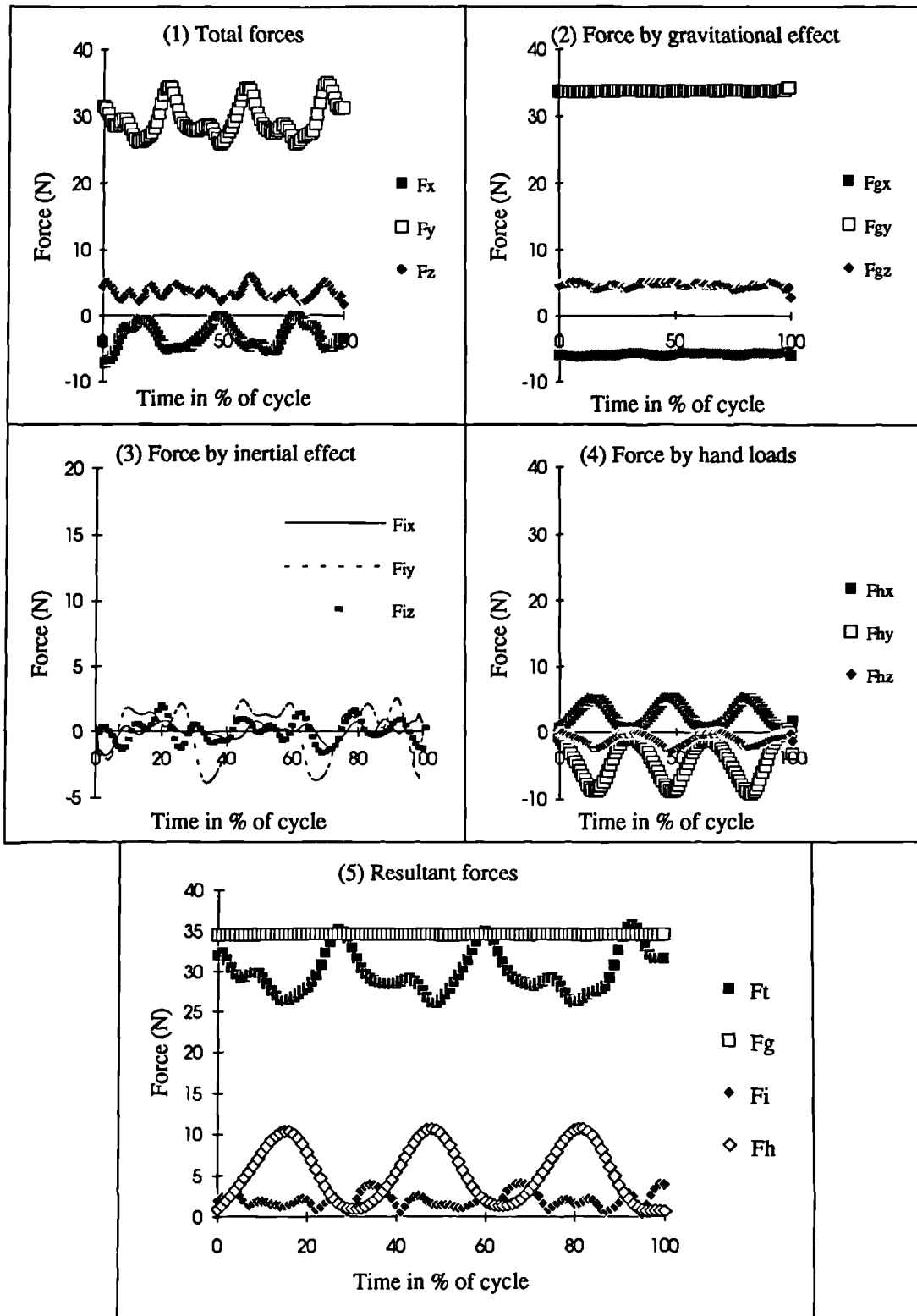


Figure 6.45 3-D shoulder forces during cutting activity

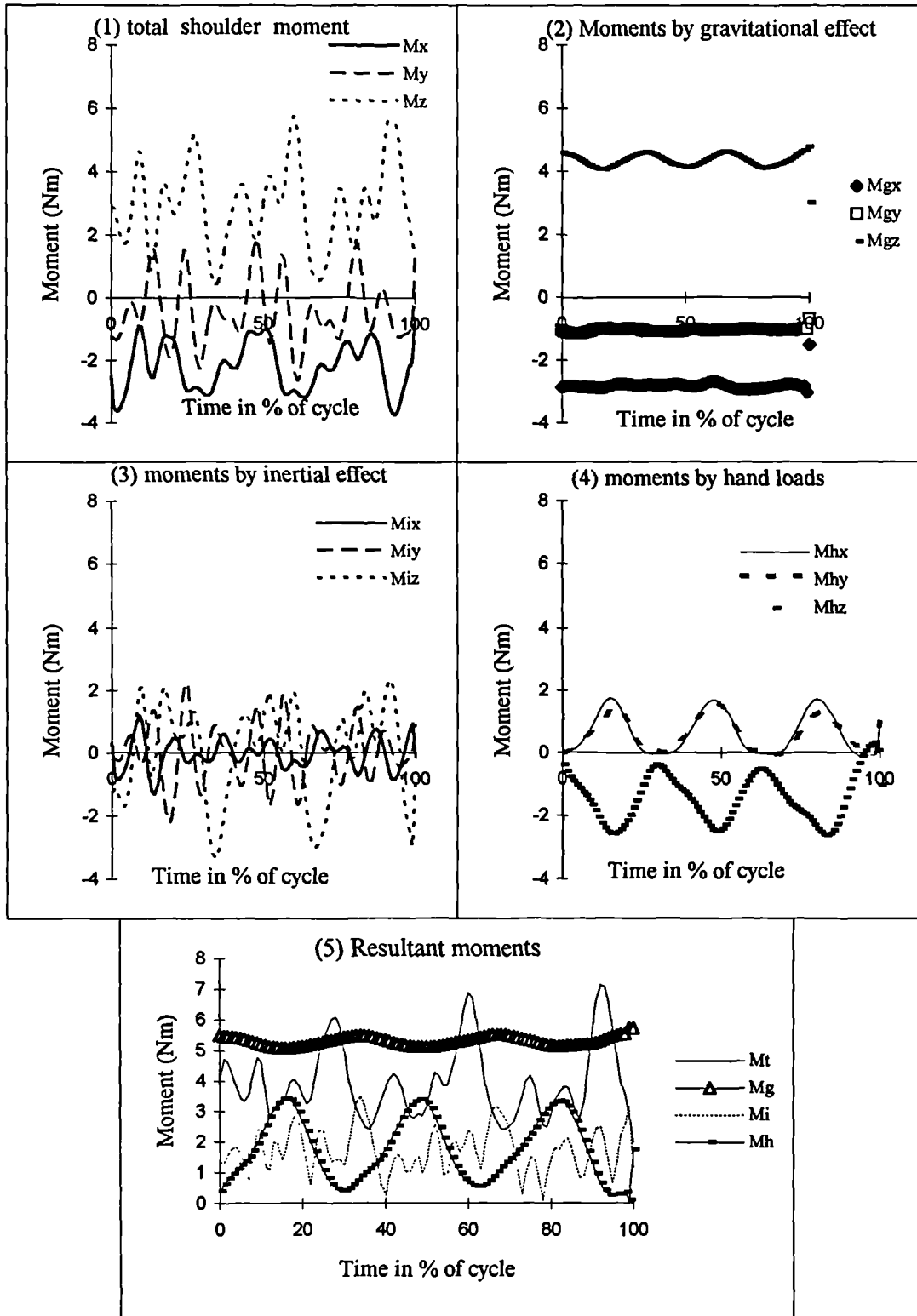


Figure 6.46 3-D shoulder moments during cutting activity

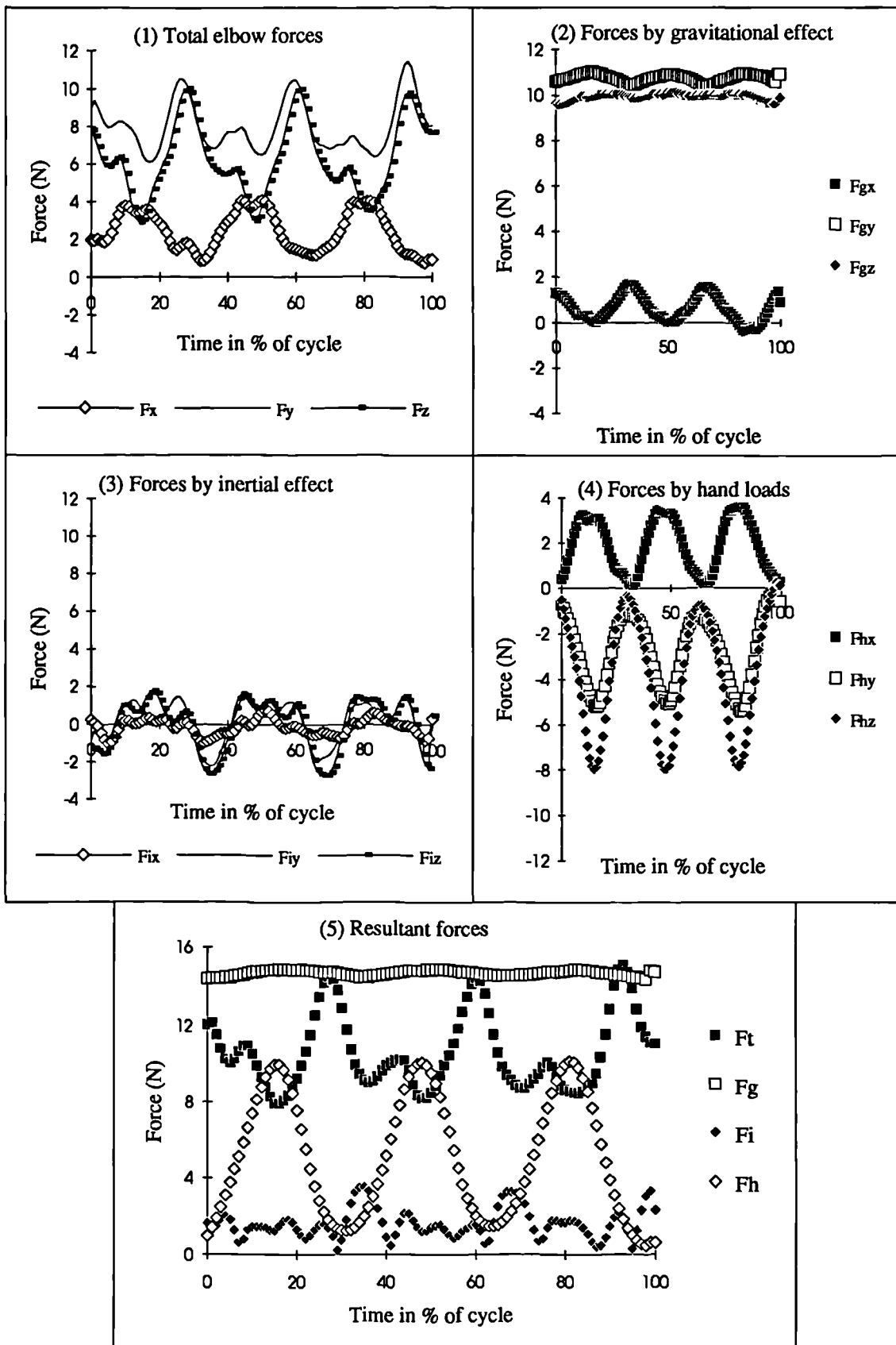


Figure 6.47 3-D elbow forces during cutting activity

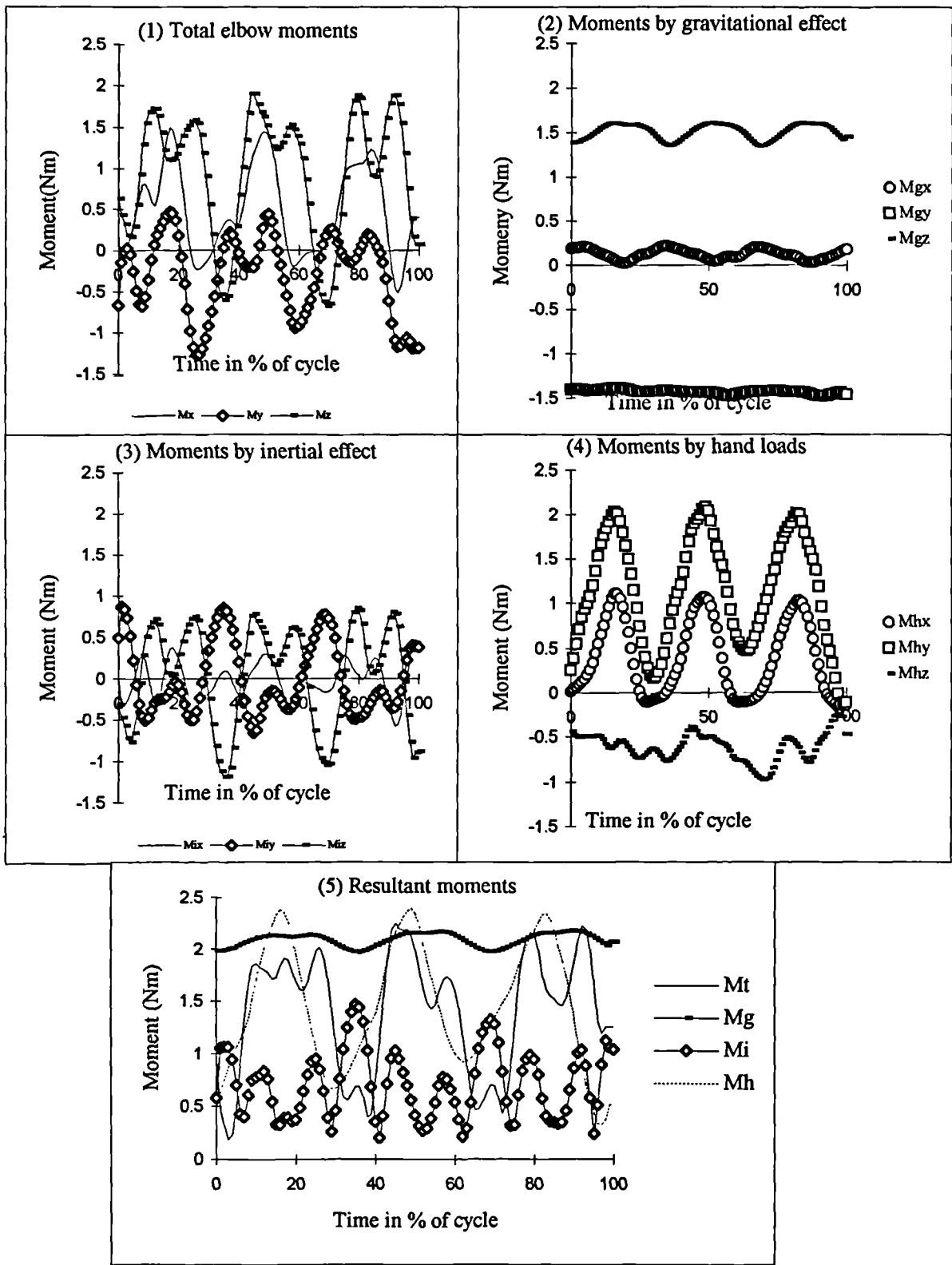


Figure 6.48 3-D elbow moments during cutting activity

the arm position during the cutting activity. The maximum magnitudes of M_x , M_y , and M_z on the shoulder are 3.75Nm, 2.67Nm, and 6.11Nm, respectively.

The magnitude of M_g (Fig. 6.46(5)) is higher than the magnitude of M_i and M_h which are of similar level of magnitude. The results show that the gravitational effect is more important than the inertial effect and the hand load effect to the total shoulder moment for the cutting activity. The inertial effect produced multi-peak values in the resultant total shoulder moment M_t (Fig. 6.46(5)) and its components (Fig. 6.46(1)) since the inertial shoulder moment and the shoulder moments caused by gravitational effect and hand loads are in similar level of magnitude. Special attention should also be paid to the inertial effect and hand load effect which can be changed greatly by the speed of cutting and the magnitude of cutting force exerted during the activity. The maximum M_t , M_g , M_i , and M_h are 7.14Nm, 5.72Nm, 3.47Nm, and 3.43Nm, respectively.

As with shoulder forces and moments, the elbow forces F_{gy} and F_{gz} (Fig. 6.47(2)) caused by the gravitational effect are greatly reduced by the hand load effect F_{hy} , F_{hz} (Fig. 6.47(4)), which cause the resultant total elbow force F_t (Fig. 6.47(5)) to be much lower than F_g the resultant gravitational elbow force. The maximum magnitude of F_h is much higher than that of F_i (Fig. 6.47(5)). The maximum magnitude of the three components of total elbow force F_x , F_y , F_z (Fig. 6.47(1)) are 4.0N, 11.4N, and 10.0N, respectively. The maximum magnitude of F_t , F_g , F_i , and F_h are 15N, 14.9N, 3.5N, and 10.1N, respectively.

The highest elbow moment is M_z (Fig. 6.48(1)), the flexion (positive) moment, which is mostly due to the gravitational effect M_{gz} (Fig. 6.48(2)). The inertial effect M_{iz} (Fig. 6.48(3)) also results in an increase of the elbow flexion moment. Although the M_{hy} (Fig. 6.48(4)) is high in magnitude, the negative M_{gy} (Fig. 6.48(2)) and M_{iy} (Fig. 6.48(3)) cause the magnitude of M_y (Fig. 6.48(1)) to be lower than that of M_x and M_z . The maximum magnitude of the three components of elbow moment M_x , M_y , and M_z are 1.50Nm, 1.27Nm, and 1.90Nm, respectively. The highest resultant elbow moment is M_h (Fig. 6.48(5)) caused by the hand load, and M_g is also high in magnitude. Although the resultant inertial elbow moment M_i (Fig. 6.48(5)) is the lowest among the three effects, its magnitude relative to M_t is much higher than that of the door opening/closing, and driving activities presented in previous sections. The maximum magnitudes of elbow moment M_t , M_g , M_i , and M_h are 2.25Nm, 2.17Nm, 1.47Nm, and 1.39Nm, respectively.

6.5 Summary of Shoulder and Elbow Moments of Different Activities.

For the purpose of comparing the loads on the shoulder and elbow joints during different activities, the mean values of the maximum shoulder and elbow moments are represented and discussed in this section in two parts. The mean values and standard deviations of maximum moment are calculated from the maximum moments of each trial before time normalisation. It should be noted that the method of calculating the mean values of the maximum moments is different with the method used in previous sections where the maximum moment is obtained from the means of normalised results. Therefore it is easier to understand that the results given below will be greater in value than the corresponding part in previous sections. There are two reasons for choosing the method to present the results of maximum moment, first it can avoid lower estimation of the maximum moments, second the standard deviations reflect the differences between maximum moments. Appendix C shows the repeatability of shoulder moments for all subjects during the lifting activity.

6.5.1 Summary of Shoulder Moments of Different Activities

The summary of shoulder moments of different activities are given in two parts. The first part summarises the 3-D results and the second part summarises the results by different effects.

3-D maximum shoulder moments

In Figure 6.49, M_r represents the mean values of the maximum resultant shoulder moment, and M_x , M_y , and M_z represent the mean values of the maximum shoulder moment about each axis of the trunk coordinate system. For simplicity, M_x , M_y and M_z given in Figure 6.49 are absolute values without considering the signs. Details of the results are given numerically in Table 6.8 with sign (Max, Min) and standard deviations.

It can be seen that the flexion/extension moment M_z is the major component of the shoulder moment for most activities investigated in this study, the only exception being the driving activity in which the inward/outward rotation moment is the major component of shoulder moment and is caused by the big moment lever arm (Fig. 6.35(3)) and hand force (Fig. 6.39(1)). The results indicate that having enough shoulder flexion/extension strength is most important for conducting most upper limb activities of daily living, although the

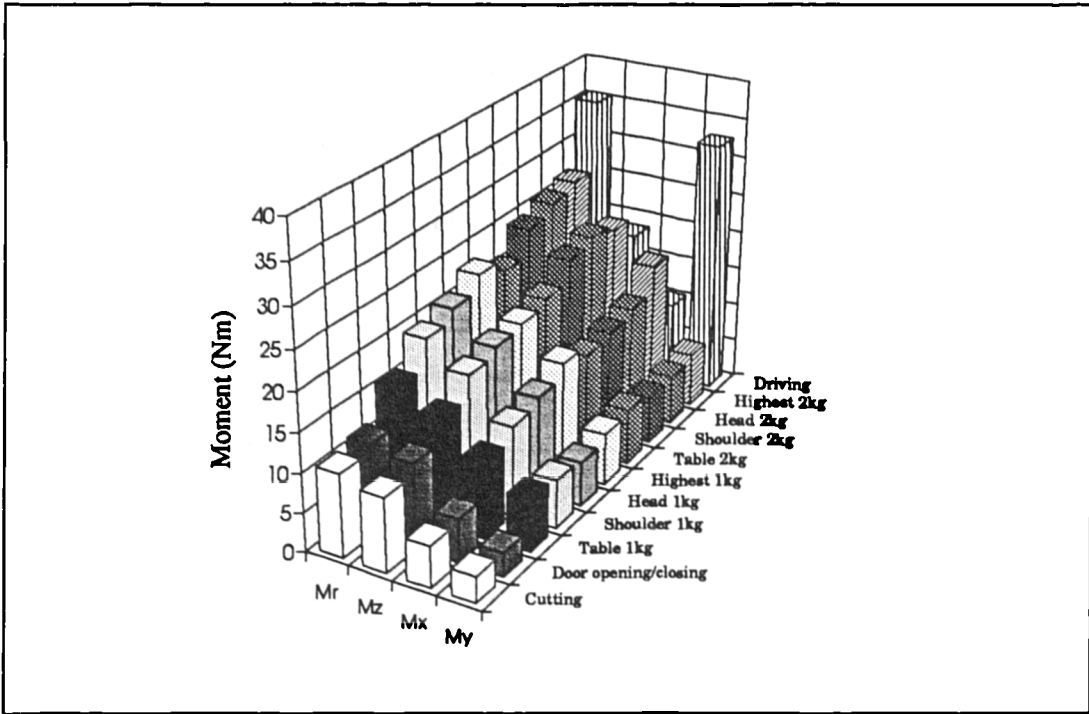


Figure 6.49 3-D mean values of the maximum shoulder moment of different activities
 Mr: resultant moment; Mx: Adduction/abduction moment
 My: Inward/outward rotation moment; Mz: Flexion/extension moment

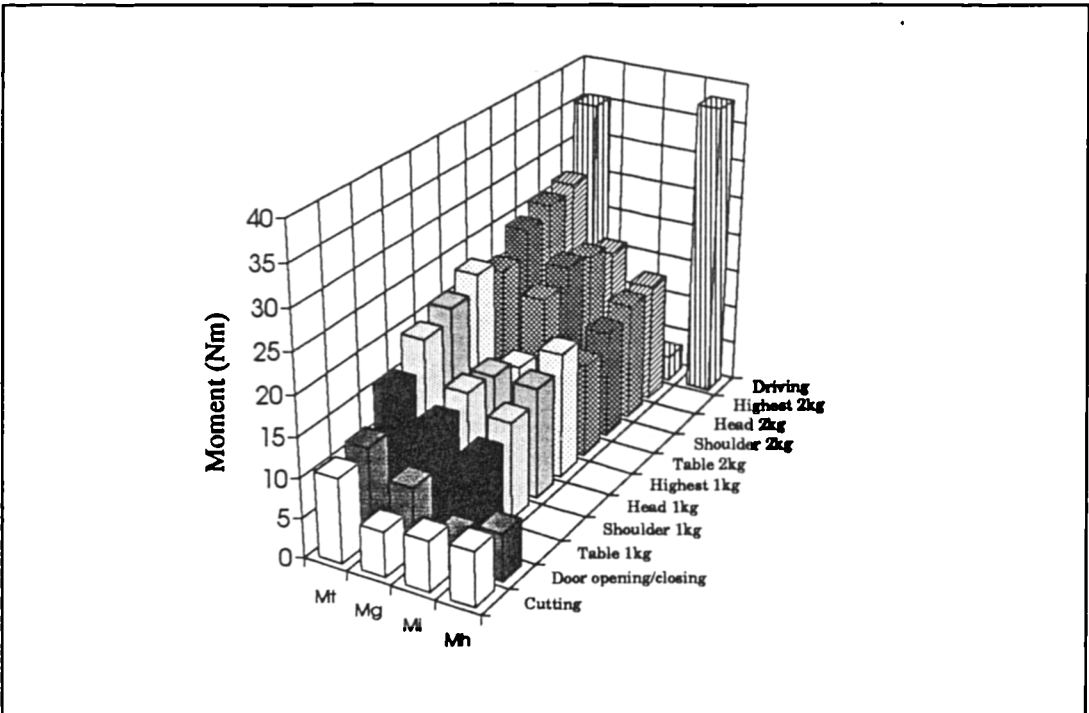


Figure 6.50 Mean values of the maximum resultant shoulder moment by different effects
 Mt: resultant total moment Mg: resultant moment by gravitational effect
 Mi: resultant moment by inertial effect Mh: resultant moment by hand loads
 Note: In Figure 6.49 to Figure 6.52, the table, shoulder, head, and highest refer to the height of the book lift.

movement patterns and the purposes of the activities may be different. For example the purpose of the lifting activity is to move an object upward and downward, the door opening/closing can be considered as moving an object forward and backward and the cutting activity can be performed with a small range of arm movement.

The second major component of the shoulder moment is M_x , the adduction/abduction moment, for most activities except driving. This result indicates that possessing sufficient adduction/abduction shoulder strength is also an important condition for the execution of most upper limb activities of daily living. It has been found in previous sections that significant adduction/abduction of the upper arm always accompanies flexion/extension. This is why the adduction/abduction shoulder strength is also important for performing upper limb activities of daily living. The results also indicate that 3-D biomechanical analysis is required for fully understanding the load patterns on the shoulder joint during various activities of daily living.

As shown in Figure 6.49, the maximum resultant shoulder moment M_r and maximum magnitude of the major components M_z and M_x of the lifting activity increase with the increase of the weight to be lifted and the increase of lifting height. The maximum values of M_r , M_x , M_y and M_z of the door opening/closing and cutting activities are lower than the corresponding part of lifting a 1kg book to table height. It can also be seen that the highest magnitude of shoulder moment occurs during the driving activity. These results provide a general image of how much moment acts on the shoulder joint for different activities. The information is very important for the assessment of loads acting on the shoulder and can be used to quantitatively grade the difficulty of each activity by the magnitude of shoulder moment. Since the shoulder moment must be generated by the muscle around shoulder joint, the information can also be used to assess the patient's ability of performing the activities of daily living.

Therefore according to the magnitude of shoulder moments (Fig. 6.49) the cutting is the easiest activity investigated in this study, and the door opening/closing is the second easiest activity. The most difficult activity is driving, it not only requires a high flexion/extension shoulder moment (M_z) but also needs a high inward/outward rotation shoulder moment (M_y) which is also the highest component of the shoulder moment among all the activities investigated in this study. For the lifting activity, it is obvious that difficulty increases with the increase of the weight to be lifted and the height of lifting.

Table 6.8 Maximum shoulder moments of different activities

Activities	Mx		My		Mz		Mt(Mr)	Mg	Mi	Mh
	Max	Min	Max	Min	Max	Min				
Lifting a 1kg book to table height	-1.87	-9.98	6.74	-5.69	13.17	-0.35	16.12	13.12	10.68	
Stdev	1.16	2.27	2.25	1.66	1.99	1.93	1.64	1.63	1.78	
Lifting a 1kg book to shoulder height	-1.34	-11.54	5.83	-6.18	16.64	-0.33	19.73	14.51	12.37	
Stdev	1.53	3.83	3.37	2.46	3.51	2.25	3.17	1.43	3.32	
Lifting a 1kg book to head height	-0.23	-12.53	5.28	-5.67	17.64	-0.85	21.14	14.01	13.97	
Stdev	2.52	3.07	2.97	1.84	3.39	2.95	3.22	1.37	3.31	
Lifting a 1kg book to highest height	0.85	-14.3	6.58	-6.45	18.08	-1.1	23.1	12.62	15.75	
Stdev	1.98	4.19	3.86	2.23	3.87	4.21	4.39	2.44	4.46	
Lifting a 2kg book to table height	-2.85	-12.88	6.24	-7.06	18.89	3.5	21.35	19	11.68	
Stdev	2.11	2.72	3.75	2.75	2.14	2.07	1.58	2.03	2.07	
Lifting a 2kg book to shoulder height	-2.07	-13.4	4.8	-6.1	21.69	3.44	24.59	20.91	13.62	
Stdev	4.41	4.2	2.71	2.77	1.91	2.77	2.54	1.64	2.88	
Lifting a 2kg book to head height	-1.22	-14.14	5.35	-6.38	22.52	3.07	25.87	20.07	14.91	
Stdev	3.35	4.7	3.98	2.28	3.71	3.22	4.95	2.15	3.98	
Lifting a 2kg book to highest height	0.07	-17.59	5.66	-6.84	21.31	1.7	26.69	18.61	15.24	
Stdev	2.74	3.95	2.18	1.92	3.85	3.03	5.29	3.35	4.22	
Door opening/closing	0.6	-5.61	3.04	-2.35	10.93	-0.9	11.61	8.27	3.79	5.94
Stdev	2.12	1.37	0.93	1.29	1.94	1.97	1.78	0.98	2.11	1.3
Driving	10.04	-9.18	32.62	-3.21	18.4	-7.5	35.44	9.42	3.22	38.07
Stdev	7.78	4.13	6.41	2.64	3.65	7.03	5.51	1.3	0.86	8.53
Cutting	1.3	-5.22	2.8	-3.3	9.51	-2.99	10.7	5.7	6.35	6.87
Stdev	2.24	2.55	1.58	1.56	2.78	3.68	2.61	1.37	2.67	3.65

Table 6.9 Maximum elbow moments of different activities

Activities	Mx		My		Mz		Mt (Mr)	Mg	Mi	Mh
	Max	Min	Max	Min	Max	Min				
Lifting a 1kg book to table height	1.09	-3.36	-0.08	-4.42	8.72	0.66	10.05	6.48	5.23	
Stdev	1.1	1.6	0.53	0.93	1.36	0.96	1.14	0.6	0.87	
Lifting a 1kg book to shoulder height	1.24	-3.93	0.32	-4.28	9.89	-0.38	11.1	6.6	5.71	
Stdev	0.74	1.09	0.64	1.18	1.91	1.26	1.69	0.55	1.3	
Lifting a 1kg book to head height	1.1	-4.82	0.1	-4.63	10.17	-0.33	11.61	6.67	6.2	
Stdev	1.27	1.2	0.85	0.81	1.88	1.76	1.66	0.66	1.46	
Lifting a 1kg book to highest height	2.06	-5.32	1.01	-5.27	10.54	-0.68	12.11	6.72	6.73	
Stdev	2.63	0.87	1.7	1.16	1.93	1.31	1.93	0.62	1.61	
Lifting a 2kg book to table height	1.07	-5.21	-1.07	-6.08	12.97	2.85	14.53	10.99	6.19	
Stdev	1.41	1.69	0.86	0.97	1.87	1.77	1.52	0.8	0.94	
Lifting a 2kg book to shoulder height	1.19	-5.38	-1.19	-6.86	15.04	1.87	16.66	11.15	7.29	
Stdev	1.67	1.67	1.1	1.53	1.47	2.88	1.19	0.91	1.05	
Lifting a 2kg book to head height	1.19	-7.06	-0.96	-7.6	14.86	0.4	16.72	11.14	7.63	
Stdev	2.47	1.45	0.94	1.71	2.34	2.89	2.03	1	1.62	
Lifting a 2kg book to highest height	1.31	-7.56	-0.06	-7.75	14.68	0.03	17.16	11.26	7.95	
Stdev	2	0.91	0.78	1.11	3.25	1.81	2.74	1.15	1.54	
Door opening/closing	0.43	-2.91	1.37	-2.72	5.61	0.69	6.28	2.73	0.98	4
Stdev	0.99	0.75	0.96	1.75	1.76	1.14	2.02	0.42	2.01	1.78
Driving	13.53	-3.44	8.27	-2.05	14.04	-1.99	21.04	2.72	1.04	22.19
Stdev	7.48	1.38	2.44	1.16	3.38	3.03	4.83	0.43	0.24	5.43
Cutting	2.39	-0.86	1.94	-2.91	4.38	-1.73	6.35	2.32	2.58	5.02
Stdev	1.3	0.98	2.66	1.19	2.16	1.8	1.83	0.34	1.12	2.73

Maximum resultant shoulder moments caused by different effects

The mean values of the maximum resultant total shoulder moment M_t and resultant shoulder moment from each effect are given in Figure 6.50. The data used in Figure 6.50 are given in Table 6.8 with standard deviations.

The activities investigated in this study can be divided into two groups, the activities without external loads on the hand (such as lifting), and the activities with external hand loads on hand (driving, door opening/closing and cutting).

Since there are no external loads on hand, the shoulder moments are only influenced by gravitational and inertial effects during lifting activity. The gravitational and inertial shoulder moments (M_g and M_i) are similar in magnitude, and M_g is slightly higher than M_i for the lifting of a 1kg book. When the lifted weight was increased, the gravitational shoulder moments (M_g) increased greatly but the inertial shoulder moments increased only slightly. Because the lifting of 1kg or below can be considered as a light weight, it can be concluded that during light weight lifting both gravitational and inertial effect are important factors for the assessment of shoulder moments. Relative to the gravitational effect the inertial effect to shoulder moment decreases with the increase of lifted weight. This finding is in agreement with the results obtained in section 6.1.

During the activities of door opening/closing, driving and cutting, not only the inertial and gravitational effects but also the hand loads will influence the shoulder moment. As shown in Figure 6.50 the shoulder moment caused by the hand loads during the driving activity is the highest shoulder moment. This result reflects the important effect of hand loads on the shoulder moment during driving and indicates that driving is more difficult than the other activities.

Compared to the driving activity, the shoulder moments caused by hand loads for the cutting and door opening/closing activities are quite low, but it is still ranked highest and second highest among the three effects for the cutting and door opening/closing activity, respectively. The difference between M_g , M_i and M_h is quite small for the cutting activity and the magnitude of M_i for the door opening/closing activity is very low. Therefore it can be concluded that all three effects are important for the assessment of shoulder moment of the

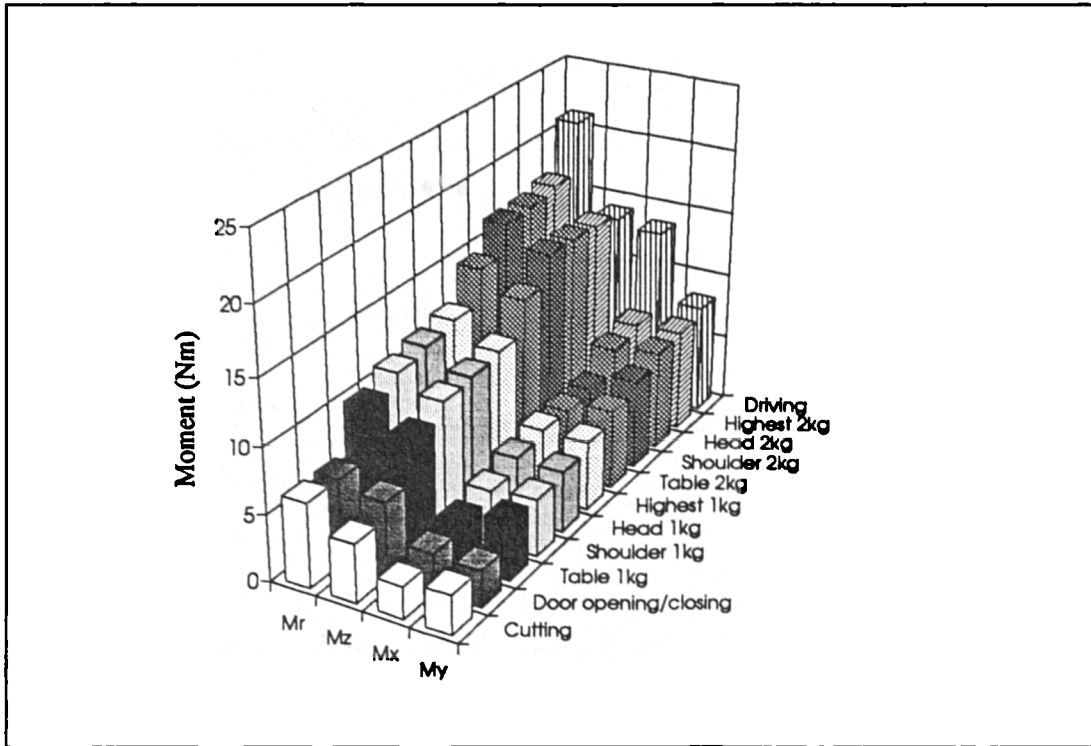


Figure 6.51 3-D mean values of the maximum elbow moment of different activities
 Mr: resultant moment; Mx, My, Mz are expressed in upper arm coordinate system

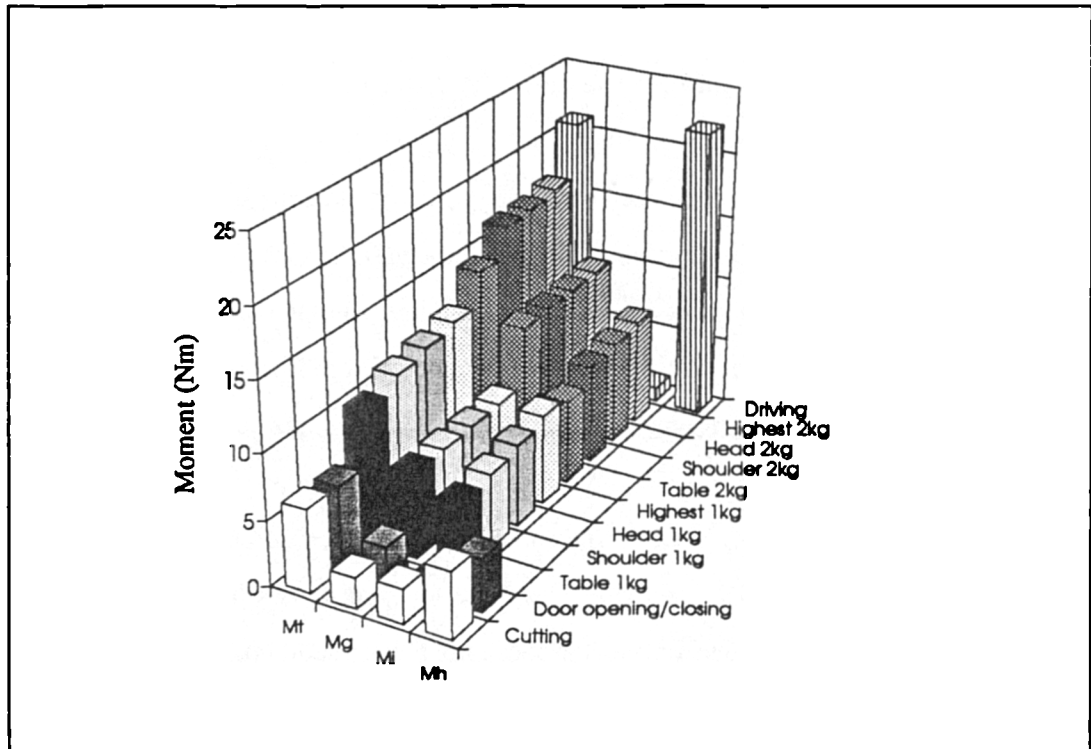


Figure 6.52 Mean values of the maximum elbow moment by different effects
 Mt: total ; Mg: by gravitational effect; Mi: by inertial effect; Mh: by hand loads

cutting activity, while the inertial effect on the shoulder moment is less important for the door opening/closing and driving activities.

6.5.2 Summary of Elbow Moments of Different Activities.

The elbow moments of the different activities are summarised in this section (Fig. 6.51, Fig. 6.52, and Table 6.9) in the same way as for the summary of shoulder moment.

3-D Maximum elbow moments

As shown in Figure 6.51, the flexion/extension elbow moment M_z (Fig. 6.51) is the major component of the elbow moment for all the activities despite the movement patterns and purposes of the activities being different as stated in above section. This indicates that sufficient elbow flexion/extension strength is required for performing most upper limb activities of daily living. The results are also in agreement with the fact that flexion/extension of the forearm is the major function of elbow joint.

It is interesting to find that M_x and M_y are at nearly same level of magnitude for all the activities except driving. Since most of the activities were performed with free style, except the driving activity in which the hand moves in a specified route, the results can be explained as that the subject adopted consciously or unconsciously a style of movement to load the major elbow moment on the z-axis (directing from medial epicondyle to lateral epicondyle) and to enable the moments on the x-axis and y-axis of the upper arm coordinate system to be as low as possible. This load pattern for the elbow may be the optimal distribution of elbow moment.

Maximum resultant elbow moments caused by different effects

As shown in Figure 6.52, for the activities with external hand loads (driving, door opening/closing and cutting) the elbow moment (M_h) caused by hand loads is higher than the elbow moments caused by gravitational and inertial effects (M_g and M_i). For the driving activity M_h is so high that the influences of M_i on the total elbow moment can be neglected in the estimation of total elbow moment. Therefore it can be concluded that the hand load is a major contributor to the elbow moment for the activities with external hand loads.

For activities without measured external hand loads, such as lifting, the gravitational elbow moment M_g and inertial elbow moment M_i are at similar levels of magnitude for the

lifting of a 1kg weight, and M_g is higher than M_i for the lifting of a 2kg weight. Therefore it can be concluded that the gravitational elbow moment increases with increase of the lifted weight, in contrast with this the inertial effect on elbow moment will increase if the lifted weight were to be reduced.

Finally, it should be noted that the above results were obtained under test conditions with the preferred style which each subject adopted while performing the activities of this study. It is clear, however, that the shoulder (or elbow) moments will be changed if the test conditions were different or the activities were performed in a specified style. For example if the relative position between the shoulder and hand (or equipment i.e. the door, steering wheel and cutting table) were different from that of this study, the shoulder moments will be changed accordingly. While the changes of shoulder moments due to this reason can be determined using Eq. B.10 in Appendix B. Generally, according to Eq. B.10, 1cm difference in x -direction (forward/backward) will cause a change of $-0.01F_z$ Nm in M_y (inward/outward rotation moment) and $0.01F_y$ Nm in M_z (flexion/extension moment) respectively, where the F_y and F_z are the components of hand force expressed in the trunk coordinate system. In the case of the door opening/closing activity, the maximum hand force of -3.405N , -23.153N , and 8.147N along the three axes of the hand coordinate system occurred at the early pulling phase when the hand coordinate system was approximately parallel to the trunk coordinate system and the x , y , z axes of the hand frame correspond to the Z , X , Y axes of the trunk frame. Therefore the three components of hand force in the trunk coordinate system are -23.153N , 8.147N , and -3.045N , respectively. If the change of the relative position of the shoulder and hand in the vertical direction is 1cm ($dy = 0.01\text{m}$ in Eq. B.10), each of the three components of shoulder moment changes -0.03Nm , 0.0Nm , and 0.23Nm , respectively. The changes of shoulder and elbow moments in other cases can also be estimated in the same way, but further investigations are beyond the purpose of this study.

Chapter Seven

Conclusions and Recommendations

7.1 Conclusions

Although the purpose of this study is to investigate the biomechanical characteristics of four upper limb activities, the most significant achievement of this study is the implementation of the residual analysis technique into the computer program which allows noisy kinematic data collected by the motion analysis system to be filtered at the auto-selected cut-off frequency for each data sequence. It therefore avoids the problems of over-filtering (cut-off frequency is too low) or allowing too much noise to pass (cut-off frequency is too high) which often occurs when using a fixed cut-off frequency for a data file or a set of data files. The expense of using this method is that it uses more computer time for selecting the cut-off frequency for each data sequence than using a fixed cut-off frequency, however it can save a lot of time for the frequency analysis during the exercise of choosing a fixed cut-off frequency, especially for users who are unfamiliar with the frequency analysis technique.

The second methodological achievement of this study is the development of the new method of representing the velocity and acceleration of points of interest in a phase plane. This method can provide more information than the conventional method of representing the velocity and acceleration in a time domain. It has proved that this method is an effective, easy and clear way of investigating the velocities and accelerations of the lifted book in the lifting activities and of the hand centre in the door opening/closing activity.

The results obtained in Chapter Six provide a lot of useful information for improving the understanding of the biomechanical nature of the four activities and for clinical reference. The information and the conclusions drawn from the results are given in the following.

Lifting activity

It was found that the upper arm rotates externally during the lifting phase and rotates internally during the lowering phase. The maximum axial rotation angle of the upper arm increased with the height of lifting.

The kinematic results show that the book moves at greater velocity and acceleration in the lifting phase than in the lowering phase, and the 2kg book was lifted at smaller velocity and acceleration than the 1kg book in the principal direction of the movement.

From the observed upper arm rotation angles it is suggested that the lifting height should be arranged a little lower than the shoulder height for minimising the scapular movement, any design of lifting to over the highest height should also be carefully considered because it may cause movement of the spinal column.

It was found that the flexion moment is the major component of the shoulder moment for the lifting activity, and the abduction moment is the second. The maximum resultant total shoulder moment and flexion shoulder moment increase with the height of lifting.

The inertial effect has a significant contribution to the total shoulder moment during the lifting activity, and the contribution increases with the height of lifting. Neglecting inertial effects in the biomechanical analysis of the lifting activity will result in up to 47% (averaged) lower estimating of the resultant shoulder moment for the lifting of a 1kg book to the highest height, and at least 30% lower (averaged) estimating of the resultant total shoulder moment for the lifting of a 1kg book to table height. For the lifting of a 2kg book the corresponding values are 36% and 25%, respectively. Results also show that the inertial to total shoulder moment ratios decrease with the increase of the lifted mass, therefore the contribution of the inertial effects to the total shoulder moment decrease with the increase of the lifted mass.

The shoulder moments are higher in the lifting phase than in the lowering phase.

The major component of elbow force is along the long axis of the upper arm., and the major component of the elbow moment is the flexion moment.

Due to the increase of the inertial effects the maximum resultant elbow moment increases with the height of lifting.

It was found that the contribution of the inertial effect to the elbow moment is similar to the contribution of inertial effect to the shoulder moment. The averaged inertial to total elbow moment ratio increases with the height of lifting and decreases with the increase of the mass to be lifted. It is concluded that neglecting inertial effects in a biomechanical analysis of the lifting activity will result in up to 49% (averaged) lower estimating the resultant total elbow moment for the lifting of a 1kg book to the highest height, and at least 24% lower estimating

the resultant total elbow moment for the lifting of a 1kg book to the table height. For the lifting of a 2kg book the corresponding values are 36% and 19% respectively

Door opening/closing activity

The major component of the 3-D shoulder moment during the door opening/closing activity is the flexion moment. The highest flexion and resultant total shoulder moments occur at the beginning and end of the door opening/closing activity. The second major component of the shoulder moment is the abduction moment. The highest abduction moment occurs at the middle of the activity. Therefore it can be concluded that 3-D analysis of the shoulder moment is required for the door opening/closing activity or pushing/pulling activities in general.

Among the three effects (hand load, gravitational and inertial effects), the weight of the arm is the major contributor to the shoulder moment. The second major contributor to the shoulder moment is the hand load. Due to the influence of these effects, it is concluded that pulling to open a door will reduce the resultant shoulder moment, while pushing to opening a door will increase the resultant shoulder moment.

It was also found that the three components of gravitational elbow force are equally distributed along the three axes of the upper arm coordinate system at the beginning and end of the door opening/closing activity when the arm is fully stretched to hold the door handle.

In the early pulling phase the maximum elbow force is along the long axis of upper arm, while in the later pulling phase the maximum elbow force is along the long axis of forearm.

The action of hand loads on elbow moment is more important than the action of gravity, which is a major difference with the shoulder force where the gravitational effect is more important than the effect of hand loads.

The flexion moment is the major component of 3-D elbow moment. The gravitational effect and hand load effect are equally important to the resultant elbow moment. The inertial effect of forearm-hand has little contribution to the resultant total elbow moment. Therefore, to neglect the inertial effect of the forearm-hand will not cause a significant difference on the estimated maximum resultant total elbow moment for the door opening/closing activity.

Driving activity

From the kinematic point of view, driving is the most complicated activity investigated in this study, because it is the only activity which requires upper arm adduction , upper arm inward rotation and a large range of forearm axial rotation.

The major component of hand force during driving acts along the transverse direction (z-axis in Figure 6.28(3)). Therefore in the assessment of driving ability more attention should be paid to the transverse hand force rather than to the grip and pushing/pulling strengths.

Among the three effects (hand load, gravitational effect and inertial effect), the hand load is the most important contributor to the forces and moments on the upper limb joints, the gravitational effect is the second, while the inertial effect can be neglected for the normal speed of turning of the steering wheel.

During driving the right hand exerts a bigger resultant force for the anticlockwise turning than the clockwise turning of the steering wheel, and the resultant forces and moments on the elbow and shoulder joints have similar patterns.

Due to the hand loads, the major component of the 3-D shoulder force acts along the lateral to medial direction. The major component of the 3-D shoulder moment is the inward rotation moment about the vertical axis of trunk coordinate system.

The major component of the elbow moment is the flexion moment.

Cutting activity

The resultant total shoulder force decreases with the increase of the cutting force, because the cutting and gravitational shoulder forces are in opposite directions. The cutting force also results in a reduction of the resultant total shoulder moment, due to the fact that the shoulder moments caused by the cutting force and the gravitational effect are in opposite directions. Although the gravitational effect is the major contributor to the total shoulder moment, the inertial and hand load effect also have a significant influence on the total shoulder moment.

The elbow force is dominated by the gravitational effect under the test conditions of this study. The inertial effect has little influence on the total elbow force.

All three components of the elbow moment are in the low level of magnitude.

Summary

According to the magnitude of the maximum resultant total shoulder moment, the difficulty of the four activities can be graded as cutting, door opening/closing, lifting, and driving. For the lifting activity the difficulty increases with the increase of the mass to be lifted and the height of lifting.

The major component of the shoulder moment is the flexion/extension moment for most of the activities except driving, therefore it is concluded that having adequate shoulder flexion/extension strength is most important for conducting most upper limb activities of daily living.

The above conclusions indicate that the biomechanical characteristics of arm movement can be used as the parameters for the assessment of the ability of doing the ADL, and that biomechanical analysis is an effective way to determine these parameters.

7.2 Recommendations For Further Work

Since only four upper limb activities were investigated in this project, more biomechanical studies on a wider range of activities are required in order to construct a data base for the assessment of the ability of performing ADL and clinical reference. The investigations can also be extended to the lower limb and whole body activities using the same method. Further investigations on the individual activity can be conducted in the following aspects.

For the lifting activity, the study of more lifted weight levels is required to find out the relationships between the loads on upper limb joints and the lifted weight. The relationship may be non-linear and is very important information for the task and work design of prevention of upper limb disorders.

For the driving activities, the loads on both hands and upper limb joints need to be investigated to find out the difference and correlation between the loads on the left arm joints and the right arm joints, because the patient may have one arm with disorders and one normal arm.

During the door opening/closing activity, the subject usually walks to the door and uses the movement of the trunk and lower extremities to assist the pulling/pushing actions of the upper limb. This assistance is extremely important for the patient with upper limb disorders,

therefore further investigations of the influence of movement of trunk and lower extremities on the load of upper limb joints is required. This investigation should involve the analysis of the whole body movement and forceplate data measured under the foot.

Finally, investigations of mechanical energy expenditure, mechanical energy transformation at joints, and muscle activities during the activities are required for the complete understanding of the biomechanical nature of these activities.

REFERENCES

- Afflect, J. W., Aitken, R. C. B., Hunter, J., McGuire, R. J., and Roy, C. W. (1988), Rehabilitation status; a measure of medica-social dysfunction. *Lancet*, **i**, 230-233.
- Alexander, M. J. I., and Colbourne, J. (1980), A method of determination of the angular velocity vector of limb segment. *Journal of Biomechanics*, **13**, 1089-1093.
- American Occupational Therapy Association (AOTA) (1979), Philosophical base of occupational therapy, Detroit, MI: Representative Assembly. *The American Journal of Occupational Therapy*, **33**, 785.
- Amirouche, F. M. L., Ider, S. K. and Trimble, J. (1990), Analytical method for the analysis and simulation of human locomotion. *ASME Journal of Biomechanical Engineering*, **112**, 379-386.
- An, K. N. & Chao E. Y. S. (1984), Kinematic analysis of human movement. *Annals of Biomedical Engineering*, **12**, 585-597.
- An, K. N., Chao, E. Y. S., Asken, L. J. (1980), Hand strength measurement instruments. *Archives of Physical Medicine and Rehabilitation*, **61**, 366-368.
- An, K.-N., Jacobsen, M. C., Berglund, L. J., and Chao, E. Y. S. (1988), Application of a Magnetic Tracking Device to Kinesiologic Studies, *Journal of Biomechanics*, **21**, 613-620.
- Andersson, G. B. J. (1981), Epidemiological aspects of low back pain in industry. *Spine*, **6**, 53-60.
- Andrews B. J., Nicol, S. M., Thynne, G. And Beale, A. Q. (1981), The strathclyde TV system for human analysis. In J. P. Paul et al (edt) *Computing in Medicine*, McMillan Press, UK.
- Asmussen, E., Poulsen, E., and Bøch Sørensen, H. E. (1964), Measurements of the muscular strength necessary for driving a motor car. *Communications from the Danish National Association for Infantile Paralysis*, Nr 19.
- Ayoub, M. M. and El-Bassoussi, M. M. (1976), Dynamic biomechanical model for sagital lifting activities. in *Proceedings of the 6th Congress of the International Ergonomics Association* (University of Maryland), 355-361.
- Ayoub, M. M. and McDaniel, J. W. (1974), Effect of operator stance on pushing and pulling tasks. *AIIE Tr.*, **6**, 185-195.

- Bammer, G. and Blignault, I. (1987), A review of research on repetitive strain injuries (RSI). in Peter Buckle (ed.), *Musculoskeletal Disorders at Work*, Taylor & Francis, London, 118-123.
- Barham, J. N. (1978), *Mechanical Kinesiology*. The C. V. Mosby Company.
- Baron, S., Milliron, M. and Habes, D.J. (1990), NIOSH, Health Hazard Evaluation Report. HETA 88-344.
- Begg, R. K. Wytch, R. and Major, R. E. (1989), Instrumentation used in clinical gait studies: a review. *Journal of Medical Engineering & Technology*, 13, 290-295.
- Bejjani, F. J., Gross, C. M. and Pugh, J. W. (1984), Model for static lifting: relationship of loads on the spine and the knee. *Journal of Biomechanics*, 17, 281-286.
- Berne, N., Cappozzo, A., and Meglan, J. (1990), Rigid body mechanics as applied to human movement studies. In Berne and Cappozzo (ed.) *Biomechanics of Human Movement: Application in Rehabilitation, Sport and Ergonomics*, Bertec Corporation, Worthington, Ohio, 89-102.
- Berne, N. and Cappozzo, A. (1990), *Biomechanics of Human Movement: Applications in Rehabilitation, Sports and Ergonomics*. Bertec Corporation, Worthington, Ohio.
- Berne, N., Lawes, P., Solomonidis, S., and Paul, J. P. (1975), A short pylon transducer for measurement of prosthetic forces and moments during amputee gait. *Engineering in Medicine*, 4(4), 6-8.
- Bernstein, N. A. (1967), *The Co-ordination and Regulation of Movement*. New York, Pergamon Press.
- Bisshopp, K. E. (1969), Rodrigues' Formula and Screw matrix, *Transactions ASME, Journal of Engineering for Industry*, 91, 179-185.
- Bjelle, A., Hagberg, M., and Michaelsson, G. (1979), Clinical and ergonomic factors in prolonged shoulder pain among industrial workers. *Scandinavian Journal of Work Environment and Health*, 5, 205-210.
- Bober, T., Putnam, C. A., and Woodward, G. G. (1987), Factors influencing the angular velocity of a human limb segment. *Journal of Biomechanics*, 20, 511-521.
- Bøgh, H. E., and Poulsen, E. (1967), Investigations on the demand/ability relation in handicapped motorists. *Communications from the Danish National Association for Infantile Paralysis*, Nr 26.
- Braune, W. & Fischer, O. (1987), *The Human Gait*. translated by Maquet, P & Furlong, R., Springer-Verlag.

- Braune, W. and Fischer, O. (1889), *On the centre of gravity of the human body*, Translated by P.G.J. Maquet and E. Furlong, 1985. Springer-Verlag, Berlin.
- Bresler, B & Frankel, J. P. (1950), The forces and moments in the leg during level walking, *Trans. Amer. Soc. Mech. Eng.*, **72**, 27-36.
- Buchalter, D. N., Kahanovitz, N., Viola, K., Dorsky, S., and Nordin, M. (1989), Three-dimensional spinal motion measurements, Part 2. A non-invasive assessment of lumbar brace immobilisation of the spine, *J. Spin Disord* **1**, 284-286.
- Buchalter, D. N., Parnianpour, M., Nordin, M., and kahnovitz, N. (1986), A non-invasive in-vivo technique for examining posture and functional spinal motion, In Karwowski, W. ed. *Trend in Ergonomic/Human Factors, III*, Elsevier, 727-737.
- Buchwald, E. (1949), Functional training. *Physical Therapy Review*, **29**, 491- 496.
- Buckle, P. W., Stubbs, D. A., Randle, I. P. M., and Nicholson, A. S. (1992), Limitations in the application of materials handling guidelines. *Ergonomics*, **35**, 955-964.
- Buckle, P. (1987), Musculoskeletal disorders of the upper extremities: the use of epidemiological approaches in industrial settings. *Journal of Hand Surgery*, **12A**, 885-889.
- Burt, S., Hornung, R. and Fine, L. J. (1990), NIOSH Health Hazard Evaluation Report, HETA 89-250-2046.
- Cailliet, R. (1981), *Shoulder Pain*. F. A. Davis Comany, Philadelphia.
- Cappozzo, A. and Berme, N. (1990), Subject-specific segmental inertial parameter determination - A survey of current methods, In Berme and Cappozzo (ed.), *Biomechanics of Human Movement: Applications in Rehabilitation, Sport and Ergonomics*. Bertec Corporation, Worthington Ohio, 178-185.
- Cappozzo, A. (1981), Analysis of the linear displacement of the head and trunk during walking at different speed. *Journal of Biomechanics*, **14**, 411-425.
- Carey, R. G. & Posavac, E. J. (1982), Rehabilitation program evaluation-using a revised level of rehabilitation scale (LORS-II). *Archives of Physical Medicine and Rehabilitation*, **63**, 367-370.
- Chaffin, D. B. and Andersson, G. B. J. (1984), *Occupational Biomechanics*. John Wiley & Sons, New York.
- Chaffin, D. B., Herrin, G. D., Keyserling, W. M. and Garg, A. (1977), A method for evaluating the biomechanical stresses resulting from manual materials handling jobs. *American Industrial Hygiene Association Journal*, **38**, 622-675.

- Chaffin, D. B. (1969), A computerized biomechanical model - development and use in studying gross body actions. *J. Biomechanics*, 2, 429-441.**
- Chandler, R. F., Clauser, C. E., McConville, J. T., Reynolds, H. M. and Young, J. W. (1975), Investigation of inertial properties of human body. *AMRL Technical Report 74-137*, Wright-Patterson Air Force Base Ohio.**
- Chao, E. Y. S. & An, K. N. (1990), Human joint and muscle force estimation, In Berme and Cappozo (ed.) *Biomechanics of Human Movement: Applications in Rehabilitation, Sport and Ergonomics*. Bertec Corporation, Worthington, Ohio, 289-303.**
- Chao, E. Y. S. (1980), Justification of tri-axial goniometer for the measurement of joint rotation. *Journal of Biomechanics*, 13, 989-1006.**
- Chiou, I. L. & Burnett, C. N. (1985), Values of activities of daily living: A survey of stroke patients and their home therapists. *Physical Therapy*, 65, 901-906.**
- Christiansen, C. (1993), Continuing challenges of functional assessment in rehabilitation: Recommended changes. *The American Journal of Occupational Therapy*, 47, 258-259.**
- Ciriello, V. M., Snook, S. H. and Hughes, G. J. (1993), Further studies of psychophysically determined maximum acceptable weights and forces. *Human Factors*, 35, 175-186.**
- Clark, F. A., Parham, D., Carlson, M. E., Frank, G., Jackson, J., Pierce, D., Wolfe, R. J., & Zemke, R. (1991), Occupational science: Academic innovation in the service of occupational therapy's future. *The American Journal of Occupational Therapy*, 45, 300-310.**
- Clarke, M. R., Robertson, J. C., Gillies, J. H., and Ellis, R. M. (1991), Effect of body posture and time on grip strength in patients with cervical spondylosis. *Clinical Biomechanics*, 6, 123-126.**
- Clauser, C. E., McConvide, J. T., and Young, J. W. (1969), Weight, volume, and center of mass of segments of the human body. *Report AMRL-TR-69-70*, Wright Patterson Air Force Base, Ohio.**
- Contini, R., Drillis, R., Hill, D. B. and Bennett, L. (1970), Body segment parameters (Pathological), *Technical Report 1584.03*. School of Engineering and Science, New York University, New York.**
- Crippen, T. E., An, K. N., and Takahashi, K. (1982), Effects of measurement errors in describing human joint motion. *Proceedings of the Tenth Annual Northeast Bioengineering Conference, IEEE*, 178-182.**

- Cunningham, D. M. & Brown, G. W. (1952), Two devices for measuring the forces acting on the human body during walking, *Proc. SESA*, 14(2), 75-90.
- Cushman, W. H. & Rosenbery, D. J. (1991), *Human Factor in Product Design*. Elsevier Science Publisher, Amsterdam.
- Dapena, J. (1981), Simulation of modified human airborne movement. *Journal of Biomechanics*, 14, 81-89.
- Davis, R. B. (1988), Clinical gait analysis. *IEEE Engineering in Medicine and Biology Magazine*, September, 35-40.
- Davis, P. R. and Stubbs, D. A. (1980), *Force Limits in Manual Work*. IPC Science and Technology Press, Guildford.
- Davis, P. R. and Stubbs, D. A. (1978), Performance Capacity Limits. *Applied Ergonomics*, 9, 33-38.
- Dempster, W. T. (1955), *Space requirements of the seated operator*. WADC-TR-55-159, Aerospace Medical Research Laboratories, Ohio.
- Donkers, M. J., An, K. N., Chao, E. Y. S., and Morrey, B. F. (1993), Hand position affects elbow joint load during push-up exercise. *Journal of Biomechanics*, 26, 625-532.
- Drillis, R., Contini, R. and Bluestein, M. (1964), Body segment parameters, A survey of measurement techniques. *Artificial Limbs*, 8(2), 44-66.
- Drillis, R. and Contini, R. (1966), *Body segment parameters*. BP174-954, Tech. Rep. No. 1166.03, School of Engineering and Science, New York University, New York.
- Dupertuis, C. W., et al. (1951), Relation of specific gravity to body build in a group of healthy men. *J. Apply. Physiol*, 3, 676-680.
- Eberhart, H. D. & Inman, V. T. (1947), Fundamental studies of human locomotion and other information relating to design of artificial limb. *University of California, Berkeley, Report to National Research Council, Committee on Artificial Limb*.
- Edwards, M. (1990), The reliability and validity of self-report activities of daily living scales. *Canadian Journal of Occupational Therapy*, 57, 273-278.
- Ellis, M. & Cutts, A. (1992), Measurement of grip strength. *Clinical Biomechanics*, 7, 187-188.
- Engin, A. E. & Tümer, S. T. (1989), Three-dimensional kinematic modelling of human shoulder complex-Part I: Physical model and determination of joint sinus cones. *ASME Journal of Biomechanical Engineering*, 111, 107-112.

- Feinstein, A., Josephy, B. R., & Wells, C. K. (1986), Scientific and clinical problems in indexes of functional disability. *Annals of Internal Medicine*, 105, 413-420.
- Fine, L. J., Punnett, L., and Keyserling, W. M. (1987), An epidemiologic study of postural risk factors for shoulder disorders in industry. In Peter Buckle (ed.), *Musculoskeletal disorders at work*, (Taylor & Francis, London), 108-109.
- Fisher, W. P. (1993), Measurement-related problems in functional assessment. *The American Journal of Occupational Therapy*, 47, 331-338.
- Forthergill, D. M., Pinder, A. D. J., Grieve, D. W. (1993), Protocol for the omnidirectional assessment of manual strength. *Clinical Biomechanics*, 8, 127-134.
- Forthergill, D. M., Grieve, D.W., and Pleasant, S. T. (1991), Human strength capabilities during one handed maximum voluntary exertions in the fore and aft plane. *Ergonomics*, 34, 565-573.
- Fox, W. F. (1967), Body weight and coefficient of friction determinants of pushing capability. *Human Engineering Special Studies Series*, No. 17, Lockheed Co. Marietta, GA.
- Freivalds, A., Chaffin, D. B., Garg, A. And Lee, K. S. (1984), A dynamic biomechanical evaluation of lifting maximum acceptable loads. *J. Biomechanics*, 17, 251-262.
- Frigo, C. (1990), Three-dimensional model for studying the dynamic loads on the spine during lifting. *Clinical Biomechanics*, 5, 143-152.
- Furnée, E. H. (1967), Hybrid instrumentation in prosthetic research. *Proc. 7th Int. Conf. on Med. & Biol. Eng.*, p446, Stockholm.
- Gagnon, D. & Gagnon, M. (1992), The influence of dynamic factors on triaxial net muscular moments at the L5/S1 joint during asymmetrical lifting and lowering. *Journal of Biomechanics*, 25, 891-901.
- Garg, A. and Herrin, G. D. (1979), Stoop or squat: a biomechanical and metabolic evaluation. *AIIE transactions*, Dec., 293-302.
- Giroux, B., and Lamontagne, M. (1992), Net shoulder joint moment and muscular activity during light weight-handily at different displacements and frequencies. *Ergonomics*, 35, 385-403.
- Goldstein, H. (1960), *Classical Dynamics*. Addison-Wesley, New York.
- Granger, C. V., Albrecht, G. L. & Hamilton, B. B. (1979), Outcome of comprehensive medical rehabilitation: Measurement by PULSES Profile and Barthel Index. *Archives of Physical Medicine and Rehabilitation*, 60, 145-154.

- Grant-Thompson, J. C. 1977, *Amputee gait analysis techniques using pylon data*. MSc thesis, University of Strathclyde, Glasgow.
- Griffin M. J. (1992), Causes of motion sickness. In *Contemporary Ergonomics 1992: Ergonomics for industry*, 2-15, Taylor & Francis.
- Grood, E. S. & Suntay, W. J. (1983), A joint coordinate system for clinical description of three-dimensional motions: application to the knee. *J. Biomech. Engng*, **105**, 136-144.
- Guo, L., Genaidy, A., Warm, J. Karwowski, W. And Hidalgo, J. (1992), Effects of job-simulated flexibility and strength-flexibility training protocols on maintenance employees engaged in manual handling operation. *Ergonomics*, **35**, 1103-1117.
- Habes, D., Carlson, W. and Badger, D. (1985), Muscle fatigue associated with repetitive arm lifts: effect of height, weight, and reach. *Ergonomics*, **28**, 471-488.
- Hagberg, M. (1986), Optimising occupational muscular stress of the neck and shoulder. In Corlett et al. (ed.) *The Ergonomics of Working Postures* (Taylor & Francis, London), 109-114.
- Hagberg, M. (1984), Occupational musculoskeletal stress and disorders of neck and shoulder: a review of possible pathophysiology. *International Archives of Occupational and Environmental Health*, **53**, 269-278.
- Hall, S. (1991), *Basic Biomechanics*, Mosby Year Book.
- Hanavan, E. P. (1964), A mathematical model of the human body. *AMRL-TR-64-102*, Wright-Patterson Air Force Base, Ohio.
- Harms-Ringdahl, K. & Ekholm, J. (1987), Influence of arm position on neck muscular activity levels during flexion-extension movements of the cervical spine. In B. Jonsson (ed.) *Biomechanics X-A* (Human Kinetics, Champaign, IL), 249-254.
- Haselgrave, C. M. (1991), Driving for handicapped people. *International Disability Studies*, **13**, 111-120.
- Hatze, H. (1980), A mathematical model for the computational determination of parameter values of anthropomorphic segments. *Journal of Biomechanics*, **13**, 833-843.
- Hatze, H. (1977), A complete set of control equations for the human musculo-skeletal system. *Journal of Biomechanics*, **10**, 799-805.
- Heinrichs, W. (1974), Eine digitale Zeitmesz-einrichtung hoher Auflösung zur Weiterentwicklung der chronocyclographischen Bewegungsaufnahme mit Prozessorrechner. *Europ. J. Appl. Physiol.*, **32**, 227-238.

- van der Helm, F. C. T. (1994), A finite element musculoskeletal model of the shoulder mechanism. *Journal of Biomechanics*, **27**, 551-569.
- van der Helm, F. C. T., Veeger, H. E. J., Pronk, G. M., Van der Wound, L. H. V. and Rozendal, R. H. (1992), Geometry parameters for musculoskeletal modelling of the shoulder system. *Journal of Biomechanics*, **25**, 129-144.
- Herberts, P., Kadefors, R., Högfors, C. and Sigholm, G. (1984), Shoulder pain and heavy manual labour. *Clinical Orthopaedics and Related Research*, **191**, 166-178.
- Herberts, P., Kadefors, R. & Broman, H. (1980), Arm positioning in manual tasks. An electromyographic study of localized muscle fatigue. *Ergonomics*, **23**, 655-665.
- Hertzberg, H. T., Dupertuis, C. W., and Emanuel, I. (1957), Stereophotogrammetry as an anthropometric tool. *Photogrammetric Engineering*, **24**, 924-947.
- Hindle, R. J., Pearcy, M. J., Cross, A. T., and Miller, D.H.T (1990), Three-dimensional Kinematics of the Human Back, *Clinical Biomechanics*, **5**, 218-228.
- Hinrichs, R. N. (1985), Regression equations to predict segment moment of inertia from antropometric measurements: an extension of the data of Chandler *et al.* (1975). *Journal of Biomechanics*, **18**, 621-624.
- Högfors, C., Sigholm, G. and Herbert, P. (1987), Biomechanical model of human shoulder-I. Elements. *Journal of Biomechanics*, **20**, 157-166.
- HSC (Health and Safety Commission) (1988), *Handling Loads at Work*. (Health and Safety Executive, London).
- ILO (International Labour Office) (1988), *Maximum Weights in Load Lifting and Carrying* (ILO Geneva).
- Inman, V. T., Saunders, J. B., and Abbott, L. C. (1944), Observation on the function of shoulder joint, *J. Bone & Joint Surg.*, **26**, 1-30.
- Inman, V. T., Ralston, H., J., and Todd, F. (1981), *Human Walking*, Willims & Wilkins, Baltimore.
- Ivergård, T. (1982), *Information Ergonomics*. Chartwell-Bratt Ltd.
- Jager, M. and Luttman, A. (1992), The load on the lumbar spine during asymmetrical bi-manual material handling. *Ergonomics*, **35**, 783-805.
- Jager, M., Luttmann, A. And Laurig, W. (1984), The load on the spine during the transport of dustbins. *Applied Ergonomics*, **15**, 91-98.
- Jarrett, M. O. (1976), Television - computer system for human locomotion analysis. *PhD Thesis, University of Strathclyde, Glasgow, Scotland, UK.*

- Johnson, R. J. & Smidt, G. L. (1969), Measurement of hip joint motion during walking: evaluation of electrogoniometric method. *Journal of Bone and Joint Surgery*, **51A**, 1083-1094.
- Jones, A. R., Unsworth, A., and Haslock, I. (1985), A microcomputer controlled hand assessment system used for clinical measurement. *Engineering in Medicine*, **14**, 191-198.
- Kapandji, I. A. (1970), *The Physiology of the Joints, Volume1 Upper limb*. Churchill Livingstone, Edinburgh.
- Karlsson, D. & Petersson, B. (1992), Toward a model for force predictions in the human shoulder. *Journal of Biomechanics*, **25**, 189-199.
- Katz, S., Ford, A. B., Moskowitz, R. W., Jackson, B. A. & Jaffe, M. W. (1963), Studies of illness in the aged. *Journal of the American Medical Association*, **12**, 914-919.
- Kiddicoal, K. and Ellis, N. (1987), A national strategy for the prevention and management of RSI, *Musculoskeletal Disorders at Work*. Taylor & Francis, London, 139-145.
- Kinzel, G. L. (1973), On the design of instrumented linkages for the measurement of relative motion between two rigid bodies. Ph.D. Thesis, Purdue University, West Lafayette, Indiana.
- Kinzel, G. L., Hall, A. S. Jr. and Hillberry, B. M. (1972), Measurement of the total motion between two body segment – I. Analytical development. *J. Biomechanics*, **5**, 93-105.
- Kinzel, G. L., Hillberry, B. M., Hall, A. S. Jr., Sickle, V., and Harvey, W. H. (1972), Measurement of the total motion between two body segments, Part II - Description of application. *Journal of Biomechanics*, **5**, 283-293.
- Kirby R. & Roberts J. A. (1985), *Introductory Biomechanics*. Movement Publication Inc. New York.
- Kivela, S. L. (1984), Measuring disability — Do self-ratings and service provider ratings compare. *Journal of Chronic Disease*, **38**, 115-123.
- Klein, R. M. & Bell, B. (1982), Self-care skills: Behavioral measurement with the Klein-Bell ADL Scale. *Archives of Physical Medicine and Rehabilitation*, **63**, 335-338.
- Kompier, M., de Vries, M., van Noord, F., Mulder, H., Neijman, T. and Broersen, J. (1987), Physical work environment and musculoskeletal disorders in the bus driver's profession. In Peter Buckle (ed.) *Musculoskeletal Disorders at Work*, Taylor & Francis, London, 17-22.

- Kondraske, G. V. (1985), Measurement of the quality of hand contractions. *Med. Biol. Eng. Comput.*, **23**, 399.
- Koppa, R. J., Make McDermott, Jr., Leavitt, L. A., and Zuniga E. N. (1978), Handicapped driver controls operability: A device for clinical evaluation of patients. *Arch Phys Med Rehabil*, **59**, 227-231.
- Kroemer, K. H. E. (1992), Personal training for safer material handling. *Ergonomics*, **35**, 1119-1134.
- Kroemer, K. H. E. and Robinson, D. E. (1971), Horizontal static forces exerted by men standing in common working postures on surfaces of various tractions. *AMARL-TR-70-114, Aerospace Medical Research Laboratory, Wright-Patterson air Force Base, Ohio*.
- Kromodihardjo, S. and Mital, A. (1987), Biomechanical analysis of manual lifting tasks. *J. Biomechanical Engineering*, **109**, 132-138.
- Kuhlmann's, A. (1986), *Introduction to Safety Science*. Springer-Verlay, New York.
- Kumar, S. (1980), Physiological responses to weight lifting in different planes. *Ergonomics*, **23**, 987-993.
- Kvarnström, S. (1983), Occurrence of musculoskeletal disorders in manufacturing industry with special attention to occupational shoulder disorders. *Scandinavian Journal of Rehabilitation Medicine*, suppl. **8**, 1-114.
- Law, M. (1993), Evaluating activities of daily living: Directions for the future. *The American Journal of Occupational Therapy*, **47**, 233-237.
- Law, M. & Letts, L. (1993), A critical review of scales of activities of daily living. *The American Journal of Occupational Therapy*, **43**, 522-528.
- Lawes P. (1982), *Alignment kinetics in patient - prosthesis matching*. PhD thesis, University of Strathclyde, Glasgow.
- Lee, K. (1982), Biomechanical Modelling of cart pushing and pulling. Unpublished doctoral dissertation, University of Michigan, Ann Arbor, MI.
- Leskinen, Y. P. F. (1985), Comparison of static and dynamic biomechanical models. *Ergonomics*, **28**, 285-291.
- LeVeau, B. (1977), *Biomechanics of Human Motion*. 2nd ed., Saunder, Philadelphia.
- Li, Q. H. (1993), *Biomechanical analysis of aided gait in total hip replacement or total knee replacement patients*. PhD thesis, University of Strathclyde, Glasgow.

- Lindholm, L. E. & Öberg, K. E. (1974), An opto-electronic instrument for remote on-line movement monitoring. *Biotelemetry*, **2**, 94-95.
- Lings, S. and Jensen, P. B. (1991), Driving after stroke: a controlled laboratory investigation. *International Disability Studies*, **13**, 74-82.
- de Looze, M. P., Toussaint, H. M., van Dieën, J. H., and Kemper H. C. G. (1993), Joint moments and muscle activity in the lower extremities and lower back in lifting and lowering tasks. *Journal of Biomechanics*, **26**, 1067-1076.
- Louis, D. S. (1990), Evolving concerns relating to occupational disorders of upper extremity. *Clinical Orthopaedics and Related Research*, **254**, 140-143.
- Lowe, P. J. (1969), *Knee mechanisms performance during amputee activities*. PhD thesis, University of Strathclyde, Glasgow.
- Lynn P. L. and Fuerst W. (1989), *Introductory digital signal processing with computer application*. John Wiley and Sons, Chichester.
- Magnissalis, E. A. (1992), *Studies of prosthetic loading by means of pylon transducers*. PhD thesis, University of Strathclyde, Glasgow.
- Mahoney, F. I. & Barthel, D. W. (1965), Functional evaluation: Barthel Index. *Maryland State Medicial Journal*, **14**, 61-56.
- Marey, E. J., (1873), Dela locomotion terrestre chez les bipedes at les quadrupedes. *J Anat, Phys.*
- Marras, W. S. and Sommerich, C. M. (1991a), A three-dimensional motion model of loads on the lumbar spine I, Model structure. *Human Factors*, **33**, 123-137.
- Marras, W. S. and Sommerich, C. M. (1991b), A three-dimensional motion model of loads on the lumbar spine, II, Model validation. *Human Factors*, **33**, 139-149.
- Marshall, R. H., Jensen, R. K. and Wood, G. A. (1985), A general Newtonian simulation of an n-segment open chain model. *Journal of Biomechanics*, **18**, 359-367.
- Martin, J. B. and Chaffin, D. B. (1972), Biomechanical computerised simulation of human strength in sagittal plane activities. *AIIE Tr.*, **4**, 19-28.
- Mathiowetz, V. (1993), Role of Physical performance component evaluations in occupational therapy functional assessment. *The American Journal of Occupational Therapy*, **47**, 225-230.
- McGill, S. M. and Norman, R. W. (1985), Dynamically and statically determined low back moments during lifting. *J. Biomechanics*, **18**, 877-855.

- Merbitz, C., Morris, J., & Grip, C. (1989), Ordinal scales and foundations of misinference. *Archives of Physical Medicine and Rehabilitation*, 70, 308-312.
- Meyer, R. H. (1987), RSI-the Australian experience. *Musculoskeletal Disorders at Work*, Taylor & Francis, London, 112-117.
- Miller, D. I. (1979), Modelling in biomechanics: an overview. *Med. Sci. Sports*, 11, 115-122.
- Miller, D. I. and Nelson, R. C. (1973), *Biomechanics of Sport*. Lea and Febiger, Philadelphia.
- MIRA (Motor Industry Research Association) (1979), Personal transport for disabled people. *MIRA Project Report K44554*, Nuneaton, UK: Motor Industry Research Association.
- Mital, N. K., and King, A. I. (1979), Computation of rigid-body rotation in three-dimensional space from body-fixed linear acceleration measurements. *ASME Journal of Applied Mechanics*, 46, 925-930.
- Mitchelson, D. L. (1977), The clinical assessment of gait using polarized light goniometer. *Paper presented at the BES Conference (Sept.) 28-30*.
- Miyazaki, S. & Ishida, A. (1991), New mathematical definition and calculation of axial rotation of anatomical joint. *J. Biomech Engng*, 113, 270-275.
- Morris, J. R. W. (1973), Accelerometry—A technique for the measurement of human body movement. *Journal of Biomechanics*, 6, 729-736.
- Morris, J. M., Lucas, D. B. and Bresler, B. (1961), Role of the trunk in stability of the spine. *Journal of Bone and Joint Surgery*, 43A, 327-351.
- Murray, P. M., Drought, B. A., and Kory, R. C. (1964), Walking patterns of normal men. *Journal of Bone and Joint Surgery*, 64A, 335-360.
- Nicol, A. C. (1987a), A new flexible electrogoniometer with wide spread application. In: Bengt Jonsson (ed.) *International Series on Biomechanics*, Human Kinetic Publishers, Inc., Champaign, IL, Vol 6B, 1029-1033.
- Nicol, A. C. (1987b), Measurement of joint motion. *Clinical Rehabilitation*, 3, 1-9.
- Nicol, A. C. (1977), *Elbow joint prosthesis design: Biomechanical aspects*. PhD thesis, Strathclyde university, Glasgow, Scotland.
- Nicol, S. (1993), *Vicon handbook for bioengineering unit*. University of Strathclyde, Glasgow.
- NIOSH (National Institute for Occupational Safety and Health) (1990), *Revised Work Practices Guide for Manual Lifting*. Draft document (NIOSH, Cincinnati).

- NIOSH (National Institute for Occupational Safety and Health) (1981), *A work practices guide for manual lifting*. Tech. Report No. 81-122, U.S. Dept. of Health and Human Services (NIOSH), Cincinnati, OH.**
- Nicholson, A. S. (1989), A comparative study of methods for establishing load handling capabilities. *Ergonomics*, 32, 1125-1144.**
- Padgaonkar, A. J., Krieger, K. W., and King, A. I. (1975), Measurement of angular acceleration of a rigid body using linear accelerometers. *ASME Journal of Applied Mechanics*, 42, 552-556.**
- Paul, J. P. (1967a). Forces transmitted by joints in the human body. *Proc. Inst. Mech. Eng.* 181(3J), 8-15.**
- Paul, J. P. (1967b), *Forces at the human hip joint*. PhD thesis, University of Glasgow, Glasgow.**
- Pheasant, S. (1986), *Bodyspace: Anthropometry, Ergonomics and Design*. Taylor & Francis, London.**
- Pinder, A. D. J., Forthergill, D. M., and Grieve, D. W. (1993), System for the triaxial measurement of manual force exertions. *Clinical Biomechanics*, 8, 120-126.**
- Poppen, N. K. & Walker, P. S. (1978), Forces at the glenohumeral joint in abduction. *Clin. Orthop. Rel. Res.* 135, 165-170.**
- Porter, J. M., Porter, C. S. and Lee, V. J. A. (1992), A Survey of car driver discomfort. In Lovesey (ed.) *Contemporary Ergonomics 1992*, (Taylor & Francis, London), 262-267.**
- Pronk, G. M. (1987), Three-dimensional determination of the position of the shoulder girdle during humerus elevation. *Biomechanics XI-B*, 1070-1076, 11th ISB-Congress, Amsterdam.**
- Pronk, C. N. A., & Niesing, R. (1981), Measuring hand-grip force, using a new application of strain gauges. *Medical & Biological Engineering & Computing*, 19, 127-128.**
- Punnett, L., Robins, J. M., Wegman, D. H. and Keyserling, M. (1985), Soft tissue disorders in the upper limbs of female garment workers. *Scandinavian Journal of Work and Environmental Health*, 11, 417-425.**
- Putz-Anderson, V. (1988), *Cumulative Trauma Disorders: A Manual for Musculoskeletal Diseases of Upper Limbs*. Taylor & Francis, London.**
- Ramey, M. R. & Yang, A. T. (1981), A simulation procedure for human motion studies. *Journal of Biomechanics*, 14, 203-213.**

- Ranney, D. (1993), Work-related chronic injuries of the forearm and hand: their specific diagnosis and management. *Ergonomics*, **36**, 871-880.
- Reed, E. S. (1982), An outline of a theory of action systems. *Journal of Motor Behavior*, **14**, 98-134.
- Reed, K. L. & Sanderson, S. R. (1983), *Concepts of occupational therapy (2nd ed.)*. Williams & Wilkins, Baltimore.
- Riley, P. O., Mann, R. W. and Hodge, W. A. (1990), Modelling of biomechanics of posture and balance. *Journal of Biomechanics*, **23**, 503-506.
- Roberson, R. E. & Schwertassek, R. (1988), *Dynamics of Multibody System*. Springer-Verlag, Berlin.
- Roebuck, J. A., Kroemer, K. H. E, and Thomson, W. G. (1975), *Engineering Anthropometry Method*. Wiley-Interscience, New York.
- Rohmert, W. (1966), *Maximalkräfte von Männern im Beuegungsraum der Arme und Beine*. Köln, Germany: Wesferdeutscher, Verlag.
- Roosbazer, A. (1975), Biomechanics of lifting. in R. C. Nelson and C. A. Morehouse (eds). *Biomechanics IV*, (University Park Press, State College, PA), 37-43.
- Rowe, M. L. (1983), *Backache at work*. Perinton, Fairport, NY.
- Rubenstein, L. Z., Schairer, C., Wieland, G. D. & Kane, R. (1984), Systematic biases in functional status assessment of elderly adults: Effects of different data sources. *Journal of Gerontology*, **39**, 686-691.
- Runciman, R. J. (1993), *Biomechanical Model of the shoulder joint*, PhD thesis, Bioengineering Unit, University of Strathclyde, Glasgow, UK.
- Sanders, M. S. and McCormick, E. J. (1987), *Human Factors in Engineering and Design*, (6th edition). McGraw-Hill Book Company, Singapore.
- Schaer, A. R. (1992), *Inertial effects in the gait of normal and CP children*. PhD thesis, University of Strathclyde, Glasgow.
- Schüldt, K., Ekholm, J., Harms-Ringdahl, K., Némeh, G. and Arborelius, U. P. (1987), Effect of arm support or suspension on neck and shoulder muscle activity during sedentary work. *Scandinavian Journal of Rehabilitation Medicine*, **19**, 77-84.
- Schüldt, K. Ekholm, J., Harms-Ringdahl, K., Németh, G., and Arborelius, U. P. (1986), Effects of changes in sitting work posture on static neck and shoulder muscle activity. *Ergonomics*, **29**, 1525-1537.

- Schultz, A., Andersson, G. B. J., Ortengren, R., Haderspeck, K. and Nachemson, A. (1982), Loads on the lumbar spine. *Journal of Bone & Joint Surgery*, 64-A, 713-720.
- Selvik, G. (1989), Roentgen stereophotogrammetry - A method for the study of the kinematics of the skeletal system. *Acta Orthopaedica Scandinavica*, Suppl. no. 232, vol. 60, Copenhagen: Munksgaard.
- Serratos-Perez, J. N. and Mendiola-Anda (1993), Musculoskeletal disorders among male sewing machine operators in shoemaking. *Ergonomics*, 36, 793-800.
- Shipman, P., Walker, A., and Bichell, D. (1985), *The Human Skeleton*. Harvard University Press.
- Simon, S. R. 1981, In: Workshop on the clinical application of gait analysis, Dundee, 30th March - 1st April, (1981).
- Singleton, W. T. (1972), *Introduction to Ergonomics*. World Health organisation, Geneva.
- Small, C. F., Bryant, J. T., and Pichora, D. R. (1992), Rationalization of kinematic descriptors for three-dimensional hand and finger motion. *Journal of Biomedical Engineering*, 14, 133-141.
- Snook, S. H. (1978), The design of manual handling tasks. *Ergonomics*, 21, 963-985.
- Statistics Canada (1991), *Work Injuries-1989* (catalogue 72-208) available from Labour Division. Statistics Canada (Queen's Printer, Ottawa, Ontario).
- Steindler, A. (1953), A historical review of the studies and investigations made in relation to human gait. *Journal of Bone and Joint Surgery*, 35A, 540-542, 728.
- Sutherland, D. H. & Hagy, J. L. (1972), Measurement of gait movements from motion picture-film. *Journal of Bone and Joint Surgery*, 54, 787-797.
- Tichauer, E. R. (1978), *The Biomechanical Basis of Ergonomics*. Wiley-Interscience, New York.
- Tichauer, E. R. (1973), In: *The Industrial Environment - Its Evaluation and Control*, National Institute for Occupational Safety and Health. Department of Health, Education and Welfare, Washington, D. D. 138-139.
- Trombly, C. (1993), Anticipating the future: Assessment of occupational function. *The American Journal of Occupational Therapy*, 47, 253-257.
- Tümer, S. T. & Engin, A. E. (1989), Three-dimensional kinematic modelling of human shoulder complex-Part II: Mathematical modelling and solution via optimization. *ASME Journal of Biomechanical Engineering*, 111, 113-121.

- Tupling, S. J., & Pierrynowski, M. R. (1987), Use of cardan angles to locate rigid bodies in three-dimensional space. *Medical & Biological Engineering & Computing*, **25**, 527-532.
- Vaughan, C. L. (1982), Smoothing and differentiation of displacement-time data: An application of splines and digital filtering. *Int. J. Biomed. Comp.*, **13**, 375-386.
- Verstraete, M. C. & Soutas-Little, R. W. (1990), A method for computing the three-dimensional angular velocity and acceleration of a body segment from three-dimensional position data. *ASME Journal of Biomechanical Engineering*, **112**, 114-118.
- Waters, T. R., Putz-Anderson, V., Garg, A. and Fine, L. J. (1993), Revised NIOSH equation for the design and evaluation of material lifting tasks. *Ergonomics*, 1993, **36**, 749-776.
- Webb Associates (1978a), *Anthropometry Source Book*, Vol. II. NASA Reference Publication 1024, Washington, D.C..
- Webb Associate (1978b), *Anthropometric Source Book* Vol. I. NASA 1024, National Aeronautics and Space Administration, Washington, D.C., PP. IV-1 to IV-76.
- Williams, M. and Lissner, H. R. (1962), *Biomechanics of Human Motion*. W. B. Saunders Company, Philadelphia.
- Winter, D. A. (1990), *Biomechanics and Motor Control of Human Movement* (second edition). John Wiley & Sons, Inc., New York.
- Winter, D. A., Sidwall, H. G., and Hobson, D. A. (1974), Measurement and reduction of noise in kinematics of locomotion. *Journal of Biomechanics*, **7**, 157-159.
- Winter, D. A, Greenlaw, R. K., and Hobson, D. A. (1972), Television - computer analysis of kinematics of human gait. *Comp. Biomed. Res.* **5**, 498-504.
- Woltring, H. J. (1994), 3-D attitude representation of human joint: A standarization proposal. *J. Biomechanics*, **27**, 1139-1414.
- Woltring, H. J. (1991), Representation and calculation of 3-D joint movement. *Human Movement Science*, **10**, 603-616.
- Woltring, H. J. (1985), On optimal smoothing and derivative estimation from noisy displacement data in biomechanics. *Human Movement Sciences*, **13**, 229-245.
- Woltring, H. J., Huiskes, R., de Lange A, and Veldpaus, F. E. (1985), Finite centriod and helical axis estimation from noisy landmark measurements in the study of human joint kinematics. *J. Biomechanics*, **18**, 379-389.

- Woltring, H. J. & Marsolais, E. B. (1980),** Opto-electronic (SELSPOT) gait measurement in two- and three-dimensional space - a preliminary report. *Bull. Prosthetics Research*, 46-52.
- Woltring, H. J. (1975),** Single- and dual-axis, lateral photodetectors of rectangular shape. *IEEE trans. Electron. Devices*, 22,581-590.
- Wood, J. E., Meek, S. G. and Jacobsen, S. C. (1989a),** Quantification of human shoulder anatomy for prosthetic arm control I. Surface modelling. *Journal of Biomechanics*, 22, 273-292.
- Wood, J. E., Meek, S. G. and Jacobsen, S. C. (1989b),** Quantification of human shoulder anatomy for prosthetic arm control II. Anatomy matrices. *Journal of Biomechanics*, 22, 319-325.
- Wood, G. A. (1982),** Data smoothing and differentiation procedures in biomechanics. *Exercise and Sport Sciences Reviews*, 10, 308-362.
- Woodson, W. E. (1970),** *Human Engineering Guide for Equipment Designers*. University of California Press.
- Yang, L. (1988),** *The influence of limb alignment on the gait of above-knee amputee*. PhD thesis, University of Strathclyde, Glasgow.
- Yeadon, M. R. and Morlock, M. (1989),** The appropriate use of regression equation for the estimation of segment inertia parameters. *Journal of Biomechanics*, 22, 683-689.

Appendix A

Derivation of Equation 5.58

The derivation of equation of 5.58 begins with the description of the rotation of a rigid body about an arbitrary axis of rotation in a three-dimensional reference frame. Instead of starting the description of the rigid body rotation by the positional changes of a particle in the rigid body as usually used in classical mechanics, the following analysis is based on the positional changes of a unit vector fixed in the rigid body. The reason is that the relative position between any two particles in the rigid body remains unchanged during the rotation of the rigid body, and the positions of the two particles form a unique vector which moves in three-dimensional space with the whole body rotation. The positional changes of a body-fixed vector with the rotation of the body can be described as a translation with its starting point and a rotation about an axis passing through the starting point and parallel to the axis of whole body rotation. If the starting point of the body-fixed vector is on the axis of whole body rotation, the translation of the vector vanishes and the rotation of the vector is the same as the whole body rotation. Therefore the rotation of a rigid body about an axis of rotation can be determined by the rotation of a body-fixed vector with starting point on the axis of rotation (or intersecting with the axis of rotation). The concept is of fundamental importance, it allows any body-fixed vector to be translated onto the axis of the whole body rotation for the analytical purpose of investigating the rotation of the rigid body without losing generality, because the translation of a vector does not change the orientation of the vector.

In Figure A.1, xyz is a reference Cartesian coordinate system with base vector $\mathbf{e} = [\mathbf{i} \ \mathbf{j} \ \mathbf{k}]^T$. $O'O''$ is the axis of rotation and \mathbf{n} is its unit vector. AB and AC represent the positions of a body-fixed unit vector \mathbf{n}_1 and \mathbf{n}_2 before and after rotation, respectively. DB is perpendicular to AD , E is the mid point of BC and DE is perpendicular to BC . A is the starting point of the body-fixed vector on the axis of rotation. θ is the rotation angle.

The purpose of the following analysis is to find \mathbf{n}_2 from the known \mathbf{n} , \mathbf{n}_1 and rotation angle θ . First some geometrical relations in Figure A.1 can be obtained by vector operations as:

$$\mathbf{BC} = \mathbf{n}_2 - \mathbf{n}_1 \quad (\text{A.1})$$

$$\mathbf{AE} = (\mathbf{n}_2 + \mathbf{n}_1) / 2 \quad (\text{A.2})$$

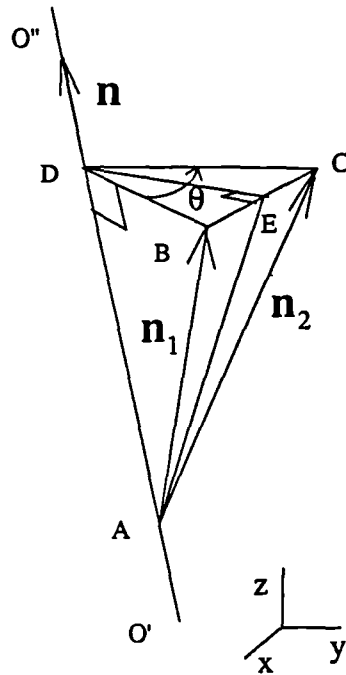


Figure A.1 The rotation of a body-fixed unit vector about an arbitrary axis (O'O'') in a three-dimensional reference frame (xyz). The \mathbf{n} is the unit vector of the rotation axis O'O'', \mathbf{n}_1 and \mathbf{n}_2 are the body-fixed vector before and after the rotation, θ is the rotation angle. The body-fixed unit vector has been transformed onto the rotation axis for the analytical purpose.

$$|BC| = 2 |DE| \tan(\theta/2) \quad (A.3)$$

Because BC is perpendicular to both \mathbf{n} and \mathbf{DE} , it can be expressed as:

$$\mathbf{BC} = a_1 \mathbf{n} \times \mathbf{DE} \quad (A.4)$$

where a_1 is a constant to be determined. The magnitude of vector BC is:

$$|BC| = a_1 |\mathbf{n}| |DE| \sin(\pi/2) = a_1 |DE| \quad (A.5)$$

because \mathbf{n} is a unit vector. From Equation A.3 and A.5, a_1 can be found as:

$$a_1 = 2 \tan(\theta/2) \quad (A.6)$$

Thus

$$\begin{aligned} \mathbf{BC} &= 2 \tan(\theta/2) \mathbf{n} \times \mathbf{DE} \\ &= 2 \tan(\theta/2) \mathbf{n} \times (\mathbf{AE} - \mathbf{AD}) \\ &= 2 \tan(\theta/2) \mathbf{n} \times \mathbf{AE} \end{aligned} \quad (A.7)$$

because \mathbf{n} and \mathbf{AD} are parallel. Combining Equations A.1, A.2, and A.7, it can be found that:

$$\mathbf{n}_2 - \mathbf{n}_1 = \tan(\theta/2) \mathbf{n} \times (\mathbf{n}_2 + \mathbf{n}_1) \quad (A.8)$$

The equation A.8 describes the relation between \mathbf{n} , \mathbf{n}_1 , \mathbf{n}_2 and θ , but it needs to be solved to find unit vector \mathbf{n}_2 . For simplicity equation A.8 is written as:

$$\mathbf{n}_2 - \mathbf{n}_1 = \mathbf{a} \times (\mathbf{n}_2 + \mathbf{n}_1) \quad (A.9)$$

where $\mathbf{a} = \tan(\theta/2) \mathbf{n}$ (A.10)

In order to solve the equation A.9, \mathbf{n}_2 is assumed to have the following form:

$$\mathbf{n}_2 = c_1 \mathbf{n}_1 + c_2 \mathbf{a} + c_3 \mathbf{a} \times \mathbf{n}_1 \quad (A.11)$$

where c_1 , c_2 , and c_3 are constants to be determined. Substituting Equation A.11, into A.9 and comparing the coefficients of corresponding vector, c_1 , c_2 , and c_3 can be found.

Finally \mathbf{n}_2 is obtained as:

$$\mathbf{n}_2 = \cos(\theta) \mathbf{n}_1 + (1-\cos(\theta))(\mathbf{n} \cdot \mathbf{n}_1) \mathbf{n} + \sin(\theta) \mathbf{n} \times \mathbf{n}_1 \quad (A.12)$$

The equation is important. Knowing the unit vector of the axis of rotation \mathbf{n} , the rotation angle θ , a body-fixed unit vector \mathbf{n}_1 before rotation, the orientation of the body-fixed unit vector \mathbf{n}_2 after rotation can be determined. The equation can also be expressed in matrix form by the following procedure. First the unit vectors \mathbf{n} , \mathbf{n}_1 , and \mathbf{n}_2 are expressed in matrix forms as:

$$\mathbf{n} = [\mathbf{n}]^T [\mathbf{e}] = [n_1 \ n_2 \ n_3] [\mathbf{e}] \quad (A.13)$$

$$\mathbf{n}_1 = [\mathbf{n}_1]^T [\mathbf{e}] = [n_1^1 \ n_2^1 \ n_3^1] [\mathbf{e}] \quad (A.14)$$

$$\mathbf{n}_2 = [\mathbf{n}_2]^T [\mathbf{e}] = [n_1^2 \ n_2^2 \ n_3^2] [\mathbf{e}] \quad (A.15)$$

$$[e] = [i \ j \ k]^T \quad (\text{A.16})$$

where $[e]$ is the base vector of the reference Cartesian coordinate system and

$$\begin{aligned} l_1, l_2, l_3, &= \text{three components of unit vector } n \text{ in the reference frame} \\ n_1^1, n_2^1, n_3^1, &= \text{three components of unit vector } n_1 \text{ in the reference frame} \\ n_1^2, n_2^2, n_3^2, &= \text{three components of unit vector } n_2 \text{ in the reference frame} \end{aligned}$$

Then by vector operation on the second term of the right hand side of equation A.12 becomes

$$\begin{aligned} (n \cdot n_1) n &= (([n]^T [e]) \cdot ([n_1]^T [e])) [n]^T [e] \\ &= ([n]^T ([e] \cdot [e]^T) [n_1]) [n]^T [e] \\ &= [n]^T [n_1] [n]^T [e] \\ &= [n_1]^T [n] [n]^T [e] \end{aligned} \quad (\text{A.17})$$

in which matrix transpose properties were used. The vector product in the last term of Equation A.12 is

$$n \times n_1 = [n_1]^T [\tilde{n}]^T [e] \quad (\text{A.18})$$

where $[\tilde{n}]^T$ is the transpose of Skew-symmetric matrix $[\tilde{n}]$ and

$$[\tilde{n}] = \begin{bmatrix} 0 & -l_3 & l_2 \\ l_3 & 0 & -l_1 \\ -l_2 & l_1 & 0 \end{bmatrix} \quad (\text{A.19})$$

Substituting Equations A.13 to A.18 into equation A.12, then equation A.12 becomes:

$$[n_2]^T [e] = \cos(\theta) [n_1]^T [e] + (1 - \cos(\theta)) [n_1]^T [n] [n]^T [e] + \sin(\theta) [n_1]^T [\tilde{n}]^T [e] \quad (\text{A.20})$$

Removing $[e]$ on each side of the above equation, it becomes:

$$[n_2]^T = \cos(\theta) [n_1]^T + (1 - \cos(\theta)) [n_1]^T [n] [n]^T + \sin(\theta) [n_1]^T [\tilde{n}]^T \quad (\text{A.21})$$

Then transposing each side of Equation A.21, it is written as:

$$[n_2] = \cos(\theta) [n_1] + (1 - \cos(\theta)) [n] [n]^T [n_1] + \sin(\theta) [\tilde{n}] [n_1] \quad (\text{A.22})$$

For simplicity, remove the square brackets and rewrite the equation in matrix and vector form as:

$$n_2 = A(\theta, n) n_1 \quad (\text{A.23})$$

where

$$A(\theta, n) = \cos(\theta) I + (1 - \cos(\theta)) n n^T + \sin(\theta) [\tilde{n}] \quad (\text{A.24})$$

is the transformation matrix, I is a unit matrix, $[\tilde{n}]$ has been given in equation A.19, and $n n^T$ can be explicitly written as:

$$\mathbf{n} \mathbf{n}^T = \begin{bmatrix} l_1 \\ l_2 \\ l_3 \end{bmatrix} (l_1 \quad l_2 \quad l_3) = \begin{bmatrix} l_1 l_1 & l_1 l_2 & l_1 l_3 \\ l_2 l_1 & l_2 l_2 & l_2 l_3 \\ l_3 l_1 & l_3 l_2 & l_3 l_3 \end{bmatrix} \quad (\text{A.25})$$

The \mathbf{n}_1 and \mathbf{n}_2 in equation A.23 can be considered as column vectors. It can be seen that the transformation matrix $A(\theta, \mathbf{n})$ is only related with the rotation axis \mathbf{n} and rotation angle θ , therefore the orientation of any body-fixed vector \mathbf{n}_2 after rotation can be determined from its orientation directed by \mathbf{n}_1 before rotation, the transformation matrix A and using Equation A.23. An alternative approach to derivation of the Eq. 5.58 and Eq. A.24 can be found in Bisshopp (1969).

Appendix B

The purpose of this Appendix is to formulate the changes of shoulder (or elbow) moments with a small shoulder displacement relative to the hand where a constant force is acted.

Considering the arm as a rigid segment, the relative position between shoulder and hand is :

$$\mathbf{r} = [x \quad y \quad z]^T \quad (\text{B.1})$$

and the hand force is:

$$\mathbf{F} = [F_x \quad F_y \quad F_z]^T \quad (\text{B.2})$$

Then the shoulder moment is:

$$\mathbf{M} = \mathbf{r} \times \mathbf{F} \quad (\text{B.3})$$

$$= M_x \mathbf{i} + M_y \mathbf{j} + M_z \mathbf{k} \quad (\text{B.4})$$

which can be written in matrix form as:

$$\mathbf{M} = [M_x \quad M_y \quad M_z]^T = [yF_z - zF_y, \quad zF_x - xF_z, \quad xF_y - yF_x]^T \quad (\text{B.5})$$

The changes of the shoulder moment is assumed as:

$$d\mathbf{M} = dM_x \mathbf{i} + dM_y \mathbf{j} + dM_z \mathbf{k} \quad (\text{B.6})$$

In case the shoulder joint has a small displacement relative to the hand:

$$d\mathbf{r} = dx \mathbf{i} + dy \mathbf{j} + dz \mathbf{k} \quad (\text{B.7})$$

then each component of $d\mathbf{M}$ in Eq. B.6 can be written as:

$$\begin{aligned}
dM_x &= \frac{\partial M_x}{\partial x} dx + \frac{\partial M_x}{\partial y} dy + \frac{\partial M_x}{\partial z} dz \\
dM_y &= \frac{\partial M_y}{\partial x} dx + \frac{\partial M_y}{\partial y} dy + \frac{\partial M_y}{\partial z} dz \\
dM_z &= \frac{\partial M_z}{\partial x} dx + \frac{\partial M_z}{\partial y} dy + \frac{\partial M_z}{\partial z} dz
\end{aligned} \tag{B.8}$$

From Eq. B.5, the partial derivatives in Eq. B.8 can be derived as:

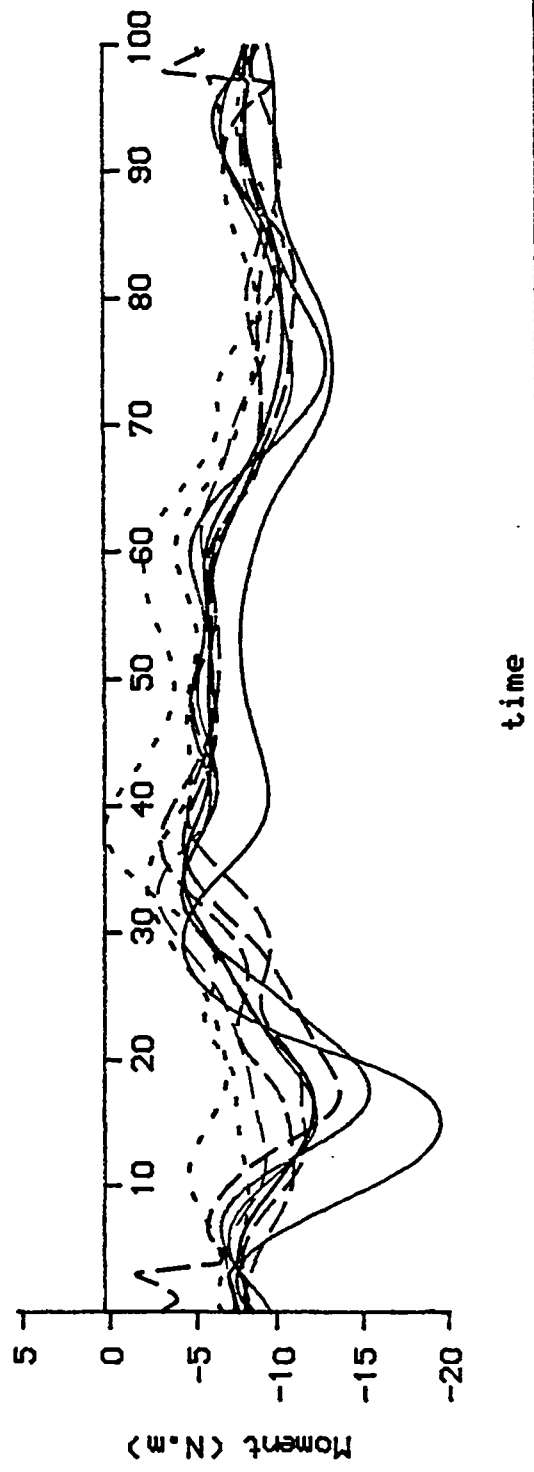
$$\begin{aligned}
\frac{\partial M_x}{\partial x} &= 0, \quad \frac{\partial M_x}{\partial y} = Fz, \quad \frac{\partial M_x}{\partial z} = -Fy \\
\frac{\partial M_y}{\partial x} &= -Fz, \quad \frac{\partial M_y}{\partial y} = 0, \quad \frac{\partial M_y}{\partial z} = Fx \\
\frac{\partial M_z}{\partial x} &= Fy, \quad \frac{\partial M_z}{\partial y} = -Fx, \quad \frac{\partial M_z}{\partial z} = 0
\end{aligned} \tag{B.9}$$

Then considering Eq. B.7 and Eq. B.8, Eq. B.6 can be written in matrix form as:

$$d\mathbf{M} = \begin{bmatrix} dM_x \\ dM_y \\ dM_z \end{bmatrix} = \begin{bmatrix} 0 & Fz & -Fy \\ -Fz & 0 & Fx \\ Fy & -Fx & 0 \end{bmatrix} \begin{bmatrix} dx \\ dy \\ dz \end{bmatrix} = [\tilde{F}] d\mathbf{r} \tag{B.10}$$

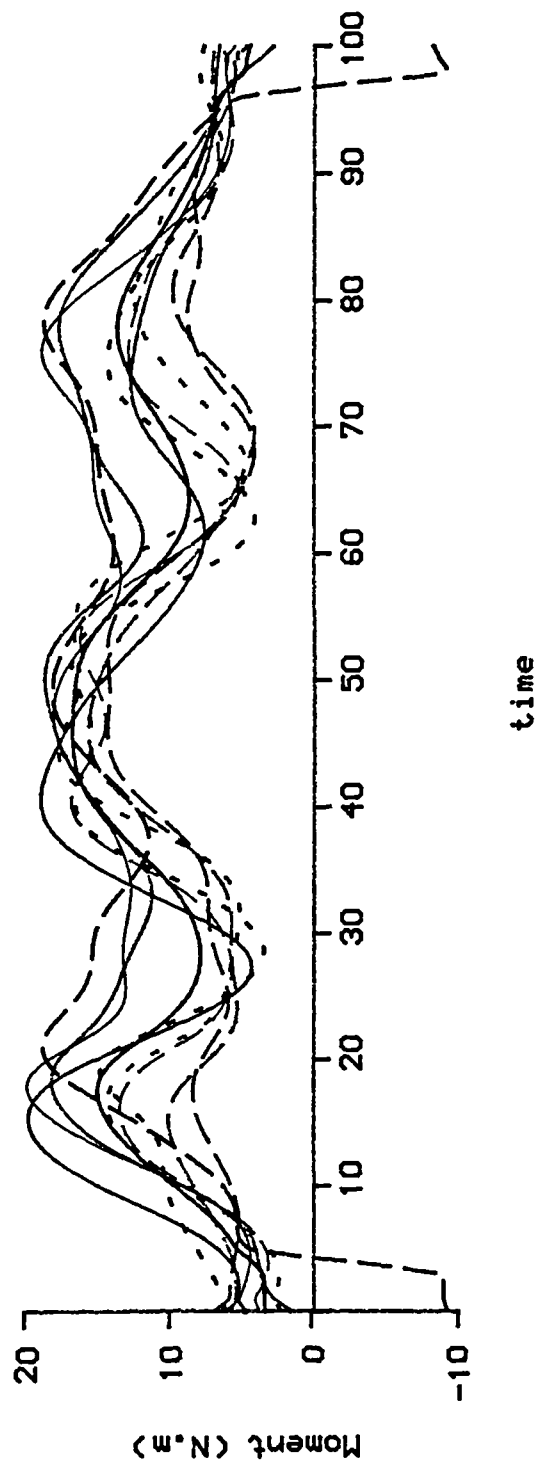
From above equation the increment of shoulder moment due to the increment of relative position between shoulder and hand can be determined, when the hand force F is constant. The $d\mathbf{M}$, F , and $d\mathbf{r}$ in Eq. B.10 are all expressed in the same coordinate system therefore if the hand force and shoulder moment are measured or expressed in different coordinate systems a coordinate transformation is required before using Eq. B.10.

Appendix C



Normalized shoulder moments (Mx) in the trunk system during the lifting of a 2kg book to the highest height.

Figure C.1



Normalized shoulder moments (M_z) in the trunk system during the lifting of a 2kg book to the highest height.

Figure C.3